POST-RIFT SEDIMENTARY EVOLUTION OF THE CENTRAL BRANSFIELD BASIN (ANTARCTIC PENINSULA)

Margarita García García

EVOLUCIÓN SEDIMENTARIA POST-RIFT DE LA CUENCA CENTRAL DE BRANSFIELD (PENÍNSULA ANTÁRTICA)

Tesis Doctoral 2008

Departament d'Estratigrafia, Paleontologia i Geociències Marines
Universitat de Barcelona
Programa de Doctorado en Ciencias del Mar
Bienio 2002-2004

Post-rift sedimentary evolution of the Central Bransfield Basin (Antarctic Peninsula)

Evolución sedimentaria post-rift de la Cuenca Central
de Bransfield (Península Antártica)

Memoria de Tesis Doctoral presentada por

Margarita García García

2008

Memoria de Tesis Doctoral presentada por

Margarita García García

para optar al título de Doctora por la Universitat de Barcelona

Tesis realizada en el Departamento de Geología Marina del
Instituto de Ciencias del Mar (ICM)
Centro Mediterráneo de Investigaciones Marinas y Ambientales (CMIMA)
Consejo Superior de Investigaciones Científicas (CSIC)
Barcelona

La doctoranda:

Margarita García García

Las directoras de la Tesis:

Dra. Gemma Ercilla Zárraga	Dra. Belén Alonso Martínez
Departamento de Geología Marina	Departamento de Geología Marina
Instituto de Ciencias del Mar	Instituto de Ciencias del Mar
CMIMA-CSIC	CMIMA-CSIC

El tutor de la Tesis:

Dr. Miquel Canals Artigas
Departament d'Estratigrafia, Paleontologia i Geociències Marines
Universitat de Barcelona

Agradecimientos

Esta Tesis es el resultado de varios años de trabajo en el Instituto de Ciencias del Mar (ICM, CSIC) de Barcelona. Pero también es el resultado de una formación científica que empezó en el Centro Oceanográfico de Málaga (IEO), prosiguió en el Departamento de Geofísica de la Universidad de Chile y continuó en este centro, aunque con otros objetivos científicos más cercanos espacialmente. Finalmente, la geología marina de la Antártida se convirtió en el centro de mis estudios, lo que ha llenado estos últimos años de grandes quebraderos de cabeza pero a su vez de grandes satisfacciones. El camino realizado antes de llegar aquí me ha ofrecido la formación científica para abordar este estudio, pero también la posibilidad de haber trabajado en diversos centros de investigación, con numerosos compañeros de los que he ido aprendiendo poquito a poco a lo largo de los años.

Mi primer agradecimiento es para las directoras de esta Tesis, Gemma Ercilla y Belén Alonso, del Instituto de Ciencias del Mar de Barcelona. A Belén le debo mi integración en el Grupo de Márgenes Continentales del Departamento de Geología Marina del ICM, desde donde he tenido la oportunidad de trabajar en numerosos proyectos y su ayuda en todos los temas científicos que he abordado, además de su apoyo total en todos los aspectos desde mi llegada a Barcelona. Por su parte, Gemma me ha transmitido la pasión por la Geología Marina que ha hecho posible, entre otros trabajos, la realización de esta Tesis. También le agradezco su energía y dedicación incansable y sus millones de ideas, cuestionamientos y propuestas, además de su increíble capacidad de transmitir su conocimiento. Aún más, le debo el sentirme respaldada y respetada como investigadora y como persona. Le agradezco, finalmente, la confianza que ha depositado en mí para trabajar sobre los datos estudiados en esta Tesis.

Quiero agradecer al tutor de esta Tesis, Miquel Canals, de la Universitat de Barcelona, las facilidades que me ha proporcionado para que todos los trámites se pudieran llevar a buen término y por su continuo interés en el tema de esta Tesis.

I want to thank John B. Anderson, from the Department of Earth Sciences of the Rice University (Houston, Texas) for his efforts in our collaboration, which has been crucial for the ellaboration of this Thesis. Also, I thank John for having invited me to participate in an Antarctic cruise, where I confirmed that the "study area" is the most beautiful place in the world. I would like to thank all the people from his Department -Julia Wellner, David C. Heroy and specially Rodrigo Fernández- for their help during my stage in Houston and during the cruise.

A mis compañeros de grupo, David Casas, Ferran Estrada, Marcel.li Farran y Jorge Iglesias, les debo un agradecimiento especial, además de por su apoyo constante en el trabajo científico y su ayuda para la finalización de esta Tesis, por los estupendos ratos pasados en campañas, viajes, y charlas a la hora del café y cigarrito.

A las técnicas de laboratorio del Instituto de Ciencias del Mar, Neus Maestro y Silvia de Diago, les agradezco su dedicación en el trabajo con las muestras analizadas para esta Tesis, y por supuesto por su amabilidad y esas sonrisas que van repartiendo por los pasillos. A José Manuel Fortuño, le agradezco su ayuda para la obtención de imágenes de microscopio electrónico y sus explicaciones sobre la "sopa de diatomeas". A mucha gente del ICM, que hace que ir a trabajar cada día sea menos duro. Al personal del Hospital Clínic Veterinari de la Universitat Autònoma de Barcelona, por su ayuda en la obtención de imágenes de Rayos X.

A Javier Hernández Molina, le agradezco un poco todo, desde haberme ayudado a dar mis primeros pasos en la investigación hasta ejercer de "guía espiritual" ante cualquier duda. Y aún más por su hospitalidad, por los buenos ratos compartidos y por haber descubierto con él los efectos de la piña sobre la capacidad intelectual.

A los colegas del instituto y "allegados"… son muchos, los que están ahora y los que ya se fueron. A Elena y Tona, por estar siempre conmigo. A Graziella, que me ayudó a prever lo que se me venía encima con esto de la Tesis. A Claudio y sus abrazos. A Cesca, por su vitalidad contagiosa. A Ruth, Frederique, Laura, Marta, Arturo y Toni, que han dado un soplo de vidilla en estos últimos tiempos.

A los amigos de la universidad y "satélites"… Muchas gracias por los estupendos ratos que he pasado con vosotros, esas celebraciones de tesis, vendimias, calçotadas, boletadas y "lo que se terciara". Me habéis hecho querer más a esta ciudad. A Tina y Joan lejos y Sergi y Eli más cerca… gracias por todo y mucha suerte!

A mis niños queridos, que tengo lejos desde hace tiempo pero aún así lo son, y cada vez más. A Marta, Miguel, Lella, Ernesto, Nico, Bea, Carmen, Aintzina. A la niña Cuca, que reparte alegría.

Y por supuesto, a mi familia, que tengo lejos desde hace tanto tiempo. A mis estupendos hermanos y hermanas, cuñaos y sobrinos. Y sobre todo a mi madre que –ya lo dije en los agradecimientos de la tesina– sigue siendo la mejor.

A la memoria de Jesús Baraza, quien me hubiera gustado que disfrutara de esta Tesis, cuyos datos fueron obtenidos gracias a su esfuerzo y dedicación.

Según el filósofo Ly Tin Wheedle, el caos se encuentra en mayor abundancia cuando se busca el orden. El caos siempre derrota al orden porque está mejor organizado

Terry Pratchett

Tiempos interesantes

INDEX

Chapter I. Introduction

Chapter II. Methodology and dataset

Chapter III. Physiography, morphology and recent sedimentary systems

Chapter IV. Post-rift seismic stratigraphic architecture of the Antarctic Peninsula margin, growth patterns and controlling factors

Chapter V. Sediment types and processes, stratigraphy and sedimentary models during the last glacial cycle

Chapter VI. Synthesis and conclusions

References

Presentation and objectives of the Ph.D. Thesis

Detailed studies of glacial and glaciomarine processes and the resulting sedimentary products in high-latitude margins started to develop only about 35 years ago, promoted by the availability of techniques and oceanographic vessels adaptable for this environment. The study of marine geology in Antarctic margin is a challenging experience, due to the inherent difficulties in dealing with glacial environments. However, it is highly required to understand climatic changes in the past and to better predict future changes that will affect the natural systems of the planet Earth, since the continental margins surrounding the Antarctic constitute a tape recorder of its ice sheet behavior, which plays an important role in regulating the world climate, atmosphere, ocean circulation and sea level changes.

The investigations of the sedimentary record of the Antarctic continental margins through seismic reflection methods and sediment cores represent the most useful tool for the study of the glacial, glaciomarine and marine sedimentary processes. These investigations make possible to recognize and differentiate criteria in order to distinguish glacial from local tectonic, physiographic/morphologic, sediment source and oceanographic effects.

A review of the state of the art about the building and evolution of the glacier-influenced sedimentation on the Antarctic continental margins reveals that most studies have been focused in specific physiographic/sedimentary domains. There is a lack of studies reconstructing the interplay among the different sedimentary systems and approaching the stratigraphic architecture of the margin and deep sea as an entire system. Likewise, the sedimentary dynamics and processes that transfer the sediment from shoreline to deep basins in high-latitude continental margins are not yet well established.

Based on the significance of the Antarctic glacial and glaciomarine environments and the state of the art of their sedimentology investigations, the present PhD Thesis aims the following objectives:

- To analyse, interpret and discuss the post-rift sedimentary evolution of the Central Bransfield. This objective is approached by three specific objectives:

  a) To establish and characterize the sedimentary systems composing the morphologic and physiographic domains of the Central Bransfield Basin during the last glacial cycle; analysing the linkages between them in a source-to-sink perspective; and studying the global and local factors that have controlled their evolution.

b) To provide new insights in the characterization and interpretation of the post-rift stratigraphic architecture and growth patterns of the Antarctic Peninsula continental margin of the Central Bransfield Basin; to analyze in detail the seismic facies, seismic sequences and units and unconformities; and to constrain the chronology of the stratigraphic evolution in order to reconstruct the Antarctic Peninsula Ice Sheet dynamics and its interaction with the physiographic and structural configuration over time.

c) To characterize the near-surface sediment types formed during the last glacial cycle in the various environments of the Central Bransfield Basin, establishing the relationships among sedimentary processes, associated sequences and sedimentary environments; to interpret the stratigraphic models in the light of the Antarctic Peninsula Ice Sheet dynamics that affected the Central Bransfield Basin during the last glacial cycle and their interaction with local factors.

- To provide improved and new models of the post-rift sedimentary-evolution with different temporal and resolution scales, in order to increase the present-day knowledge of sedimentation on the Central Bransfield Basin; and to compare the models of both margins of the CBB in order to refine the understanding of the role played by the factors controlling the basin infilling (who, how and when).

This Ph. D. thesis is structured in six chapters. Chapter I presents the state of the art in the knowledge of marine geology in high-latitude continental margins and in particular of the study area, the Central Bransfield Basin and the Antarctic Peninsula.

Chapter II explains the dataset studied in this Thesis and the methodology applied for the data obtaining, processing, visualization and interpretative analyses.

Chapter III deals with the physiography and morphology of the Central Bransfield Basin. Specifically, this investigation characterizes the sedimentary systems forming the Antarctic Peninsula and South Shetland Islands margins and adjacent basin, through an integrated study from a source-to-sink point of view. The results of this chapter have been submitted for publication:

García, M., Ercilla, G., Alonso, B. Morphology and sedimentary systems in the Central Bransfield Basin (Antarctic Peninsula). Basin Research. Accepted with moderate revisions.

Chapter IV presents the stratigraphic architecture and growth patterns of the Antarctic Peninsula margin of the Central Bransfield Basin and the post-rift sedimentary evolution. The results of this chapter have been published in:

García, M., Ercilla, G., Anderson, J.B., Alonso, B., 2008. New insights on the post-rift sedimentary evolution of the Antarctic Peninsula margin (Central Bransfield Basin). Marine Geology 251, 167-182. DOI: 10.1016/j.margeo.2008.02.006.

Chapter V analyses the last glacial sedimentation and near-surface stratigraphy in the Central Bransfield Basin, in order to recognize the sedimentary mechanisms in the different environments of the study area.

Finally, Chapter VI includes the synthesis of the results and conclusions of this PhD Thesis and proposes new models for the post-rift sedimentary evolution of the Central Bransfield Basin. Some outstanding questions that have risen from this study are also proposed in this chapter.

This PhD Thesis is presented during the International Polar Year (IPY 2007-2009) and the International Year of the Planet Earth (IYPE 2007-2009). It shares with the IPY scientific programme the intention of enhancing the knowledge about changes in ice sheets, global linkages between ice dynamics and climate, and developing a new understanding of processes occurring in polar margins. Likewise, the objectives of this thesis have much in common with the philosophy behind the IYPE since the erosional and depositional landscape of the Central Bransfield Basin may be translated into the narrative of the geological history of the Antarctic Ice Sheet dynamics. Also, this thesis pursues providing a piece of knowledge about the mechanisms occurring in the natural systems development, which may help to improve the natural environment policies to preserve the planet.

Abstract

The Central Bransfield Basin is located at the northernmost tip of the Antarctic Peninsula (West Antarctica). This investigation, focused in the morphology, stratigraphy and near-surface sedimentation, and based on acoustic, seismic and sedimentological methods, reveals the main sedimentary systems and processes involved in the stratigraphic architecture and growth pattern of the basin. Likewise, it provides clues about the interplay of the global and local factors that have controlled the basin sedimentary evolution during the post-rift stage and allows the reconstruction of depositional models.

The most striking physiographic characteristic of the Central Bransfield Basin is the presence of slope platforms composing the middle domain of the slope, in both the Antarctic Peninsula and South Shetland Islands margins. This favors the occurrence of glacial and glaciomarine processes on this domain, representing a difference with other high-latitude margins, where these processes are restricted to the continental shelf. The morphologic elements identified on the Central Bransfield Basin may be grouped into four major sedimentary systems (glacial-glaciomarine, slope-basin, seabed fluid outflow and contourite). The development of these systems has occurred during the last glacial cycle and has been controlled by the glacial cyclicity, tectonics, physiography and oceanography.

The post-rift seismic stratigraphy of the Antarctic Peninsular margin consists on two seismic sequences, S1 and S2, of glacial and glaciomarine origin, overlying the syn-rift record. S2 was deposited during the post-rift to the Mid-Pleistocene and can be subdivided into four seismic units composed of prograding wedges. S1 was deposited after the Mid-Pleistocene and is composed of prograding/aggrading deposits. This sequence is composed of five seismic units whose distribution was mostly governed by variations in the thermal regimes of the Antarctic Peninsula Ice Sheet. Climate and physiography are interpreted as the major factors controlling the stratigraphic architecture and growth pattern of the margin.

The near-surface sedimentary record of the Central Bransfield Basin corresponds to the last glacial cycle and offers a high-resolution definition of sediment sequences, including subglacial diamicton, compound glaciomarine, turbid glacial meltwater, proglacial diamicton, flow-in and contourite sequences, and a characterization of the sedimentary paleoenvironments during the deglaciation and interglacial stage. Likewise, the identification of sedimentary processes allows the establishment of several stratigraphic models (glacial trough, slope platforms, lower slope and basin) in the Central Bransfield

Basin, in relation to sedimentary processes that were directly controlled by climatic factors and modulated by the physiography/morphology, sediment source and oceanography.

This PhD Thesis has allowed the definition of post-rift sedimentary models by different scale, resolution and temporal approaches. Likewise, the interpretation of the interplay among the different depositional systems has been done considering the margin and deep sea as an entire system, to analyze the inherent sedimentary dynamics and processes that transfer the sediment from the shoreline to the deep basin.

Resumen

Presentación y objetivos de la Tesis Doctoral

Los estudios de procesos glaciales y glaciomarinos y sus productos sedimentarios en márgenes continentales de altas latitudes comenzaron a desarrollarse hace apenas 35 años, favorecidos por la disponibilidad de técnicas y buques oceanográficos adaptados a estos medios. A pesar de que el estudio de la geología marina en la Antártida presenta serias dificultades debidas al entorno, dicho estudio es necesario para la comprensión de los cambios climáticos en el pasado y para la predicción de los cambios que afectarán en el futuro a los sistemas naturales del planeta, ya que los márgenes continentales de la Antártida registran el comportamiento de los mantos de hielo, que tiene una gran repercusión en la regulación del clima, atmósfera, circulación oceánica y cambios del nivel del mar a escala global.

El empleo de técnicas indirectas, acústicas y sísmicas, y técnicas directas como la obtención de testigos de sedimento es útil para investigar los procesos glaciales, glaciomarinos y marinos en márgenes continentales de altas latitudes, y posibilitan el reconocimiento y la diferenciación de criterios para discernir los efectos climáticos globales de otros efectos locales como la tectónica, la fisiografía y morfología, el aporte de sedimento y la oceanografía. La mayor parte de trabajos científicos desarrollados en este tipo de márgenes se han centrado en dominios fisiográficos específicos, de modo que las reconstrucciones de la inter-relación entre distintos sistemas sedimentarios y el enfoque de la arquitectura estratigráfica de margen y cuenca como un sistema completo son escasos en la literatura. Basándose en la importancia del estudio de los ambientes glaciales y glaciomarinos de la Antártida, y el estado actual de las investigaciones sedimentarias en estos ambientes, la presente Tesis Doctoral tiene como objetivos:

- Analizar, interpretar y discutir la evolución sedimentaria post-rift de la Cuenca Central de Bransfield. Este objetivo se aborda mediante tres objetivos específicos:

  a) Definir y caracterizar los sistemas sedimentarios que componen los dominios morfológicos y fisiográficos de la Cuenca Central de Bransfield durante el último ciclo glacial; analizar las interacciones entre ellos en una perspectiva de "*source to sink*"; y estudiar los factores globales y locales que han controlado su evolución.

  b) Caracterizar en detalle y refinar la interpretación de la arquitectura estratigráfica del margen de la Península Antártica de la Cuenca Central de

Bransfield; Analizar en detalle las facies sísmicas, secuencias y unidades sísmicas y disconformidades que las limitan; y acotar la cronología de la evolución estratigráfica, con el objeto de reconstruir la dinámica del Manto de Hielo de la Península Antártica y su relación con la configuración fisiográfica y estructural a lo largo del tiempo.

c) Caracterizar los tipos de sedimento superficial depositados durante el último ciclo glacial en los diferentes ambientes de la Cuenca Central de Bransfield, estableciendo las relaciones entre procesos sedimentarios, secuencias asociadas y ambientes sedimentarios; interpretar los modelos estratigráficos en base a la dinámica del Manto de Hielo de la Península Antártica que afectó a la Cuenca Central de Bransfield durante el último ciclo glacial, y su inter-relación con factores locales.

- Proponer modelos mejorados y nuevos para la evolución post-rift, a diferentes escalas temporales y espaciales, con el objeto de aumentar el conocimiento de la sedimentación de la Cuenca Central de Bransfield; y comparar los modelos de los dos márgenes de la cuenca para refinar la comprensión del papel jugado por los diferentes factores de control en el relleno y evolución de la cuenca.

CAPÍTULO I. Introducción

1.1. Estado del arte

Los ambientes glaciales muestran una gran sensibilidad a los cambios climáticos, ya que reciben la influencia directa del avance y retroceso del hielo a lo largo de los ciclos glaciales. El ambiente glacial se define como aquel área con algún tipo de contacto con glaciares (Reading, 1986) y actualmente ocupa aproximadamente un 10% de la superficie terrestre, aunque en periodos pasados llegaron a ocupar hasta el 30%.

El hielo representa el agente principal de erosión y sedimentación en ambientes glaciales, por lo que resulta de gran interés conocer las modalidades en las que se presenta. Los *casquetes o mantos de hielo* representan las mayores acumulaciones de hielo; las *plataformas de hielo* son masas de hielo parcialmente flotantes que se desarrollan en los bordes del continente y se extiende sobre el océano. Las *corrientes de hielo* representan la parte más rápida de los casquetes de hielo. Se forman allí donde este se mueve más rápido (> 1 m/a). Son los puntos por donde se produce el principal drenaje de la masa de hielo del casquete; Las *lenguas de hielo* forman masas de hielo flotantes estrechas y largas.

Finalmente, los *icebergs* son fragmentos de hielo que se desprende de los glaciares o plataformas de hielo, que suelen ser transportados por las corrientes.

En medios glaciomarinos, se pueden diferenciar cuatro ambientes sedimentarios, en relación con su posición respecto a la capa de hielo. Estos ambientes se denominan, de proximal a distal: subglacial, zona de anclaje, proglacial (proximal y distal o sub-plataforma de hielo) y marino.

1.2. Procesos y facies sedimentarias

Los procesos sedimentarios en márgenes continentales de altas latitudes incluyen, de forma general, la erosión glacial de la plataforma continental por el efecto directo del avance de la capa de hielo, y el depósito y retrabajamiento del sedimento erosionado a través de procesos glaciales y glaciomarinos en la plataforma externa y margen distal durante los intervalos glaciales (Alley et al., 1989; Anderson et al., 1999). Durante los intervalos interglaciales la capa de hielo retrocede hacia costa y predominan los procesos glaciomarinos, como las capas de turbidez por derretimiento, caída de derrubios glaciales y los procesos marinos, como la caída vertical de sedimento, los flujos de gravedad y el retrabajamiento por corrientes de contorno.

En el ambiente subglacial, localizado bajo la base de hielo, predomina la erosión subglacial. Este proceso depende del estado termal en la base del hielo (Eyles, 2006). En glaciares templados el movimiento del hielo se produce por la deformación interna y el movimiento está favorecido por las capas de agua que se forman entre la base del hielo y el sustrato, produciéndose un movimiento relativamente rápido y la formación de una capa basal de till fácil de deformar. Los glaciares polares permanecen congelados hasta su base, y los glaciares sub-polares contienen zonas discretas donde el hielo está derretido. Las capas de hielo suelen contener flujos de hielo (*ice streams*) que drenan la masa helada con velocidades relativamente altas y erosionan los denominados surcos glaciales (*glacial troughs*) (Vorren y Laberg, 1997). Bajo las capas y flujos de hielo el agua derretida suele formar valles de túnel (*tunnel valleys*) que drenan el exceso de agua hacia el frente del glaciar, mediante flujos que pueden ser catastróficos (Shaw, 2002; Domack et al., 2006). El principal producto sedimentario en el ambiente subglacial es el diamicton glacial (*till*), compuesto del debris erosionado y transportado por la masa de hielo. Se trata de un sedimento generalmente no clasificado que no presenta estratificación, y se diferencian dos tipos (Anderson, 1999). El till de carga se forma por el aplastamiento del sedimento contra el sustrato bajo el peso del hielo y se caracteriza por valores altos de resistencia a la cizalla. El till de deformación se forma en la capa basal de glaciares templados y presenta estructuras lineales de deformación y clastos orientados. El till de deformación puede resultar del retrabajamiento y deformación del till de carga (Evans et al., 2005).

El ambiente de zona de anclaje es la franja de transición donde el hielo se separa del fondo para formar una plataforma de hielo. Se trata de una zona muy dinámica, ya que avanza y retrocede con el movimiento de la capa de hielo. En la parte frontal de la zona de anclaje el sedimento se acumula formando cuerpos progradantes similares a los prodeltas y que se denominan cuñas de zona de anclaje. Generalmente, estos depósitos son erosionados por el posterior avance del hielo, de modo que sólo se preservan aquellas cuñas formadas durante los máximos glaciales o durante paradas en el retroceso del hielo (Bart y Anderson, 1995). El sedimento en este ambiente es similar al till de carga, pero presenta menor compactación y tiene una fábrica de clastos más aleatoria (Anderson et al., 1991).

El ambiente proglacial es la continuación hacia el mar de la zona de anclaje y en él predominan procesos glaciomarinos ya que están afectados tanto por el manto de hielo cercano como por la plataforma de hielo suprayacente. Se puede subdividir en dos subambientes: proglacial proximal y proglacial distal o sub-plataforma de hielo. En el ambiente proglacial proximal predominan los procesos relacionados con el manto de hielo. Parte del sedimento se deposita a partir de plumas de turbidez formadas con agua de deshielo en la zona de anclaje (Hesse et al., 1997). También se deposita materia basal desde la zona proximal de la plataforma de hielo, así como sedimento residente en la columna de agua. Como resultado, el sedimento proglacial proximal presenta diferentes grados de laminación y estratificación. Los depósitos característicos formados en el ambiente proglacial cuando la zona de anclaje alcanza el borde de plataforma son las cuñas progradantes que se acumulan en el talud (Alley et al., 1989; Vorren y Laberg, 1997).

El ambiente proglacial distal o de sub-plataforma está mayoritariamente afectado por la plataforma de hielo. Este ambiente registra una variedad de procesos glaciomarinos como la caída de sedimento desde la base del hielo al fundirse y desde icebergs desprendidos de la plataforma de hielo. Asimismo, se registran procesos marinos como flujos de gravedad y retrabajamiento por corrientes de contorno que redistribuyen el sedimento. Como resultado, se producen distintos tipos de sedimento, siendo los más importantes los sedimentos glaciomarinos compuesto y residual, que contienen distintas proporciones de material bioclástico y clastos glaciales (*ice-rafted debris, IRD*), y suelen presentar diversos grados de estratificación y bioturbación (Anderson ,1999).

Finalmente, el ambiente marino no tiene influencia directa de la capa y plataforma de hielo, salvo la posible caída vertical de IRD desde icebergs y las plumas de sedimento subglacial diluidas que proceden del manto de hielo. En este ambiente predominan los procesos marinos, como la caída vertical de sedimento residente en la columna de agua, flujos de gravedad y procesos relacionados con las corrientes de fondo.

1.3. Elementos morfosedimentarios

Los márgenes continentales de altas latitudes presentan una gran variedad de elementos morfosedimentarios particulares, con diferentes niveles de jerarquía, escala espacial y distribución. Se puede distinguir, como primera aproximación, entre elementos erosivos, que ocurren fundamentalmente en las áreas proximales del margen, y elementos de origen mixto y deposicional, que predominan en las áreas media y distal.

Los elementos erosivos incluyen: Disconformidades glaciales (*glacial unconformities*), producidas en la plataforma continental por la erosión subglacial e indicativas de los sucesivos avances del manto de hielo a lo largo de los ciclos glaciales; surcos glaciales, excavados en la plataforma continental por las corrientes de hielo. Alcanzan profundidades de centenares de metros y longitudes de decenas de kilómetros y presentan generalmente perfiles en forma de U. Los surcos glaciales suelen presentar una asociación de morfologías que incluye pequeños surcos (*grooves*), resaltos estructurales (*knickpoints*), canales de agua de deshielo, *drumlins* y la parte proximal de lineaciones glaciales de gran escala (*mega-scale glacial lineations*). La distribución de estos elementos está relacionada con el tipo de sustrato (Wellner et al., 2006); las marcas de icebergs (*iceberg plough marks*) son el producto de la erosión de icebergs desprendidos de la plataforma de hielo que se mueven por la acción de corrientes termohalinas (Pudsey et al., 1997) o por el empuje de la capa de hielo (Lien et al., 1989); finalmente, los valles de túnel o canales sub-glaciales se forman bajo la capa de hielo y son producidos por el flujo de agua de deshielo (Eyles, 2006).

El principal elemento de origen mixto (erosivo-deposicional) son los drumlins, que se componen de till subglacial y se pueden formar alrededor de irregularidades topográficas en zonas que limitan el basamento rocoso con el recubrimiento sedimentario (Wellner et al., 2001).

Los elementos deposicionales incluyen: las lineaciones glaciales de gran escala, que son esculpidas en till subglacial por el avance rápido del hielo e indican la dirección del movimiento del mismo (Anderson, 1997; Clark et al., 2003); las estructuras en haz (*bundle structures*), que tienen un carácter similar a las lineaciones glaciales pero presentan mayor inter-espaciado, formas sinuosa y patrones convergentes (Canals et al., 2003; Willmott, 2007); las morrenas, de muy diversos tipos, son depósitos no clasificados y sin estratificación que se forman por la acción directa de la masa de hielo (Bennet and Glasser, 1996); las cuñas de zona de anclaje pueden considerarse un tipo especial de morrenas; las cuñas progradantes, como se ha descrito anteriormente, son depositadas a través de flujos de derrubios desde la zona de anclaje cuando ésta alcanza el borde de plataforma (Alley et al., 1989; Punkari, 1997). En las desembocaduras de los surcos glaciales estos elementos

alcanzan proporciones mayores, y se denominan abanicos de desembocadura de surcos (*trough mouth fans*) (Dahlgren et al., 2005); los depósitos glaciomarinos subtabulares se forman por procesos glaciomarinos y marinos, que incluyen la caída de IRD desde icebergs y la capa de hielo, plumas de sedimento subglacial y sedimentación hemipelágica (Anderson et al., 2002); otros elementos morfosedimentarios de origen fundamentalmente marino son los depósitos contorníticos, los depósitos de movimiento de masas y los *pockmarks* o cráteres asociados al escape de fluidos.

1.4. Arquitectura sedimentaria de márgenes continentales de altas latitudes

Los márgenes de altas latitudes registran en su arquitectura sedimentaria el apilamiento vertical de secuencias relacionadas con ciclos glaciales completos, y limitadas entre sí por disconformidades erosivas interpretadas como superficies de erosión subglacial (Bart y Anderson 1996, 1997a). La plataforma continental registra depósitos agradantes formados por las cuñas de zona de anclaje y la parte proximal de las cuñas progradantes, mientras que las zonas distales se caracterizan por la progradación de las cuñas y abanicos de desembocadura de surcos glaciales (Cooper et al., 1991; Bart and Anderson, 1996; Dowdeswell et al., 1996). El nivel de progradación y agradación depende de diversos factores como la fisiografía del margen, el levantamiento o la subsidencia tectónica, el aporte de sedimento y el régimen glacial (Dahlgren et al., 2005). El talud inferior y el ascenso continental presentan crestas sedimentarias que pueden formarse por sedimento fino procedente del talud superior (Rebesco et al., 1996, 1997).

2. El área de estudio: encuadre geográfico y geológico

La Antártida es el continente más austral, situado en su mayor parte a latitudes superiores a 70ºS, y está cubierto en un 98% por la Capa de Hielo Antártica, experimentando un clima polar con bajas precipitaciones, bajas temperaturas y fuertes vientos (Anderson, 1999). La Península Antártica se orienta en dirección S-N y se extiende entre las latitudes 61-74ºS y las longitudes 55-80ºW. Tiene una forma alargada y sinuosa, estrechándose hacia el norte, y su geografía es muy irregular por la presencia de bahías y fiordos a lo largo de la costa. La Cuenca de Bransfield se localiza entre el extremo norte de la península y el archipiélago de las islas Shetland del Sur. Está dividido en tres sub-cuencas, Occidental, Central y Oriental, por escarpes morfológicos a las alturas de las islas de Decepción y Bridgeman (Jeffers y Anderson, 1991).

El clima de la Península Antártica es polar en su mayor parte, pero los cambios climáticos afectan a esta zona de forma importante, registrándose calentamientos regionales rápidos en comparación con el cambio climático global (Vaughan et al., 2003). La oceanografía del área está determinada por las condiciones atmosféricas y dominada por la Corriente Circumpolar Antártica y los frentes asociados (Orsi et al., 1995), así como por los

giros de Weddell y del Mar de Ross que se desarrollan a ambos lados de la península. La oceanografía de la Cuenca de Bransfield no está totalmente establecida. La circulación general es ciclónica, con una corriente relativamente fuerte hacia el NE en el margen de las Islas Shetland del Sur y un flujo más débil dirigido hacia el SW en el margen peninsular (Gomis et al., 2002). Las corrientes profundas son afectadas por los relieves topográficos submarinos (López et al., 1999).

Estructuralmente, la Península Antártica es uno de los bloques de corteza que componen la Antártida Occidental (Anderson, 1999). Su separación del bloque sudamericano y de la Cresta Septentrional de Scotia por su desplazamiento relativo hacia el SE (Barker, 1972), llevó a la apertura del Estrecho de Drake que comenzó hace alrededor de 29 Ma, permitiendo el establecimiento de la Corriente Circumpolar Antártica entre 23.5 y 17 Ma (Barker y Burrell, 1977; Barker, 2001). El margen Pacífico de la Península Antártica sufrió la subducción de la placa Sudamericana bajo la placa Antártica durante 150 Ma, que terminó con la colisión de la dorsal Phoenix-Antártica, entre 6 y 3 Ma y progresivamente desde el sur hacia el norte (Barker, 1982; Barker y Camerlenghi, 2002). La Cuenca de Bransfield se abrió al finalizar el proceso de subducción hace aproximadamente 3.3 Ma, como resultado de procesos de *roll-back* que produjeron la migración hacia el noroeste del bloque de las Shetland del Sur y la propagación a lo largo de su límite suroriental de rasgos estructurales asociados con el límite de las placas de Scotia y Antártica (Barker y Dalziel, 1983; Galindo-Zaldívar et al., 2004, Maestro et al., 2007).

La Cuenca de Bransfield tiene una orientación SW-NE y está marcada fisiográficamente por la asimetría de sus márgenes, con un margen noroccidental estrecho y escarpado, correspondiente a las islas Shetland del Sur y un margen suroriental más ancho y suave, correspondiente a la Península Antártica (Jeffers and Anderson, 1991; Lawver et al., 1996). En ambos márgenes, la plataforma continental está formada por bancos planos que alcanzan profundidades de hasta 250 m, limitados por surcos glaciales. Un escarpe estrecho conecta los bancos de plataforma con una plataforma de talud que se extiende entre 750 y 900 m de profundidad, y que pasa a la cuenca a través de otro estrecho escarpe. La cuenca alcanza profundidades de cerca de 1900 m.

Los rasgos morfológicos identificados en la Cuenca Central de Bransfield son de origen sedimentario, volcánico y oceanográfico (Ercilla et al., 1998; Prieto et al., 1998). El margen peninsular presenta surcos glaciares, estructuras en haz, marcas de icebergs y una variedad de depósitos de movimientos en masa, incluyendo el Valle Gebra en la zona oriental de la cuenca (Ercilla et al., 1998; Canals et al., 2002; Imbo et al, 2003; Canals et al., 2004). El rasgo más destacable de la cuenca es el alineamiento de edificios volcánicos submarinos en dirección paralela a la cuenca (Gràcia et al., 1996; Lawver et al., 1996).

La estratigrafía de la Cuenca Central de Bransfield está caracterizada por dos secuencias solapantes en el talud, separadas por una disconformidad regional y caracterizadas por una variación en el grado de solapamiento. (Gamboa y Maldonado, 1990; Jeffers y Anderson, 1990). La secuencia inferior ha sido interpretada por estos autores como una secuencia sin-rift, mientras que la superior se relaciona con procesos glaciomarinos post-rift. Trabajos posteriores han identificado la sucesión de tres secuencias tectonoestratigráficas (TU1 a TU3, de más antigua a más reciente), en relación con los procesos de apertura de la cuenca, correspondiendo TU2 y TU3 a la secuencia glaciomarina superior (Prieto et al., 1998). Finalmente, esta misma secuencia ha sido subdividida en unidades progradantes de talud y unidades agradantes de cuenca (Prieto et al., 1999).

Los estudios sobre la sedimentación holocena en los márgenes de la Cuenca Central de Bransfield indican la sucesión de tres unidades estratigráficas (Yoon et al., 1997; Heroy et al., 2008). La unidad más antigua es subglacial y se compone de diamicton sobreconsolidado. La unidad intermedia es de origen mixto, proglacial y subglacial, y se compone de fango arenoso laminado con clastos. La unidad más reciente tiene origen marino y se compone de fango de diatomeas. La sedimentación en la cuenca durante los últimos 2850 años está representada por limos arcillosos de origen hemipelágico y turbiditas volcanoclásticas (Fabrés et al., 2000).

La historia climática durante el Pleistoceno Superior y Holoceno en el margen de la Cuenca Central de Bransfield ha sido establecida a través del estudio de asociaciones de foraminíferos en testigos de sedimento, diferenciándose cinco regímenes climáticos (Heroy et al., 2008). El periodo de Deglaciación llegó hasta los 9000 años, durante el cual una plataforma de hielo dominó la Cuenca de Bransfield. Durante el Holoceno inferior a medio (9000-6800 años) la plataforma de hielo retrocedió y se comenzó a establecer el patrón actual de circulación oceanográfica. Durante el Óptimo Climático del Holoceno medio (6800-5900 años) se produjo un derretimiento rápido del hielo marino, con la estabilización de la columna de agua. El Holoceno medio-superior (5900-2600 años) se caracterizó por un incremento en la cubierta de hielo marino y la entrada de masas de agua frías. Finalmente, el periodo Neoglacial (desde 2600 años) se caracteriza por eventos de tormenta frecuentes que desestabilizan la columna de agua, en un ambiente marino.

CAPÍTULO II. Metodología y datos

Los datos estudiados en esta tesis se obtuvieron en su mayor parte durante dos campañas geológicas (GEBRA93 y MAGIA99). Los datos consisten en batimetrías multihaz, perfiles sísmicos de reflexión monocanal de alta y muy alta resolución (cañones de aire y TOPAS, respectivamente) y testigos de gravedad. Asimismo, se han utilizado datos

batimétricos regionales (Polish Polar Academy of Sciences, 1990) y datos batimétricos multihaz disponibles en internet (http://marine-geo.org).

1. Datos batimétricos

Los datos de batimetría fueron obtenidos con ecosondas multihaz y procesados con los programas informáticos Neptune y Caraibes. Los programas Surfer y Fledermaus han facilitado su visualización y la producción de distintos tipos de mapas y modelos batimétricos.

2. Datos geofísicos

2.1. TOPAS

La sonda paramétrica (*topographic parametric sonar*, TOPAS) trabaja con una combinación de frecuencias acústicas que producen una señal secundaria de baja frecuencia (0.5-5 kHz) que permite obtener perfiles sísmicos de muy alta resolución de los primeros 50-80 m de la columna sedimentaria.

2.2. Perfiles sísmicos de alta resolución

El sistema de sísmica monocanal de reflexión con cañones de aire obtiene perfiles sísmicos de alta resolución usando como fuente acústica aire a presión que se dispara desde un conjunto de cañones de aire comprimido, a la vez que los ecos se registran en hidrófonos dispuestos en un *streamer* remolcado tras el barco. Tras el procesado de los datos, los perfiles sísmicos se interpretaron con la ayuda del programa informático Kingdom Suite 8.0 (http://seismicmicro.com).

La interpretación estratigráfica de los perfiles sísmicos se ha hecho en base a la identificación de secuencias y unidades sísmicas y las disconformidades que las limitan, el análisis del carácter de las reflexiones, la identificación de facies sísmicas y su interpretación en términos geológicos (Vail, 1987; Damuth, 1980; Posamentier et al., 1988, entre otros).

3. Datos sedimentológicos

Los testigos de gravedad estudiados en esta tesis, de un máximo de 3 m de longitud, fueron abiertos, descritos, fotografiados y muestreados, para ser sometidos posteriormente a distintos análisis. Estos análisis incluyeron estudios granulométricos, análisis de contenido de carbonatos, contenido en agua, propiedades físicas (densidad y susceptibilidad magnética), rayos X y fotografías en microscopio electrónico de barrido.

CAPITULO III. Fisiografía, morfología, sistemas sedimentarios y su dinámica

1. Fisiografía

Este estudio fisiográfico se ha realizado en base a los estudios previos y teniendo en cuenta la nueva y detallada información batimétrica disponible. La CCB tiene una orientación SW-NE y un carácter marcadamente asimétrico, con un margen noroccidental, adyacente a las Islas Shetland del Sur, estrecho y abrupto y un margen suroriental adyacente a la Península Antártica, más ancho y suave. Pese a esta asimetría, y tomando como criterio la pendiente, ambos márgenes pueden dividirse en los mismos dominios fisiográficos: plataforma continental y talud continental el cual está a su vez compuesto de talud superior, plataformas de talud y talud inferior.

El margen de las Islas Shetland del Sur presenta una plataforma continental compuesta de bancos relativamente planos (<2º), con una anchura de hasta 10 km y profundidades de hasta 300 m. Estos bancos están separados por hasta 11 surcos glaciales. El talud tiene una anchura máxima de 15 km y alcanza profundidades de 1750 m. El talud superior es escarpado (hasta 23º) y tiene una anchura máxima de 4 km, alcanzando profundidades de 450 a 525 m. El talud medio está formado por cuatro plataformas de talud con gradientes de menos de 3º, que alcanzan profundidades entre 625 y 850 m, y tienen una anchura media de 5 km. El talud inferior es una rampa escarpada (hasta 26º) que se ensancha hacia el este hasta alcanzar anchuras de 10 km, y alcanza profundidades que aumentan hacia el este, desde 1350 hasta 1750 m.

El margen de la Península Antártica se caracteriza por una plataforma continental más ancha y menos escarpada (hasta 50 km de anchura, 300 m de profundidad y 1.5º de pendiente), también formada por bancos planos separados por surcos. El talud superior es estrecho, con una anchura máxima de 10 km, profundidades de hasta 800 m y pendientes de hasta 15º, y conecta con el talud medio, que está formado por dos amplias plataformas de talud, occidental y oriental. Las plataformas de talud tienen anchuras máximas de 35 km y alcanzan profundidades de hasta 1100 m, con pendientes en torno a 2º. El talud inferior tiene anchuras de hasta 10 km, pendientes de hasta 20º y conecta con la cuenca a profundidades entre 800 y 1500 m.

Finalmente, los márgenes conectan con la cuenca, que tiene una anchura de hasta 45 m y profundidades que aumentan hasta valores de 1900 m hacia el este con gradientes medios de 2º.

2. Caracterización morfosedimentaria y acústica

La gran variedad de rasgos morfológicos identificados en la CCB se pueden clasificar según su origen como glaciales (superficies de erosión, surcos glaciales, *grooves*, *drumlins*, lineaciones glaciales y cuñas de zona de anclaje), glaciomarinos (marcas de icebergs, abanicos de desembocadura de surcos glaciales, cárcavas y capa glaciomarina) y marinos (campos de *pockmarks*, inestabilidades sedimentarias ,complejos de cicatriz y lóbulo, canales turbidíticos, depósitos contorníticos y edificios volcánicos).

2.1. Rasgos de origen glacial

Las superficies de erosión son el resultado de la erosión directa subglacial y se localizan en los bancos de la plataforma continental, el talud superior las áreas proximales de los surcos glaciales. Los surcos glaciales (once en el margen de las islas Shetland del Sur y ocho en el margen peninsular) tienen orientaciones que varían de NE a N, longitudes de hasta 60 km, profundidades de hasta 600 m y perfiles en forma de U. El fondo de los surcos glaciales presenta la sucesión hacia cuenca de elementos morfológicos de dimensiones kilométricas, incluyendo pequeños surcos (*grooves*), resaltos estructurales, drumlins y la parte proximal de lineaciones glaciales. Estas lineaciones se continúan en las plataformas de talud y alcanzan longitudes de hasta 50 km, tienen relieves entre 20 y 40 m, y están espaciadas entre sí 4-6 km, por lo que pueden ser clasificadas como estructuras en haz. En general, las lineaciones tienen la dirección de los surcos glaciales (N-NNW) hasta que, llegadas a las plataformas de talud, cambian la dirección hacia el NE. También se observa la superposición de un grupo de lineaciones en la plataforma occidental con una tendencia más marcada hacia el E. Finalmente, se identifican dos escarpes sinuosos en la plataforma occidental, que constituyen cuñas de zona de anclaje.

2.2. Rasgos de origen glaciomarino

Las marcas de icebergs muestran una orientación ENE y se identifican en las áreas distales de las plataformas de talud del margen peninsular, sobre todo al este de las desembocaduras de los surcos glaciales. Estas marcas tienen longitudes de hasta 15 km y relieves de hasta 25 metros. Los abanicos de desembocadura de surco ocupan la parte distal de las plataformas de talud en ambos márgenes, y se forman en posiciones ligeramente desplazadas hacia el este respecto a las desembocaduras, afectando áreas de hasta 150 km². Las cárcavas se localizan en la parte superior del talud inferior de ambos márgenes, especialmente afectando a las áreas donde las lineaciones glaciales alcanzan el borde de las plataformas de talud. Los gullies tienen longitudes de entre 2 y 5 km y profundidades de decenas de metros. Por último, la capa sedimentaria cubre la parte distal de los surcos glaciales, las plataformas de talud y la cuenca, con espesores máximos de decenas de metros.

2.3. Rasgos de origen marino

Los campos de *pockmarks* se localizan en la parte distal de los surcos glaciales y plataformas de talud del margen peninsular. Las inestabilidades sedimentarias se distribuyen fundamentalmente en los bordes de las plataformas de talud, en el talud inferior y en la cuenca. El rasgo más señalado es el complejo Gebra-Magia, situado en la parte oriental del margen peninsular de la CCB. Este complejo está formado por dos valles de deslizamiento (Gebra y Magia) y una extensa zona de depósitos de flujos en masa y turbiditas. El valle de Gebra mide 30 km de largo y 5-12 km de ancho, y alcanza profundidades de incisión de hasta 150 m (Imbo et al., 2003; Casas et al., 2008). Los complejos de cicatriz y lóbulo ocupan el talud inferior de los dos márgenes y la parte proximal de la cuenca. Los lóbulos tienen dimensiones de 1-4 km de largo y 1-1.5 km de ancho y ocurren o bien en el talud inferior o bien en la cuenca. Los canales turbidíticos se observan en la transición desde el talud inferior a la cuenca en la parte occidental de la CCB. Se han identificado dos depósitos contorníticos asociados a fosas, adosados al pie del talud inferior del margen peninsular. Finalmente, la cadena de edificios volcánicos a lo largo del eje de la cuenca es el rasgo más particular de este dominio fisiográfico (Gràcia et al., 1996; Lawver et al., 1996).

3. La morfología como clave para la definición de sistemas sedimentarios y su dinámica

La caracterización morfológica de la CCB permite la interpretación de los elementos arquitectónicos de los sistemas sedimentarios, en relación con los procesos responsables de su formación y distribución. Los dos sistemas principales son el sistema glacial-glaciomarino y el sistema de talud-cuenca. Otros dos sistemas secundarios son el sistema de escape de fluidos y el sistema contornítico.

El sistema glacial-glaciomarino incluye la mayoría de los elementos identificados en plataforma y talud. Los elementos arquitectónicos principales son las superficies erosivas y los surcos glaciales, resultados de la erosión subglacial. Los surcos glaciales representan el elemento jerárquico de primer orden en un sistema que incluye otros elementos secundarios como las superficies erosivas del fondo de los surcos, los *grooves*, los resaltos estructurales, los drumlins y las lineaciones glaciales, cuya sucesión está relacionada con el tipo de sustrato bajo el hielo (Wellner et al., 2001, 2005). Los *drumlins* y las lineaciones glaciales indican una velocidad relativamente alta del hielo y también la dirección de su movimiento, la cual presenta un cambio de dirección de flujo de N-NW a NE al llegar a las plataformas de talud. Las cuñas de zona de anclaje indican paradas o reavances del manto de hielo durante el retroceso general en la última deglaciación, mientras que las marcas de icebergs sugieren una dirección ENE para el desplazamiento de los mismos. Por último, la capa

glaciomarina que cubre la mayor parte de las plataformas de talud y la cuenca se interpreta como un depósito glaciomarino originado tras la retirada del hielo.

El sistema de talud-cuenca incluye los elementos relacionados con procesos gravitativos en los dominios distales de los márgenes y la cuenca: abanicos de desembocadura de surcos glaciales, formados por el aporte de sedimento desde los surcos glaciales por las corrientes de hielo (Alley et al., 1989); complejos de cicatriz-lóbulo que forman distintos sistemas de *slope-apron* en relación con el tipo de sedimento (Llave et al., 2008); el complejo de inestabilidad Gebra-Magia, posiblemente relacionado con diversos factores como las altas tasas de sedimentación durante el último periodo glacial, el rebote isostático por la retirada del hielo, la fábrica tectónica preexistente y la sismicidad (Imbo et al., 2003; Casas et al., 2004); y los sistemas turbidíticos (cárcavas y canales turbidíticos).

El sistema de escape de fluidos está formado por los campos de *pockmarks*, originados por el escape de fluidos durante la consolidación del sedimento depositado en la parte distal de los surcos y en las plataformas de talud del margen peninsular, durante el último avance glacial (Judd and Hovland, 2007). El sistema contornítico está formado por surcos erosivos y crestas sedimentarias asociados en la cuenca, y se relaciona con el forzamiento de las corrientes oceanográficas de fondo por el efecto de los relieves topográficos de la cuenca, en particular, los edificios volcánicos (Ercilla et al., 1998; Faugères et al., 1999; López et al., 1999).

4. Factores de control

Los cuatro principales factores de control que afectan a los sistemas sedimentarios en la CCB son la ciclicidad glacial/interglacial, la tectónica, la fisiografía y la oceanografía.

La ciclicidad glacial/interglacial controla el desarrollo de la mayoría de sistemas sedimentarios desarrollados durante el último ciclo, aunque los surcos glaciales, los abanicos de desembocadura de surcos y el complejo de inestabilidad de Gebra-Magia se han desarrollado a lo largo de sucesivos ciclos. De este modo, los elementos arquitectónicos se formaron durante dos periodos diferenciados: el último avance glacial y máximo glacial, y el retroceso glacial e interglacial. Durante el primero de estos periodos se desarrollan la mayor parte de los elementos morfológicos observables hoy día en la CCB (superficies de erosión, surcos glaciales, *grooves*, resaltos estructurales, *drumlins*, lineaciones glaciales, abanicos de desembocadura de surcos y cárcavas). Durante el periodo que incluye la deglaciación y el interglacial se depositan las cuñas de zona de anclaje, las marcas de icebergs y los campos de *pockmarks*. Las inestabilidades sedimentarias se favorecieron probablemente durante este periodo, y las cárcavas posiblemente continuaron activas en los dos periodos.

La tectónica afecta a la localización y dirección de los surcos glaciales de ambos márgenes, quizás con la excepción de los surcos más occidentales del margen peninsular. La actividad tectónica reciente también se propone como uno de los mecanismos que producen las inestabilidades sedimentarias, pudiendo afectar el desarrollo de los elementos del sistema de talud-cuenca (Bryn et al., 2005; Solheim et al., 2005). También la localización y desarrollo de los edificios volcánicos está determinada estructuralmente. La subsidencia/levantamiento de origen tectónico también han podido influir en la evolución sedimentaria de la CCB. La fisiografía de la CCB, resultante de los procesos de apertura de la misma (Jeffers y Anderson, 1990), tiene un gran efecto en las diferencias entre el margen de las islas Shetland del Sur y el margen peninsular. La mayor parte de los elementos morfológicos presentan un mayor desarrollo en el margen peninsular, y muchos de ellos sólo han sido identificados en éste. Esto puede relacionarse con la diferencia de tamaño entre los dos márgenes, que produce una diferencia en la escala de los procesos sedimentarios, aunque no en la naturaleza de los mismos. La fisiografía también tiene un efecto importante en el desarrollo de los sistemas de *slope-apron* en el talud inferior, ya que muchas inestabilidades se generan sólo en áreas donde se han depositado previamente abanicos de desembocadura de surcos.

CAPÍTULO IV. Arquitectura estratigráfica post-rift de la Península Antártica, estilos de edificación y factores de control

1. Estratigrafía sísmica

El estudio de estratigrafía sísmica incluye un análisis de las facies acústicas y la identificación del registro post-rift desde la plataforma continental a la cuenca en el margen de la Península Antártica. Las facies acústicas diferenciadas son: estratificada (paralela, oblicua, ondulada e irregular), caótica (indistinta o monticular), semitransparente, prolongada e hiperbólica.

Se han identificado dos secuencias sísmicas limitadas por disconformidades regionales. Estas secuencias yacen sobre una secuencia basal syn-rift, que aflora en la plataforma y talud superior y se caracteriza por facies acústicas prolongadas y estratificadas irregulares. Las secuencias se han denominado Secuencia Inferior (S2) y Secuencia Superior (S1), de más antigua a más moderna, y se correlacionan con las secuencias S2 y S1 de Jeffers y Anderson (1991), respectivamente.

1.1. Secuencia Inferior, S2

S2 está limitada en su base por la disconformidad U2, y tiene terminaciones solapantes en la parte proximal de las plataformas de talud, y terminaciones biselantes hacia cuenca. S2 se depositó en un margen caracterizado por un talud abrupto en el área oriental y con forma de rampa en el área occidental. Su distribución indica que su depósito representó el inicio del desarrollo de las plataformas de talud actuales. El principal depocentro (700 ms) se sitúa en la plataforma oriental, mientras que en la plataforma occidental, el grosor es generalmente inferior a 300 ms. S2 se caracteriza por facies estratificadas oblicuas formando cuñas que progradan hacia cuenca y, localmente, por facies caóticas y onduladas que forman cuerpos monticulares o irregulares, respectivamente. La secuencia S2 se puede subdividir en cuatro unidades sísmicas, S2d a S2a que pueden diferenciarse sólo en la plataforma oriental. Las unidades más antiguas (S2d a S2b) presentan pequeños depocentros (200 ms) en las desembocaduras de los surcos glaciales, mientras que la más reciente se concentra en un depocentro más amplio (450 ms).

1.2. La Secuencia Superior, S1

S1 se deposita sobre la disconformidad U1 y tiene el fondo marino como límite superior. Se desarrolla en la parte distal de los surcos glaciales, plataformas de talud y talud inferior. Esta secuencia se depositó sobre una plataforma de talud ya desarrolladas, con una tendencia más rectilínea que la actual, a lo largo del margen. Los principales depocentros de S1 se localizan en el borde de las plataformas de talud, especialmente en la occidental (700 ms). La secuencia S1 se subdivide en cinco unidades sísmicas, denominadas S1d a S1a, de más antigua a más reciente. Las unidades S1e, S1c y S1a presentan depocentros en las partes distales de las plataformas de talud, desplazados hacia el este de las desembocaduras de los surcos, mientras que las unidades S1d y S1b tienen sus depocentros en las plataformas de talud, frente a las desembocaduras de los surcos. Todas las unidades presentan un carácter común en cuanto a las facies acústicas. Sobre la disconformidad que forma el límite basal de cada unidad se desarrollan paquetes masivos tabulares de facies caóticas indistintas y localmente cuerpos monticulares de facies caóticas. El techo de las unidades se caracteriza por un tapiz de facies estratificada paralela. En los bordes de las plataformas de talud y en el talud inferior se identifican paquetes con forma de cuña compuestos por cuerpos apilados verticalmente separados por disconformidades y caracterizados por facies estratificada oblicua. Sólo localmente se identifican las facies transparente y estratificada ondulada en el borde de las plataformas de talud y al pie de escarpes.

2. Cuerpos sísmicos deposicionales y erosivos

En el registro sísmico se puede diferenciar una serie de cuerpos deposicionales y erosivos formando parte de las unidades y secuencias sísmicas. Estos cuerpos son: cuñas de till, morrenas, valles de túnel, cuñas progradantes, abanicos de desembocadura de surcos, tapices de depósitos glaciomarinos y depósitos de flujos de gravedad.

Las cuñas de till se localizan sobre las disconformidades, en la base de las unidades sísmicas que componen la secuencia superior S1 y se interpretan como el producto de la sedimentación subglacial. Las morrenas ocurren en la mayoría de las unidades de S1 y son el resultado del depósito en los márgenes de las corrientes de hielo o en la zona de convergencia de dos ellas en las que las morrenas laterales conforman una morrena central (Anderson, 1999). Los valles de túnel son canales erosionados por el agua de fusión bajo el manto de hielo y excavados en el till subglacial. Se han identificado sólo en la unidad S1d en la plataforma de talud occidental. Las cuñas progradantes forman los límites distales de todas las unidades de S1 y forman enteramente las unidades de S2 en los bordes de las plataformas de talud y en el talud inferior. Incluyen clinoformas que progradan hacia cuenca, y son interpretadas como el resultado del depósito proglacial desde la zona de anclaje del manto de hielo cuando ésta alcanza el borde de las plataformas de talud. Los abanicos de desembocadura de surcos se consideran un tipo especial de cuñas progradantes, que se desarrollan en la desembocadura de las corrientes de hielo. La mayor velocidad de éstos y su mayor carácter erosivo producen un mayor aporte sedimentario puntual. Estos abanicos se desarrollan siempre ligeramente desplazados hacia el este respecto a la desembocadura de los surcos glaciales. Los tapices de depósitos glaciomarinos se encuentran en el techo de todas las unidades de la secuencia superior, y aparecen formando capas finas sobre las cuñas de till y las morrenas. Su origen es una combinación de procesos de caída de derrubios desde icebergs y plataformas de hielo y procesos marinos. Finalmente, los depósitos de flujos de gravedad se identifican en la secuencia superior y, particularmente, en la unidad más reciente S1a.

3. Procesos sedimentarios a lo largo de un ciclo glacial en la CCB

La distribución de cuerpos sísmicos dentro de las unidades sísmicas indica que cada una de ellas es el resultado de un ciclo glacial-interglacial completo, en el que se pueden distinguir dos periodos: el avance glacial y máximo glacial, y el retroceso glacial e interglacial.

Durante el primer periodo el manto de hielo avanzó a lo largo de la plataforma continental, talud superior y plataformas de talud, generando las disconformidades glaciales que limitan las unidades sísmicas. El sedimento transportado en las capas basales del

manto de hielo se depositó en forma de cuñas de till en las plataformas de talud, y de cuñas progradantes en el borde de plataforma y talud inferior, mientras que en las zonas donde desembocaban los corrientes de hielo se formaron abanicos de desembocadura. Estos abanicos se localizan hacia el este respecto a la desembocadura de los surcos glaciales de la plataforma continental. La identificación de abanicos en la secuencia inferior S2 indica que los surcos glaciales fueron activos desde el comienzo de la actividad glacial en la CCB. Las crestas de límite de corrientes de hielo se formaron en la confluencia de flujos adyacentes en la plataforma occidental. En condiciones de climas glaciales menos severos la fusión en la base del manto de hielo originó la excavación de valles de túnel que drenaban el exceso de agua.

Durante el retroceso glacial y el periodo interglacial se formaron las morrenas por la retirada del hielo y las capas glaciomarinas. También los procesos de flujo de gravedad ocurrieron preferentemente durante este periodo, como resultado del exceso de presión de poro en los sedimentos depositados durante el avance del manto de hielo y por el levantamiento isostático tras la retirada del hielo (Bryn et al., 2005; Solheim et al., 2005).

4. Factores de control en la arquitectura sedimentaria del margen peninsular de la CCB

Teniendo en cuenta la interpretación de cada unidad sísmica como resultado de un ciclo completo de avance y retroceso del manto de hielo de la Península Antártica, la distribución de sedimento y la arquitectura sedimentaria pueden entenderse como el resultado de dos factores de control principales: la fisiografía y configuración estructural del margen y el clima.

4.1. Fisiografía y configuración estructural del margen

La arquitectura estratigráfica del margen peninsular de la CCB está definida por el apilamiento de cuñas progradantes y prominentes abanicos de desembocadura de surcos, indicando que el crecimiento del margen es el resultado de un aporte sedimentario lineal, el borde del Manto de Hielo de la Península Antártica, con fuentes puntuales representadas por las corrientes de hielo. La fisiografía del margen al comienzo de cada secuencia controló la distribución de las secuencias sísmicas S2 y S1. La distribución espacial de los sedimentos está determinada por la progresiva apertura de la cuenca, que produjo una migración hacia el NW de los depocentros (Prieto et al., 1998). La apertura de la cuenca se produjo más rápidamente y/o durante más tiempo en el área oriental, dando lugar a un mayor espacio de acomodación en esta área respecto al área occidental.

La secuencia S2 se depositó tras la apertura de la cuenca. En este momento, la cuenca era relativamente somera y la fisiografía estaba caracterizada por un talud estrecho

y escarpado en la zona oriental, donde el sedimento se depositó en gruesas cuñas progradantes y abanicos de desembocadura de surcos que formaron la plataforma oriental ancestral. Por el contrario, el área occidental se caracterizaba por un talud más ancho y menos escarpado, donde la mayor área de distribución del sedimento dio lugar a depósitos con menor carácter progradante (Solheim et al., 1998) que formaron la plataforma occidental ancestral.

Posteriormente, durante el depósito de S1, el manto de hielo de la Península Antártica avanzaba a lo largo de plataformas de talud ya desarrolladas. El mayor espacio de acomodación en la zona oriental explica que en esta zona la progradación sea menor, lo que también estaría relacionado con el menor aporte sedimentario debido a la menor entidad de la cuenca de drenaje del citado manto de hielo.

4.2. Clima

El clima ha sido el principal factor en el control de la evolución sedimentaria del margen peninsular de la CCB (Jeffers y Anderson, 1990; Prieto et al., 1999). El clima afectó a la arquitectura sedimentaria a dos escalas: de unidades sísmicas y de secuencias. En primer lugar, las diferencias entre la distribución de las unidades sísmicas dentro de cada secuencia puede explicarse por variaciones en el patrón del flujo de hielo, que controlan el aporte y depósito de sedimento. Respecto a la secuencia S2, las unidades más antiguas, S2d a S2c presentan depocentros pequeños y aislados, probablemente relacionados con un bajo aporte sedimentario dada la poca disponibilidad de sedimento erosionable. En cambio, la unidad más reciente, S2a, presenta un depocentro más amplio, resultado de un mayor aporte de sedimento, disponible tras el depósito de las unidades anteriores. Respecto a la secuencia superior, S1, se diferencian dos tipos de unidades. S1e, S1c y S1a forman depocentros elongados en los bordes de plataforma de talud, y desplazados hacia el este respecto a las desembocaduras de los surcos glaciales. El depósito de estas unidades se relaciona con una capa de hielo relativamente gruesa y una dirección general hacia el NE en las plataformas de talud. Las corrientes de hielo tienen una dirección N-NNW en los surcos glaciales de la plataforma continental, pero al desembocar en las plataformas de talud son desviadas hacia el NE por la tendencia general del manto de hielo de la Península Antártica. En cambio, el depósito de las unidades S1d y S1b se produce frente a la desembocadura de los surcos, indicando capas de hielo relativamente menos potentes y corrientes de hielo con una dirección de flujo marcada por la dirección estructural de los surcos glaciales.

En segundo lugar, el tipo de oscilaciones glacio-eustáticas se interpreta como el responsable de las diferencias entre las dos secuencias, S2 (progradante) y S1 (progradante-agradante). Un cambio similar a nivel regional ha sido correlacionado con un cambio en el

carácter del manto de hielo de la Península Antártica, de más templado a más polar, ocurrido hace 3.0 Ma (Rebesco et al., 2006). Sin embargo, la edad de apertura de la cuenca (3.3 Ma, Galindo-Zaldívar et al., 2004) y el espesor de las secuencias sugieren que en la CCB este cambio se debió producir más tarde. El cambio en el tipo de oscilaciones climáticas ocurrido durante el Pleistoceno Medio (*Mid Pleistocene Revolution*, MPR) explica la variación en la arquitectura estratigráfica entre S2 y S1. Antes del MPR las oscilaciones climáticas estaban dominados por ciclos de 100 ka, moduladas por ciclos de 41 ka (Shackleton et al., 1990; Berger et al., 1994). Esta combinación de frecuencias dio lugar a ciclos glaciales reforzados, con la formación de capas de hielo más gruesas y de mayor carácter erosivo, que produjeron depósitos progradantes, a la vez que erosionaban la parte proximal de los mismos. En cambio, tras el MPR, los ciclos fueron de 100 ka, y aumentó la frecuencia de los eventos de avance y retroceso del hielo. Este aumento favoreció la formación de secuencias progradantes/agradantes debido a la reducción de la capacidad erosiva del manto de hielo, y la preservación de los depósitos más proximales (Solheim et al., 1996), que también pudo ser favorecida por un incremento en la subsidencia.

Capítulo V. Tipos de sedimento y procesos sedimentarios, estratigrafía y modelos durante el último ciclo glacial

Los testigos de sedimento analizados son representativos de los distintos ambientes deposicionales de la CCB: áreas proximales de los surcos glaciales (TG37 y TG39), áreas distales de los surcos glaciales (TG38, TG36, TG27 y TG26), plataformas de talud (TG50, TG34, TG15, TG14 en el margen peninsular y TG11 en el margen de las islas Shetland del Sur), talud inferior (TG3, TG4, TG29 y TG56) y cuenca (TG32, TG2, TG10, TG51, TG52 y TG54).

Se han identificado cuatro tipos de sedimento, en base a su estructura sedimentaria, tamaño de grano y estructuras internas. También se han caracterizado según otros parámetros cualitativos y cuantitativos, como la textura del sedimento, composición de la fracción arena, composición cualitativa de la fracción fina, contenido de carbonato, color y propiedades físicas. Estos tipos de sedimento son: sedimento brechoide, sedimento laminado (en el que se distingue entre laminado regular, finamente laminado, con estructuras de flujo e indistinto), sedimento bioturbado y sedimento masivo.

1. Definición de secuencias sedimentarias

Se definen siete tipos de secuencias sedimentarias, en función de las afinidades sedimentológicas que resultan de procesos sedimentarios específicos (flujos de turbidez de agua de fusión, flujos turbidíticos, flujos en masa) o de una asociación de procesos a mayor

escala (cambios climáticos, producción biológica). Las secuencias diferenciadas se denominan: diamicton subglacial, secuencia glaciomarina compuesta, secuencia de flujos de turbidez densos de agua de fusión, diamicton proglacial, turbiditas, secuencia de sedimento deformado y contornitas.

El diamicton subglacial se identifica en la base de los sedimentos de la parte proximal de los surcos glaciales y está compuesto por sedimento brechoide con un alto porcentaje en clastos, que se interpretan como IRD. Esta secuencia es el resultado de la erosión, deformación y retrabajamiento del sedimento por parte del manto de hielo.

La secuencia de sedimento glaciomarino compuesto es la secuencia predominante en los surcos glaciales y plataformas de talud. Está formada mayoritariamente por sedimento con IRDs aislados y laminaciones de distinta escala. Este sedimento aparece intercalado con niveles ricos en IRDs y sedimento bioturbado. Estos niveles proceden de dos tipos de procesos glaciomarinos: flujos de turbidez diluidos de agua de fusión procedentes de la zona de anclaje y la caída de derrubios desde la plataforma de hielo proximal. Los niveles bioturbados se relacionan con disminuciones en la tasa de sedimentación (Dowdeswell y Pudsey, 2001).

La secuencia de flujos de turbidez densos de agua de fusión se identifica en los surcos glaciales y plataformas de talud, formando niveles de 3 a 20 cm de espesor de sedimento finamente laminado, e intercalados en la secuencia glaciomarina compuesta. Estos niveles presentan granoselección positiva y laminaciones cruzadas o paralelas en la base, que cambian a laminaciones indistintas y ausencia de estructuras hacia el techo. Esta secuencia se interpreta como sedimento glaciomarino depositado, como su nombre indica, por pulsos de flujos de turbidez densos de agua de fusión procedente de la zona de anclaje. Estos procesos ocurren como eventos esporádicos, según sugiere la intercalación de la secuencia con la secuencia glaciomarina compuesta.

El diamicton proglacial se identifica exclusivamente en el talud inferior. Está formado por sedimento brechoide intercalado con niveles centimétricos de fango laminado. Los altos porcentajes de IRDs y su relativo mayor tamaño, son los rasgos característicos de esta secuencia, que se deposita por la caída masiva de derrubios desde el frente del manto de hielo, cuando la zona de anclaje alcanza el borde de las plataformas de talud.

La secuencia turbidítica se identifica en el talud inferior y la cuenca, y está formada por niveles centimétricos de sedimento regularmente laminado en el que se distinguen los niveles de la secuencia de Bouma (1962) desde Tb a Te. Dentro de la secuencia turbidítica se identifican niveles de sedimento volcánico, de espesor entre 1 y 4 cm. El nivel más reciente es correlacionable en la parte occidental de la cuenca. La secuencia turbidítica es el resultado de flujos turbidíticos con distinto tipo de concentración y capacidad energética.

La secuencia de sedimento deformado se identifica en la parte proximal de los surcos glaciales, en la plataforma de talud del margen de las islas Shetland del Sur, en el talud inferior y en la cuenca y está compuesta por el tipo de sedimento laminado afectado por estructuras de deformación. Los contactos angulares de esta secuencia y sus estructuras sedimentarias primarias altamente disturbadas indican su origen por deformación plástica del sedimento.

La secuencia contornítica se identifica en la cuenca, al pie del talud inferior, en una zona caracterizada morfológicamente por la presencia de un surco contornítico. Está compuesta de sedimento brechoide, con algunos niveles ricos en IRDs orientados, lo que permite su interpretación como el resultado del retrabajamiento de sedimento glacigénico por parte de corrientes de contorno.

2. Modelos estratigráficos

La distribución superficial de las secuencias sedimentarias y su distribución vertical indican que las secuencias sólo pueden ser correlacionadas, y de forma parcial, en cada dominio fisiográfico de la CCB. Por tanto, se han definido cuatro modelos estratigráficos generales: de surcos glaciales, de plataformas de talud, de talud inferior y de cuenca.

Los surcos glaciales presentan dos sub-modelos estratigráficos diferenciados. En las zonas proximales, la estratigrafía comprende una secuencia basal de diamicton subglacial, seguida por secuencias de sedimento glaciomarino compuesto por numerosas secuencias de flujos de turbidez diluidos de agua de fusión y una secuencia de sedimento deformado intercalada. En las zonas distales, la estratigrafía comprende exclusivamente secuencias glaciomarinas compuestas intercaladas con secuencias de flujos de turbidez densos de agua de fusión intercalados.

El modelo estratigráfico de las plataformas de talud comprende secuencias glaciomarinas compuestas con distinto grado de intercalación de secuencias de flujos turbios de agua de fusión. La mayor variabilidad se da en la zona distal de las plataformas. En este dominio, la secuencia de sedimento glaciomarino compuesto se caracteriza por la presencia de numerosos niveles ricos en IRDs y bioturbación.

El talud inferior se caracteriza por dos modelos estratigráficos: a) predominio de la secuencia de diamicton proglacial con intercalaciones de secuencias de sedimento deformado; y b) un modelo donde predomina la secuencia turbidítica con intercalaciones de de secuencias de sedimento deformado de distinta frecuencia, en la zona oriental del área de estudio.

La cuenca se caracteriza por dos modelos estratigráficos: a) secuencias turbidíticas predominantes con intercalaciones locales de secuencias de sedimento deformado. Este

modelo se identifica prácticamente en toda la cuenca; y b) secuencia contornítica. Este modelo se identifica en las zonas de surco contornítico.

3. Factores de control

La estratigrafía y la distribución espacial y temporal de secuencias son los criterios geológicos que permiten distinguir entre los factores globales (ciclos glaciales) y locales (morfología, área fuente del sedimento y oceanografía) que han gobernado la historia sedimentaria reciente de la CCB.

3.1. Variabilidad climática

La variabilidad climática durante el último ciclo glacial se considera un factor principal en la sedimentación reciente. Durante el último avance glacial y máximo glacial, el manto de hielo avanzó a lo largo de los surcos de la plataforma continental y plataformas de talud. El único registro sedimentario de este periodo es el diamicton subglacial depositado en la parte proximal de los surcos glaciales. Este sedimento sólo se ha identificado en esta zona porque posiblemente estuvo dominada por un ambiente subglacial mientras que en las zonas distales del margen se producía la deglaciación. El talud inferior recibió el depósito de las secuencias proglaciales durante el periodo en que la zona de anclaje del manto de hielo permaneció en el borde de las plataformas de talud.

Durante la deglaciación y el interglacial, los procesos subglaciales fueron sustituidos progresivamente hacia tierra por procesos proglaciales, glaciomarinos y marinos. Las estructuras sedimentarias indican que el depósito de la secuencia de sedimento glaciomarino compuesto estuvo marcado por variaciones en la tasa de sedimentación que dieron lugar a niveles ricos en IRD y bioturbación, y se vio frecuentemente interrumpida por eventos de flujos de turbidez densos de agua de fusión. Estos eventos son más frecuentes en las zonas más proximales, debido a la mayor cercanía relativa al manto de hielo. En este intervalo, el talud inferior actúa como área de transferencia de sedimento y en su parte inferior registra movimientos en masa. En la cuenca, el principal proceso sedimentario en este periodo es la sucesión de numerosos eventos de flujos turbidíticos, procedentes fundamentalmente del talud inferior, pero también desde los edificios volcánicos. En particular, el volcán Tres Hermanas, situado en la zona occidental de la cuenca, puede considerarse el área fuente de las capas de sedimento volcanoclástico identificadas en las secuencias turbidíticas. También se producen en la cuenca procesos de inestabilidad sedimentaria y procesos relacionados con las corrientes de contorno.

El margen de las islas Shetland del Sur presenta una mayor variabilidad sedimentológica, que puede explicarse por una mayor sensibilidad a los cambios climáticos y

sedimentarios en un manto de hielo de la Península Antártica de dimensiones mucho más reducidas que el peninsular.

3.2. Factores locales: Morfología/fisiografía, área fuente y oceanografía

La variabilidad de los rasgos morfológicos en los distintos dominios fisiográficos indica la actuación que un rango amplio de procesos sedimentarios en la CCB, que se ven reflejados también en el registro sedimentario. En general, la fisiografía determina en la CBB el dominio de procesos subglaciales y proglaciales proximales en las plataformas de talud, ya que en la mayoría de márgenes de altas latitudes estos procesos se restringen a la plataforma continental. Las diferencias entre los modelos estratigráficos del talud inferior también se relacionan con la variabilidad fisiografía, y en particular con la presencia o no de plataformas de talud, que posibilitan que la zona de anclaje del hielo se sitúe en zonas más distales.

El área fuente es un factor de control para el talud, ya que la principal fuente de sedimento son los mantos de hielo y en particular las corrientes de hielo, que se disponen de forma semirradial alrededor de la CCB. En cuanto a la cuenca, el sedimento procede de las plataformas de talud y talud inferior, que tienen una configuración radial. Los edificios volcánicos también actúan como fuente de sedimento para las turbiditas volcanogénicas, pero a su vez limitan la distribución espacial de los flujos turbidíticos.

Finalmente, la oceanografía ejerce un control local en la sedimentación reciente en la zona de la cuenca al pie del talud inferior del margen peninsular.

CAPITULO VI. Síntesis y Conclusiones

1. Evolución post-rift de la CCB: fisiografía, sistemas sedimentarios, estratigrafía y depósitos

Este trabajo aborda el estudio de la evolución de la CCB a través de aproximaciones multi-escala, multi-resolución y multi-temporal, como resultado de la utilización de una gran variedad de técnicas y de distintas escalas de estudio. Se establecen tres niveles de estudio temporal: a) la aproximación temporal del Plioceno-Cuaternario aborda la arquitectura estratigráfica del margen de la Península Antártica de la CCB; b) la aproximación temporal del Pleistoceno superior-Holoceno estudia la morfología y los sistemas sedimentarios desarrollados durante el último ciclo glacial en la CCB; y c) la aproximación temporal del Holoceno estudia los procesos sedimentarios ocurridos durante el periodo de deglaciación e interglacial en la CCB.

Este estudio indica que la CCB tiene como característica especial el desarrollo de plataformas de talud relacionadas con procesos glaciales, a diferencia de otros márgenes de altas latitudes.

La dinámica sedimentaria de la CCB durante el último ciclo glacial dio lugar al desarrollo de cuatro sistemas sedimentarios: el sistema glacial-glaciomarino, el sistema de talud-cuenca, el sistema de escape de fluidos y el sistema contornítico. El principal factor de control de la dinámica sedimentaria es el clima, mientras que la tectónica, fisiografía y oceanografía juegan un papel secundario.

La sedimentación reciente en la CCB indica que los procesos sedimentarios subglaciales, proglaciales, glaciomarinos y marinos se han desarrollado en relación con los ambientes sedimentarios y dominios fisiográficos. La mayor parte del registro sedimentario estudiado corresponde al periodo de deglaciación e interglacial.

La arquitectura sedimentaria del margen peninsular de la CCB está controlada por la fisiografía y por factores climáticos, que produjeron el desarrollo del relleno sedimentario post-rift en dos periodos separados por el evento climático del Pleistoceno Medio (MPR, *Middle Pleistocene Revolution*). El primer periodo dio lugar a depósitos eminentemente progradantes, mientras que durante el segundo periodo se desarrollaron depósitos progradantes/agradantes. Durante este segundo periodo se han diferenciado cinco ciclos glaciales que muestran una alternancia entre dos tipos de régimen climático con diferentes espesores del manto de hielo de la Península Antártica, que produjeron variaciones en la distribución de los depósitos glaciales.

2. Contribución a los modelos sedimentarios glaciales: refinando y ampliando el conocimiento de la evolución sedimentaria de la CCB

Los resultados de este estudio permiten refinar los modelos sedimentarios de la CCB, ya que proporcionan una caracterización detallada y de alta resolución de los sistemas y procesos sedimentarios y de la arquitectura estratigráfica del área.

2.1. Modelos sedimentarios en la CCB

Se proponen dos modelos sedimentarios, de margen y de cuenca, basados en la arquitectura estratigráfica, los elementos arquitectónicos que forman los sistemas sedimentarios y la estratigrafía sedimentaria reciente de dichos ambientes.

El modelo sedimentario de margen incluye la plataforma, el talud superior, las plataformas de talud y el talud inferior. En estos dominios se reflejan los cambios más importantes como resultado del efecto de procesos glaciales y glaciomarinos. La arquitectura estratigráfica se caracteriza por la erosión glacial de la plataforma, talud superior y zonas

proximales de las plataformas de talud, y el depósito de sedimento glaciogénico formando las plataformas de talud y el talud inferior. La sucesión de ciclos glaciales produjo el crecimiento progresivo del margen hacia cuenca y determinó que los procesos glaciales y glaciomarinos ocurrieran tanto en las plataformas de talud como en el talud inferior. Este hecho constituye la característica más distintiva de la CBB respecto a otros márgenes de altas latitudes. Este dominio constituye un sistema de dispersión de sedimento afectado por erosión subglacial y deposición proglacial, glaciomarina y marina, e indica que las rutas del sedimento desde su fuente hasta su depósito están gobernadas por los ciclos glaciales. Dentro de los ciclos glaciales, es durante el periodo de avance de hielo y máximo glacial cuando se desarrolla el grueso de los productos sedimentarios en este dominio. Esta interpretación se basa en la identificación de disconformidades glaciales regionales, el carácter de los cuerpos sísmicos que forman parte de las unidades sísmicas y el carácter de los elementos morfológicos y sistemas sedimentarios identificados en la CCB.

El modelo sedimentario de cuenca está principalmente afectado por procesos marinos y oceanográficos que predominan cuando el manto y las corrientes de hielo retroceden hacia tierra. En este dominio las rutas del sedimento desde su fuente hasta su depósito están gobernadas por factores locales, y los principales procesos son los movimientos de masas y las corrientes de contorno.

2.2. Margen peninsular *vs.* Margen de las Islas Shetland del Sur

Las diferencias entre los dos márgenes que componen la CCB pueden resumirse en su caracterización como dos tipos de margen: un margen pobremente alimentado (margen de las islas Shetland del Sur) y un margen construccional (margen peninsular). El modelo sedimentario del margen de las islas Shetland del Sur resulta del desarrollo de procesos glaciales y glaciomarinos en un margen estrecho y escarpado, donde el manto y corrientes de hielo son de tamaño limitado. En este escenario, el desarrollo de los sistemas sedimentarios es menor, y se forman elementos arquitectónicos de menor orden de magnitud. También la variabilidad sedimentológica responde al menor tamaño de las masas de hielo en este margen. Por el contrario, el margen peninsular permite el desarrollo de grandes masas de hielo y una mayor área fuente de sedimento glacigénico. Por ello, en este margen se desarrollan elementos arquitectónicos de mayor orden de magnitud cuyo desarrollo ha favorecido un mayor crecimiento del margen.

2.3. Inter-relaciones entre factores globales y locales que controlan la evolución post-rift de la CCB

La fisiografía, morfología y estratigrafía sísmica y sedimentaria de la CCB son el resultado de las inter-relaciones entre varios factores de control. El clima es el factor principal y está modulado por otros factores locales que incluyen la tectónica, la fisiografía,

el aporte de sedimento y la oceanografía. El clima controla la sucesión de ciclos glaciales. Las características de estos ciclos determinan la frecuencia de los eventos de anclaje del Manto de Hielo de la Península Antártica en ambos márgenes de la CCB, el régimen termal, espesor y extensión del mismo. Estos factores inciden en el patrón de arquitectura estratigráfica, en las facies y en la distribución de los sistemas sedimentarios. En particular, es el periodo de avance de hielo y de máximo glacial en el que ocurre la mayor parte de los procesos que han dado lugar a actual configuración de la CCB.

La tectónica afecta a la fisiografía de la CCB, que ha determinado las diferencias entre los dos márgenes que la componen. También las diferencias en la tasa de apertura de la cuenca han afectado a los patrones arquitecturales del margen peninsular. La tectónica también determina la localización de los edificios volcánicos y de los surcos glaciales erosionados por las corrientes de hielo.

El control fisiográfico se relaciona con la tasa de migración de los dominios sedimentarios a lo largo del margen con el movimiento del manto de hielo de la Península Antártica. Las provincias fisiográficas están claramente correlacionadas con la distribución de los sistemas sedimentarios y con los modelos sedimentarios establecidos en la CCB (modelo de margen y modelo de cuenca).

El aporte de sedimento está influenciado por el tamaño de las áreas de drenaje del manto de hielo, y determina la tasa de sedimentación y el espesor de los depósitos. El tipo de sustrato sedimentario también afecta a la velocidad del avance del manto y corrientes de hielo, así como su capacidad erosiva. También tiene un efecto en el desarrollo de los sistemas sedimentarios, especialmente en el talud inferior y cuenca.

Por último, la oceanografía tiene un papel local en el desarrollo de elementos contorníticos y su acción está a su vez controlada por la presencia de edificios volcánicos.

3. Cuestiones por resolver

Este estudio, además de producir una mejora en el conocimiento de la evolución sedimentaria post-rift de la CBB, ha puesto de manifiesto una serie de cuestiones que deberían ser estudiadas.

En relación al estudio fisiográfico y morfológico (Capítulo III), la relación entre los rasgos de inestabilidad (especialmente el complejo de valles de deslizamiento Gebra-Magia) con la ciclicidad glacial aún está por clarificar. La caracterización de las corrientes profundas en la CBB también puede ser refinada a partir del análisis de algunos rasgos morfológicos en la cuenca, especialmente los rasgos contorníticos. Finalmente, este estudio provee una mayor comprensión de los procesos sedimentarios especialmente durante la fase

de avance del hielo y máximo glacial, mientras que la fase de deglaciación no puede ser caracterizada apropiadamente, al menos con las técnicas empleadas.

El estudio estratigráfico (Capítulo IV) también arroja algunas cuestiones. En primer lugar, la definición del límite inferior de la Secuencia S2 debería ser refinada y definida en toda la cuenca, para entender el efecto de la subsidencia y/o levantamiento tectónicos y sedimentarios, las diferencias entre la evolución de los dos márgenes de la CBB y el control estructural de la estratigrafía estratigráfica, y poder así definir la reconstrucción paleogeográfica del desarrollo de la CBB en relación con la paleoestructura y los paleoambientes durante la apertura de la cuenca. Finalmente, la aplicación de los conceptos de la estratigrafía secuencial a los márgenes continentales de altas latitudes presenta dificultades, que podrían ser superadas mediante una mejor definición de las disconformidades en los registros sísmicos.

Por último, el estudio sedimentológico (Capítulo V) plantea la necesidad de establecer la cronología de los depósitos para datar la deglaciación y correlacionar los resultados de este trabajo con otros de áreas similares. Por último, el desarrollo de estudios detallados de las asociaciones de diatomeas en los testigos disponibles produciría un importante avance en las reconstrucciones paleoclimáticas y paleoceanográficas de la CBB.

I. Introduction

1. Geology of high-latitude continental margins

High-latitude continental margins are characterized as glacial environments, which comprise all the areas that have some form of contact with glaciers (Reading, 1986). At present, these areas cover about a 10% of the earth's surface, mostly on the Antarctic continent and in the northern hemisphere at latitudes higher than 56º, but they are estimated to have covered up to 30% during past glacial episodes. Advances and retreats of the ice cover were determinant in the evolution of human civilization, since they have forced or facilitated different episodes of human migrations throughout history (Gribchenko and Kurenkova, 1997; Mandryk et al., 2001; Fagan, 2001). The glacial environment has proven to be one of the most sensitive areas to climatic changes. The direct influence of ice sheets and ice streams on the sedimentary record makes geological studies in glacial environments a powerful tool for inferring how climatic changes have interacted with other geological controlling factors such as tectonics, physiography and sediment supply and how this interaction has varied over time and space.

1.1. Ice

Glacial environments are affected by a variety of sedimentary processes, of which the glacial and glaciomarine processes are the most important ones in the modeling of the hinterland and continental margins via glacial-related erosion and deposition. The main actors in these processes are ice sheets with ice streams, ice caps, glaciers, ice shelves, icebergs and sea ice (Fig.1.1).

- *Ice sheets* are extensive glacial ice and snow masses that cover more than 50.000 km^2 and occur in Greenland and Antarctica. The Antarctic Ice Sheet covers an area of 13.6 x 10^6 km^2. In some areas it rests at up to 2.5 km below sea level, due to the weight of the ice. The most dynamic component of ice sheets are *ice streams*, which flow within the ice mass at least one order of magnitude faster (Stokes and Clark, 2001).

- *Ice caps* are dome-shaped glaciers that spread out in all directions, usually covering less than 50.000 km^2. They are highly dynamic components of the glacial environment due to their extreme sensitivity to climatic changes (Bart and Anderson, 2000; Hillenbrand and Ehrmann, 2005).

- *Glaciers* are flowing masses of natural ice that move due to gravity and show a rapid response to short-term climatic changes (Anderson, 1999). Mountain glaciers occur in high mountainous regions and drain ice fields from mountain ranges. Valley glaciers originate from mountain glaciers or ice fields and flow down along valleys, sometimes reaching the sea level (Fig. 1.1). Piedmont glaciers are fan or lobe-shaped ones that

occur due to the spreading of steeper valley glaciers when they reach flat plains. Tidewater glaciers reach the sea and are responsible for icebergs calving.
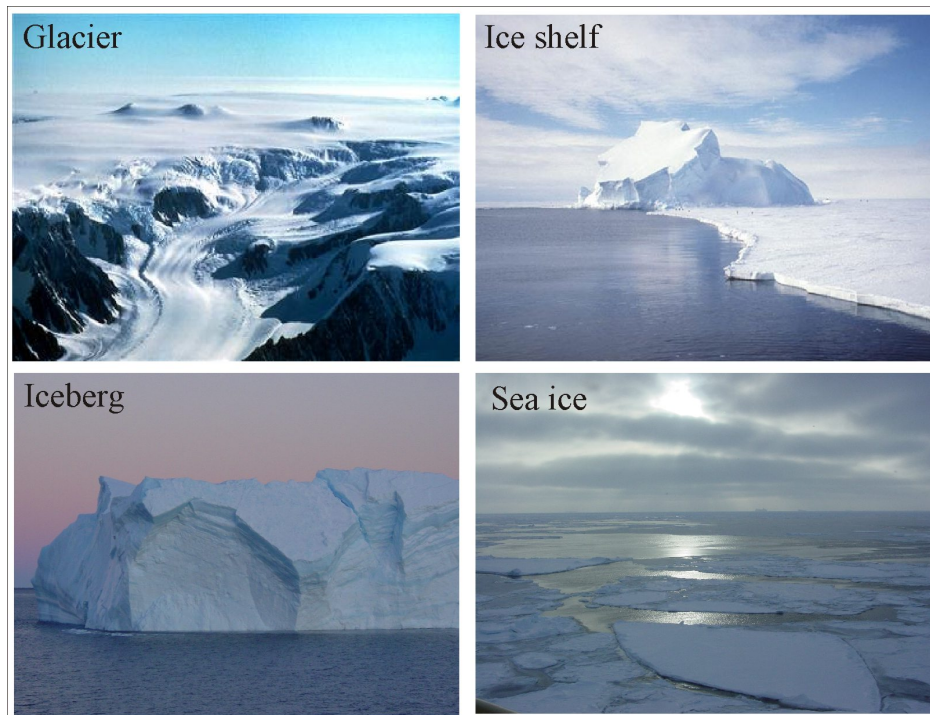

Figure 1.1. Images of different ice forms that contribute to the glacial and glaciomarine processes on high-latitude continental margins.

- *Ice shelves* are platforms of floating ice that constitute the prolongation of ice sheets and glaciers where they move out into the oceans (Fig. 1.1). They provide a constraint for the flow of the ice mass (Anderson, 1999; De Angelis and Skvarca, 2003). Massive collapses of ice shelves have been reported in the Antarctic Peninsula, such as those that recently affected the Larsen Ice Shelf (Rott et al., 1996; Rack and Rott, 2004; Scambos et al., 2004).

- *Icebergs* are fragments of ice that break off glaciers and ice shelves and drift into open water, forced by winds and currents. They have a wide variety of sizes and shapes including tabular icebergs (plateau-shaped, with flat top and steep sides), and dome-, wedge- and pinnacle-shaped icebergs (Fig. 1.1).

- *Sea ice* forms when sea water freezes and salt is forced out of the ice, thus decreasing its salinity and increasing that of the water (Fig. 1.1).

1.2. Sedimentary environments

Four environments are differentiated on the basis of the dominant sedimentary processes (glacial, glaciomarine and marine) and include, from a proximal to a distal position from the ice mass: subglacial, grounding zone, proglacial and open-marine environments (Fig.

1.2). These environments vary in location from the inner continental shelf to the slope as the of ice mass advances and retreats.
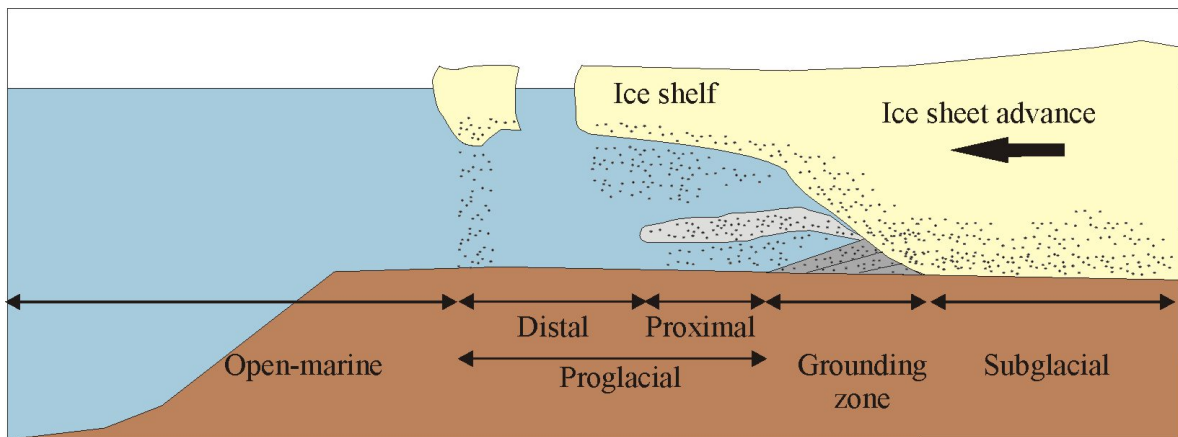

Figure 1.2. Sedimentary environments defined according to their location respect to the grounding line of the ice sheet. These environments are, from proximal to distal: subglacial, grounding zone, proglacial (proximal and distal) and open-marine. The effect of the ice sheet on these environments decreases towards the distal areas.

- The subglacial or basal environment occurs at the lower part of the ice sheet where both erosion and deposition are influenced by the glacier's contact with the bedrock or sedimentary cover underneath. The type of substrate underlying the ice mass and the convergent or divergent ice flow pattern are critical for determining the velocity of the ice flow (Anderson, 1999; Wellner et al., 2001). This environment is dominated by glacial erosive processes.

- The grounding zone environment is the area where ice sheet decouples from the seafloor and an ice shelf may form the seaward prolongation of the ice mass. This is a highly dynamic setting, since it is transitional between the subglacial and the proglacial environments and it advances and retreats with the ice sheet. Glacial erosive and mostly glaciomarine depositional processes occur in this environment.

- The proglacial environment occurs adjacent to the grounding zone and can be subdivided into two sub-environments: proximal and distal. The proximal sub-environment is more affected by the ice mass and the distal sub-environment is more affected by the overlying ice shelf. Glaciomarine depositional processes dominate in both sub-environments.

- The open-marine environment is the area that is not affected directly by the ice sheet or ice shelf. Marine processes are dominant in this environment, but it may also be affected by glaciomarine processes.

1.3. Sedimentary processes and facies

In a general scheme, sedimentary processes on high-latitude continental margins include the glacial erosion of the continental shelf due to the direct effect of the ice sheet advance, and the deposition of the eroded sediment due to glacial and glaciomarine processes (including the deposition of subglacial till, grounding zone wedges and prograded wedges) on the outer shelf and distal areas of the margin during the glacial stages (Fig. 1.3). During interglacial stages, the ice sheet retreats to proximal areas of the margin. The predominant processes are glacial and glaciomarine processes such as turbid meltwater flows and rain-out of debris, and marine processes such as sediment settling, gravity flows and contour current reworking (Fig. 1.3). A more detailed characterization of these processes and their sedimentary products may be made in the different environments.
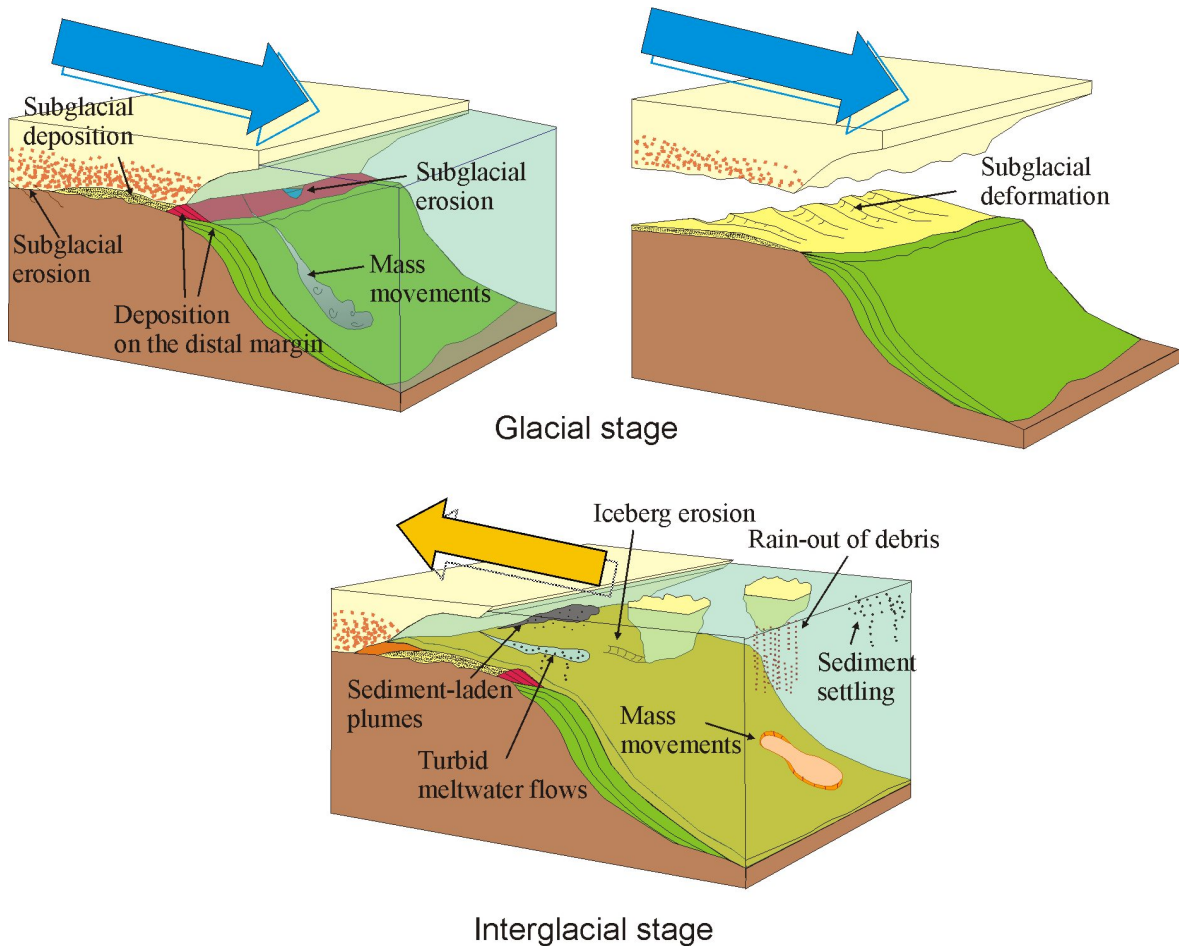

Figure 1.3. Scheme of the sedimentary processes in high-latitude continental margins during the glacial and the interglacial stages.

1.3.1. Subglacial environment

Sedimentary processes occurring in the basal zone involve the glacial advance in direct contact with the bedrock or sedimentary cover and are dependent on the thermal state at the base of the ice sheet (Eyles, 2006). In *temperate glaciers*, where ice temperatures are close to melting point, the ice movement occurs through internal deformation and basal sliding favored by the water film at the base. The ice flow is relatively rapid as a the result of the deformation of basal till layers, which can be as much as ten meters thick. Subglacial till in the basal zone is probably incorporated into the ice by "freeze-on" processes (Bougamont et al., 2003). Net freezing of the subglacial water layer continues to add ice to the base of the ice sheet, thereby lifting debris further into the ice sheet. The moving ice erodes the sediment beneath and transports most of the debris (Alley et al., 1989; Licht et al., 1999). combined with the isostatic effect of the ice weight, this results in overdeepened and landward dipping continental shelves on high-latitude continental margins (Clausen, 1998; Anderson, 1999; Weaver et al., 2000). The ploughing action of the flowing ice and the incorporation of lubricating sediment into the ice mass increase the ice sheet velocity (Stokes and Clark, 2001, 2002). *Sub-polar glaciers* have thawed parts and patches that remain frozen to the substrate. The refreezing of the thawed parts incorporates large volumes of englacial debris. *Polar glaciers* have temperatures below the pressure melting point, and the movement of the ice takes place through internal creep.

Ice sheets are drained by ice streams that excavate glacial troughs as the result of the increased erosion by the relatively faster ice flow (Fig. 1.4) (Vorren and Laberg, 1997). Meltwater under the ice sheet drains towards the ice mass front eroding tunnel valleys (Boulton et al., 1996; Piotrowski, 1997a,b; Domack et al., 2006; Eyles, 2006). This flow may occur in the form of catastrophic floods events (Shaw et al., 1989; Shaw, 2002).
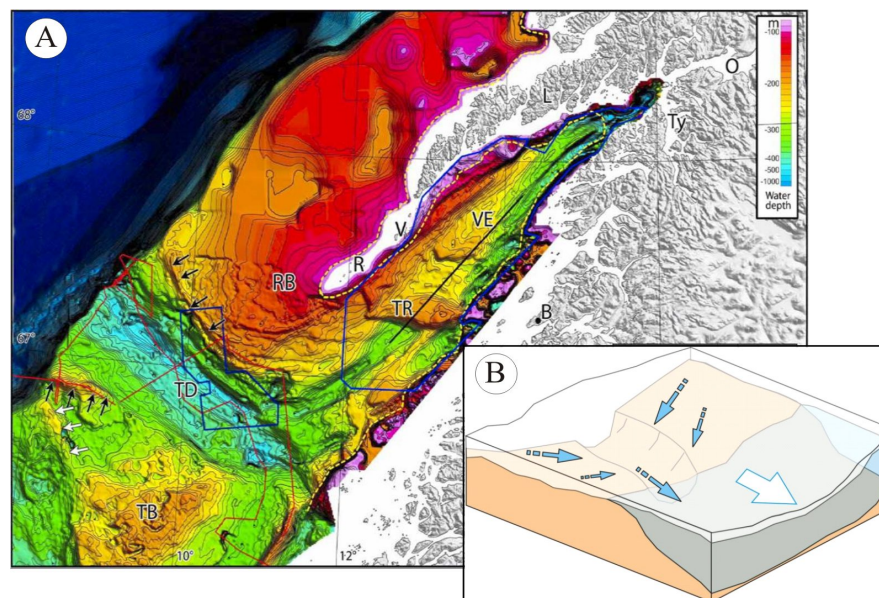

Figure 1.4. A) Glacial troughs eroded on the mid-Norwegian continental shelf, with depths of up to 600 m (modified from Ottesen et al., 2005). B) Cartoon showing the ice stream flow within an ice sheet.

The main product in the subglacial environment is glacial diamicton (till), composed of the debris transported within an ice mass. Diamicton is generally unsorted and unstratified sediment characterized by the absence of fossils, random pebble fabric, a rounded pebble shape, textural and mineralogenic homogeneity within individual units, little or no organic carbon and petrographic similarity within a given province (Anderson, 1999). It is deposited by four primary processes, including lodgement, melt-out, sublimation and subglacial deformation (Bennett and Glasser, 1996). The interplay of these processes produces two types of glacial diamicton: lodgement and deformation till (Anderson, 1999; Wellner et al, 2001). Lodgement till forms by sediment plastering onto the substrate through pressure-melting processes under the weight of the ice mass and shows high values of shear strength (Heroy et al., 2008). Deformation till is formed in a subglacial deforming layer and is differentiated from lodgement till by its lower shear strength values, high porosity, linear structures interpreted as 'shear' planes, attenuated and inclined mud and debris clasts, folded pods of gravel and a general lack of clast fabric (Dowdeswell and Sharp, 1986; Hart and Roberts, 1994; Benn, 1995; Benn and Evans, 1996; Evans et al., 2005). Soft deformation till may be produced from lodgement till due to reworking and deformation (Evans et al., 2005).

1.3.2. Grounding zone environment

Ice sheets advance and retreat between the inland and the marine environment, and the grounding zone changes its position along the margin during the glacial cycle (Fig. 1.5). Conceptualized ice sheet grounding models indicate that the erosion and deposition processes associated with grounding events occur in a similar manner on all Antarctic margins (Cooper et al., 1991; Bart and Anderson, 1995; Saanumi, 2006). During the advance of an ice sheet from the continent the ice-covered inner continental shelf becomes a zone of net erosion as sediments are eroded by the ice mass. These eroded sediments are subsequently transported
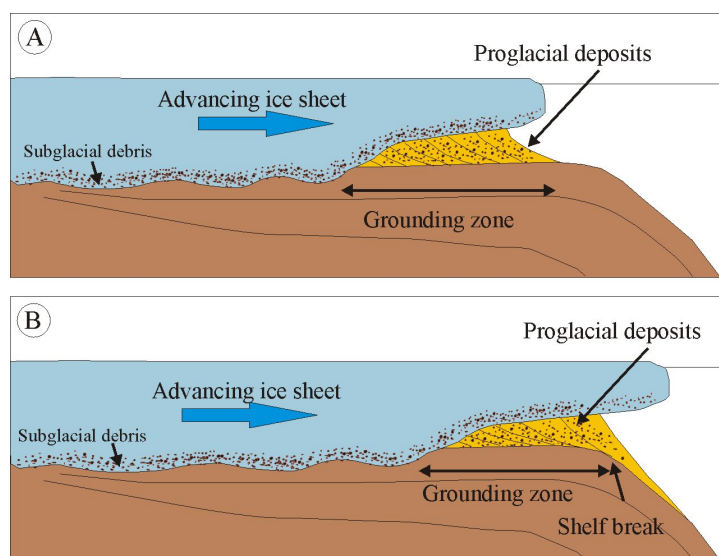

Figure 1.5. Deposition of proglacial deposits. A) The grounding zone and proglacial environments migrate with the ice sheet advance.   B) As the grounding zone reaches the shelf edge, proglacial deposits form prograded wedges on the slope.

8

as subglacial debris and re-deposited in the grounding zone as prograding foresets, which downlap onto pre-existing topography on the outer-continental shelf (Bartek et al., 1991; Bart and Anderson, 1995). As the ice sheet continues its advance the sediment deposited on the grounding zone is continuously stripped from the inner shelf and the distal toes of truncated prograding foresets are only preserved on the outer shelf (Fig. 1.5B) (Bart and Anderson, 1995).

Sediment deposited in the grounding zone environment is similar to lodgement till, but it is not overcompacted and has a more random pebble fabric (Anderson et al., 1991; Anderson, 1999). Also, it may have some structures such as laminations and lenses (Lucci et al., 2002).

1.3.3. Proglacial environment

The proglacial environment is dominated by glaciomarine processes, since sedimentation is influenced by the ice sheet, the ice shelf and marine processes. It preserves a combination of sub-aqueous outwash, glaciomarine sediments, and vertical settling of debris (Powell, 1984; Reading, 1986). The proglacial environment can be divided into proximal and distal (sub-ice shelf) sub-environments.

The proximal proglacial sub-environment is affected by glaciomarine processes, but the major sediment source is the ice mass. As the ice sheet advances, ablation in the grounding zone releases debris that washes down the ice sheet and falls through the water column. Because the debris is melted/washed out, it is distributed over a large area. This sub-environment contains sediment with a different degree of lamination and stratification, as the result of size fractionation by ice-margin processes, including meltwater turbid plumes and superficial, intermediate or bottom sediment-laden plumes (Hesse et al., 1997, 1999; Dowdeswell et al., 2000; Lucchi et al., 2002; Escutia et al., 2003; Leventer et al., 2006; Murdmaa et al., 2006; Heroy et al., 2008; Willmott et al., in press). As the grounding zone reaches the shelf break, the glacigenic sediment is deposited by sediment mass transport processes forming thick prograded wedges that accumulate on the slope (Damuth, 1978; Anderson et al., 1986; Alley et al., 1989; Laberg and Vorren, 1995; Dowdeswell et al., 1996; Punkari, 1997; Vorren and Laberg, 1997; Anderson, 1999; Barker et al., 1999; Dahlgren et al. 2005; Evans et al., 2005; Rise et al., 2005).

The distal proglacial (sub-ice shelf) sub-environment shows a variety of glaciomarine and marine sedimentary processes. The relatively longer distance from the ice mass enhances the predominance of processes related to the ice shelf, such as the vertical settling from melt-out of the basal debris zone, settling from icebergs at the calving line of the ice shelf and vertical settling, while marine processes include mass movements and current reworking, among others (Grobe and Mackensen, 1992; Harris and O'Brien, 1998; McKay et al., 2008).

The sedimentary record in this sub-environment includes a variety of sediment types (Anderson et al., 1991; Anderson, 1999). Compound glaciomarine sediments are the result of combined ice rafting and suspension settling and are composed of terrigenous and diatomaceous mud with less than 10% of clasts (Ice Rafted Debris, IRD). These sediments are better sorted than basal till and show stratification and bioturbation. Residual glaciomarine sediments consist of IRD and bioclastic material, and are the result of the combination of ice rafting and marine current reworking (Anderson, 1999). IRD layers reflect vertical rain-out of IRD from the base of the ice shelf, massive episodes of iceberg rafting (Lucchi et al., 2002; Heroy et al., 2008) and/or quasi-instantaneous dumping of sediment accumulated on the iceberg surface produced by the iceberg overturning (Dowdeswell et al., 1994). Other types of sediments in this environment include siliceous mud and ooze, carbonates, traction current deposits, eolian sediments, mass movement deposits and iceberg turbates (Anderson, 1999).

1.3.4. Open-marine environment

The open-marine environment is not affected directly by the ice sheet and ice shelf influence. Marine sedimentary processes predominate, including the vertical settling of sediment, mass movement processes and contour current-related processes. The sedimentary record of this environment includes a variety of sediment types, similar to that of mid-latitude areas (mass movement deposits, turbidites, pelagites/hemipelagites, contourites, among others), although this environment may also receive the rain-out of debris from drifting icebergs and the distal, diluted parts of sediment plumes that escape from the grounding zone area.

1.4. Morphosedimentary elements

High-latitude continental margins are characterized by a wide variety of morphosedimentary elements of different levels of hierarchy, spatial scale and distribution. Some of these elements are common with other types of margins, but most of them have a glacial or glaciomarine origin. Some of these elements may occur associated in morphosedimentary systems, based on their distribution and the sedimentary processes involved in their development. A first-approach element classification regarding their origin distinguishes between erosive, mixed and depositional elements. Generally, erosive features occur in the proximal areas of the continental margin and mixed and depositional features predominate in the middle and distal areas.

1.4.1. Erosive morphosedimentary elements

Glacial unconformities are irregular erosive surfaces that truncate underlying strata and are the direct result of deep glacial erosion by the advancing ice sheet on continental shelves (Alley et al., 1989; Anderson, 1999). These unconformities can be traced along large

10

areas (100s km), and their succession in the stratigraphic record indicates repeated episodes of glacial erosion on the inner continental shelf (Fig. 1.6) (Alonso et al., 1992; Bart and Anderson, 1997a). The repeated episodes of glacial erosion produce the outcropping of crystalline basement substrate in the inner areas of many glacial troughs (Wellner et al., 2001).
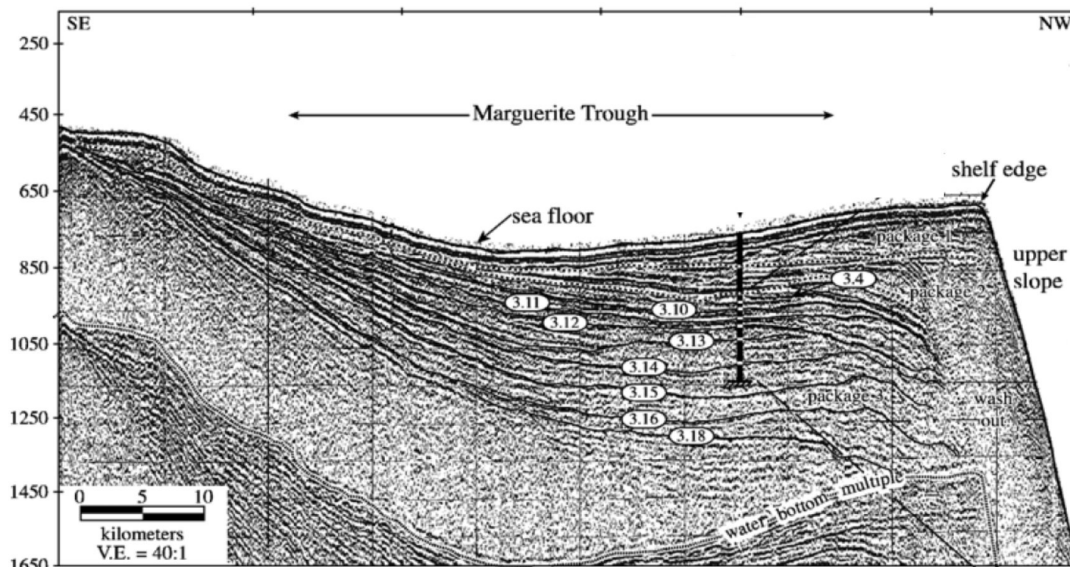

Figure 1.6. Glacial unconformities on the Antarctic Peninsula outer continental shelf. Unconformities record the expansion of the ice sheet and grounding events on the outer continental shelf during the Late Miocene-Early Pliocene in this area (Bart and Anderson, 1997a).

Glacial troughs are the most prominent erosive features in many glaciated continental shelves. They are characterized by their steep walls and relatively flat, seawards-shallowing seafloors and reach depths of hundreds of meters and lengths of tens to hundreds of kilometers. Glacial troughs are eroded by ice streams, which concentrate relatively high-velocity flows within the ice sheet (Figs. 1.4 and 1.7) (Josenhans, 1997; Stokes and Clark, 2001; Ottesen et al., 2005). Their location and orientation is commonly determined by geologic boundaries, especially at their proximal reaches, such as the limits between basement rocks of different resistance to erosion or structurally-controlled weak zones (Anderson, 1999; Camerlenghi et al., 2001). The glacial trough seafloor is characterized by a series of morphological features of minor hierarchy (grooves, knick-points, meltwater channels, drumlins and megascale glacial lineations) that are related to the type of subglacial substrate (Fig. 1.7A) (Anderson et al., 2001; Wellner et al., 2001; Lowe and Anderson, 2003; Wellner et al., 2006).

Erosional grooves are irregular lineations with lengths of tens of km that result from the direct subglacial erosion into outcropping bedrock (Fig. 1.7A,B) (Wellner et al., 2001). In some cases they indicate the direction of the ice flow, and their formation may also be favored by the flow of melting water beneath the ice sheet (Domack et al., 2006).

Knick-points are linear relief irregularities resulting from the subglacial erosion and bulldozing of resistant bedrock horizons of the seafloor (Barnes and Reimnitz, 1997; O'Brien et al., 1997).

Plough marks are typically straight or winding V-shaped depressions with random to preferred orientations, lengths of several kilometers, and levees on their sides. They result from erosion exerted by calving icebergs that move due to the action of thermohaline currents (Belderson et al., 1973; Polyak et al., 1997; Pudsey et al., 1997; Kuijpers et al., 2007) or under the influence of direct push by the advancing ice shelf (Lien et al., 1989). Plough marks may also result from the erosion of a thinning ice sheet in the areas where it is lifted off the seafloor to become an ice shelf (Gilbert et al., 2003). In this case, they have a more consistent trend, controlled by the direction of the ice sheet. Plough marks at high depths (>450 m) may be the result of fast-flowing ice sheet outlet glaciers, high flux and mechanically constrained ice shelf settings or large events of ice sheet collapse (Dowdeswell and Bamber, 2007).
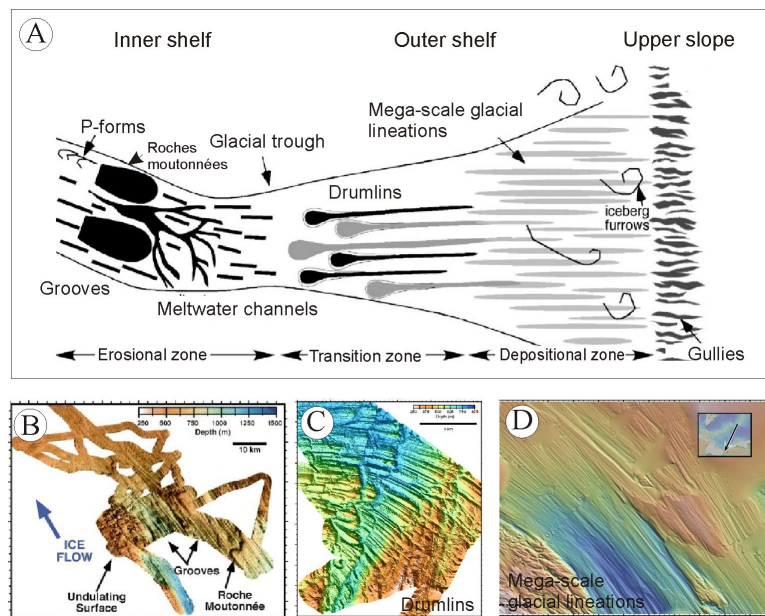

Figure 1.7. Morphological features in glacial troughs. A) Scheme of their development in relation with the substrate, modified from Wellner et al. (2006). B) to D) Examples of these features in swath bathymetry images.

Tunnel valleys or *sub-glacial channels* are channel-like reliefs that may reach lengths of several kilometers and have trends that may follow the regional gradient or be adapted to the irregularities of the lower surface of the ice sheet and the topography (Fig. 1.7A,B). They are eroded by high-energy subglacial meltwater flows beneath the ice sheets where the excess of meltwater cannot be drained through an impermeable bed (Boulton et al., 1996; Gataullin and Polyak, 1997; Josenhans, 1997; Piotrowski, 1997a,b; Eyles and de Broekert, 2001; Eyles, 2006). They may erode bedrock or till deposits with low transmisivity to drain the meltwater.

They usually form networks of anastomosing channels that represent transitional, short-lived features, or systems of relatively stable features in terms of lateral migration and temporal continuity (Piotrowski, 1997b).

1.4.2. Mixed erosive and depositional morphosedimentary elements

Drumlins are smooth, asymmetric oval-shaped hills with the long axis in the direction of the ice flow and a tail pointing in the down-ice direction (Fig. 1.7A,C). They may be tens of meters high and kilometers long. They are composed of subglacial till, but may form around topographic irregularities, being erosional in this sense (Wellner et al., 2001). They occur in areas that form the limit between bedrock and sedimentary cover and are indicative of the flow direction. Their presence suggests the acceleration of the ice flow (Anderson, 1999; Wellner et al., 2001; Evans et al., 2005; Ó Cofaigh et al., 2005; Wellner et al., 2006).

1.4.3. Depositional morphosedimentary elements

Mega-scale glacial lineations are elongated, relatively straight features of hundreds of kilometers that form a "ridge and runnel" relief on the glaciated continental shelves and seafloor of glacial troughs (Fig. 1.7A,D). They are sculptured into soft deformation till by the advancing ice sheet or rapid flowing ice streams (Anderson, 1997). Their morphology and relief suggest high flow velocity (Shipp et al., 1999; Stokes and Clark, 2001; Wellner et al., 2001; Stokes and Clark, 2002; Clark et al., 2003) and indicate the direction of the ice flow. In the Antarctic Peninsula continental margin, mega-scale glacial lineations show consistent morphologic characteristics, including straight and parallel trends, elongation ratios of >80:1 and spacing of 200–600 m (Heroy and Anderson, 2005).

Bundle structures are ice-bed contact till deposits that are similar in scale, character and location to mega-scale glacial lineations but they display sinuous and convergent trends, larger spacing (1-5 km) and a higher longitudinal continuity of up to 100 km (Fig. 1.8) (Canals et al., 2000; Willmott et al., 2003; Willmott, 2007). These structures are related to fast-flowing ice streams, their upstream portions are carved into bedrock, and they occur in an irregular topographic setting. The topographic influence and the character of the substrate are interpreted as the cause of the morphologic differences with mega-scale glacial lineations (Stokes and Clark, 2001; Heroy and Anderson, 2005).

Moraines are unsorted ice-marginal deposits of sediment with no stratification, formed by the direct action of the ice mass both on land and on continental margins. They are very common features that display a variety of morphologies and sizes. In relation to the phase of the glacial cycle, moraines can be divided into *terminal moraines* formed in front of a glacier during its maximum extension, *recessional moraines* formed during pauses in the ice sheet retreat, and *push moraines* formed during glacial readvances (Solheim, 1997). According to the
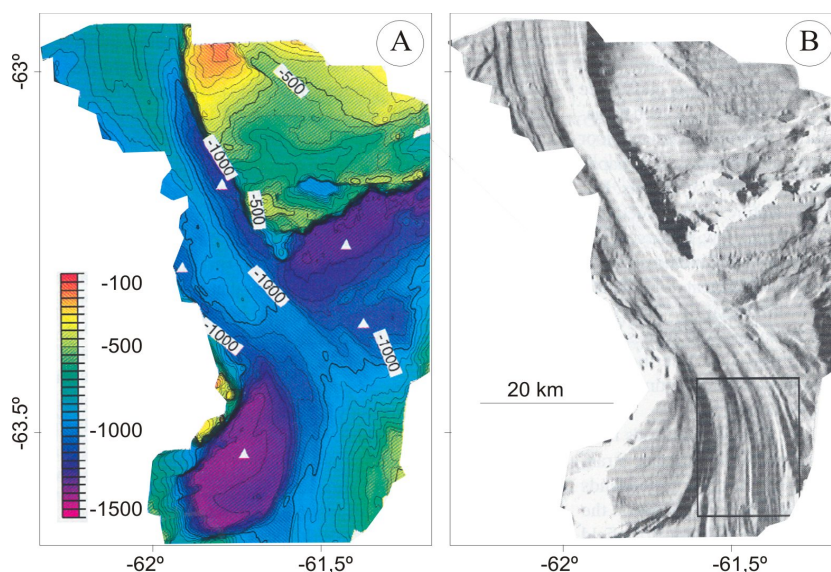
Figure 1.8. Bundle structures in the Gerlache Strait (Western Bransfield Basin). A) Swath bathymetry contour map. B) Shaded relief model. Modified from Canals et al. (2000).

processes involved in their origin, an initial classification differentiates *push moraines*, *ablation moraines* and *dump moraines* (Bennet and Glasser, 1996). *Push moraines* are caused by the glacier advance, which pushes the proglacial sediment to form a ridge; *ablation moraines* are the result of the concentration of material on the surface of a glacier; and *dump moraines* are formed by debris accumulated at the side (lateral moraines) or in front of a glacier. Lateral moraines may occur along the margins of glaciers and ice streams (MacLean, 1997), isolated within glacial troughs or in the areas of confluence of two adjacent ice streams; in this case they are denominated *ice stream boundary ridges* (Anderson et al., 1992; Anderson, 1999). *Grounding zone wedges* can be considered as frontal moraines deposited in the grounding zone (Fig. 1.9). They are formed by glacigenic sediment transported at the base of the ice sheet and deposited forming till deltas (Alley et al., 1989; Banfield and Anderson, 1997; Bart and Anderson, 1997b; Anderson, 1999). Their formation is related to vertical accretion at the glacial bed, together with progradation by sediment gravity flows (O'Brien et al., 1999). Their identification indicates deposition during the glacial maximum stage or during pauses or short readvances during the recession of the ice sheet (Larter and Vanneste, 1995; Ó Cofaigh et al, 2005; Ottesen et al., 2005; McMullen et al., 2006).

Prograded wedges are line-sourced features characterized as basinward-prograded clinoforms. They are deposited seaward of the grounding zone of the ice sheet (Alley et al., 1989; Punkari, 1997; Anderson, 1999; Dahlgren et al. 2005) and they comprise glacigenic sediments transported and deposited by sediment mass transport processes (Damuth, 1978; Anderson et al., 1986; Laberg and Vorren, 1995; Vorren and Laberg, 1997). Prograded wedges are deposited on the outer continental shelf and slope, when the ice sheet is grounded on the

14

continental shelf break (Dowdeswell et al., 1996; Barker et al., 1999; Evans et al., 2005) and their vertical stacking indicates the succession of glacial/interglacial cycles.
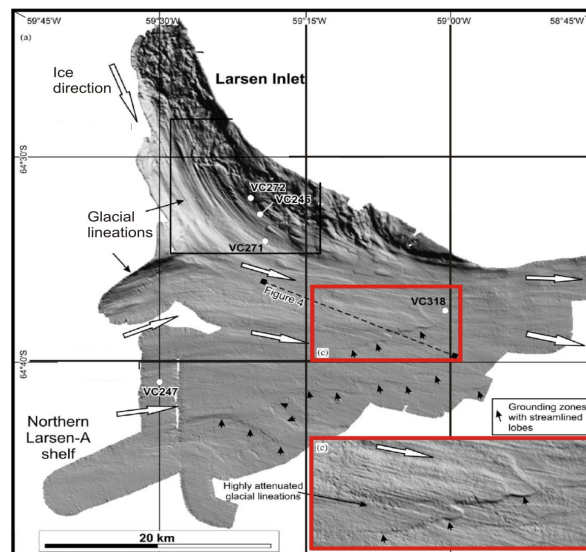

Figure 1.9. Grounding zone wedges in a shaded relief model from the Larsen Inlet (Antarctic Peninsula). Modified from Evans et al. (2005).

Trough mouth fans are a special type of prograded wedges formed primarily by sediment transported by ice streams, channelized along glacial troughs and deposited seaward of the grounding zone (Fig. 1.10) (Alley et al., 1989; Punkari, 1997; Vorren and Laberg, 1997; Dahlgren et al. 2005). They are fed by ice streams, and are therefore point-sourced. The high velocity of ice streams increases their erosive capacity and the sediment supplied to trough
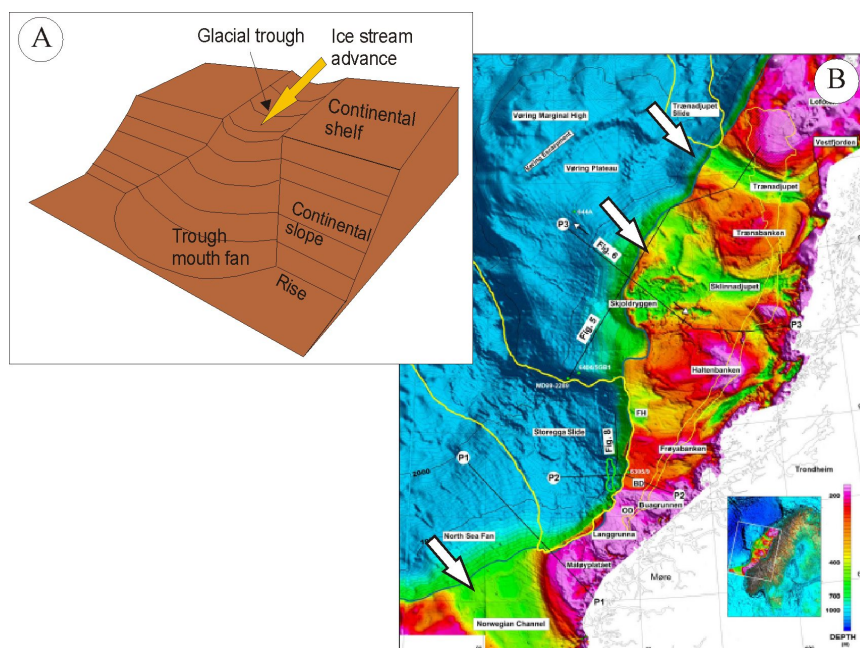

Figure 1.10. A) Scheme of the formation of a trough mouth fans at the mouth of a glacial trough, modified from Vorren and Laberg (1997). B) Trough mouth fans on the Norwegian continental margin, modified from Rise et al. (2005). Arrows mark the trough mouth fans.

15

mouth fans is also higher than in surrounding areas, where prograded wedges are deposited. The high sedimentation rates at the mouths of glacial troughs, together with the occurrence of earthquakes, the over-steepening of the shelf break and the excess pore pressure in sediments, generate instabilities that lead to the submarine glacigenic debris flows and related flows that form the trough mouth fans (Laberg and Vorren, 1995; King et al., 1998).

Contourites are mostly represented by sediment ridges or drifts and associated moats that occur commonly on the continental rise of high-latitude margins, affecting the high amount of sediment supplied to the continental slope during the glacial stages (Fig. 1.11). Contourite drifts are also fed by hemipelagic supply, IRD input and sediment deposited and removed by contour currents (Hepp et al., 2004) and they may undergo slumping and turbidity current flow down the slope and suspension as nepheloid layers within bottom currents (Pudsey, 2000; Weaver et al., 2000; Barker and Camerlenghi, 2002). Sediment waves may also develop due to the effect of deep currents (Maldonado et al., 2003).
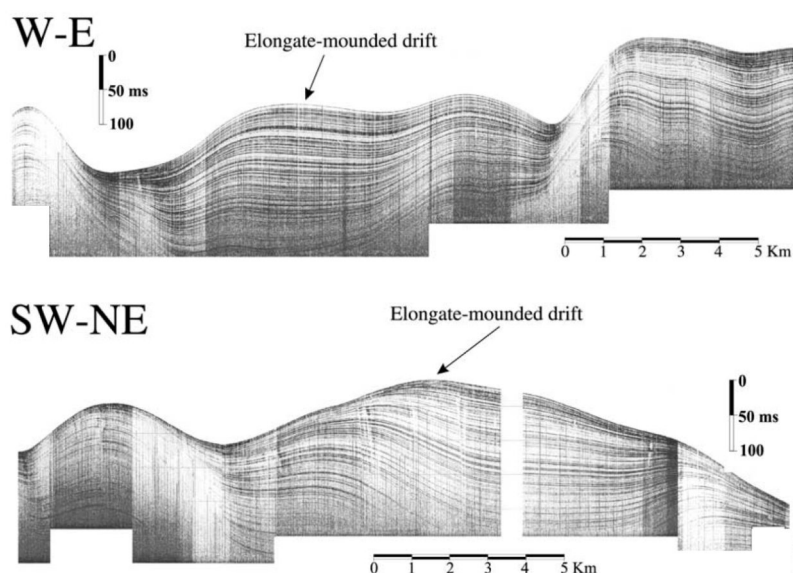

Figure 1.11. Seismic profiles showing contourite deposits in the central Scotia Sea, modified from Maldonado et al. (2003).

Sediment mass movement features of different scales commonly occur on high-latitude continental margins. Submarine landslides such as the Storegga slide on the North Sea margin are related to the rapid accumulation of unconsolidated sediment during the glacial stages and the subsequent destabilization by different triggering mechanisms, including gas hydrate destabilization and isostatic rebound (Fig. 1.12) (Bugge et al., 1988; Haflidason et al., 2004). Smaller-scale sediment mass movement processes include debris flows and small-scale slumps on the upper slope that may evolve to turbidity currents (Pudsey and Camerlenghi, 1998). Small line-sourced gullies on the continental shelf break are formed by sediment flows from an ice sheet grounded at the shelf break (Canals et al., 2002; Dowdeswell et al., 2004;

Heroy and Anderson, 2005). The upper parts of trough mouth fans may be affected by V-shaped canyons and turbidite valleys, as in the case of the Weddell Fan (Anderson et al., 1986). Trough mouth fans may also be affected by large canyons and channels with the development of turbidite channel-levee systems. This is the case of the Crary Fan, in the Weddell Sea, which has channel-levee complexes up to 140 km wide (Kuvaas and Kristoffersen, 1991).
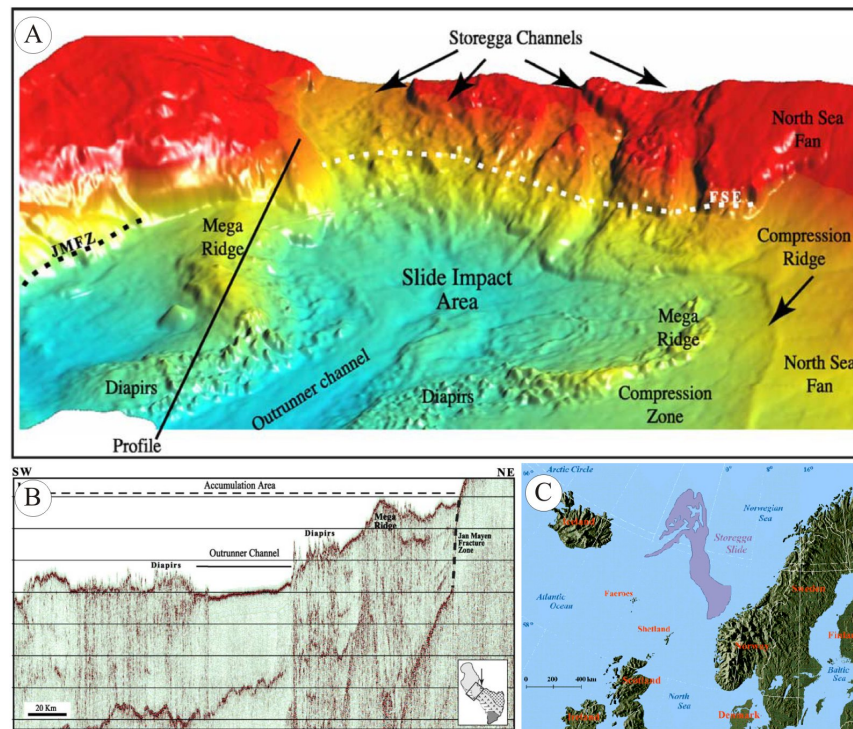

Figure 1.12. Images of the Storegga Slide in the Norwegian margin. A) Relief model of the slide area. B) Seismic profile crossing the slide (modified from Haflidason et al., 2004). C) Areal extension of the Storegga Slide that affects about 95000 km^2.

Finally, *pockmarks* are crater-like features that result of the escape of excess pore fluid from the sediment (Judd and Hovland, 2007). In glacially-influenced margins this process occurs due to the consolidation of the abundant water-saturated sediment deposited during glacial stages (Harrington, 1985; Kelley et al., 1994; Ussler et al., 2003; Judd and Hovland, 2007).

1.5. Sedimentary architecture of high-latitude continental margins

The high-latitude continental margin growth patterns reflect the vertical stacking of sequences associated with complete glacial/interglacial cycles, bounded by widespread unconformities interpreted as subglacial erosional surfaces (Bart and Anderson, 1996, 1997a). On the continental shelf the sequences consist of aggrading deposits formed by grounding zone wedges and the proximal parts of prograded wedges. These bodies are eroded by the subsequent ice sheet expansions (ten Brink et al., 1995; Bart and Anderson, 1996; Clausen,

1998). The sedimentary architecture from the continental slope to deep areas is characterized by the vertical stacking of prograded wedges that continue laterally to those deposited on the continental shelf. These prograding slope units result from proglacial deposition, and develop preferentially near the mouths of glacial troughs, where glacial erosion concentrates along the axes of ice streams (Cooper et al., 1991; Bart and Anderson, 1996; Dowdeswell et al., 1996; Vorren et al., 1998; Barker et al., 1999; De Santis et al., 2003; Nygård et al., 2005). The general pattern of sedimentary sequences is prograding, prograding-aggrading or aggrading, depending on the interplay of factors such as the margin physiography, tectonic uplift/subsidence, sediment supply and glacial regime. The continental slope and rise are characterized by large sediment ridges that may be composed of the fine grained part of the unstable sediments from the uppermost continental slope (Kuvaas and Leitchenkov, 1992; Rebesco et al., 1996, 1997; Clausen, 1998; Lucchi et al., 2002; De Santis et al., 2003; Dowdeswell et al., 2004; Hepp et al., 2004, 2006).

2. The study area

Antarctica is the southernmost continent, with most of its area lying at latitudes higher than 70ºS (Fig. 1.13). It is surrounded by the Southern Ocean and has an area of 14.4 million km². About 98% of its surface is covered by the Antarctic Ice Sheet, which currently has 25-30 million km² of ice (Drewry et al., 1982; Anderson, 1999). Antarctica is divided into two by the Transantarctic Mountains, which form a mountain range from northern Victoria Land to the Weddell Sea (Fitzgerald et al., 1986; Gleadow and Fitzgerald, 1987). This range is 3500 km long and 100-200 km wide, has elevations of up to 4500 m and constitutes the division of East and West Antarctica (Fitzgerald et al., 1986). East Antarctica is covered by the East Antarctica Ice Sheet, which rests predominantly above sea level, while the West Antarctic Ice Sheet is, mostly characterized as a marine ice sheet (Anderson, 1999). Most of the Antarctica has a true polar climate, with little precipitation, low temperatures and strong katabatic winds (Anderson, 1999).
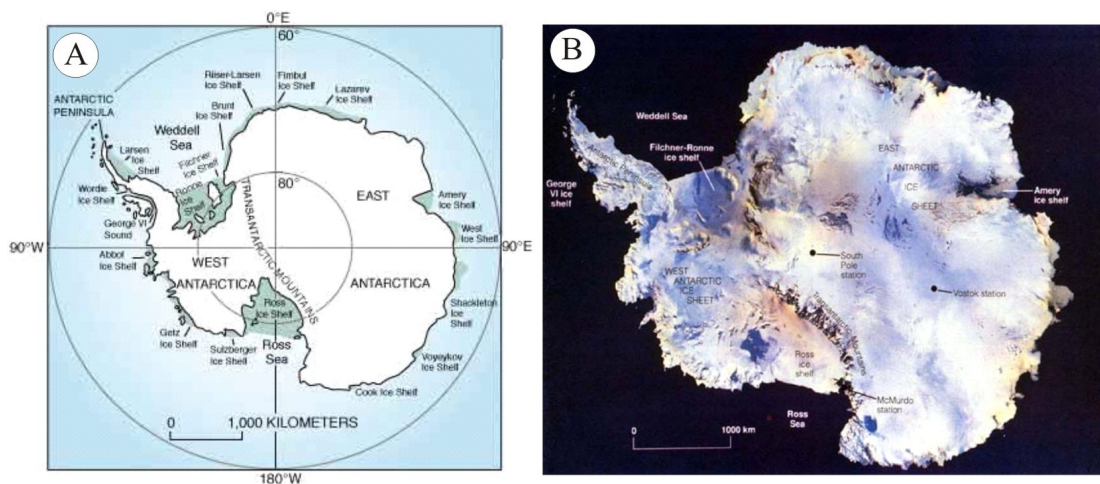

Figure 1.13. A) Map of the Antarctic continent which is divided by the Transantarctic Mountains into two parts: West and East Antarctica. B) Satellite image of the Antarctic Continent. From www.geos.ed.ac.uk.

The Antarctic Peninsula (AP) is a south-north oriented plateau that extends between the latitudes 61 and 74ºS and the longitudes 55 and 80ºW (Fig. 1.14). It narrows towards the north and extends from West Antarctica facing South America. The peninsula has a mountain ridge, with peaks that rise to approximately 2800 metres. The geography of the AP is very irregular and most of the coast is cut by fjords. Several islands surround the peninsula, including the South Shetland Island archipelago about 120 km from the northwest tip of the peninsula composed of eleven major SW-NE aligned islands. Several ice shelves occupy embayments along the AP coast, the most important being the Larsen Ice Shelf in the Weddell Sea, on the eastern peninsula coast, which has undergone several episodes of breakup (Rott et al., 1996; Rack and Rott, 2004; Scambos et al., 2004; www.nasa.gov). Other ice shelves surrounding the AP are George VI Ice Shelf and Wilkins Ice Shelf on the western peninsula coast, and the Filchner-Ronne Ice Shelf in the southeast of the peninsula.

The Bransfield Basin is located in the northernmost part of the AP (Fig. 1.14C). It is defined by a narrow NE-SW-oriented strait which separates the AP to the southeast and the South Shetland Islands (SSI) to the northwest. The basin is divided into three sub-basins, the Eastern, Central and Western Basins, limited by morphological steps off Deception and Bridgeman Islands (Jeffers and Anderson, 1990).
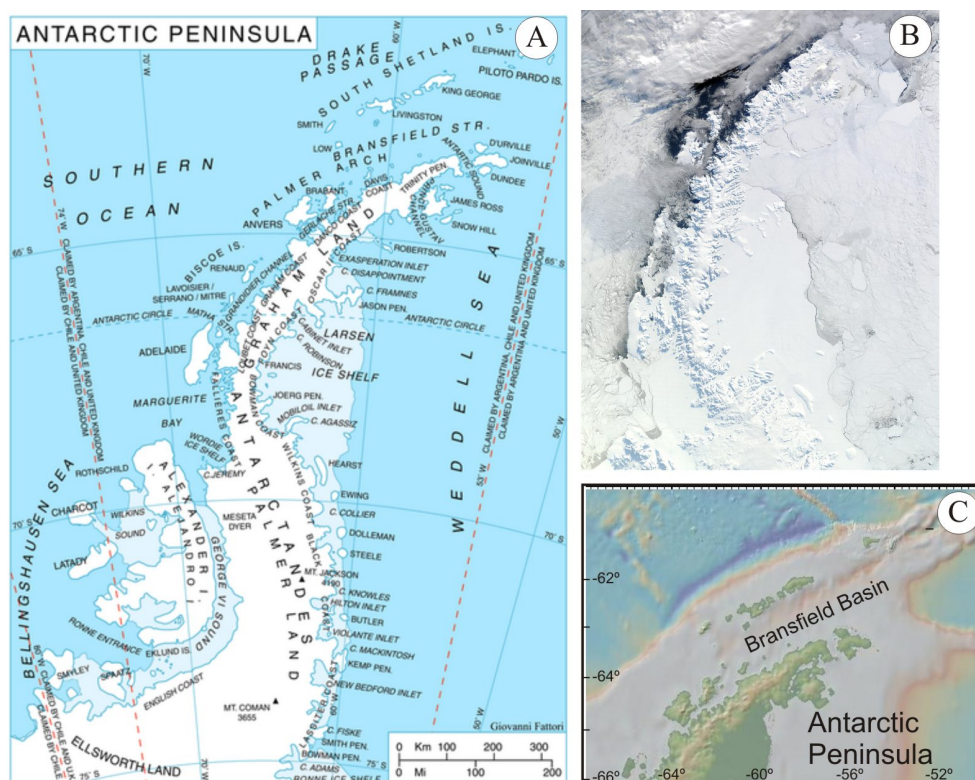

Figure 1.14. A) Map of the Antarctic Peninsula. B) Satellite image of the Antarctic Peninsula showing the ice cover in September 2002 (from NASA/GFS). C) Location of the Bransfield Basin, at the northern tip of the Antarctic Peninsula (bathymetric map from http://marine-geo.org).

2.1. Climate

Most of the AP has a fully polar regime (Fig. 1.15) (Barker and Camerlenghi, 2002). The AP mountain ridge constitutes an obstacle for the east or southeast-flowing air masses, leading to high snowfall, estimated at 25% of the total of the Antarctic continent (Drewry and Morris, 1992). The AP shows a high climatic sensitivity, since rapid regional warming in the AP is exceptionally high in comparison with the mean global warming (Vaughan et al., 2003). Also, the drainage of the AP ice sheet has increased during the past half-century due to the loss of ice shelves (Cook et al., 2005).
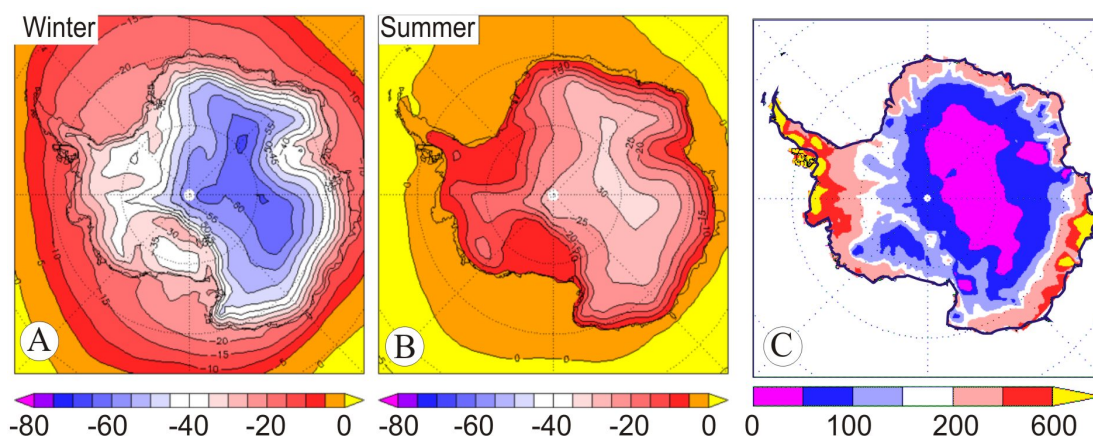

Figurre 1.15. A) Surface temperature (ºC) of the Antarctic Continent during the winter (December to February). B) Surface temperatures during the summer (June to August). C) Average annual precipitations (mm), from www.antarctica.ac.uk.

2.2. Oceanography

The oceanography of the Antarctic continent is strongly controlled by the atmospheric circulation. The main oceanographic structure is the Antarctic Circumpolar Current, ACC (Fig. 1.16A) (Orsi et al., 1995), which flows in an eastwards direction, forced by the strong eastward winds. It surrounds Antarctica, flowing from the sea surface to depths down to 4000 m. The surface flow of the ACC is driven primarily by the wind. The wind stress and the Coriolis force create a northward component in the surface current, which results in the formation of high-speed currents separated by broad, quiescent zones (Hofmann, 1985). From north to south, major fronts include the Subantarctic Front, the Polar Front, and the Southern ACC Front (Gordon et al., 1977; Whitworth, 1980; Orsi et al., 1995). Mean near-surface speeds vary between the three frontal regions and the Subantarctic and Polar Front regions have approximately twice the speed of that associated with the Subtropical Front (Hofmann, 1985). Because the Antarctic currents extend all the way down to the bottom, they are influenced by topographic steering that generates substantial mesoscale eddy activity (Marshall, 1995; Rintoul et al., 2001; Naveira-Garabato et al., 2004). Close to the continent, the Polar Current flows westwards as a counter current.

The Southern Ocean is regionally characterized by several major water masses (Fig. 1.16B) (Orsi et al., 1995, 1999; Naveira-Garabato et al., 2002a,b, 2003, 2004; Hernández-Molina et al., 2006).

- The Antarctic Surface Water (AASW) forms during the winter in the coastal areas of the continent and flows northwards at depths of up to 200 m toward the Polar Front, where it sinks.

- The Circumpolar Deep Water (CDW) flows with the ACC and is internally divided into Upper and Lower Circumpolar Deep Water (UCDW and LCDW, respectively).

- The Warm Deep Water (WDW) is formed in the Weddell Sea by warming of CDW.

- The Antarctic Bottom Water (AABW) is formed in the Weddell Sea by a combination of two local water masses. The first one is the Weddell Sea Bottom Water, which originates from the mixing of WDW with cold local water masses (Weiss et al., 1979). The second one is the Weddell Sea Deep Water (WSDW), which is the youngest and densest of the water masses that escapes from the Southern Ocean forming a deep western boundary current (Orsi et al., 1999).
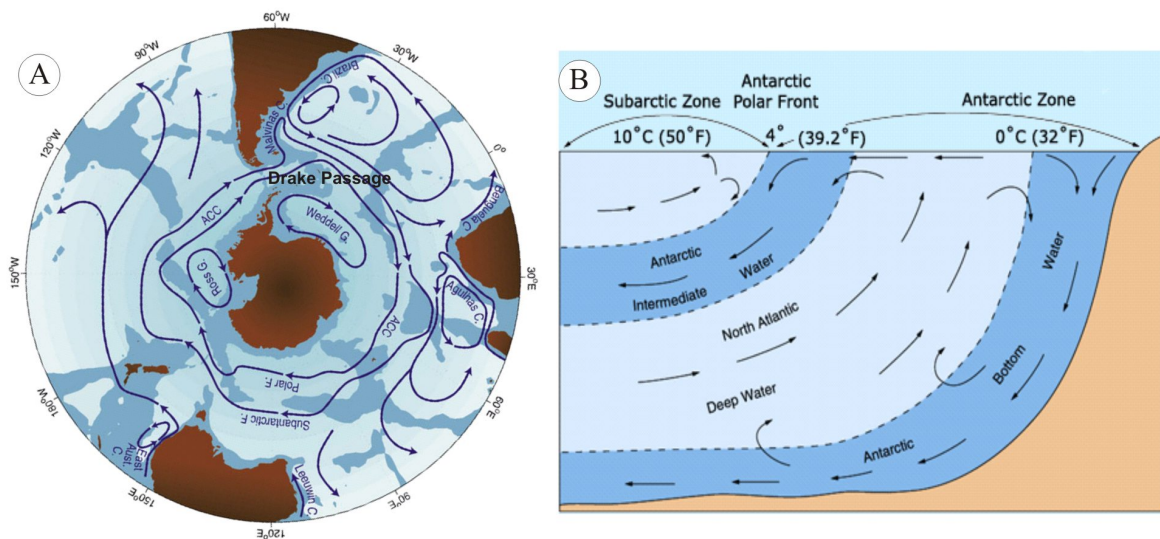

Figure 1.16. A) Scheme of the oceanographic circulation in the Southern Ocean. B) Scheme of the circulation of water masses around the Antarctic continent. (From www.science-in-salamanca.tas.sciro.au and www.nerc.ac.ak). Legend: ACC: Antarctic Contour Current.

The oceanography of the AP region is dominated by the interaction between the ACC and the seafloor topography, especially the Pacific-Antarctic Ridge and the Drake Passage (Marshall, 1995) (Fig. 1.17). In this area all properties show sharp horizontal gradients throughout the water column, the fronts are narrow relative to the total width of the current, and most of the transport occurs within the frontal zones (Whitworth and Nowlin, 1987). Fossil mounded contourite deposits on the AP Pacific margin suggest that the direction of the

ACC flow has not been consistent over time, but a reversal of the bottom currents occurred during the Miocene (Hernández-Molina et al., 2004, 2006).

Two cyclonic gyres occur on the western and eastern sides of the AP (Figs. 1.16A and 1.17). The Weddell Gyre is a large, elongated cyclone located south of the Antarctic Circumpolar Current (ACC), extending northeastward from the AP (Orsi et al., 1993). The Ross Sea gyre characterizes the circulation on the southwest side of the peninsula (Jaeger et al., 1996; Bindoff et al., 2000; Assmann et al., 2003).
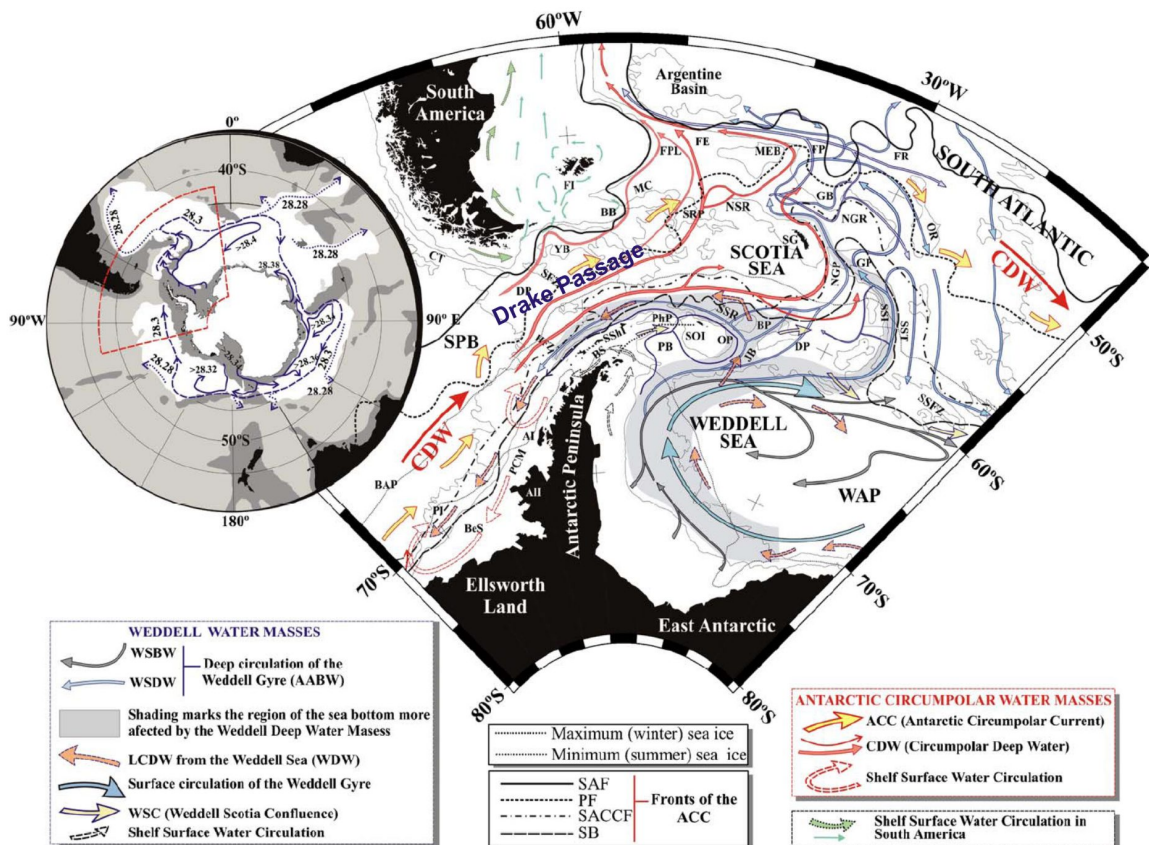

Figure 1.17. Summary of the regional oceanographic dynamics of currents and water masses around the Antarctic Peninsula (from Hernández-Molina et al.,2006).

Deep circulation on the Bransfield Basin is not well established, but hydrographic and hydrodynamic studies in the area indicate that the circulation has a general cyclonic trend, with weak flows directed to the west on the AP margin and the northeast-trending stronger flow of the Bransfield Current on the SSI margin, associated with the Bransfield Front (Grelowski et al., 1986; López et al., 1994, 1999; Gomis et al., 2002). The bottom topography affects the deep flow and creates mesoscale flow structures such as eddies and splitting of the deep flow into different branches (López et al., 1999).

Three distinct water masses have been identified in the Bransfield Basin, reflecting a high influence of the water inflow from adjacent zones (García et al., 2002).

- The warm and fresh Transitional Zonal Waters with Bellingshausen Sea Influence (TBW) are confined to a narrow band in the northern half of the Bransfield Basin.

- The cool, more saline Transitional Zonal Waters with Weddell Sea Influence (TWW) are distributed throughout almost the entire area of the Bransfield Basin and occupy the whole water column in some areas.

- The Bransfield Deep Water (BDW) is the deepest water mass in the CBB. It is the result of the turbulent mixing of waters from the Weddell Sea shelf and the WDW that entrains the basin from the Weddell Sea area. The mixing processes occur in the deep areas of the basin, and the resultant water mass is distributed along the entire basin by spilling over the shallow sills (Wilson et al., 1999).

2.3. Structural setting

The AP is one of the crustal blocks composing West Antarctica (Anderson, 1999). It was once joined to southern South America, together with the islands and submarine ridges now distributed along the Scotia Ridge (Hawkes, 1962; Barker, 2001). The AP and South Scotia Ridge were definitively separated from South America by their southeastward relative movement away from South America and the North Scotia Ridge (Fig. 1.18A) (Barker, 1972). The opening of the Drake Passage started about 29 Ma, allowing the onset of the Antarctic Circumpolar Current circulation at about 23.5-17 Ma (Barker and Burrell, 1977; Barker, 2001). The subduction of the South American ocean floor resulted from a southward migration of the pole of South American-Antarctic plate rotation, modulated by the collision of ridge crest sections of the South American-Antarctic plate boundary with the east-advancing trench (Barker, 2001). Subduction of the Pacific Ocean floor that occurred for at least 150 Ma ended with the collision of the Phoenix-Antarctic ridge crest at the trench, between 6 and 3 Ma and progressively from the southwest to the northeast (Barker, 1982; Larter and Barker, 1991; Barker and Camerlenghi, 2002). A major uplift of the opposing section of the margin followed the Neogene ridge crest-trench collisions for 1-4 Ma, and a period of steady subsidence has continued to the present day (Larter and Barker, 1991).

The BB developed in a complex tectonic setting, after the cessation of the spreading of the Phoenix-Antarctic Ridge (Barker and Burrell, 1977; Jeffers and Anderson, 1990; Barker, 2001; Jin et al., 2002; Galindo-Zaldívar et al., 2004). The opening of the basin began about 3.3 Ma and is related to roll-back processes (Barker and Dalziel, 1983; Larter and Barker, 1991; Maldonado et al., 1994; Galindo-Zaldívar et al., 2004) that resulted in northwestward

migration of the South Shetland Block and the propagation along its SE boundary of structural features associated with the Scotia/Antarctic plate boundary (Galindo-Zaldívar et al., 1996; González-Casado et al., 2000; Galindo-Zaldívar et al., 2004). Regional left-lateral strike-slip motion related to the convergence between the Phoenix and Antarctic plates and ongoing subduction by a rollback mechanism are the main processes that controlled extension in the basin (Fig. 1.18) (Maestro et al., 2007).
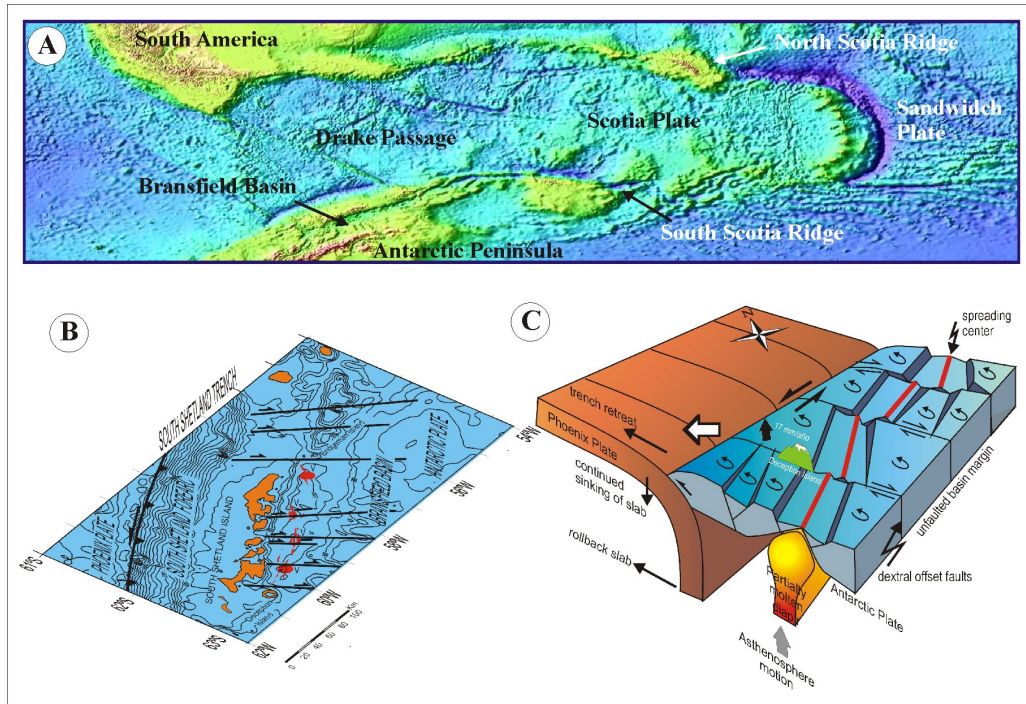

Figure 1.18. A) Structural setting of the Antarctic Peninsula (topographic map from walrus.wr.usgs.gov). B) and C) Scheme of the structural setting of the Bransfield Basin, from Maestro et al. (2007).

The Bransfield Basin is divided into three sub-basins –Western, Central and Eastern– by morphological steps that have been interpreted as the morphological expression of tectonic scarps produced by NW-trending faults (Jeffers and Anderson, 1990; Gràcia et al., 1996; Prieto et al., 1999), or as the result of regional doming in association with the largest submarine edifices (Lawver et al., 1996). The Central Bransfield Basin (CBB) structure is defined by two families of faults, NE- and NW-trending, as the result of the NW extension regime of the basin. It is marked by incipient seafloor spreading, in which the formation of new oceanic crust is related to submarine volcanism (Gràcia et al., 1996; Prieto et al., 1998). The volcanic activity of Deception Island is evidenced by tephra layers in sediment cores, and at least four events have been documented from 6.86 ka to 3.31 ka (Willmott et al., 2006). The northeastwards migration of extensional tectonics, from the AP to the SSI margins, and a left-lateral rotation of the structures, as the result of the oblique subduction of the Phoenix plate and the sinistral strike-slip movement of the South Scotia Ridge, affected the sedimentary infilling on the CBB (Prieto et al., 1998).

24

2.4. Physiography and morphology

The AP Pacific continental margin has a continental shelf located at depths of 400-1000 m that decreases in width towards the northern end. The shelf consists of banks dissected by glacial troughs displaying different orientations and containing numerous basins eroded by distinct ice stream systems (Canals et al, 2000; Camerlenghi et al., 2001; Domack et al., 2006). The continental slope consists of a series of trough mouth fans deposited at the outlets of major ice drainage areas (Larter and Barker, 1989). The continental rise of the AP occurs at depths higher than 1400 and shows major sediment drifts affected by slumping and turbidite currents (Rebesco et al., 1996, 1997; Anderson, 1999; Barker and Camerlenghi, 2002).

The physiography of the CBB is characterized by its asymmetry, with a narrow and steep northwestern SSI margin and a wider southeastern AP margin (Jeffers and Anderson, 1990; Canals et al., 1994; Klepeis and Lawver, 1994; Gràcia et al., 1996; Lawver et al., 1996; Ercilla et al., 1998; García et al., 2006a). The continental shelf reaches depths of about 250 m and is formed by flat banks dissected by SE-NW trending glacial troughs. A second platform deepens from 750 to about 900 m, and a steeper slope connects with the basin floor, which reaches depths of about 1900 m and is characterized by the presence of a linear chain of volcanic edifices (Gràcia et al., 1996; Lawver et al., 1996).

Near-surface morphosedimentary features in the Bransfield Basin are related to recent sedimentary, volcanic and oceanographic processes (Ercilla et al., 1998; Prieto et al., 1998) (Fig. 1.19). The proximal margins are characterized by the presence of paleo-ice streams and bundle structures (Canals et al., 2000, 2002; Willmott et al., 2003; Evans et al., 2004). A basinwards succession of features occur on the margin in relation to the glacial advance, including onshore and coastal erosion, erosion-deposition of glacial and glaciomarine features on the inner shelf, deposition of a continuous till cover with streamlined bundles on the outer shelf, and deposition of a debris apron on the slope and base of slope (Canals et al., 2002). Stratified deposits drape the previous morphologies from the middle parts of the margin to the basin and result from sedimentation from hemipelagic suspension and nepheloid layers. Very irregular furrows occur down to 600-700 m water depth and are related to iceberg scouring processes. The slope is mostly characterized by mass-wasting deposits, including trough mouth fans, valleys and a great variety of instability features (Ercilla et al., 1998; Casas et al., 2004). The most prominent of these features is the Gebra Slide at the eastern part of the CBB, which affects an area of about 160 km^2 down to the basin (Fig. 1.19) (Imbo et al., 2003). The basin is affected by mass transport processes, with the development of gravity flows and turbidity currents. Bottom currents in the basin result in the development of contourites at the foot of the slope. Finally, a series of volcanic edifices are distributed along the axis of the basin, with

a SW-NE direction (Gràcia et al., 1996; Lawver et al., 1996). The development of volcanic edifices has occurred during three volcano-tectonic stages in relation to the seafloor spreading, which include the formation and extension of circular volcanoes, and finally the along-axis propagation of volcanism (Gràcia et al., 1996).
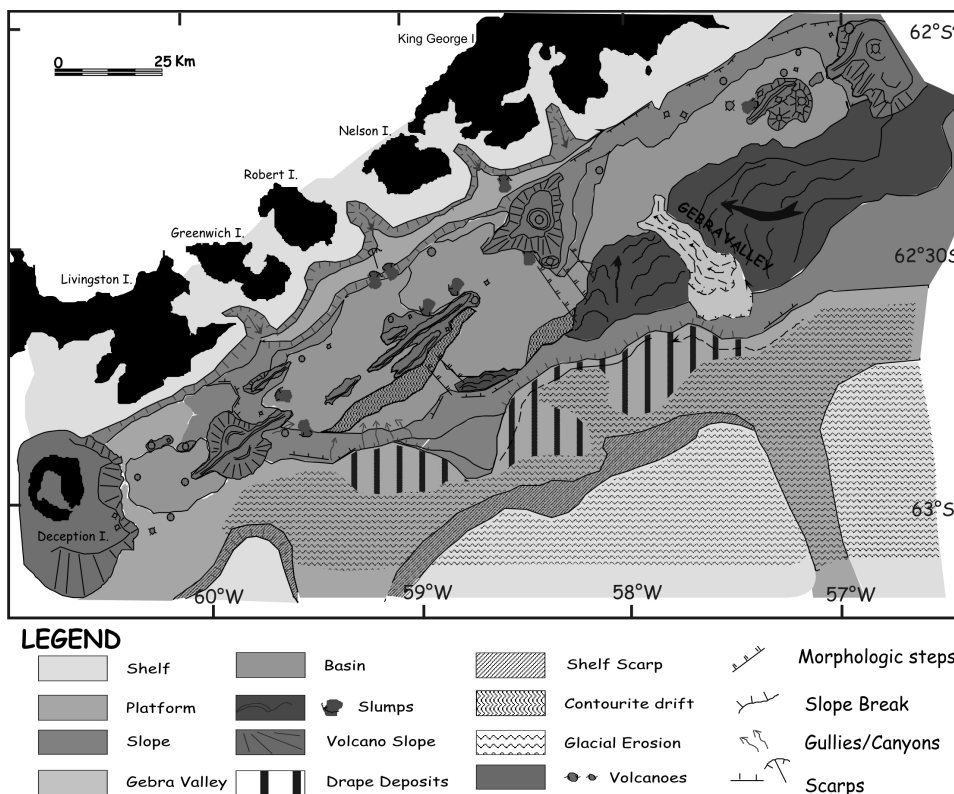

Figure 1.19. Physiographic and morphosedimentary characterization of the Central Bransfield Basin, from Ercilla et al. (1996).

2.5. Stratigraphy

The AP stratigraphy is defined by two units, S2 and S1, of Plio-Pleistocene age (Larter and Barker, 1989). They are mostly progradational (especially S2) and are focused in four lobes of thick prograding foresets and topsets. A seismic stratigraphic study by Bart and Anderson (1995) divides the stratigraphic section into four seismic packages. The oldest one is S4, which occupies almost the entire stratigraphic section on the shelf and is interpreted as being formed prior to and during ridge-trench collisions. S4 is overlaid by three packages: a lower aggradational S3, a middle progradational S2 and an upper aggradational S1, which forms a draping sequence.

The seismic stratigraphy of the CBB has been studied with different resolutions (Table 1.I, Gamboa and Maldonaldo, 1990; Jeffers and Anderson, 1990; Banfield and Anderson, 1995; Prieto et al., 1998, 1999). Two major onlapping stratigraphic units, designated S2 and S1, from older to younger, have been defined on the continental slope and are differentiated by a basinward shift in onlap (Jeffers and Anderson, 1990). These units may be correlated with the

Lower and Upper units of Gamboa and Maldonado (1990), separated by a prominent regional unconformity. S2 and S1 were interpreted as representing two complete third-order glacial/eustatic cycles. The basinal stratigraphic record consists of strong, continuous reflectors that drape units of nearly constant thickness, and packages of weaker discontinuous reflectors that onlap and thin toward the slope. These units are interpreted as a syn-rift sequence and a glaciomarine sequence, respectively (Jeffers and Anderson, 1990).

The structure and stratigraphy of the CBB were studied by Prieto et al. (1998), who identified three tectonostratigraphic units, Tu1, Tu2 and Tu3 (from oldest to youngest) (Fig. 1.20A,B). Tu1 forms a wedge of stratified sediments that occupies the southernmost area system. It onlaps the basement in the onshore direction and downlaps onto it offshore, and is affected by the NE-trending bounding normal faults. Tu1 is interpreted as a syn-rifting unit. Tu2 is composed of packages of stratified facies that onlap Tu1 on the margins and downlap the basement on the basin floor. It extends further northwestwards than Tu1 and essentially fills the intermediate graben system. Tu3 is composed of packages of stratified deposits that onlap Tu2 and the basement. It was identified over most of the CBB, and marks the initiation of the infill of the northernmost area. Tu2 and Tu3 are interpreted as having being deposited in a glacially-controlled sedimentary regime.
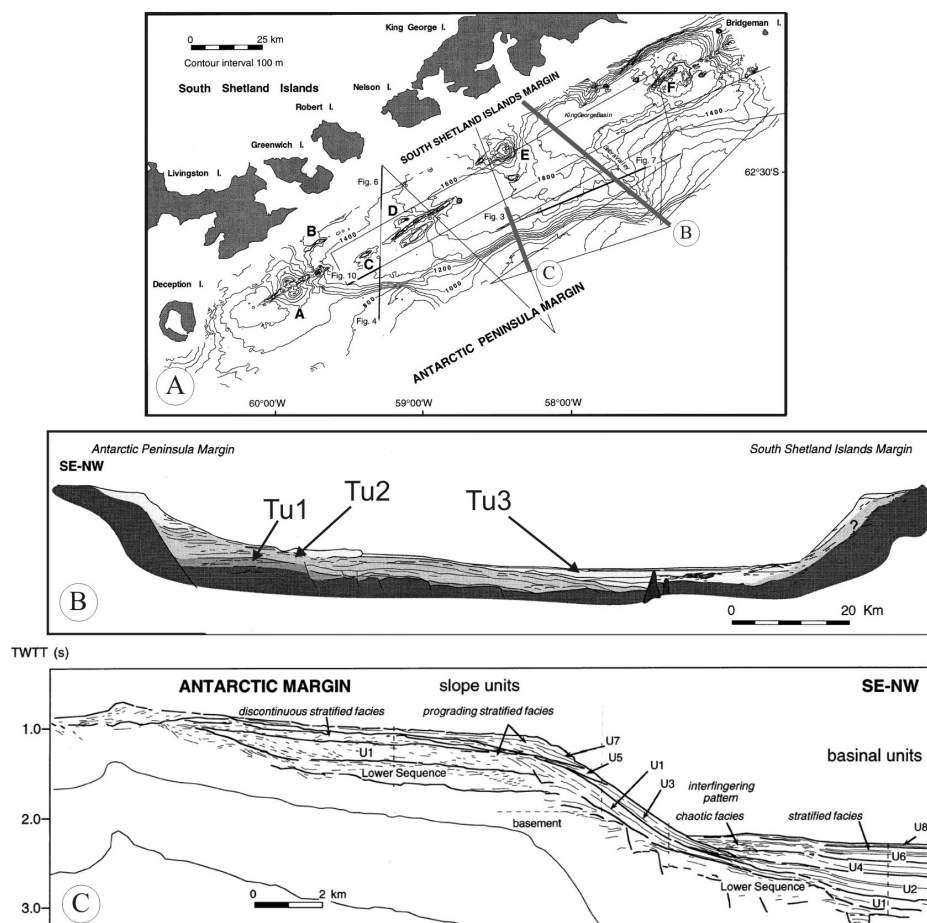

Figure 1.20. Stratigraphic framework of the CBB. A) Map with the location of the seismic lines shown in B and C. B). Sketch showing the three tectonostratigraphic sequences Tu1, Tu2 and Tu3 (from Prieto et al., 1998). C) Line drawing of the slope and basinal units. From Prieto et al., 1999).

Finally, Prieto et al. (1999) studied a larger seismic dataset, which led to the recognition of additional stratigraphic units within the Upper Sequence (Table 1.I). They interpreted the overall stratigraphic package as being composed of two main sequences, Lower and Upper, overlying the deformed acoustic basement (Fig. 1.20A,C). The Lower Sequence onlaps the basement onshore and downlaps it offshore. It is interpreted as a syn-rift sequence, deposited after the initial fragmentation, rotation, subsidence and extension of the continental basement blocks. The Upper Sequence is interpreted as a post-rift sequence. It is composed of eight seismic units, including four slope progradational units and four basinal aggradational units. Slope progradational units form sedimentary wedges extending from the slope platform edge and are interpreted as diamicton and debris flow deposits along the grounding line during the glacial periods. In contrast, basinal aggradational units fill the basin floor and their acoustic character changes from proximal chaotic and undulated seismic facies to stratified facies. They are interpreted as being formed by meltwater processes and sediment-laden underflows during the interglacial periods (Prieto et al., 1999).

Larter and Barker (1989)	Gamboa and Maldonado (1990)	Jeffers and Anderson (1990)	Prieto et al. (1998)	Prieto et al. (1999)	
S1	Upper	S1	Tu3	Upper	Basinal aggrading and slope prograding units
			Tu2		
S2	Lower	S2	Tu1	Lower	

Table 1.I. Correlation between the different stratigraphic studies carried out in the AP and the CBB.

2.6. Recent sedimentation

Sedimentation on the CBB shows several cycles of advance and retreat of the West Antarctic Ice Sheet since its opening (Jeffers and Anderson, 1990; Banfield and Anderson, 1995; Prieto et al., 1999; García et al., 2006b). Several studies have approached the study of sedimentation during the last glacial cycle, which is characterized by the ice sheet advance along the margin and the grounding zone advance reaching depths of about 900 m during the Last Glacial Maximum, LGM (Banfield and Anderson, 1995; Bentley and Anderson, 1998).

Banfield and Anderson (1995) identified seven lithofacies in the CBB, ranging from mud to pebbly sand with different contents of volcanic ash layers and disseminated volcanic ash, diatoms and pebbles, and pebbles with sand, mud and volcanic ash matrix.

Three stratigraphic units have been identified in the CBB margin, representing the sedimentation during the Holocene period (Yoon et al., 1997, 2002; Heroy et al., 2008). The

older unit is of subglacial origin, and consists of over-compacted diamicton. The second unit is of glacial proximal/sub-ice shelf origin and is characterized as a pebbly sandy stratified mud unit. The recentmost unit is interpreted as open marine and is composed of diatomaceous mud. Two significant tephra layers are related to volcanic episodes from Deception Island at 3870 and 5500 cal yr BP.

Recent sedimentation in the deep CBB basin is represented by olive clayey hemipelagic silts with different degrees of centimetric to millimetric parallel laminations (Fabrés et al., 2000). This hemipelagic sediment is interpreted as being composed of planktonic-derived sediment and terrigenous sediment from subglacial discharge from tidewater glaciers, overflow plumes, ash-rich layers and IRD.

2.7. Climatic history

The studies related to the stratigraphy, morphology and sedimentation have allowed the climatic history of the AP to be reconstructed. Glaciations on the AP and SSI have been documented to occur at least since the Early Oligocene, ~30 Ma (Dingle and Lavelle, 1998). This age is younger than the ~34 Ma considered for the onset of glaciations in other areas of Antarctica (O'Brien et al., 2001).

During the Late Miocene, the AP underwent a major cooling and glaciation, as indicated by biogenic opal records (Hillenbrand and Fütterer, 2001) and ^{18}O concentrations (Miller et al., 1991). The glacial conditions translated into the ice mass growth and ice sheet advances to the outer continental shelves of the Peninsula (Larter and Barker, 1991).

During the Pliocene several climatic oscillations characterized the climatic regime, with glacial advances and retreats that were recorded as prominent glacial unconformities on the continental shelves (Larter and Cunningham, 1993; Bart and Anderson, 1995). A warm climatic regime during the Early Pliocene (3.2–4.5 Ma) with open ocean conditions during glacial stages (Hepp et al., 2006) is suggested by high productivity values that indicate the retreat of the ice (Hillenbrand and Fütterer, 2001). The presence of ice-rafted debris implies that the AP was not deglaciated for any significant period during the "warm Pliocene". During the Pliocene-Pleistocene boundary a major cooling event took place in Antarctica (Anderson, 1999; Barker and Camerlenghi, 2002). The climatic deterioration is suggested by a productivity decrease (Hillenbrand and Fütterer, 2001) and ocean $\delta^{18}O$ values that suggest a transition from terrestrial ice margins to marine-based ice sheets (Raymo et al., 2006). A change in the stratigraphic architecture along the Pacific margin of the AP, from progradational to aggradational/progradational, has been associated with this event and interpreted as the result of a change in the character of the ice sheet, from more temperate to more polar (Rebesco et al., 2006).

The mid-Pleistocene is marked by a change in the strength and frequency of glacial-interglacial cyclicity (Cowan, 2001). A change from strong 41-ka frequency cycles to 100-ka cycles at 1.0 Ma is suggested by $\delta^{18}O$ records (Raymo et al., 2006).

After the glacial Late Pleistocene, the climatic record comprises four climatic intervals (Domack, 2002). These intervals were established in the Palmer Deep in an inner shelf trough on the Pacific margin of the AP, and are the following:

- During the Deglacial interval (~13.2-11.5 ka) ice-proximal conditions resulted in deposition of varves reflecting the intercalation of diatom ooze and siliciclastic-rich diatom mud (Leventer et al., 2002).

- The Climatic Reversal stage (11.5-9.07 ka) is indicated by enhanced terrigenous deposition, massive turbidite activity and diatom assemblages corresponding to persistent sea ice (Taylor and Sjunneskog, 2002).

- The Holocene Climatic Optimum (9.07-3.36 ka) can be divided into two phases, with a cooling interval from ~7–5 ka (Sjunneskog and Taylor, 2002; Taylor and Sjunneskog, 2002). Reduced sea-ice formation is indicated by high accumulation rates of diatoms and benthic foraminifers (Osterman et al., 2001). On the outer shelf of the AP the Climatic Optimum has been dated at 6–2.5 ka, based on sedimentological and diatom evidence (Yoon et al., 2002).

- Finally, the onset of the Neoglacial interval occurred at 3.36 ka in Palmer Deep (Domack, 2002). Changes in the surface water productivity indicated by diatom assemblages suggest the major role of fluctuating water masses, with increased meltwater stratification of the shelf water and expansion of sea ice conditions (Osterman et al, 2001).

The Late Pleistocene-Holocene studies based on sediment cores recovered from the Bransfield Basin reflect the climatic history after the last ice sheet retreat, dated at 17340 cal yr BP, and includes three stratigraphic units (Heroy and Anderson, 2005, 2008). The older subglacial unit is composed of diamicton deposited as subglacial till. This unit is overlaid by a pebbly sandy stratified mud unit which is interpreted as being deposited in a sub-ice shelf environment. The most recent unit is composed of diatomaceous mud and is interpreted as being deposited in an open-marine environment. Five climatic regimes of minor scale have been inferred from diatom assemblages (Heroy and Anderson, 2008).

- During the Deglacial period (>9 ka) a sub-ice shelf environment dominated the Bransfield Basin, with restricted open ocean circulation.

- During the early to mid-Holocene (about 9-6.8 ka) the ice shelf retreated and the present-day oceanographic circulation patterns started to develop.

- The mid-Holocene Climatic Optimum that occurred at about 6.8-5.9 ka and was characterized by the improved climatic conditions, rapid melting of sea ice and stabilization of the water column. This interval is shorter in the Bransfield Basin than in other areas of the AP.

- During the mid- to late-Holocene (about 5.9-2.6 ka) colder water masses entrained into the Bransfield Basin and the sea ice cover was increased.

- Finally, the Neoglacial (about 2.6 ka to present) was characterized by frequent storm events and decreased water column stratification in an open marine environment.

II. Methodology and dataset

1. Oceanographic cruises and dataset

The dataset studied in this work was obtained during two oceanographic cruises (GEBRA93 and MAGIA99) and comprises seafloor multibeam maps, single-channel reflection seismic profiles of different resolution, and sediment cores in the CBB area (Figs. 2.1 and 2.2, Table 2.I). Also, the regional bathymetric map published by the Polish Polar Academy of Sciences (1990) and swath bathymetric data provided by the Marine Geoscience Data System (available online, http://marine-geo.org) have been used.

Swath bathymetry data were obtained with the Simrad EM12 and EM1000 multibeam echosounder, covering an area of about 17.000 km^2 of seafloor (Fig. 2.1C). This system operated with 81 beams working at a frequency of 13 kHz, and a pulse length of 2-10 ms. Navigation was with a Global Positioning System (GPS).

Very high-resolution seismic profiles used in this work were obtained with a Simrad topographic parametric sonar (TOPAS) operating at a frequency range of 4-2 kHz. High-resolution single-channel seismic profiles were collected using four 40 in^3 sleeve-guns, arranged at a depth of 3.5 m and with a shot frequency of 8 s. The penetration of the acoustic signal was 2-3 s TWTT, and the resolution was tens of meters. Data were acquired with a SIG streamer of 150 m of active section, including three independent channels with 40 hydrophones each. A GeoAcoustics Sonar Enhancement System (SES) was used for data acquisition and processing. Sampling frequency was 1 ms and the recording window was from 4 to 8 s. Sediment gravity cores with a maximum length of 3 m were recovered during the MAGIA99 cruise. The drilling sites were selected based on the seismic and bathymetric data, covering depths between 285 and 1940 m.

2. Multibeam bathymetric data

Multibeam echosounders are based in the emission of a series of acoustic pulses directed towards the seafloor and arranged in fan of narrow acoustic beams (Fig. 2.3). The main advantage of this system is that it provides a 100% of coverage of the seafloor, and therefore the resulting seabed maps are more detailed than those obtained using single-beam mapping. The maps are also produced faster, reducing ship survey time. In addition to the soundings, the multibeam echosounders produce seabed image data similar to a sidescan sonar image, with information of the backscattering seafloor signal, which can be used for characterizing the seabed material properties and sometimes for detecting small features not visible in the sounding data. Multibeam echosounders are connected to positioning equipment, heading and motion sensing instruments, as well as sound velocity sensors in order to position the soundings correctly.
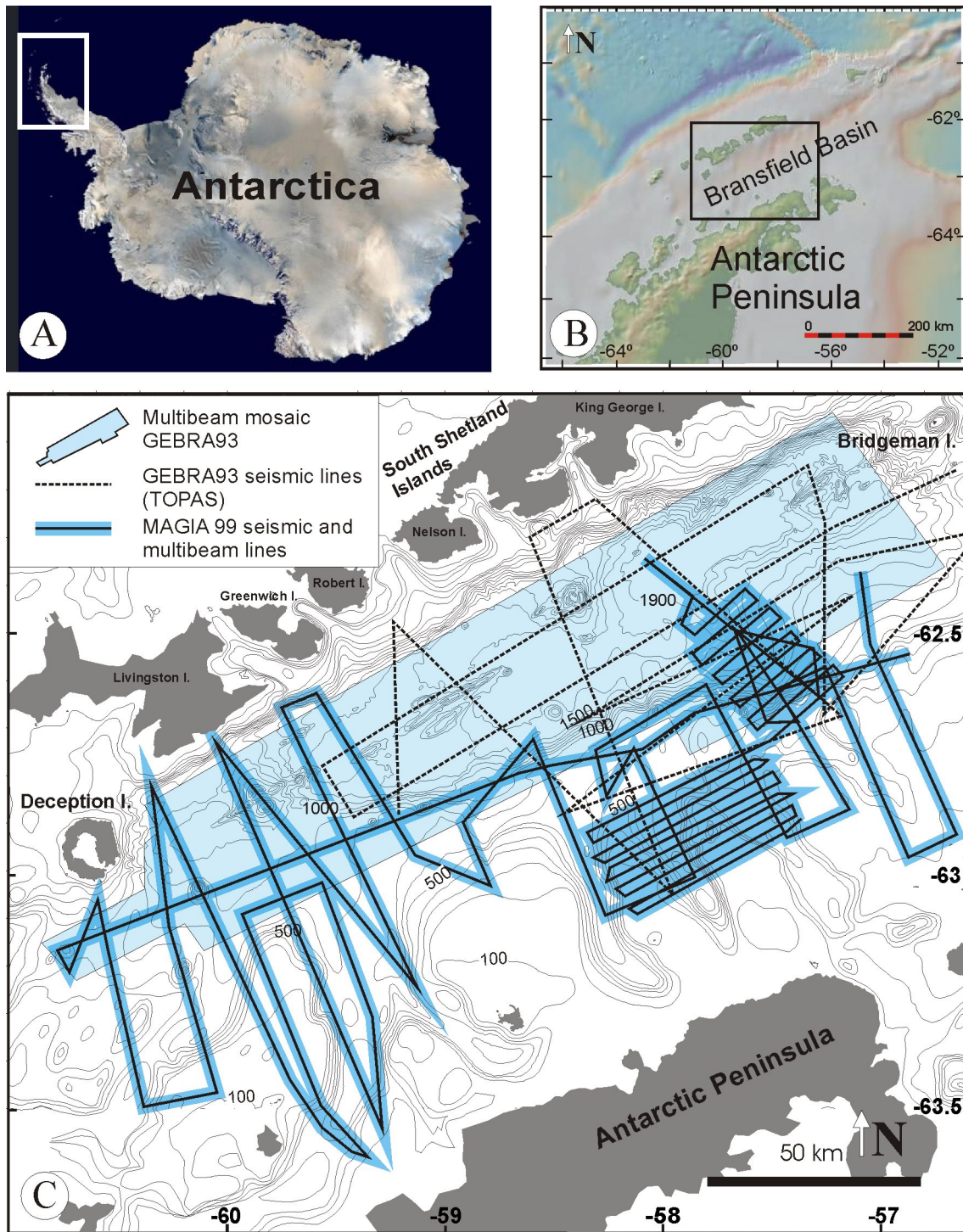
Figure 2.1. A) and B) Location of the study area. C) The dataset studied in this thesis includes a multibeam bathymetric mosaic and different resolution single-channel reflection seismic profiles and multibeam lines obtained in the CBB during the GEBRA93 and MAGIA99 geological cruises.
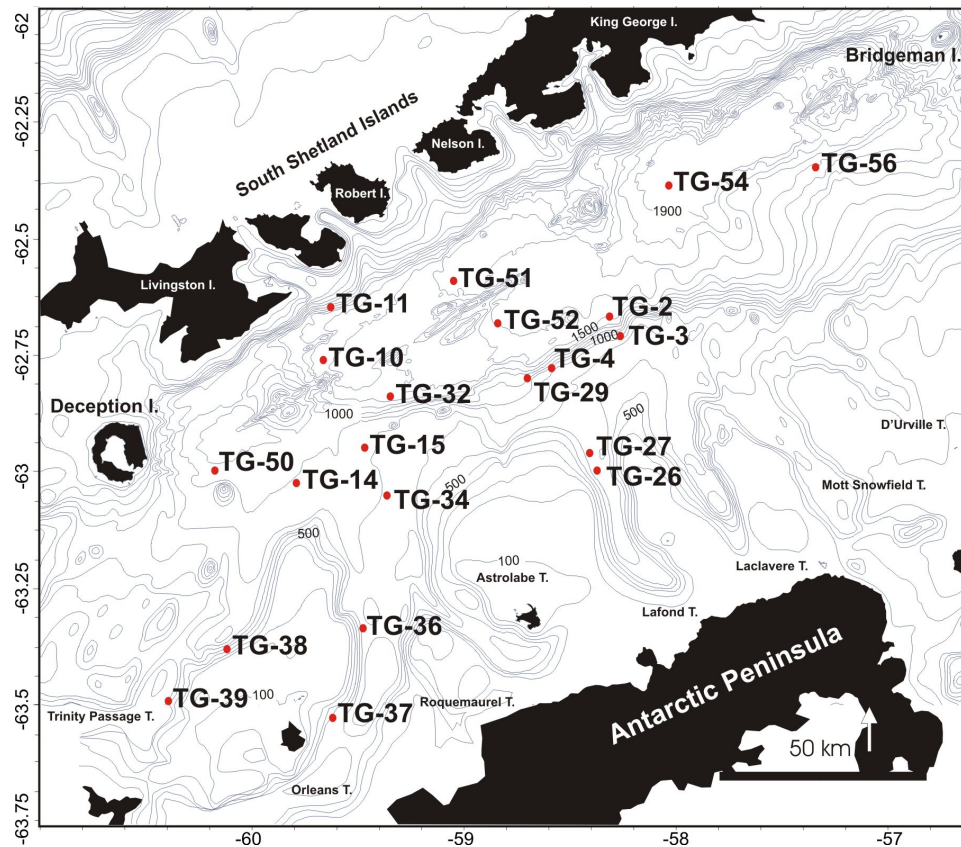
Figure 2.2. Location of the sediment gravity cores studied in this work. Sediment cores were recovered from the different physiographic and sedimentary environments of the CBB.

Core	Length (cm)	Latitude	Longitude	Water depth (m)	Core	Length (cm)	Latitude	Longitude	Water depth (m)
TG2	148	-62.6501	-58.3209	1575	TG34	264	-63.0337	-59.36	765
TG3	84	-62.6912	-58.2742	1200	TG36	300	-63.319	-59.4777	864
TG4	230	-62.7611	-58.5905	1200	TG37	232	-63.5071	-59.610	822
TG10	209	-62.744	-59.6561	1366	TG38	295	-63.363	-60.1052	1053
TG11	268	-62.6296	-59.6215	790	TG39	214	-63.4745	-60.3799	684
TG14	261	-63.0062	-59.7804	903	TG50	83	-62.981	-60.1616	965
TG15	250	-62.9319	-59.4631	880	TG51	265	-62.5743	-59.048	1548
TG26	220	-62.9779	-58.3796	806	TG52	324	-62.6646	-58.8403	1625
TG27	250	-62.9418	-58.4119	755	TG54	76	-62.3695	-58.0463	1930
TG29	120	-62.7827	-58.7051	1200	TG56	240	-62.3303	-57.36	1500
TG32	151	-62.8216	-59.3435	1391					

Table 2.I. Summary of the sediment cores studied in this thesis, including their denomination, core length, location and water depth. See cores location in Fig. 2.2.

Multibeam data are displayed in real-time on board, and afterwards they are processed to apply calibrations and corrections. After structuring and formatting data, they are stored and processed with NEPTUNE and CARAIBES softwares and Surfer and Fledermaus softwares for the production of bathymetric maps, topographic profiles, backscattering imagery and different types of terrain digital models (Fig. 2.3).
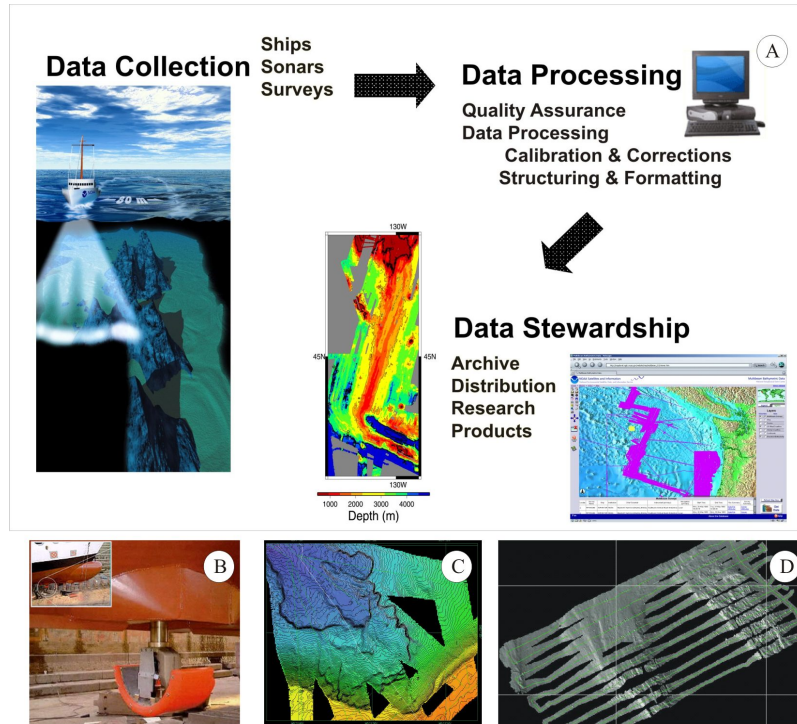

Figure 2.3. A) Scheme of the multibeam operations, from the data recovery during geological cruises to the elaboration of the final products. B) Multibeam sounders mounted under the hull of the vessel. Examples of a bathymetric mosaic (C) and shaded mean depth relief map (D).

3. Geophysical methods

3.1. TOPAS

The TOPAS system transmits two primary acoustic signals of 15 and 18 kHz that interfere with the water column generating a secondary signal of low frequency (0.5-5 kHz), providing a good vertical resolution of the upper 50-80 m of the sediment column (Webb, 1993). The TOPAS system may work with different types of pulse shapes (simple pulse, continuous wave and chirp modes). The main advantage of this system is that it provides a narrow (generally from 3º to 7º) low frequency beam from a reduced transducer surface. The system provides a stabilized acoustic beam by the application of pitch, roll and heading corrections. Generally, the TOPAS system includes a real-time processing and presentation of the raw and processed data in a monitor. These data may also be printed and stored in the adequate digital formats or their posterior processing and analysis.
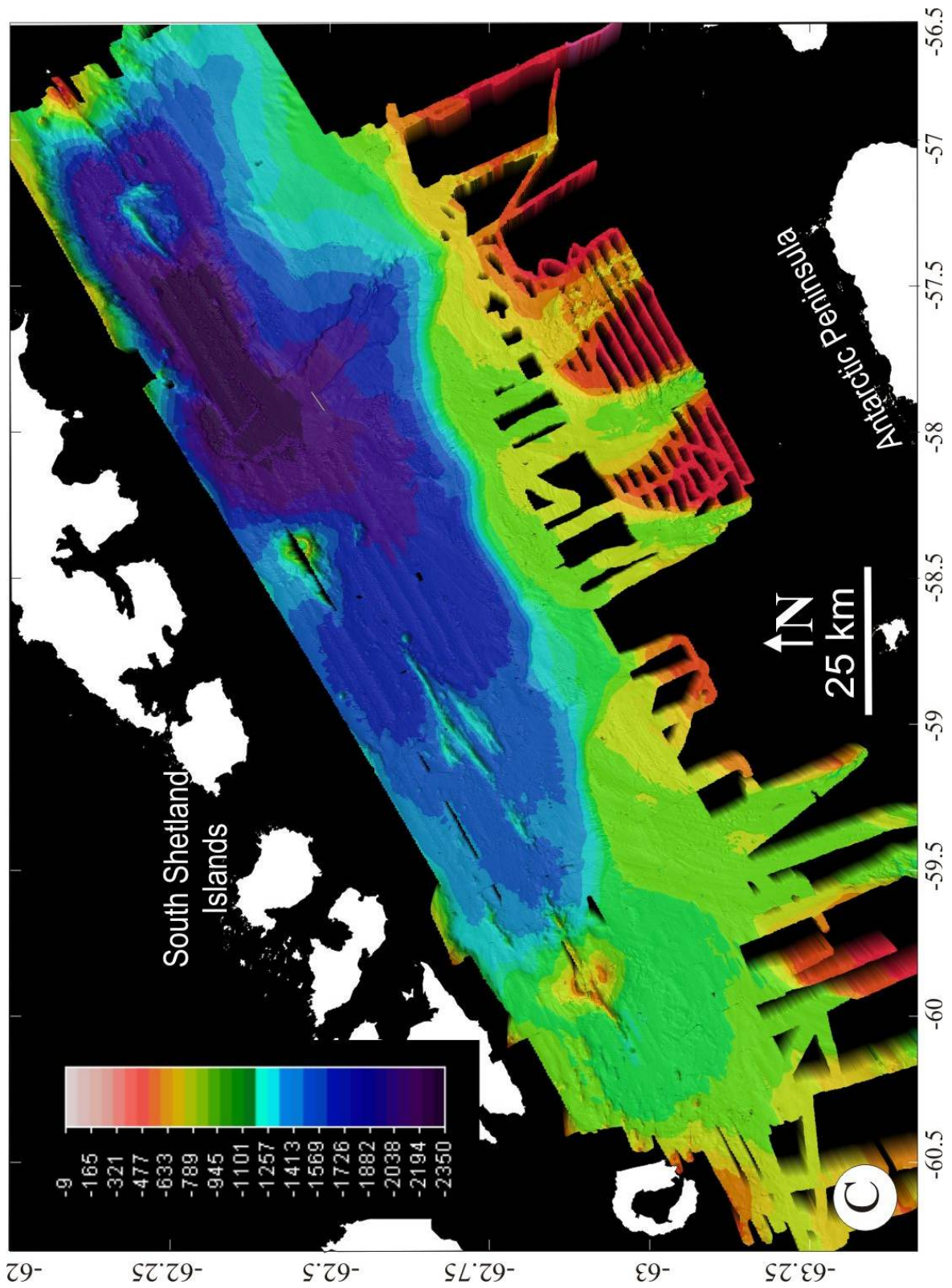
Figure 2.4. Bathymetric mosaic of the CBB obtained from the data obtained during the GEBRA93 and MAGIA99 cruises.
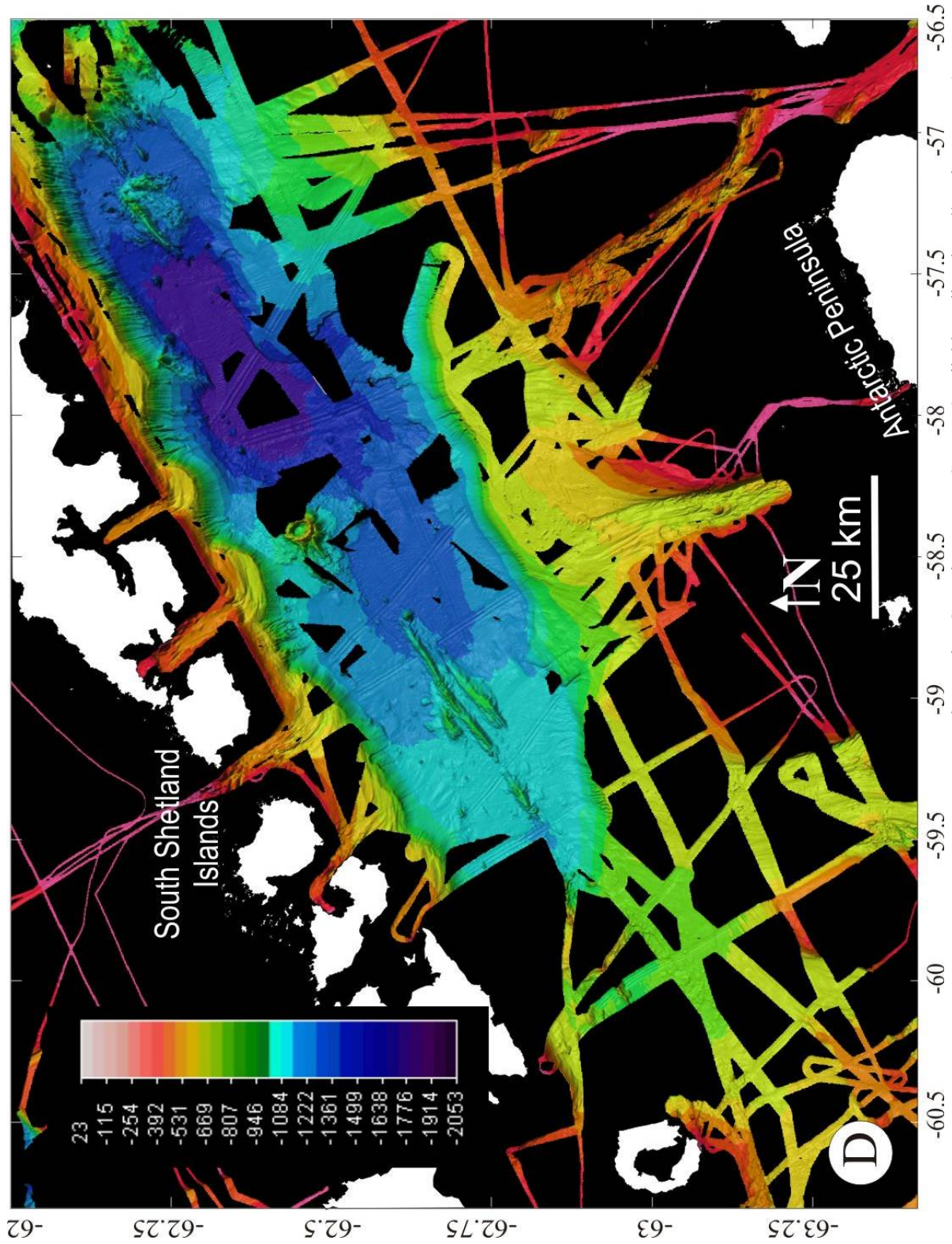
Figure 2.5. Bathymetric mosaic obtained from the data provided by the Marine Geoscience Data System (available online, http://marine-geo.org).

3.2. Airgun systems

In the airgun system the seismic sources are one or more pneumatic chambers that are pressurized with air. The airgun array is submerged below the water surface to 1.5 m water depth, and is towed behind the vessel. When the airgun is fired, a bolt is retracted, allowing the air to escape the chamber and to produce a pulse of acoustic energy. The reflected pulse is received in hydrophones displayed in a SIG streamer. The resultant seismic signal is then registered and recorded. Real-time raw data may be displayed in monitors and may also be printed on board in EPC and Dowty printers. The recorded raw data are processed to apply different types of corrections and filters.

3.3. Stratigraphic analysis

The visualization and interpretation of the seismic data were made with the aid of the Kingdom Suit software Version 8.0 (Seismic Micro-Technology, http://www.seismicmicro.com). This software allows picking horizons, correlating different seismic profiles and calculating surfaces and isopachs. It also provides visualization tools that help to get a better spatial understanding of the stratigraphy. Contour maps of isopachs were made with the Surfer software.

Seismic stratigraphy aims the identification of genetic sedimentary units and sequences, and their interpretation is done in terms of geochronological correlations, thickness, depositional environments, paleotopography, paleogeography and geologic history (Vail et al., 1977). The interpretation of seismic data is approached by the determination of seismic sequences and units and the analysis of seismic facies (Vail et al., 1977a,b; Vail, 1987; Posamentier et al, 1988; Van Wagoner et al., 1988; Vail et al., 1991).

Seismic sequences and units are defined by the subdivision of the seismic section in groups of deposits limited by discontinuities and formed by reflections of similar characteristics. Seismic sequences are defined as depositional sequences identified in a seismic section, and seismic units are groups of genetically-related reflections, limited by discontinuities and their correlative continuities, within the seismic sequences (Mitchum et al., 1977a).

The seismic facies analysis consists on the characterization of the seismic units in function of their acoustic response and geometry. This analysis includes the characterization of the reflections terminations (baselap –downlap and onlap-, concordance, toplap, erosive truncation, structural truncation), the definition of the internal reflections configuration, the classification of the reflections acoustic character and the outline of the external morphology (Mitchum et al., 1977b; Damuth, 1980; Vera et al., 1994). The study of the seismic facies allows the interpretation of the depositional environments and systems, deducing the energy

of the environments, lithology, sediment supply, sediment dispersion, paleogeographic and paleoceanographic reconstructions and the geological emplacement of the seismic units (Mitchum et al., 1977b; Vera, 1994).

4. Sampling methods

4.1. Gravity corer

The gravity corer is composed of a 3 m steel drilling pipe attached to a weight (Fig. 2.6A). They are linked by coupling sleeves and terminated by a core catcher system. The lead weight is hanging from a lever arm that counterweights the corer with a cable. The landing of the counterweight releases the lead weight and the corer falls by gravity to drill the near-surface sediment (Fig. 2.6B). Inside the coring pipes, a PVC liner is placed to recover the sedimentary column.
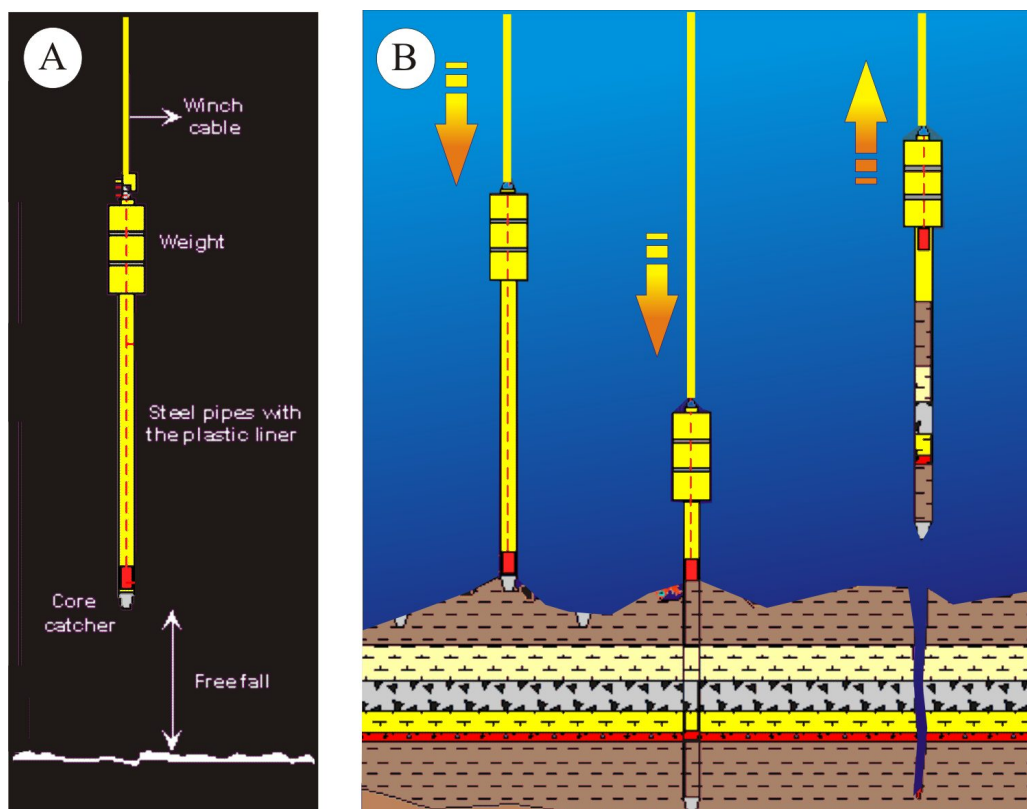

Figure 2.6. A) Scheme of the parts that compose a gravity corer. B) Scheme of the operation of a gravity corer (modified from http://www.mnhn.fr).

4.2. Sedimentological analyses

Once onboard, the cores were capped, wrapped in cheesecloth, coated with parafin and stored on board at 4ºC. In the laboratory, cores were opened and photographed with a 35 mm reflex camera, with a fixed objective of 50 mm (Fig. 2.7). The following sedimentological analyses have been carried out on the sediment samples: grain size, sand fraction composition,

carbonate content and electronic microscope imagery. X-ray technics and physical analyses were also applied to the sediment core sections (Figs. 2.8 to 2.11).
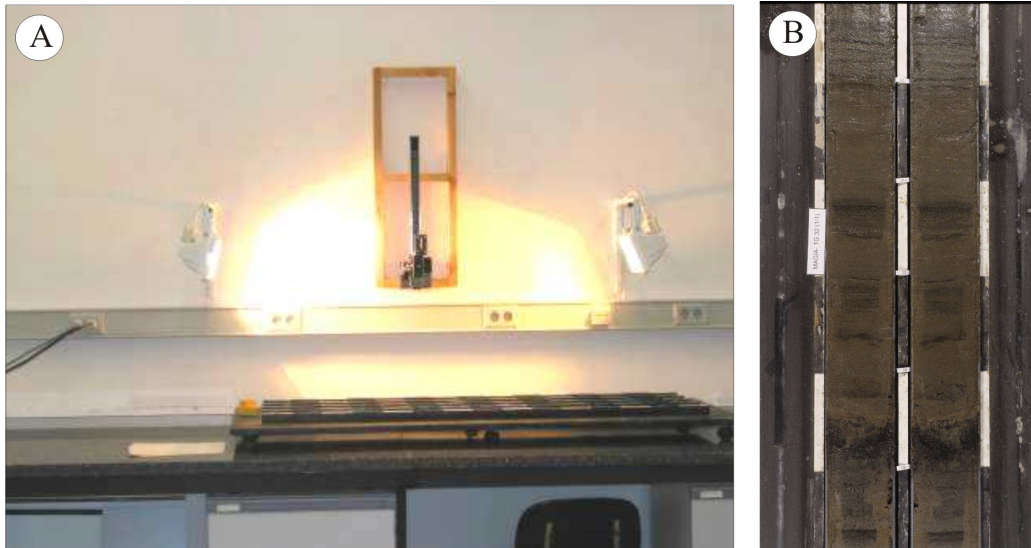

Figure 2.7. A) Equipment for core photography in the Institute of Marine Sciences (ICM-CSIC). B) Example of the photograph of a sediment core.

4.2.1. Grain size analysis

The grain-size distribution provides information on the texture of the depositional system and on the type and competency of the processes operating in the system. Grain size analysis of selected sub-samples was conducted using a hand sieve and settling tube for the greater than 50 micron fraction and by the Sedigraph prodedure (Micromeritics model 5100) for the <50 µm fraction (Fig. 2.8). Sand fraction and very coarse silt components (>50 µm) were identified using a binocular microscope, and relative abundances of components were estimated
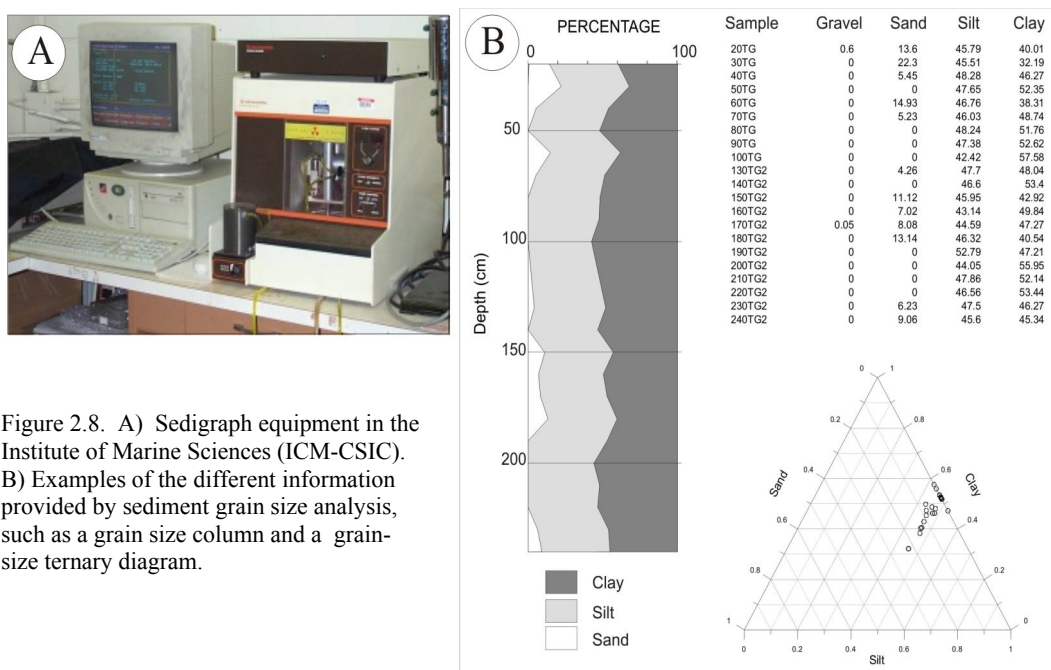

Figure 2.8. A) Sedigraph equipment in the Institute of Marine Sciences (ICM-CSIC). B) Examples of the different information provided by sediment grain size analysis, such as a grain size column and a grain-size ternary diagram.

43

4.2.2. Carbonate content

The carbonate content was obtained using a calcimeter of Bernard (Vatan, 1967). This system is based in the chemical reaction of chloridric acid with the carbonate of the sample, with the loosening of carbonic anhydride. This gas displaces a volume of an indicator liquid (sodium chloride-saturated water, acidulated water or oil) that is quantified and used to calculate the carbonate content.

4.2.3. Physical properties

Physical properties were obtained using a GEOTEK Multi Sensor Core Logger (MSCL) which measures bulk density (by Gamma Ray Attenuation) and magnetic susceptibility (MS) at 1 cm interval (Fig. 2.9). Bulk density is a measure of the weight of the sediment per unit volume (g/cc) and it depends of the relative proportion and specific gravity of solid organic and inorganic particles and to the porosity of the sediment. It is estimated from the attenuation suffered by gamma-rays passing through the sediment (Evans, 1965; Tittman and Whal, 1965). MS measures the degree to which a material can be magnetized in an external magnetic field (Blum, 1997) and has been classically used as a proxy for the concentration of magnetic minerals. MS is measured using a Bartington loop sensor.
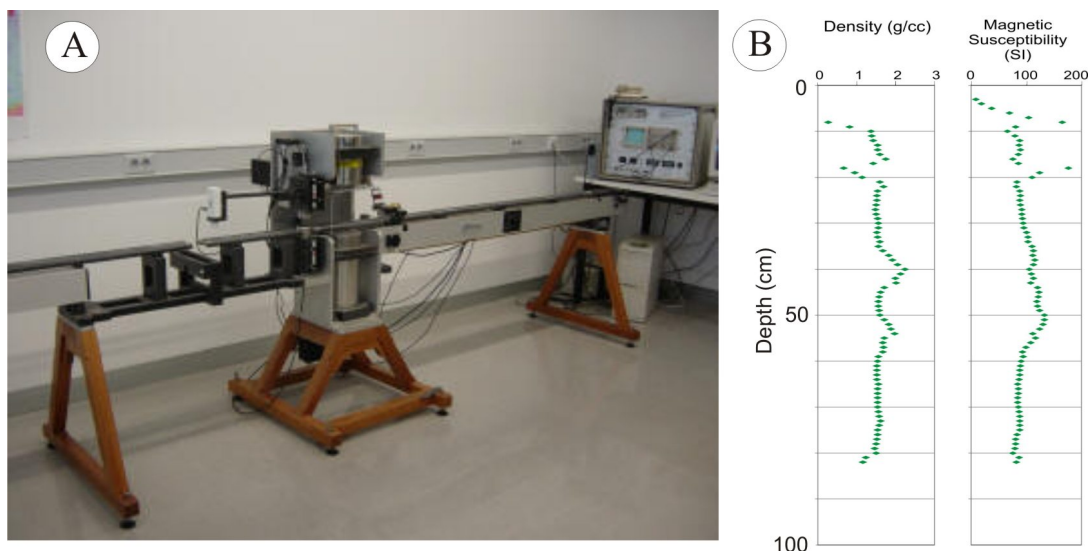

Figure 2.9. A) Multi Sensor Core Logger equipment in the Institute of Marine Sciences (ICM-CSIC). B) Example of the data obtained from the MSCL.

4.2.4. X-Ray images

X-ray images were made in the Veterinary Clinic Hospital of the Universitat Autónoma de Barcelona with a Sedecal APR-VET equipment. The equipment was used with a voltage of 45 kVp and energy of 300 mAs. A software application was applied to the X-radiography images to enhance the signal and improve the visualization of detailed sedimentary structure and disturbance features (Fig. 2.10).
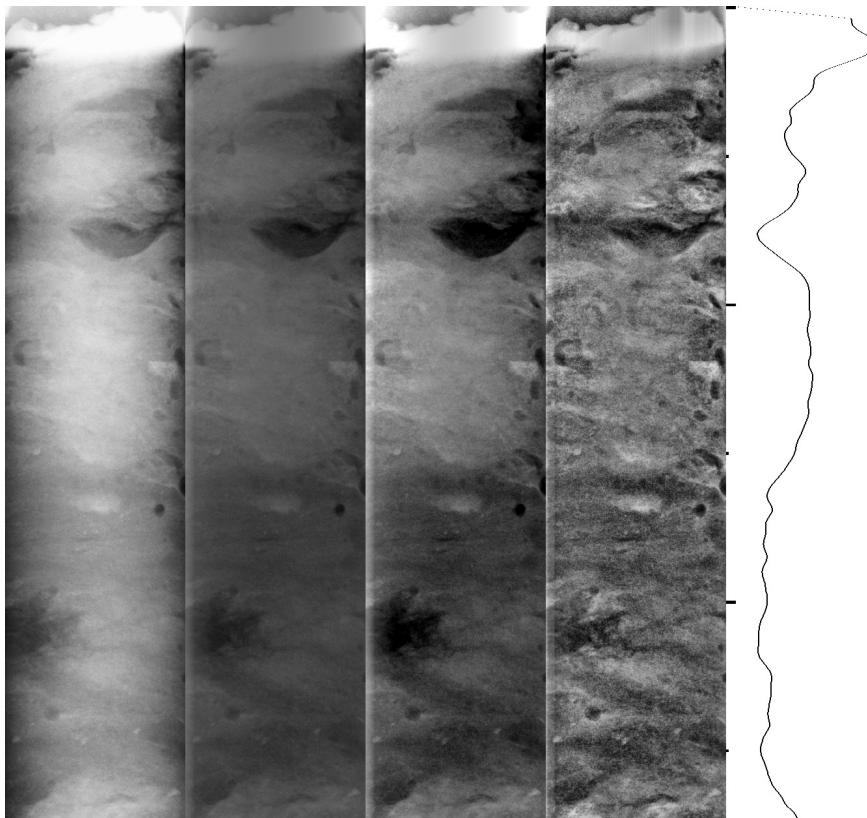
Figure 2.10. Example of a X-radiography of a sediment core and the treated images that enhance the contrast to improve the visualization of structures and features within the sediment.

4.2.5. Scanning Electronic Microscope

Samples were treated for the Scanning Electronic Microscope (SEM) imaging (Fig. 2.11). After separating the finer fraction of sediment samples by sieving, samples were filtered in policarbonate filters of 0.8 µm pore. The dry filters were fixed in the microscope support with a conductive adhesive tape. They were sputtered with a 200 Å of gold-paladium film, with the Polaron SC500 system. A Hitachi S3500N SEM system with variable pressure that allows microscopy of wet, oily and non-conductive samples was used to obtain very high resolution images of the sediment samples. This system produces a magnified image by using a beam of electrons instead of light rays, as in an optical microscope. An electron lens is an arrangement of electromagnetic coils that control and focus the beam. Electrons are detected in a fluorescent screen or a photographic plate on which the electrons form an image. The wavelength of the electron beam is much shorter than that of light, so much greater magnification and resolution (ability to distinguish detail) can be achieved. The system was operated with accelerating voltage of 5 kV.
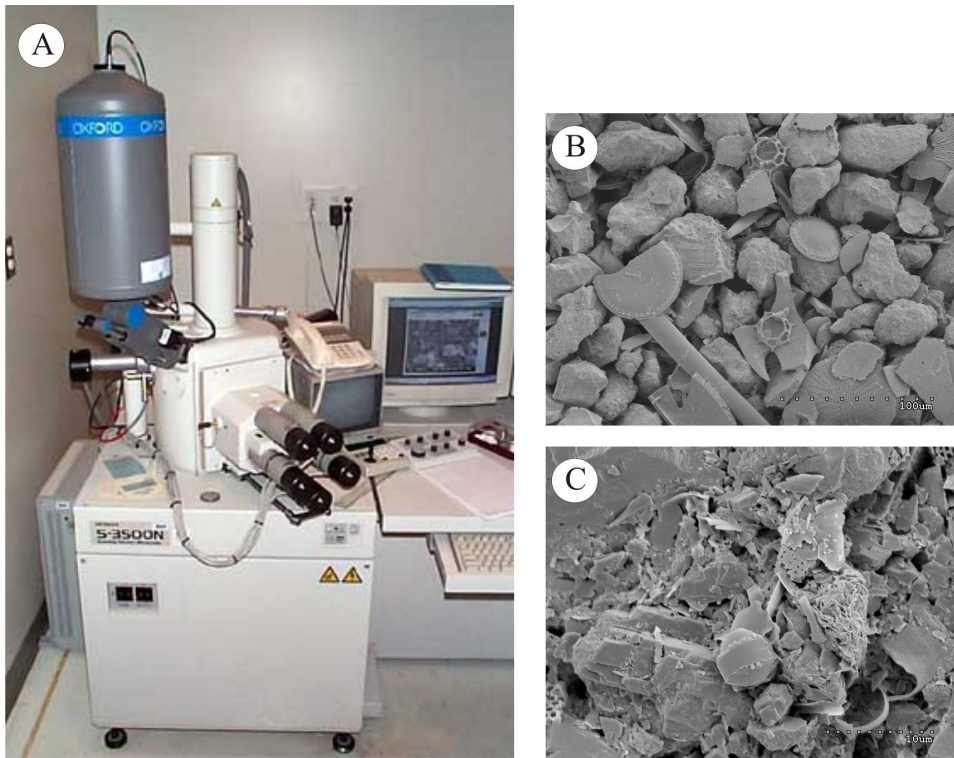
Figure 2.11. A) Scanning Electronic Microscope equipment in the Institute of Marine Sciences (ICM-CSIC). B) and C) Example of the images obtained from the fine fraction of the sediment samples.

III. Physiography, morphology, recent sedimentary systems and their dynamics

1. Introduction and methodology

This chapter is focused on the identification, classification and analysis of the wide variety of morphological features of the CBB. The present-day morphology of the study area reflects the sedimentary processes occurring during the last glacial/interglacial cycle, because the relative scarcity of postglacial sediment supply in the CBB since the Last Glacial Maximum (LGM) has allowed the preservation of these features (Canals et al., 2002).

Several studies have presented a general (Ercilla et al., 1998; Prieto et al., 1999) or local (Canals et al., 2002) overview of the near-surface features and geological processes and their controlling factors (Jeffers and Anderson, 1990; Banfield and Anderson, 1995; Prieto et al., 1998, 1999; García et al., 2006a,b). However, detailed regional studies that tackle the most recent sedimentary evolution of the basin and the relationships between the controlling factors are still lacking. This detailed morphological characterization allows:

- Integrating different features in sedimentary systems, based on their distribution, spatial linkages and sedimentary processes;

- Establishing the linkages between the sedimentary systems, in order to analyze the complex interplay among processes acting within the entire shelf-to-basin sediment distribution systems; and

- Analysing the controlling factors that govern the recent sedimentary evolution and proposing sedimentary models for the AP and SSI margins and a reconstruction of the sedimentary processes during the last glacial cycle.

For this purpose, the studied dataset includes high-resolution swath bathymetry maps and high- and very high-resolution seismic reflection profiles obtained during the GEBRA 93 and MAGIA 99 cruises. This study also integrates the regional bathymetric map published by the Polish Polar Academy of Sciences (1990) and the multibeam bathymetric dataset provided by the Marine Geoscience Data System (available online, http://marine-geo.org) (Fig. 3.1).
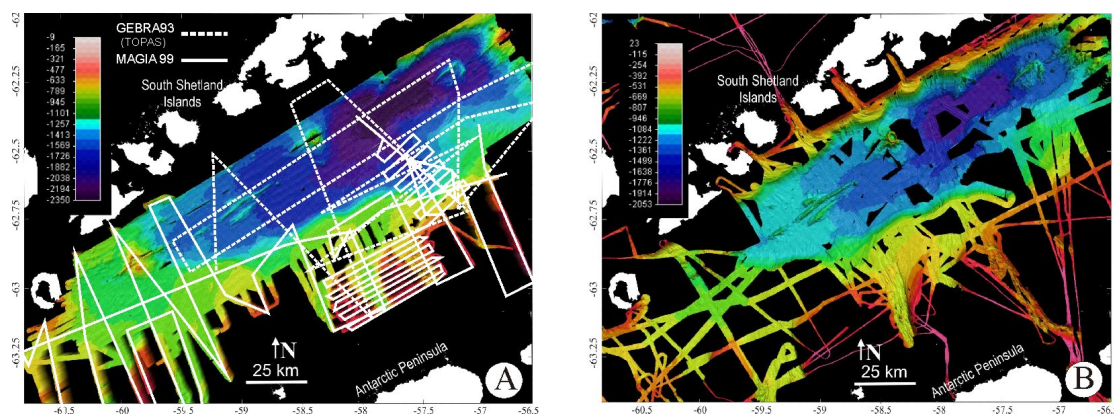

Figure 3.1. Dataset studied in this work. A) Seismic lines (TOPAS and airgun) and multibeam surveyobtained during the MAGIA99 and GEBRA93 cruises. B) Bathymetric multibeam data provided by the Marine Geoscience Data System (http://marine-geo.org).

2. Physiography

The detailed physiographic characterization of the study area (Fig. 3.2) was defined based on the high-resolution swath bathymetry datasets and it also integrates the information from previous works (Jeffers and Anderson, 1990; Canals et al., 1994; Klepeis and Lawver, 1994; Gràcia et al., 1996; Lawver et al., 1996; Ercilla et al., 1998; García et al., 2006a). The CBB is a markedly asymmetric basin, with a narrow northwest margin adjacent to the SSI and a relatively wide southeastern margin adjacent to the AP (Table 3.I). The physiography of the CBB margins is atypical in several aspects when compared with other glacial margins: a) the continental shelf is not overdeepened and has a basinwards sloping profile; b) the slope is composed of upper, middle and lower sectors; c) the middle slope is composed by isolated relatively flat slope platforms; and d) the lower slope connects sharply with the basin, and no continental rise can be observed. The geometric parameters, including width, depth and gradients of the different domains, are summarized in Table 3.I.

		Maximum width (km)	Maximum depth (m)	Average Gradient (º)
SSI	Shelf	10	300	2
	Upper slope	4	525	23
	Middle slope	5	850	3
	Lower slope	10	1750	26
AP	Shelf	50	300	1.5
	Upper slope	10	800	15
	Middle slope	35	1100	2
	Lower slope	10	1500	20
Basin		45	1960	2

Table 3.I. Geometric parameters of the physiographic domains.

The SI margin corresponds to the South Shetland Islands archipelago, which consists of a series of islands, arranged a NE direction and separated by narrow straits (Fig. 3.2). The margin has a relatively narrow *continental shelf* with an average width of 5 km that reaches depths of 100 to 300 m and is cut by NW-trending glacial troughs (Fig. 3.2). The *slope* has a maximum width of 15 km and reaches depths of 1750 m. The *upper slope* is steep (up to 23º), has maximum widths of 4 km and reaches depths of 450 to 525 m. The *middle slope* is represented by four slope platforms with gradients <3º and depths and widths that decrease eastwards. The westernmost slope platform is located off Greenwich, Roberts and Nelson Islands (Fig. 3.2). It is about 50 km long, has a maximum width of 9 km and reaches a maximum depth of 625 m. To the east, two relatively small, semi-circular slope platforms are located off King George Island. They are about 15 km long, up to 5 km wide and extend down to 850 and 700 m, respectively. The easternmost slope platform is located off the eastern part of King George Island. It is 50 km long and <5 km wide, and extends down to 625 m. The *lower slope* consists of a steep scarp that widens towards the east to up to 10 km and has gradients

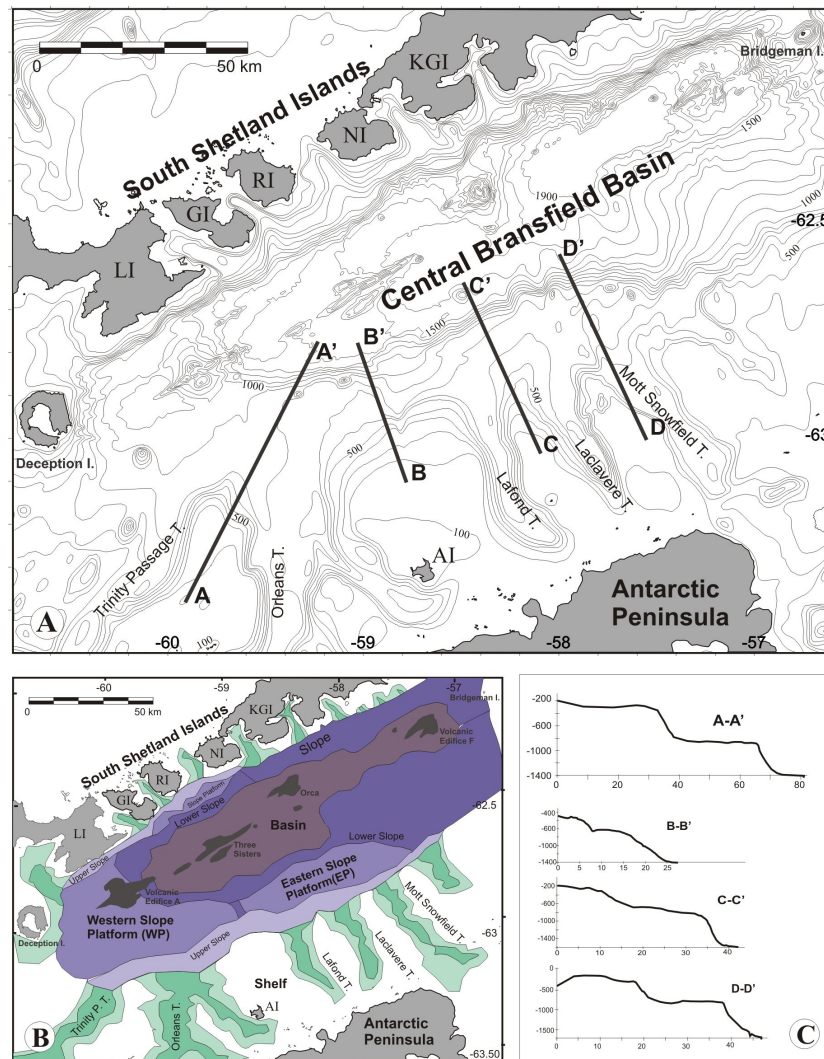of up to 26º. The lower slope reaches depths that increase from west to east (1350 to more than 1750 m).

Figure 3.2. A) Bathymetric map of the Central Bransfield Basin and location of topographic profiles. B) Physiographic characterization of the Central Bransfield Basin. Physiographic domains include continental shelf, continental slope (upper, slope platforms and lower) and basin. C) Slope cross-sections along the AP margin. Legend: LI: Livingstone Island; GI: Greenwich Island; RI: Robert Island; NI: Nelson Island; KGI: King George Island; AI: Astrolabe Island.

The AP *continental shelf* has an average gradient of 1.5º and a maximum width of 50 km, and extends down to 200-300 m, shallowing and narrowing towards the northeast (Fig. 3.2). It consists of flat banks dissected by N- to NW-trending troughs. The *AP upper slope* is characterized by a narrow (<10 km wide) and steep (up to 15º) ramp at depths between 200 and 800 m. The *AP middle slope* is composed of two relatively wide and flat slope platforms with an average gradient of 1.5º. The slope platforms have been designated Western Platform (WP) and Eastern Platform (EP). The WP has a maximum width of 35 km and extends down

to 700-1100 m water depth (Fig. 3.2). The EP is separated from the WP by a NNW-oriented scarp located at about 59ºW. This scarp is about 3 km wide and has gradients of 7-15º. The WP is up to 16 km wide and occurs at depths between about 500 and 800 m. The *lower slope* is relatively steep and narrow with gradients of up to 20º and widths of 5-10 km. It occurs at depths of 800-1500 m and has a sinuous trend in plan view (Fig. 3.2). In the boundary area between the WP and the EP the lower slope profile is gentler, with relatively lower gradients of 3-12º and maximum widths up to 10 km. East of 57º 30'W the lower slope is about 30 km wide, with a very irregular seafloor and gradients of 1-15º.

The SSI and AP margins connect with the basin, which has an averaged gradient of 2º and occurs at 1500-1900 m water, deepening towards the NE (Fig. 3.2). An almost linear chain of volcanic edifices is located along the axis of the basin, related to the formation of new crust (Gràcia et al., 1996). Deception and Bridgeman Islands are located at the ends of the volcanic chain, while the rest of the features form 300- to 600-m-high submarine relief, labeled Volcanic Edifice A, Three Sisters, Orca and Volcanic Edifice F (Lawver et al., 1996).
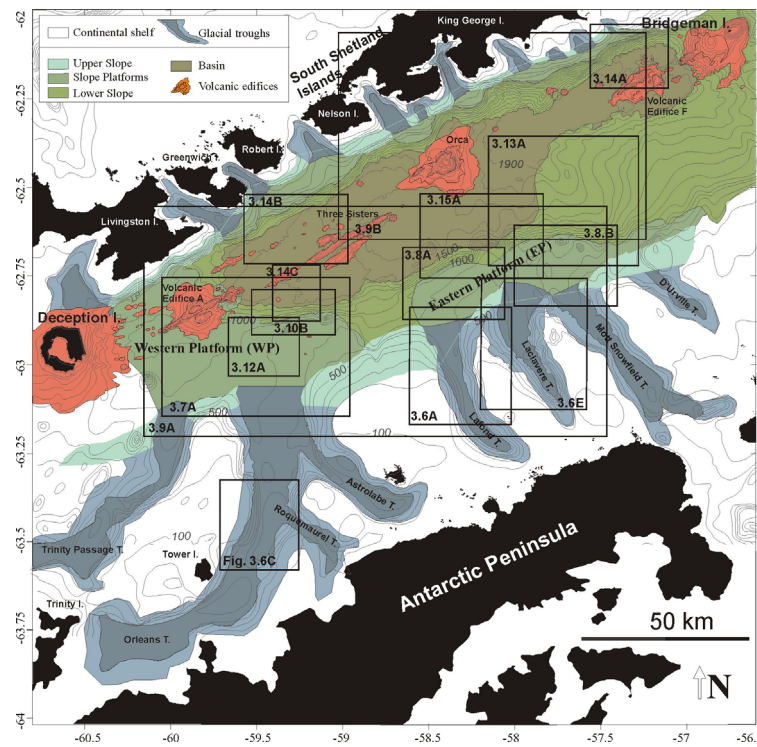
Figure 3.3. Location of the bathymetric maps and models presented in this chapter.

3. Morphologic and near-surface acoustic characterizations of the CBB

The morphological features on the CBB have been classified as glacial (erosion surfaces, glacial troughs, erosional grooves, knickpoints, drumlins, glacial lineations and grounding zone wedges), glaciomarine (furrows, trough mouth fans, gullies and draping sheet) and marine (pockmark fields, contourites, sediment mass movements, turbidite channels and

volcanic edifices). The different morphological features identified on the CBB show a clear zonation along the physiographic domains. Generally, erosional features of glacial origin predominate on the continental shelf, depositional features of glacial and glaciomarine origin and locally marine features predominate on the continental slope, and features of marine origin predominate on the basin (Fig. 3.4).

3.1. Morphological features of glacial origin

The *erosion surfaces* are located on the continental shelf banks, the upper slope and the proximal areas of the seafloor of the glacial troughs (Fig. 3.5). On the shelf banks and upper slope, these surfaces are relatively flat and characterized by indistinct non-penetrative bottom reflections on the TOPAS profiles and by prolonged echoes eroding very deformed and irregular subbottom layered reflections on the airgun profiles (Fig. 3.5B,C). On the proximal parts of the troughs, the erosion surfaces are very irregular and show hyperbolic bottom echoes eroding subbottom chaotic reflections on the airgun profiles (Fig. 3.5B) and hyperbolic, prolonged bottom echoes on the TOPAS profiles (Fig. 3.5D).

Eleven NW- to NNW-trending *glacial troughs* dissect the SSI continental shelf and upper slope and mouth into the SSI slope platforms (Figs. 3.2 and 3.4). They occur in the narrow straits between Livingstone, Greenwich, Roberts, Nelson and King George Islands and in the fjords and bays of King George Island. They are up to 500 m deep, 3-20 km long and up to 9 km wide, and have V- to U-shaped transversal profiles. They are irregular and deepen basinwards with gradients of up to 1°.

Eight *glacial troughs* dissect the AP continental shelf and upper slope (Fig. 3.4). They are up to 500 m deep and have U-shaped transversal profiles, with flat seafloor and steep walls (up to 12°). These walls are characterized by rough, non-penetrative echoes on both TOPAS and airgun profiles. The bottom depths vary from more than 900 m to about 400 m from the western to the eastern troughs. The troughs generally shallow basinwards and have a very irregular depth gradient. Two families of glacial troughs are differentiated on the basis of their morphological characteristics: (1) two large troughs (Trinity Passage and Orleans) located in the western area, with a general NE to N trend and opening into the WP and (2) six smaller troughs (Roquemaurel, Astrolabe, Lafond, Laclavere, Mott Snowfield and D'Urville), with a general NNW to NW trend and opening into the WP and the EP.

Starting from the westernmost trough, Trinity Passage Trough is 45 km long, up to 10 km wide and 300 m deep. It is NE- to N-trending and connects with the Gerlache Strait at the N of Trinity Island (Fig. 3.4). The Orleans Trough has a length of about 60 km, widths of up to 15 km and depths of more than 650 m, and it is the largest glacial trough in the CBB. The head is located at the E of Trinity Island and trends ENE for the first 30 km, turning N at the
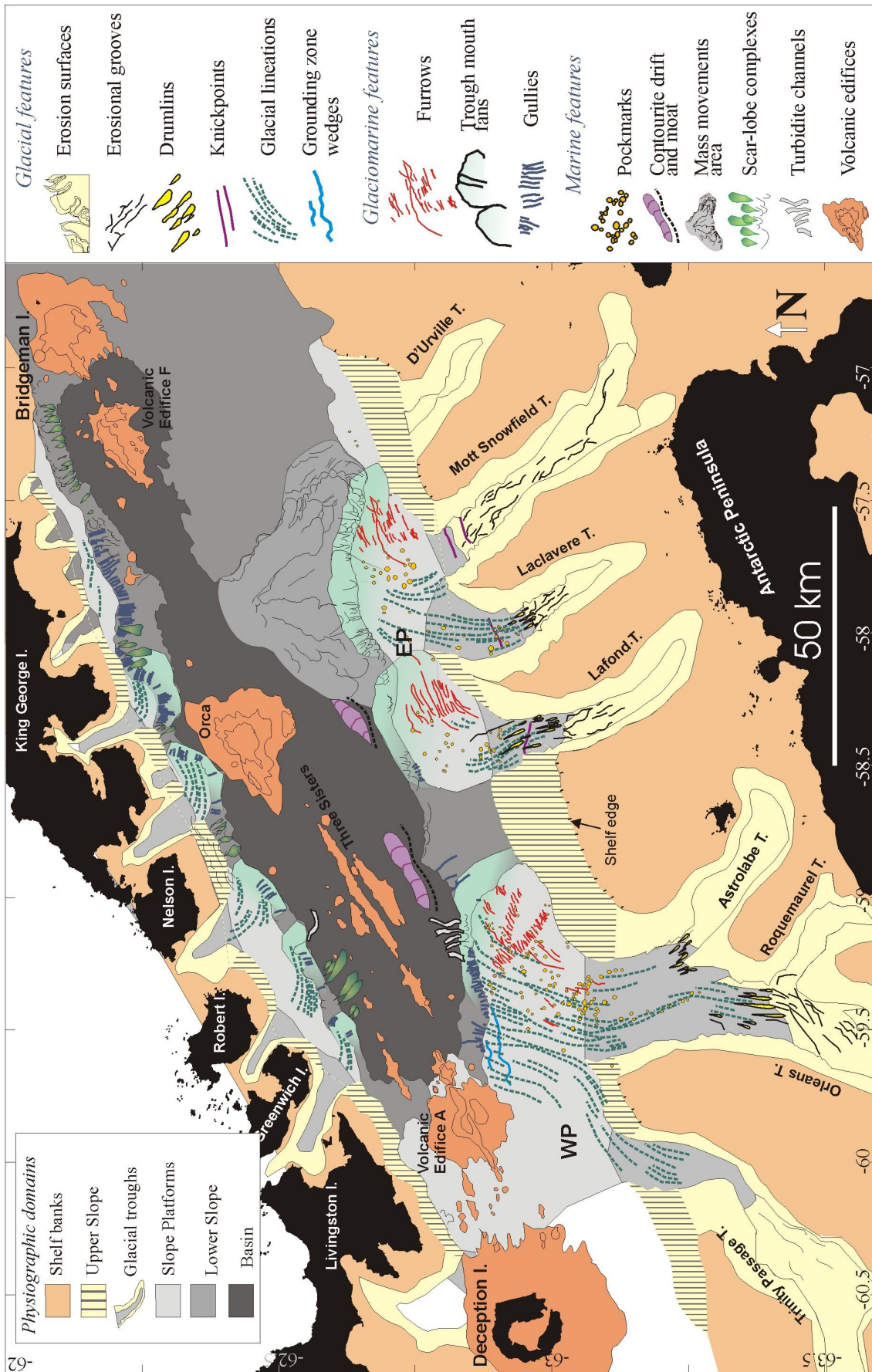
Figure 3.4. Morphological map of the CBB, showing the zonation of glacial, glaciomarine and marine features along the physiographic domains. The shelf is characterized by erosion surfaces and the presence of glacial troughs, where erosional grooves, drumlins and knickpoints occur. The distal areas of glacial troughs and slope platforms present a variety of features, including glacial lineations, pockmarks and furrows. On the lower slope, gullies, trough mouth fans and scar-and-lobe complexes predominate. The basin is characterized by the presence of contouritic features, scar-and-lobe complexes, turbidity channels and volcanic edifices.

distal part. The troughs in the eastern area are almost parallel and straight, with a NNW to NW trend. The Astrolabe and Roquemaurel Troughs mouth into the Orleans Trough. They are 15 and 25 km long, respectively, up to 13 km wide and reach depths down to 400 m. The easternmost troughs—Lafond, Laclavere, Mott Snowfield and D'Urville Troughs—open directly into the EP. They are 10-20 km long, 5-8 km wide and up to 600 m deep.

As it has been mentioned before, *erosion surfaces* characterize the proximal parts of the glacial troughs (Figs. 3.5A,B and 3.6). Moreover, irregular *erosional grooves* are identified on the proximal parts of the Trinity Passage, Orleans, Lafond, Laclavere and Mott Snowfield Troughs, at depths of 500-800 m. These features have a relief of 60-100 m and widths of 1-2 km, and their orientation ranges from parallel to oblique to the axis of troughs (Figs. 3.4 and 3.6A-D). *Knick points* were identified on the middle and distal reaches of the Lafond, Laclavere and Mott Snowfield Troughs at depths of 500-800 m. They produce a change in the depth profile with an increase in the gradient, forming trough-perpendicular oriented depressions of up to 50 m relief (Fig. 3.6A,B). *Drumlins* were previously identified in the Lafond and Laclavere Troughs (Canals et al., 2002), but the new map has allowed them to be also recognized on the middle reaches of the Trinity Passage and Orleans Troughs at depths of 750-850 m (Figs. 3.4 and 3.6).
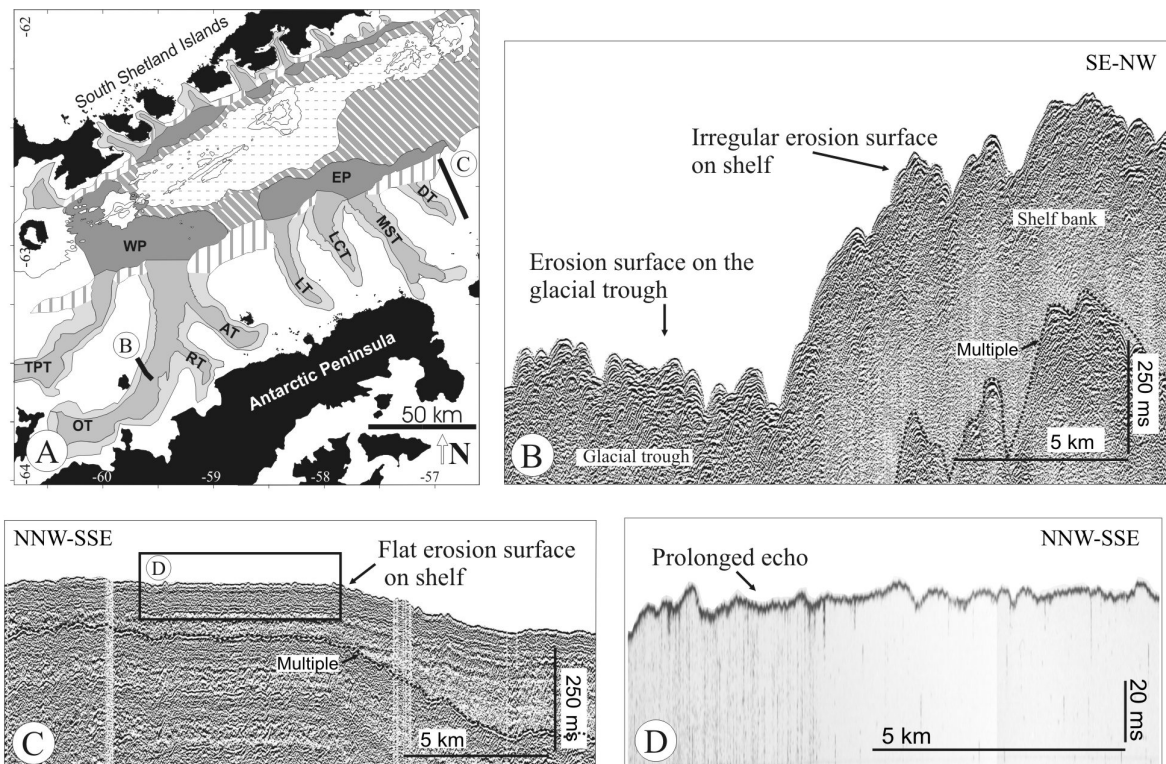

Figure 3.5. Erosion surfaces on the continental shelf banks and glacial troughs. A) Location of the seismic profiles. B) and C) Airgun profiles showing prolonged echoes on deformed and irregular subbottom layered reflections on erosion surfaces. D) TOPAS profile showing indistinct prolonged echoes.
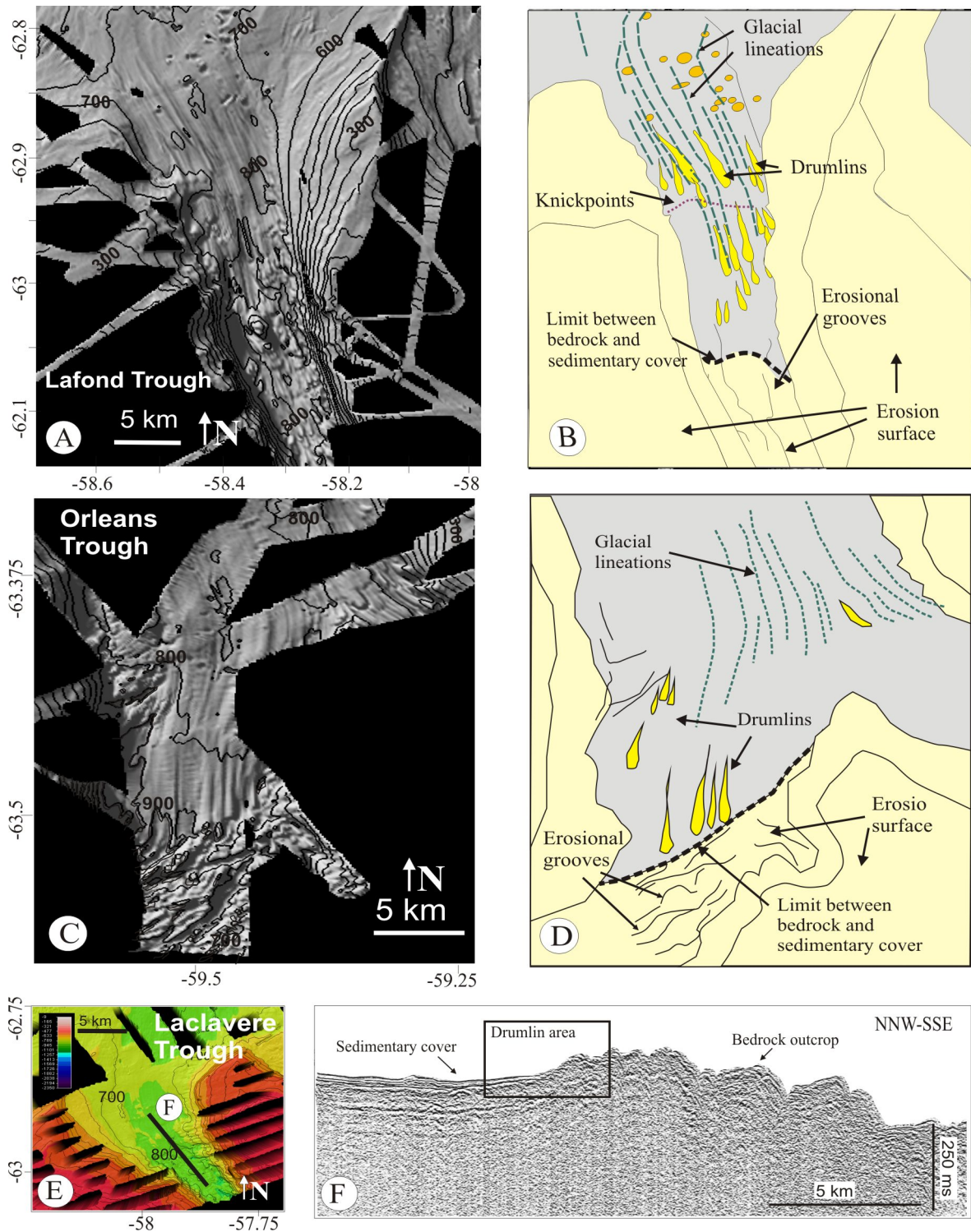
Figure 3.6. A), C) and E) Shaded relief multibeam models of the Lafond, Orleans and Laclavere glacial troughs. B) and D) Morphosedimentary interpretations based on dataset. The inner parts of the troughs seafloor is characterized by erosion surfaces with erosional grooves. Seaward of the limit between outcropping bedrock and the sedimentary cover, dominant features are knickpoints, drumlins and glacial lineations. F) Airgun seismic profile on the seafloor of Laclavere Trough, with irregular hyperbolic echoes with chaotic subbottom reflections on the erosive surface and layered reflections on the distal area with sedimentary cover. See location of bathymetric maps in Figure 3.3.

Drumlins are elongated and asymmetric features with positive relief and the steeper and wider side oriented towards the coast while the smoother narrow side is oriented basinwards. They are parallel to the troughs axis, measure up to 3.5 km long, are less than 0.5 km wide, and have a relief of up to 30 m (Figs. 3.4 and 3.6). The acoustic response of erosional features and drumlins is very similar on the seismic profiles, consisting of hyperbolic non-penetrative echoes on the TOPAS profiles and irregular hyperbolic echoes with chaotic subbottom reflections on the airgun profiles (Fig. 3.6F).

The *glacial lineations* are elongated features of very high lateral continuity that form a ridge-and-valley topography from the distal reaches of the troughs to the slope platform edge on both the SSI and AP margins (Figs. 3.4 and 3.7A). They have lengths of more than 50 km, are typically spaced 4-6 km apart and have vertical relief of 20-40 m. These lineations are characterized by a marked eastwards change of trend, from a trough-parallel trend at the troughs' seafloor to a basin-parallel trend (almost perpendicular to the troughs) on the slope platforms (Fig. 3.4) On the WP off Orleans Trough, a set of glacial lineations with a more pronounced NE trend form a tongue that overlaps older glacial lineations and ends at a more proximal position (about 800 m) on the slope platform (Fig. 3.7A). The area is acoustically characterized by discontinuous reflections on the airgun profiles (Fig. 3.7B) and transparent echoes on the TOPAS profiles (Fig. 3.7C), locally overlaid by very continuous layered reflections in both cases (Fig. 3.7B,C).

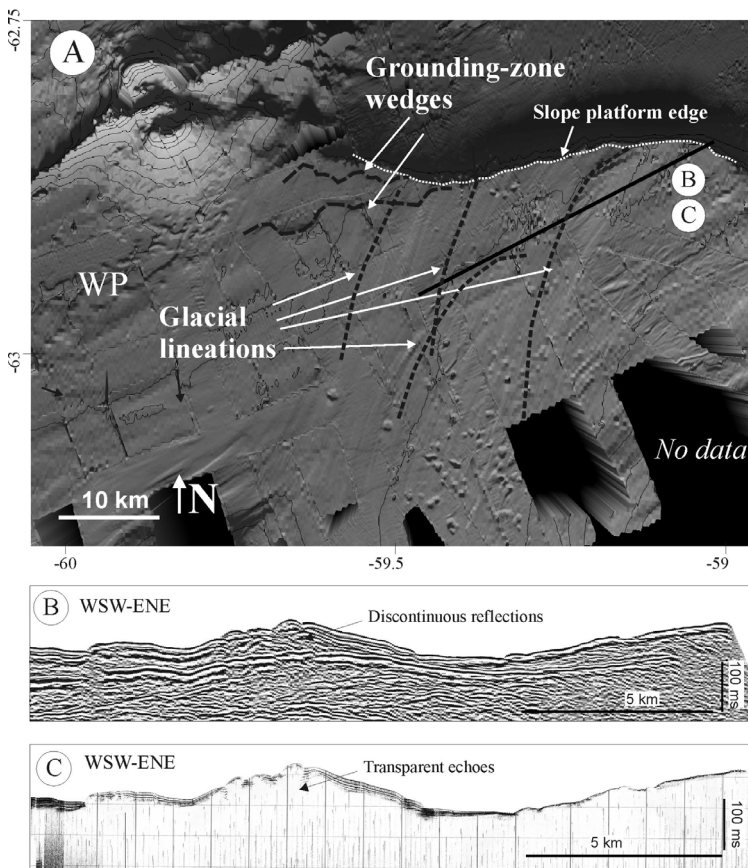
Figure 3.7. A) Shaded relief multibeam model of the WP showing the glacial lineations and grounding zone wedges on the WP slope platform. An eastwards turn of the ice flow at the slope platform is observed, as well as the overlapping of lineations with different directions. See location of the map in Figure 3.3. B) Airgun and C) TOPAS profiles show the acoustic character of glacial lineations.

The *grounding zone wedges* have been identified on the outer part of the WP, at the southern side of the Volcanic Edifice A (Fig. 3.7A). They represent two sinuous bathymetric scarps in plan view, up to 50 m in height and with a lateral continuity of up to 15 km.

3.2. Morphological features of glaciomarine origin

Furrows were identified in the distal eastern areas of the AP margin slope platforms, mostly at the E of the mouths of the Orleans, Lafond and Mott Snowfield Troughs, at 650-750 m water depth (Figs. 3.4 and 3.8). They are superimposed on the glacial lineations and represent elongated, U- or V-shaped negative relief, with a very consistent ENE trend. They are up to 15 km long, 0.5-1 km wide and up to 25 m deep, and are spaced 0.3-1 km apart (Fig. 3.8C to E). The furrows end abruptly close to the slope platform edges and have positive relief on the flanks and at the distal eastern end, up to 10 m higher than the surrounding seafloor (Fig. 3.8C). On the airgun profiles furrows are incised into the near-surface continuous layered reflections and on the TOPAS profiles they are cut into transparent deposits and covered by continuous layered reflections (Fig. 3.8D,E).
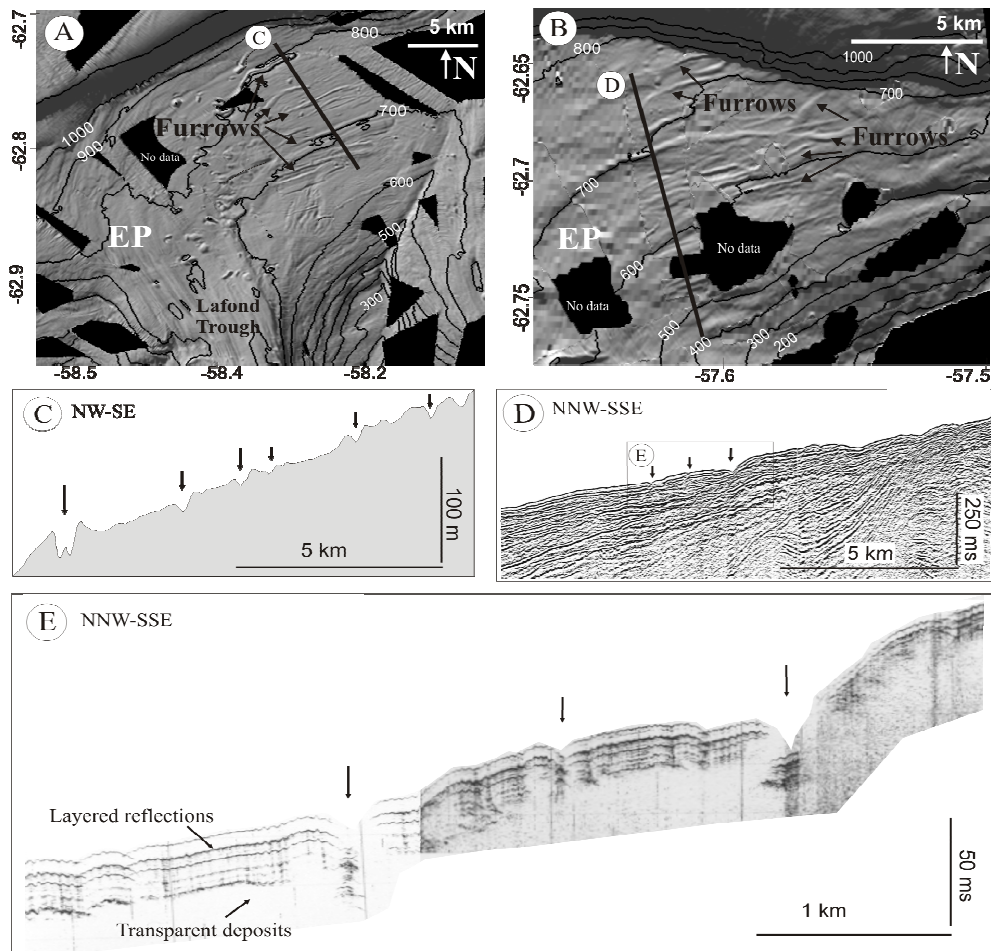

Figure 3.8. A) and B) Shaded relief multibeam models of the Eastern Platform off Lafond Trough and Mott Snowfield Trough, showing the location of furrows. Topographic profile (C) and airgun (D) and TOPAS (E) seismic profiles showing the characteristics of these features. Arrows indicate the location of furrows. See location of bathymetric maps in Figure 3.3.

Trough mouth fans occur on the distal ends of the slope platforms and the lower slope of the SSI and AP margins, displaced to the E of the mouths of the glacial troughs (Figs. 3.4 and 3.9). Individual trough mouth fans form the semi-circular slope platforms off King George Island and the rest of them coalesce resulting in the sinuous shape of the slope platforms,
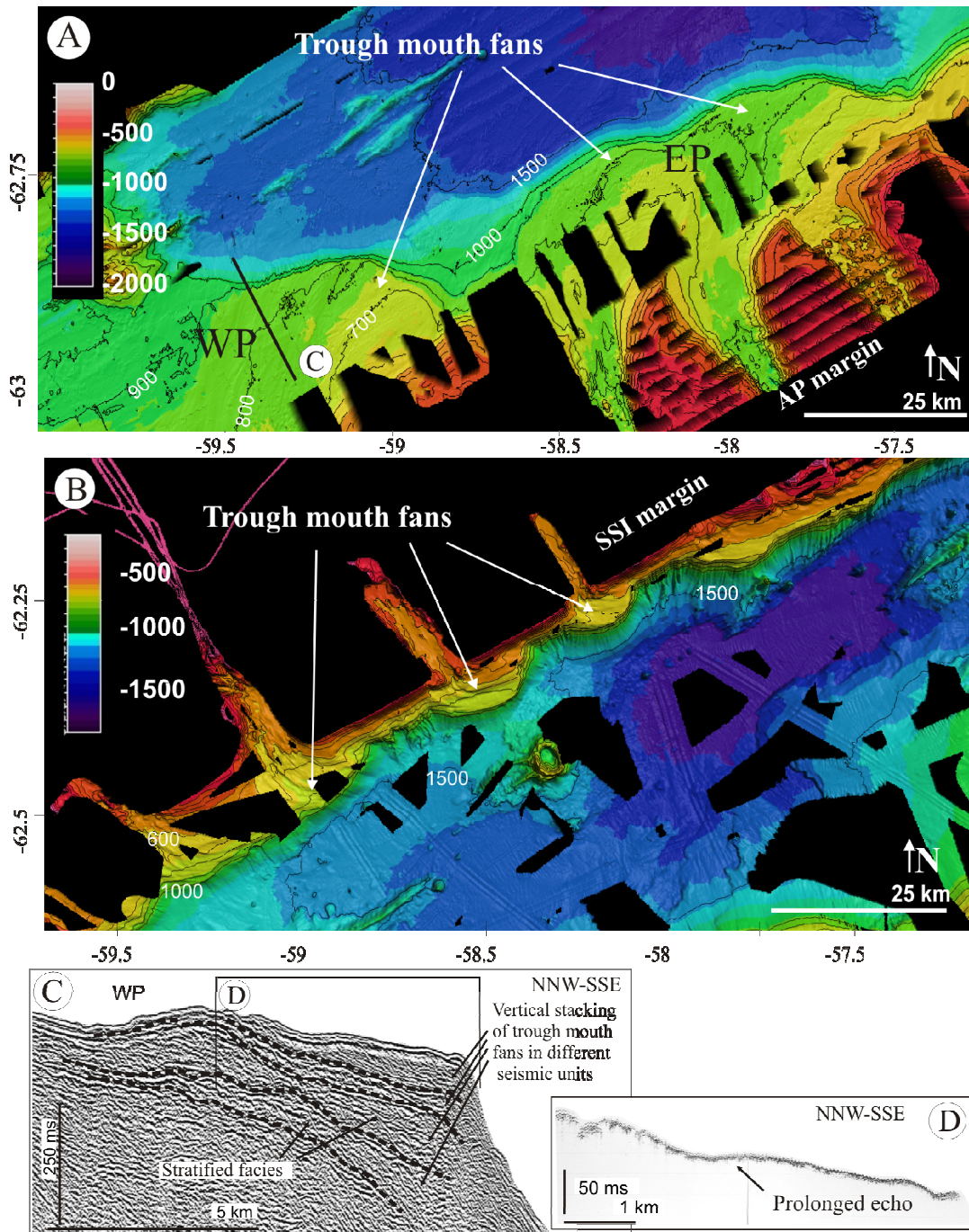

Figure 3.9. A) and B) Colour scaled shaded relief multibeam models of the AP margin and SSI margins, showing the trough mouth fans. C) Airgun seismic profile and D) TOPAS profile showing the acoustic characteristics of a trough mouth fan off Orleans Trough on the WP. See location of bathymetric maps in Figure 3.3.

which protrude basinwards off the mouths of the troughs. The trough mouth fans are characterized on the airgun profiles by the vertical stacking of units composed of layered reflections that form a prograding stratigraphic pattern on the slope platform edges and lower slope (Fig. 3.9C). On the TOPAS profiles they are characterized by indistinct non-penetrative bottom echoes or by transparent echoes covered by continuous layered reflections that pinch out towards the slope platform edge (Fig. 3.9D).

Gullies were identified in the bathymetric data, on the lower slope of the SSI margin and on the WP on the AP margin (Figs. 3.4 and 3.10). They are 2-5 km long, hundreds of meters wide and tens of meters deep. The heads of these gullies cut the platform edge at depths of 700-1000 m and they extend down to the middle part of the lower slope. The gullies occur mostly in areas where glacial lineations reach the slope platform edge.
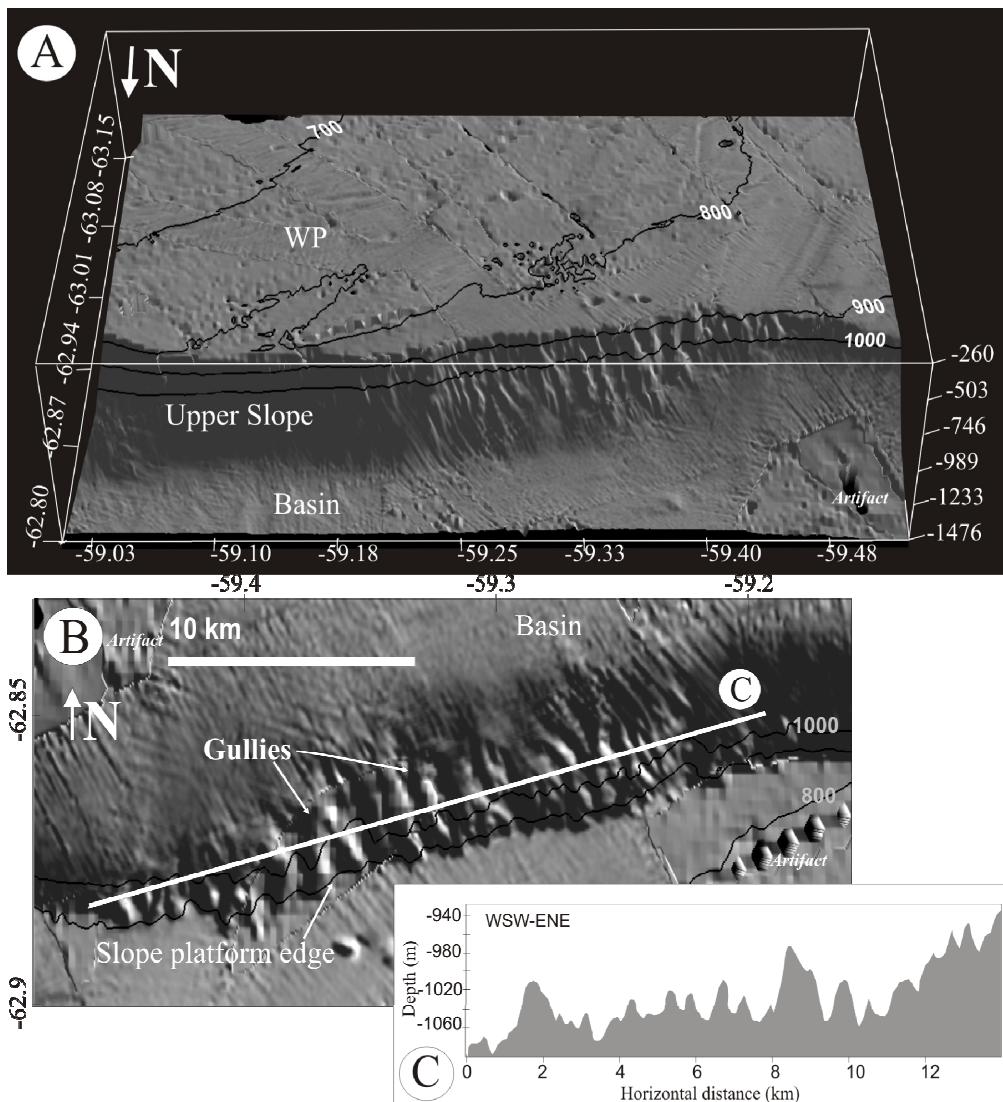

Figure 3.10. A) 3D block (looking towards the south) showing the location and morphology of gullies. B) Shaded relief multibeam model of the WP-edge and lower slope, looking towards the north. C) Topographic profile on the gully area, perpendicular to the direction of gullies. See location of bathymetric maps in Figure 3.3.

60

A thin *draping sheet* covers the distal parts of the troughs, the AP slope platforms and the basin, being very thin or absent on the continental shelf, upper slope and outer parts of the slope platforms (Figs. 3.4 and 3.11A). Its distribution was defined based on seismic profiles, since it only smooths and/or mimics the underlying topography. It is characterized by continuous parallel layered reflections on both TOPAS and airgun profiles (Figs. 3.11), with a thickness of tens of ms.
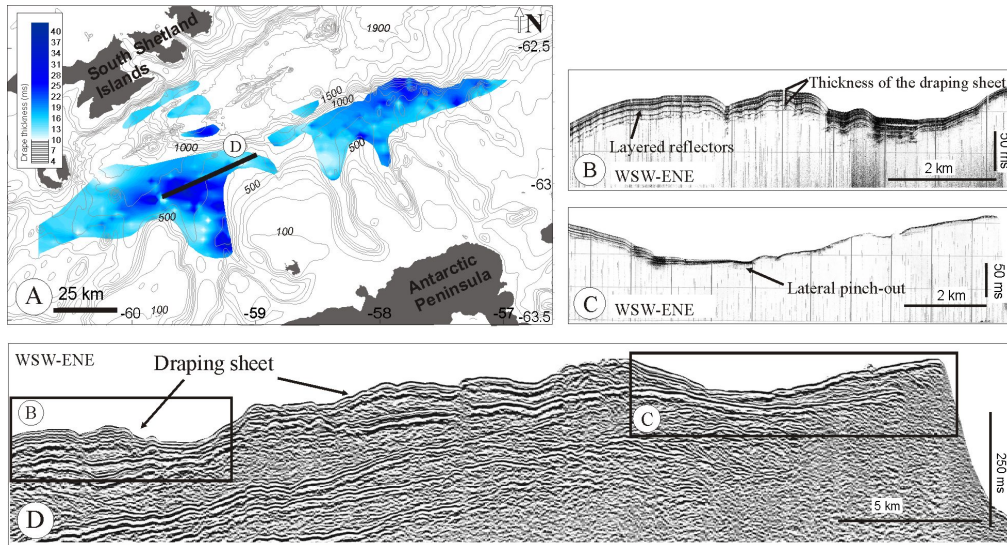

Figure 3.11.A) Isopach map of the thickness of the draping sheet. B) and C) TOPAS profiles, and D) airgun profile showing the layered reflections that characterize the drape.

3.3. Morphological features related to marine processes

Pockmark fields are located on the trough seafloor distal areas and on the slope platforms of the AP margin, off the glacial troughs (Figs. 3.4 and 3.12). The largest one is located on the eastern part of the WP and outer part of the Orleans Trough, and is formed by more than 130 pockmarks. The pockmarks are typically round- or elliptic-shaped, with diameters up to 1 km and depths of up to 35 m. Acoustically, the pockmarks occur on the TOPAS profiles as V- or U-shaped incisions into transparent deposits, filled in some cases with layered reflections. In airgun profiles they appear as V-shaped incisions into the near-surface continuous layered reflections.

Sediment mass movement features occur on the slope platform edges, lower slope and basin. They are represented by a slide valley complex (the Gebra-Magia slide complex) and several scar-and-lobe complexes (Figs. 3.4 and 3.13). The Gebra-Magia slide complex is a large area (up to 2000 km²) of mass wasting identified on the lower slope of the eastern part of the AP margin. It comprises a great variety of mass movement features that define a rough seafloor surface, including two large debris flow valleys, Gebra and Magia. The Gebra Valley is 30 km long and 5-12 km wide. It has a U-shape cross-section and a NW trend, with depths of
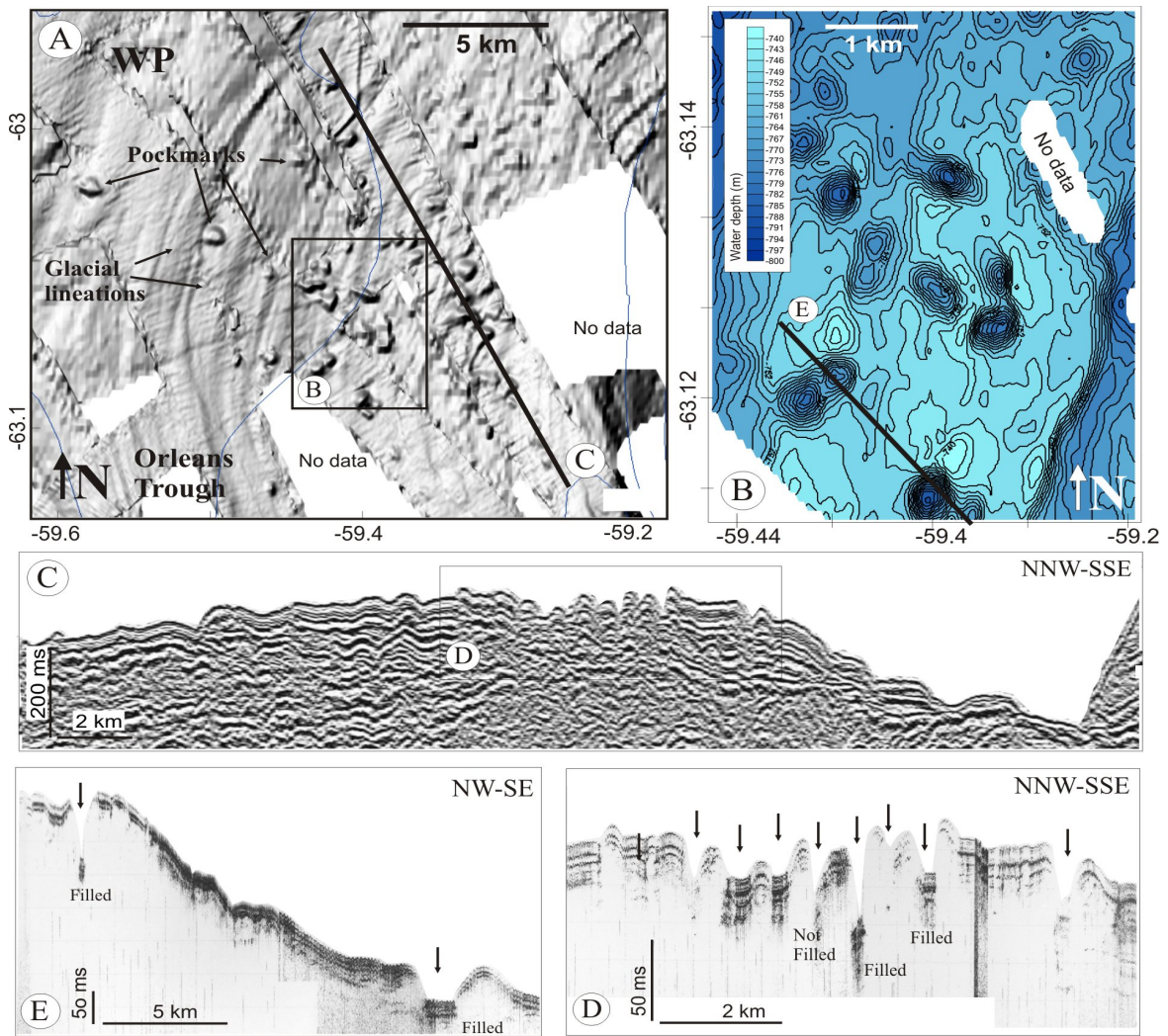
Figure 3.12. Morphosedimentary characterization of pockmarks. A) Shaded relief model and B)contour bathymetry on the WP. C) Airgun profile and D) TOPAS profile showing the acoustic character of pockmarks and the presence of sedimentary infilling in some of them. See location of bathymetric maps in Figure 3.3.

up to 150 m. It was studied in detail by Imbo et al. (2003) and more recently by Casas et al. (2004). The Magia Valley is located to the west of the Gebra Valley. It is 17 km long and has a sinuous trend with a general NE direction. The width decreases from about 3.8 km at the head to 2.2 km at the mouth. The transversal profile is U-shaped, with walls formed by laterally continuous slide scars with depths of 10-30 m (Fig. 3.13B,C). The Magia Valley seafloor displays convergent and divergent downslope-oriented lineations. The heads of the Gebra and Magia valleys are formed by several steep headwalls on the EP-edge and lower slope, suggesting a complex failure history (Fig. 3.13A). The Gebra and Magia valleys are surrounded by slide scars, slides, and mass transport sediments probably resulting from complex events involving elements of slumping and mass flows (Fig. 3.13). Acoustically, the Gebra-Magia slide complex is characterized by the stacking of chaotic, transparent and hyperbolic echoes on TOPAS and airgun profiles (Fig. 3.13C).
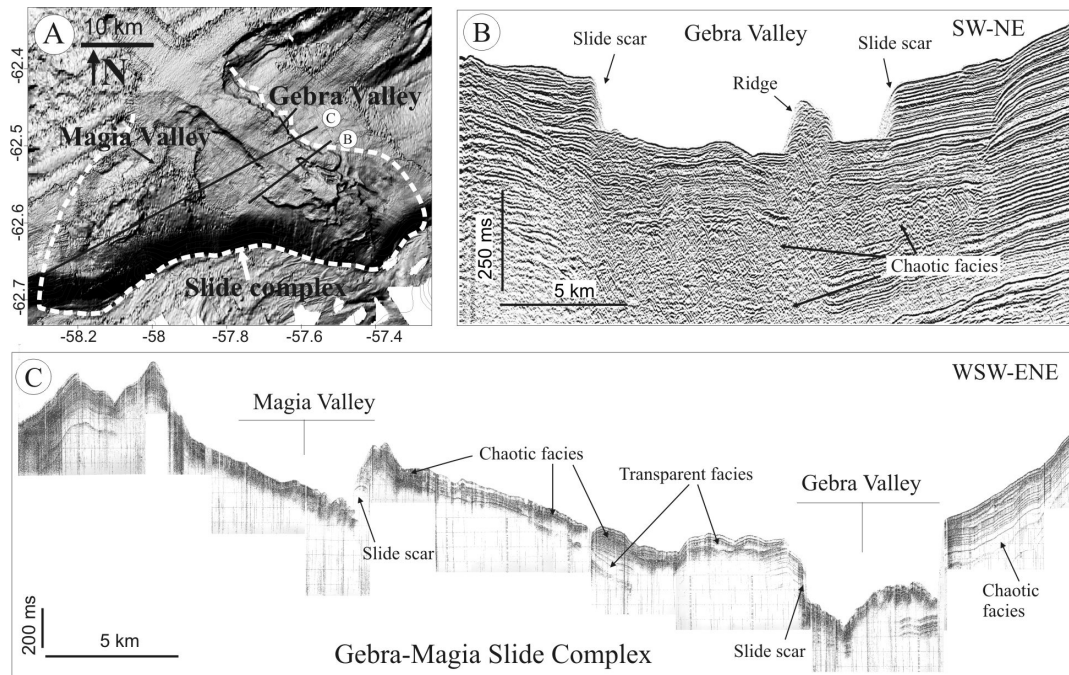
62

Figure 3.13. Morphosedimentary characterization of the Gebra-Magia slide complex. A) Shaded relief map. B) Airgun seismic profile of the Gebra Valley, showing the vertical stacking of chaotic bodies. C) TOPAS seismic profile along the slide complex, showing the chaotic and transparent acoustic character of the seismic reflections. See location of bathymetric maps in Figure 3.3.

Scar-and-lobe complexes were differentiated on the AP and SSI lower slope and basin (Figs. 3.4 and 3.14). The scars are isolated or coalescent 1- to 7-km-long features identified on the upper portion of the lower slope. Two types of lobes have been differentiated according to locations and morphologies. The first type is restricted to the distal part of the lower slope, off Nelson and King George Islands on the SSI margin, where the slope platforms are narrow or absent and the trough mouth fans are not well developed (Figs. 3.4 and 3.14A). These lobes are 1-4 km long and 1-1.5 km wide, elongated and with irregular shape. The second type is identified on the lower slope and basin of the SSI and AP margins, in areas that correspond to well-developed slope platforms and trough mouth fans. These lobes are characterized as more regular and elongated features, up to 5 km long and 1-2 km wide, that are located at the foot of the lower slope, extending down to the basin (Figs. 3.4 and 3.14B).

Turbidite channels were identified on the lower slope and basin in the western part of the study area (Fig. 3.4). On the SSI margin, one 7-km-long, 1.5-km-wide channel occurs at the foot of the lower slope, with a NW to WNW trend (Fig. 3.14B). It is asymmetric, with incision depths of about 15 m at the NE flank and less than 8 m at the SW flank. On the AP margin five symmetrical channels are identified (Figs. 3.4 and 3.14C,D). They are up to 8 km long, 2 km wide and 20 m deep. Their trend is NNE to N, following the general regional slope. Acoustically, the turbidite channels occur as incisions into undisturbed, stratified reflections on the TOPAS profiles (Fig. 3.14D).
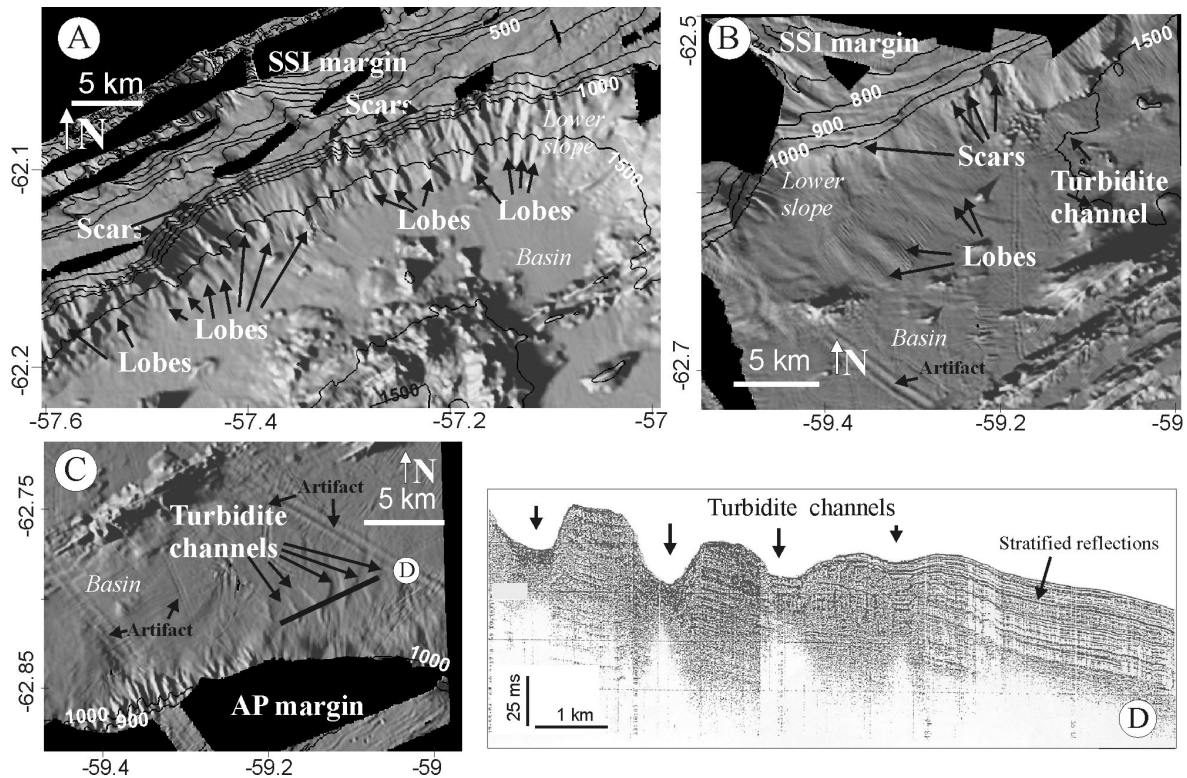
Figure 3.14. A) and B) Shaded relief models showing scar-and-lobe complexes on the distal part of the lower slope and on the basin. C) Shaded relief models showing turbidite channels. D) TOPAS profile crossing turbidite channels on the AP margin, modified from Ercilla et al. (1998). See location of bathymetric maps in Figure 3.3.

Contourite deposits have been previously described at the foot of the lower slope (Ercilla et al., 1998; Casas et al., 2004) (Figs. 3.4 and 3.15). The new detailed bathymetric data indicate that one of the mounds defined by Ercilla et al. (1998) is not contouritic in origin, but corresponds to one of the elongated lobes of the above-mentioned scar-and-lobe complexes. Likewise, the new map has allowed a better definition of the distribution and geometry of two contourite deposits, located at the foot of the AP lower slope. The westernmost contourite drift occurs south of the Three Sisters volcanic edifice (Fig. 3.4). It has an ENE-oriented elongated shape (14 km long and up to 7 km wide) and a relief of up to 15 m. It is also associated with a contourite moat at the foot of the lower slope that is about 3 km wide and has a relief of more than 50 m from the drift crest. The easternmost contourite drift occurs south of the Orca volcanic edifice (Figs. 3.4 and 3.15). It is elongated, 7 km long and less than 3 km wide, and has a relief of up to 60 m over the basin floor. It is associated with a 2-km-wide, flat floored contourite moat at the foot of the lower slope. This drift is characterized on the TOPAS profiles by laterally continuous sub-parallel layered reflections that show internal discontinuities and prograde towards the associated contourite moat at the foot of the lower slope. The moat is characterized by prolonged non-penetrative echoes (Fig. 3.15B).
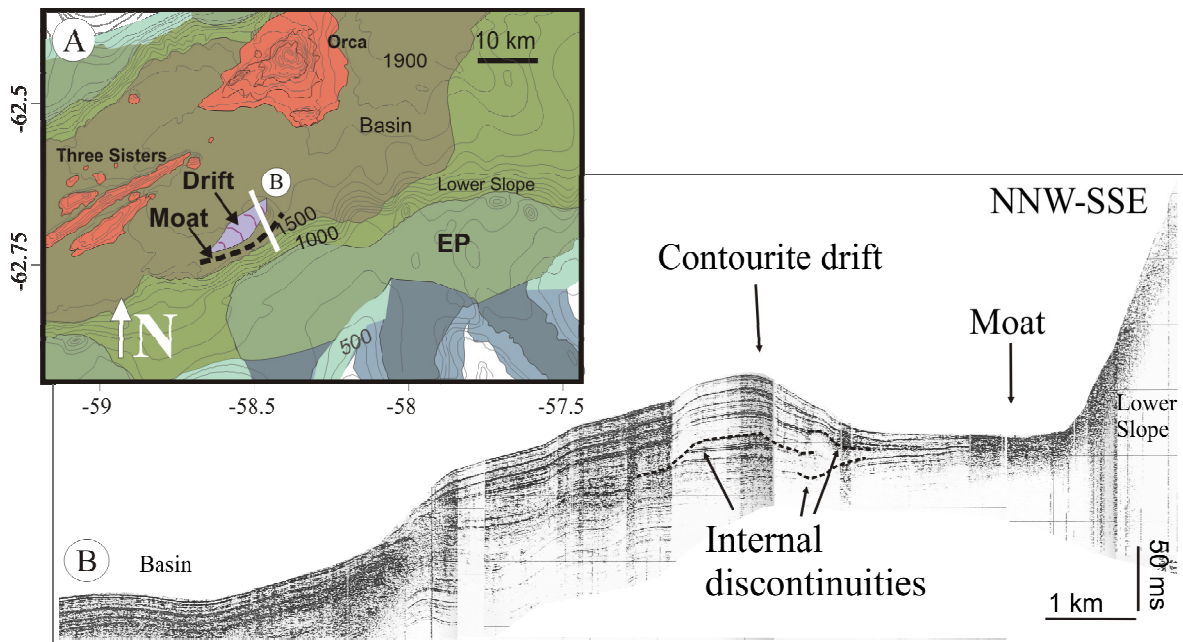
Figure 3.15. A) Morphologic map showing the location of the contourite features (drift and moat) at the base of the lower slope off the Eastern Platform on the AP margin. B) TOPAS profile (B) across the contourite drift and moat, showing their seismic facies and stratal pattern. See location of bathymetric maps in Figure 3.3.

A linear chain of *volcanic edifices* with a general NE orientation occurs at the axis of the CBB (Fig. 3.4). Both ends of the chain are formed by two volcanic islands, Deception Island (539 m above sea level) and Bridgeman Island (240 m above sea level). The most prominent submarine volcanic edifices are Edifice A, located on the WP and lower slope, and Three Sisters, Orca and Edifice F, located on the CBB basin (Gràcia et al., 1996; Lawver et al., 1996). Volcanic Edifice A consists of a circular cone, 14 km wide and about 500 m high, cut by a 28-km-long, NW-oriented ridge. Three Sisters volcano is composed of three elongated ridges with the same NW orientation. The central one is 30 km long and 400 m high, and the lateral ones are less than 14 km long and less than 300 m high. Orca Volcano is conical in shape, 7 km wide, and more than 700 m high. It has a central caldera 400 m deep. Volcanic edifice F is very irregular in shape but shows an elongate central ridge, 16 km long and 650 m high, oriented in the direction of the basin axis. Numerous smaller isolated or grouped volcanic edifices were identified, mostly on the basin and WP. In general, the volcanic edifices are characterized by non-penetrative echoes on the TOPAS profiles and very irregular, hyperbolic bottom echoes with chaotic to transparent subbottom echoes on the airgun profiles (Fig. 3.16).
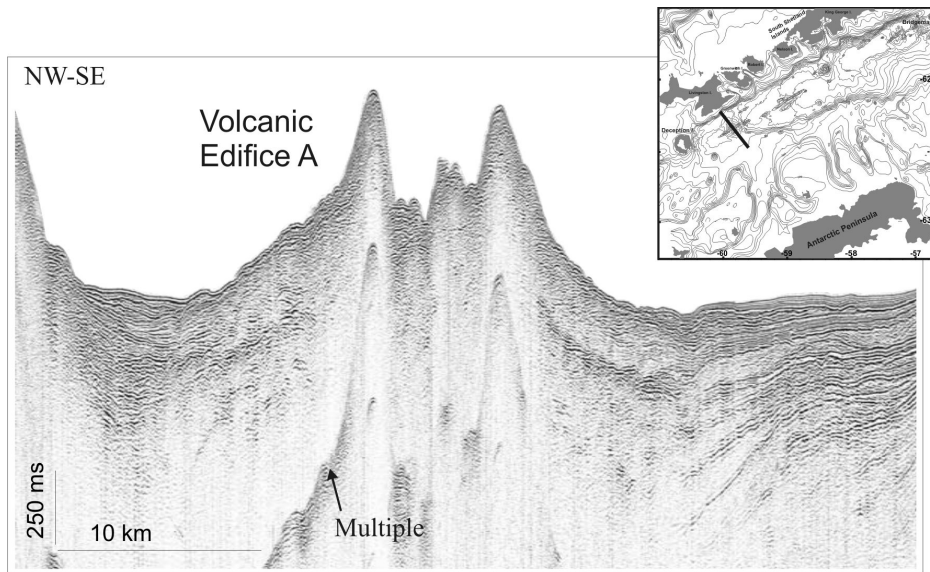
Figure 3.16. Airgun profile showing the acoustic character of the Volcanic Edifice A.

4. Discussion: Morphology as a key for the definition of sedimentary systems and their dynamics

The new morphological map offers a great variety of features representing architectural elements which can be grouped into sedimentary systems according to the processes responsible for their formation and distribution. The new data give information about the linkages between sedimentary systems and also between elements within a system. These linkages are deduced from the character of the erosional, depositional and reworking features and from the spatial connection of the features and systems. All these facts can be translated into the spatial and temporal evolution of the sedimentary processes and controlling factors, within the entire sediment dispersal pattern from shelf to basin.

4.1. Sedimentary systems: characterization, dynamics and spatial linkages

Two major systems are identified in the CBB, affecting the entire AP and SSI margins. These systems are: (1) the glacial-glaciomarine sedimentary system and (2) the slope-basin sedimentary system. Other minor systems that locally affect the margin and basin are (3) the seabed fluid outflow system and (4) the contourite system.

4.1.1 Glacial-glaciomarine sedimentary system

This system includes most of the glacial and glaciomarine morphological features on the shelf and slope (Fig. 3.4). The major architectural elements in this system are erosion surfaces, glacial troughs (which include erosion surfaces, erosional grooves, knickpoints, drumlins and the proximal part of glacial lineations as minor-hierarchy elements), glacial lineations, grounding zone wedges, furrows and the draping sheet.

The *erosion surfaces* that characterize the shelf banks and upper slope are acoustically defined by prolonged facies and lack of acoustic penetration on the seismic profiles (Fig. 3.5B to D), suggesting that they have developed on consolidated deposits by direct subglacial erosion exerted by the ice sheet (Alley et al., 1989; Anderson, 1999).

The *glacial troughs* are the result of subglacial erosion of ice streams, in which fast-flowing ice streams drain the ice sheet (Vorren and Laberg, 1997). Ice streams are channelized developing seaward-shallowing profiles characteristic of glacial margins (Anderson, 1999). In the CBB, glacial troughs erode both the inner shelf and upper slope (Fig. 3.4). The glacial troughs represent the first-order element of a series of minor-scale architectural elements which display a seaward succession, including proximal *erosion surfaces*, *erosional grooves*, *knickpoints*, *drumlins* and *glacial lineations* (Figs. 3.4 and 3.6). This succession of elements was identified on the glacial troughs of the AP margin and is governed by the type of substrate. This has been widely documented to occur in other areas around Antarctica where the contact between bedrock and sedimentary cover occurs (Shipp and Anderson, 1997; Anderson et al., 2001; Wellner et al., 2001, 2006; Domack et al., 2006). Where bedrock outcrops, the ice streams erode the seafloor directly, creating rough erosion surfaces and erosional grooves, which may also be eroded by meltwater at the base of the ice streams (Domack et al., 2006). Knickpoints are the result of direct erosion by ice keels on resistant bedrock horizons (Barnes and Reimnitz, 1997; O'Brien et al., 1997), since they occur at similar positions along the different glacial troughs (Figs. 3.4 and 3.6). Drumlins develop on the glacial troughs at the limit between bedrock and sedimentary cover (Wellner et al., 2001), at depths that range from 700 to 850 m (Figs. 3.4 and 3.6). They indicate an ice flow direction parallel to the troughs axes, and their presence suggests the acceleration of the flow.

The *glacial lineations* occur on the distal reaches of the glacial troughs and on the slope platforms of the AP and SSI margins and are fully developed on the sedimentary cover (Figs. 3.4, 3.6 and 3.7). Their transparent and discontinuous acoustic character suggests that they are composed of reworked sediment. They also suggest high flow velocity (Wellner et al., 2001) and indicate the direction of the ice flow (Gilbert et al., 2003), providing evidence for a prominent turn of the flow towards the east at the slope platforms (Fig. 3.7A). This change in trend suggests that the ice stream direction is topographically controlled by troughs, but it is controlled by a different factor on the slope platforms. In the CBB, the flow direction is interpreted as controlled by the regional profile of the ice sheet, which would slope towards the northeast on the AP margin and towards the SE on the SSI margin. Glacial lineations on the CBB are similar to the "bundle structures" described on the Boyd-Gerlache Strait and characterized as a set of subparallel ridges and grooves, up to 40 m high and 1-3 km wide (Canals et al., 2000; Heroy and Anderson, 2005). The overlapping between glacial lineations with different directions observed off the Orleans Trough on the WP (Fig. 3.7A) is interpreted

as the result of a reactivation phase of ice stream advance during the last ice sheet retreat, which was more affected by the northeastward turn of the flow.

The *grounding zone wedges* identified on the WP were deposited as morainal ridges during stillstands that punctuated the last ice sheet retreat. This is suggested by their preservation in an area where glacial lineations indicate that the grounding zone reached the slope platform-edge (Fig. 3.7A) (Alley et al., 1989; Banfield and Anderson, 1997; Bart and Anderson, 1997b; Anderson, 1999; Evans et al., 2005; McMullen et al., 2006).

The *furrows* occur on the AP slope platforms (Figs. 3.4 and 3.8). Their morphology and their position in the stratigraphic record, affecting glacial lineations and covered by stratified deposits, suggest that they are giant iceberg plough marks resulted from iceberg erosion on the seafloor (Kuijpers et al., 2007). The levees bordering the furrows and forming positive relief are interpreted to be composed of ice-pushed sediment (Fig. 3.8E). The trend of furrows is indicative of ENE-trending iceberg drifting.

Finally, the *draping sheet* that covers most of the slope platforms and basin is interpreted as a glaciomarine sheet (Fig. 3.11). It was deposited by a combination of ice-rafting (including sediment settled from ice shelves and icebergs), sediment plumes of subglacial origin and a range of marine processes, such as hemipelagic deposition (Anderson, 1999). Hemipelagic sedimentation may include fine terrigenous particles with different sources, such as subglacial discharge from tidewater glaciers, fluvial discharge from land-based glaciers and volcanic dust, and biogenic particles provided by the surface plankton productivity (Fabrés et al., 2000). The absence of the draping sheet on the continental shelf, upper slope and outer parts of the slope platforms (Fig. 3.11A) indicates that the contribution of hemipelagic sedimentation is less relevant than the glaciomarine contribution, which occurred mostly on the inner parts of the slope platforms.

4.1.2. Slope-basin sedimentary system

This system includes several types of features related to gravity processes in the distal domains of the CBB margins and basin: *trough mouth fans*, *slope aprons*, the *Gebra-Magia slide complex* and *turbidity systems* (*gullies* and *turbidity channels*).

The *trough mouth fans* on the slope platform-edge and lower slope are formed by sediment transported within the ice streams, channelized along glacial troughs and deposited seaward of the grounding zone (Alley et al., 1989; Punkari, 1997; Dahlgreen et al. 2005). These features have also been called *till deltas* or *glacier-fed fan systems* (Laberg and Vorren, 1995; Davies et al., 1997; Dowdeswell et al., 1998). They comprise glacigenic sediments which moved downslope through the action of gravity flows (Laberg and Vorren, 1995; Vorren and Laberg, 1997; Casas et al., 2004). Trough mouth fans are point-sourced features, and they are

responsible for the sinuous shape of the platform-edges of the SSI and AP margins (Figs. 3.4 and 3.9A,B). Slope platforms protrude off the mouths of troughs (especially on troughs of the SSI margin and the Orleans, Lafond, Laclavere and Mott Snowfield troughs on the AP margin), with a marked displacement to the east. The vertical stacking of stratified units observed in the airgun seismic records indicates that they have developed through several glacial cycles, favoring the progradation and sinuosity of the margin (Fig. 3.9C).

The *slope aprons* are composed of the scar-and-lobe complexes and are responsible for the dismantlement of the slope as the result of submarine instabilities related to the high gradients of the lower slope, which reach values higher than 25º. Scar-and-lobe complexes differ along the CBB margin regarding the morphology and location of the sedimentary lobes: irregular lobes on the lower slope and elongated lobes on the basin (Figs. 3.4 and 3.14). The type of sediment involved in the instability processes may control the resultant lobe morphology (Llave et al., 2008). In this sense, the hunging irregular lobes on steep areas of the SSI lower slope lacking trough mouth fans (Fig. 3.14A), would be related with instabilities affecting relatively coarse and unsorted sediment. The mass transport (e.g. debris flows and related dense mass flows) would undergo very short displacement and deposition would take place at short distances from the scars (less than 5 km). In contrast, more elongated and gentle lobes that reach the basin in areas with well-developed trough mouth fans (Fig. 3.14B) are interpreted as the result of turbidity flows or diluted mass flows that involve reworked, finer-grained sediment from the trough mouth fans.

The *Gebra-Magia slide complex* consists of a complex system of submarine mass movements in the eastern sector of the AP lower slope and basin that has been revealed for the first time in this work (Fig. 3.13). The major features are the Gebra and Magia slides, but the surrounding area displays a variety of minor features also controlled by gravity-driven sediment transport processes (e.g. slides, turbidites and mass flow deposits). The downslope-oriented lineations on the Gebra and Magia valley seafloor indicate the trajectories followed by the mass flows. They may be interpreted as the result of differential movements within single mass flow deposits and/or as ridges and scours formed by the contact between different sediment mass flow deposits (Masson et al., 1993; Cochonat and Piper, 1995; Ercilla et al., 2000). Neither the age of these slides nor their relation to the glacial history are properly constrained, but several triggering mechanisms have been proposed for the Gebra slide, which could also be generally considered for the Magia slide and the rest of gravity-driven features. The initiation of the Gebra slide is attributed to a combination of factors, such as high sedimentation rates during the last glacial period, the unloading effect of a retreating ice sheet during deglaciation, the pre-existing tectonic fabric and seismicity (Imbo et al., 2003; Casas et al., 2004).

Finally, the *turbidite system* comprises two architectural elements: gullies and isolated channels. *Gullies* are more frequent at locations where glacial lineations reach the platform edge with a perpendicular orientation, and are interpreted as the result of the erosion by sediment supplied by the ice sheet during its advance and glacial maximum when the ice sheet grounded at the slope platforms edge (Figs. 3.4 and 3.10). The gullies occur as "fresh features" with a present-day morphologic expression, suggesting their recent formation and/or activity. The *turbidity channels* are the result of channelized mass wasting processes on the lower slope (Figs. 3.4 and 3.14A,B). This is suggested by their occurrence in areas where trough mouth fans and numerous scars are identified on the slope platform and lower slope. Turbidity channels are interpreted as the result of gravity processes that affect sediment deposited on trough mouth fans, which—in contrast with slope apron systems—would be finer and/or more sorted sediment. Turbidity channels may have developed along the course of successive events.

4.1.3. Seabed fluid outflow sedimentary system

The presence of pockmarks suggests the occurrence of fluid flow events. The concentration of pockmarks on the outer parts of the AP glacial troughs and on the AP slope platforms off troughs indicates that fluid flow events affected the sediment supplied by ice streams (Figs. 3.4 and 3.12). This process is related to the excess pore fluid (gas or pore water) pressure in the sediment, which caused the fluidization of the sediment and its ejection through the overbearing sediments into the water column with the gas and/or water during the consolidation processes (Judd and Hovland, 2007). The formation of pockmarks affecting glaciomarine till has been documented in several glacial settings (Harrington, 1985; Kelley et al., 1994; Ussler et al., 2003; Judd and Hovland, 2007). The seismic record does not offer evidence of gas intervention (e.g. wipe-outs, bright spots and blanking), but it indicates that the pockmarks are recent features affecting near-surface sediment, and also that some pockmarks are filled with sediment while others remain unfilled. This suggests that these features developed at different times and/or that some of them are inactive and have been covered by the glaciomarine draping sheet.

4.1.4. Contourite sedimentary system

Contourite drifts in the CBB can be classified as mounded and elongated separate drifts (Faugères and Stow, 1993; Faugères et al., 1999) (Figs. 3.4 and 3.15). The drifts and the associated contourite moats are the result of the activity of contour currents on the seafloor (McCave and Tucholke, 1986; Faugères et al., 1993, Faugères and Stow, 1993; Faugères et al., 1999; Stow et al., 2002). The moat was created by localized erosion beneath cores of constrained currents (Stoker et al., 1998), generally parallel to upslope- and alongslope-migrating mounded and elongated separate drifts (Faugères and Stow, 1993; Faugères et al., 1999). Mesoscale flow structures such as eddies and splitting of the deep flow into different

branches as a result of the bottom topographic control (López et al., 1999) may be responsible for accelerations and concentration of the bottom currents that caused erosion of the lower slope, excavation of the contourite moat at the foot of the lower slope and deposition of the contourite drift at its right side. The most prominent topographic highs that would affect deep currents at the basin floor are the Three Sisters and Orca volcanic edifices. Internal unconformities in the layered sub-parallel reflections on the TOPAS profiles indicate that contourite drifts developed during different phases, probably related to changes in the deep current circulation (Fig. 3.15).

4.2. Controlling factors and their interplay within the sedimentary systems of the CBB

The characterization of the CBB sedimentary system, in terms of architectural elements, processes and their spatial linkages, suggests that four factors have controlled the recent sedimentary evolution of the CBB. Glacial/interglacial cyclicity is interpreted as the main controlling factor, followed by physiography. However, tectonics and oceanography also play a role in controlling sediment distribution and the development of some morphological features.

4.2.1. Glacial/interglacial cycles

Glacial/interglacial cyclicity controlled the development of most of the sedimentary systems on the CBB, which are interpreted to have developed during the last glacial/interglacial cycle, although the glacial troughs, the trough mouth fans and the Gebra-Magia slide valley complex are the result of successive cycles. The glacial troughs and trough mouth fans are the result of erosion by ice streams on the shelf and upper slope and the corresponding deposition of prograding mass wasting deposits on the outer slope platforms and lower slope, respectively. The vertical stacking of these deposits indicates that they are the final product of successive cycles (Jeffers and Anderson, 1990; Prieto et al., 1999; García et al., 2006b). The Gebra-Magia slide complex is also interpreted as the result of numerous mass movement events, as indicated by the thickness of sediment involved (scars up to 150 m high) which affect the whole post-rift stratigraphy (Prieto et al., 1999; García et al., 2006b) and by the presence of erosive and depositional mass movement-related features, both buried ancient and recent (Casas et al., 2008). These processes could have occurred during the initial interglacial stages, when melting of the ice sheet favored the discharge of a large volume of sediment, and during the full interglacial stages due to isostatic rebound. This complexity and previous works on these slides indicate a long record of slope failures in this sector of the AP margin, but further studies are required to understand the multiple phases of failure that have occurred in this area.

The architectural elements/sedimentary systems were formed in two different stages during the last glacial/interglacial cycle (Fig. 3.17): (a) last ice sheet advance and Last Glacial Maxima (LGM); and (b) ice sheet retreat and present interglacial.

a) Ice sheet advance and LGM

During the last advance of the ice sheet, the shelf suffered intense erosion which was enhanced along glacial troughs, where fast-flowing ice streams were channelized (Fig. 3.17A). The typical occurrence of erosional grooves, knickpoints, drumlins and glacial lineations developed at the seafloor of the glacial troughs of the AP margin according to the type of substrate. The grounding line reached the most distal position at the slope platform edges (750 to 950 m on the WP, 700 to 1000 m on the EP and 540 to 1000 m on the SSI slope platforms), as indicated by the glacial lineations, which suggest a general NE direction of the ice flow on the AP margin and an E-SE direction on the SSI margin. Gravity-related features (trough mouth fans and gullies) developed on the outer slope platforms and lower slope, as a result of the high amount of sediment supplied by the ice sheet and ice streams. The location of trough mouth fans, displaced to the E of the trough mouths, also suggests the general eastwards trend of the ice flow.

b) Ice sheet retreat and interglacial

The ice sheet started to retreat 17340 cal yr B.P. in the CBB area (Heroy and Anderson, 2005). A later re-advance of the ice stream that flowed along the Orleans Trough is interpreted to have occurred as suggested by the set of glacial lineations that overlap older ones and have a more pronounced NE trend on the WP. Moreover, grounding zone wedges on the WP suggest that the ice retreat was punctuated by at least two stillstand periods. During this stage, glaciomarine and marine processes predominated in the CBB (Fig. 3.17B). Furrows formed by iceberg ploughing during the start of the ice sheet retreat, as indicated by their location at present-day water depths of 650-750 m. The concentration of these features on the eastern part of the slope platforms of the AP margin at similar depths and the homogeneity in their morphological parameters suggest that they were created contemporaneously in different areas, probably in relation to a massive ice sheet calving event at the start of the ice sheet retreat. Gullies may have been active also during this stage, as conduits that channelized sediment-laden flows produced by the melting of the ice sheet. Pockmark fields developed on the slope platforms of the AP margin, affecting the sediment deposited during the previous stage. Sediment deposited on trough mouth fans was affected by instabilities and developed gravity-related features such as slope aprons and turbidity channels. A combination of glaciomarine processes (sub-ice shelf and open-marine processes) deposited the draping sheet during this stage.

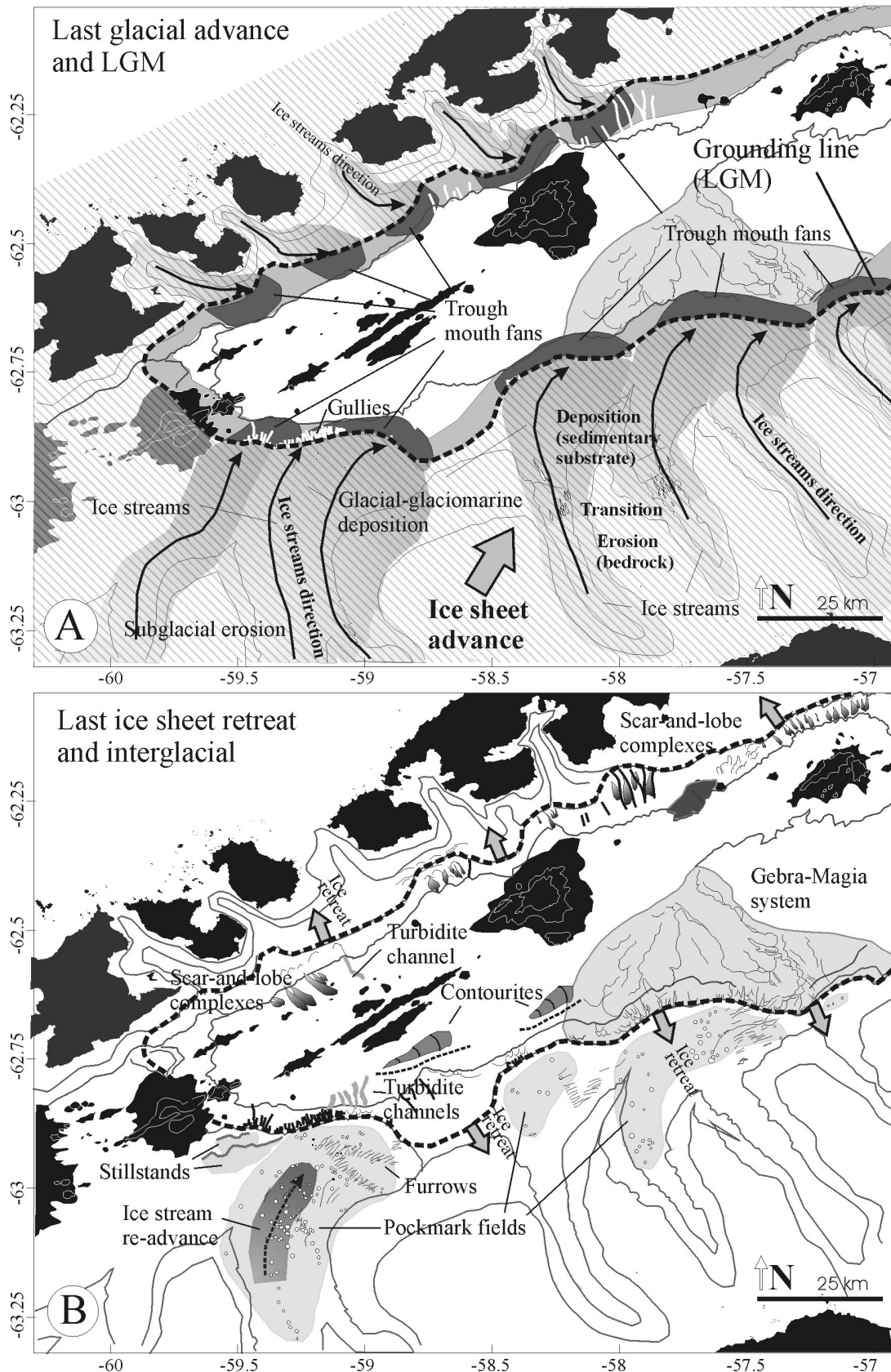Figure 3.16. Sedimentary reconstruction during the last glacial cycle. A) During the last glacial advance and Last Glacial Maximum the ice sheet grounding line reached the slope platform edge and sedimentary features of glacial and glaciomarine origin developed. B) During the last ice sheet retreat and interglacial stage glaciomarine and marine features developed in the study area. See legend in Figure 3.4.

4.2.2. Tectonics

The main tectonic control on the CBB affects the location and trend of glacial troughs, especially in the eastern area, where the most recent tectonic deformation is concentrated (Prieto et al., 1998). The troughs in the eastern area of the AP margin and the troughs on the SSI margin have a NNW trend, oblique to the ice-sheet flow direction indicated by the glacial lineations and trough mouth fans (Fig. 3.4). This indicates that the troughs have a structural control, which can be related to a set of NNW-SSE strike-slip transfer faults (Jeffers and Anderson, 1990; Barker and Austin, 1994; Gràcia et al., 1996; Maestro et al., 2007). A similar tectonic control on the glacial troughs trend has been reported in other areas of the AP margin (Camerlenghi et al., 2001). In contrast, on the WP the trend of the Orleans and Trinity Passage troughs is approximately parallel to the direction of the ice flow indicated by the glacial lineations and suggests that the troughs are glacially-controlled.

A combination of recent tectonic activity and high sediment accumulation on the trough mouth fans may have been the cause for the development of the Gebra-Magia instability complex. Earthquakes associated with the isostatic rebound after the ice sheet retreat may have acted as a triggering mechanism (Bryn et al., 2005; Solheim et al., 2005). At the same time, the recent tectonic deformation mostly concentrated in this area (Prieto et al., 1998) would explain the occurrence of the complex.

The location of the most important volcanic edifices seems to be structurally determined by the set of NNW-SSE strike-slip faults (Gràcia et al., 1996; Maestro et al., 2007). The evolution of volcanic edifices has been explained as a multi-stage process during three successive phases in relation to the extension of the basin (Gràcia et al., 1996) or as the result of eruptive activity along rift structures (Lawver et al., 1996). This work has provided evidence that, although volcanic edifices represent striking structural features on the basin, their activity and formation have not substantially affected the development of the sedimentary system. They have only played a local role in the distribution of the sediment that finally reached the basin (e.g. contourite systems).

Finally, the role of tectonic subsidence or uplift in the sedimentary processes of the CBB can not be properly constrained with the dataset used in this study, but it is likely to have had an effect in the sedimentary evolution. Tectonic subsidence and structural or lithological weakness have been interpreted as an important control on nearby and similar areas of the AP (Camerlenghi et al., 2001).

4.2.3. Physiography

The asymmetry of the basin and the general physiographic scenario is inherited from the processes involved in the basin opening (Jeffers and Anderson, 1990; Maestro et al., 2007). The physiography of the margin controls the high gradients of the lower slope, up to 25º, where most of the slope apron systems occur due to the succession of small-scale slides on the upper parts of the lower slope and the deposition of sedimentary lobes on the lower parts.
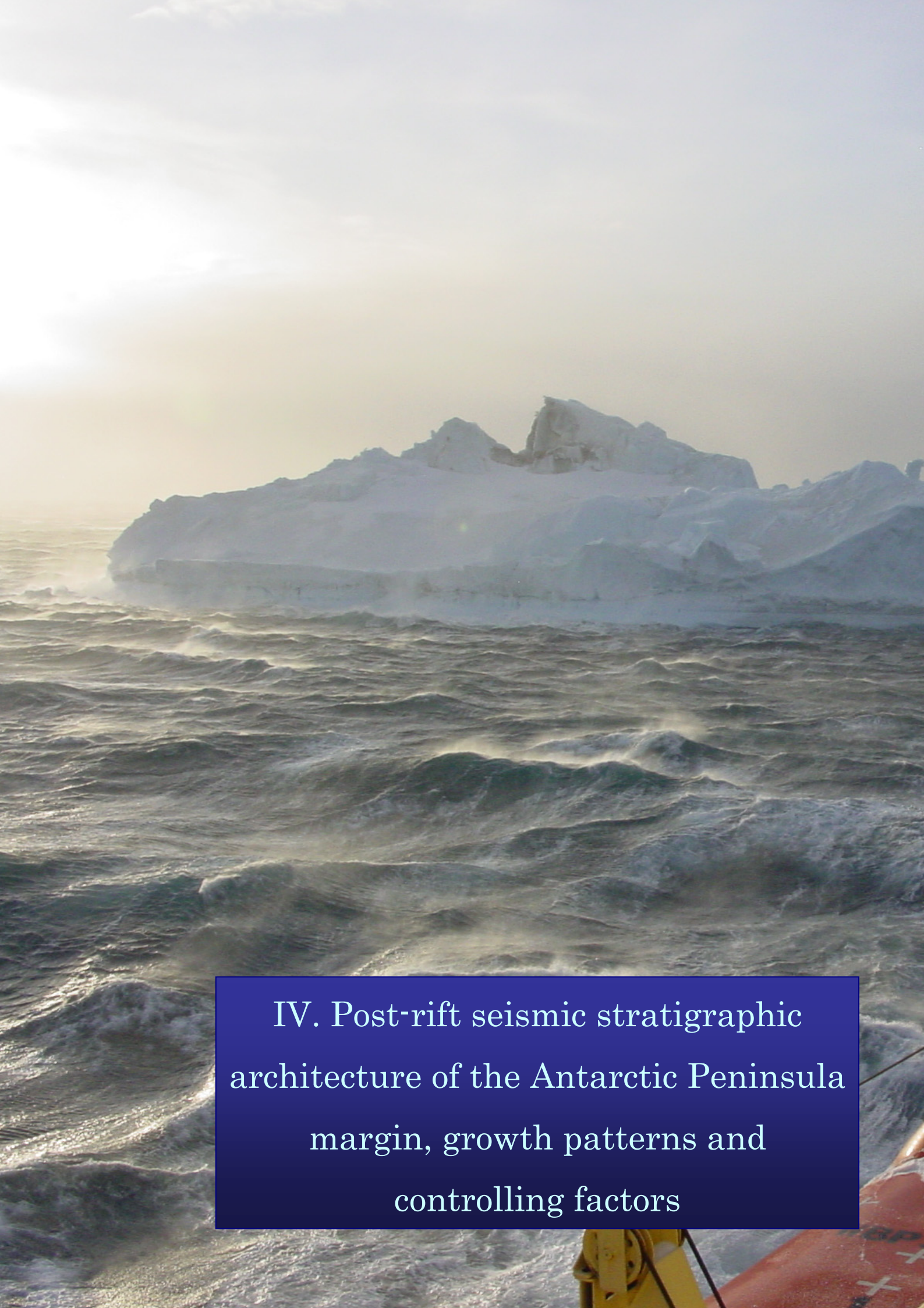
4.2.4. Oceanography

Oceanography exerts a local control on the morphology of the CBB basin, where contourite deposits occur as the result of the erosive and depositional capability of deep currents. Oceanographic studies of the deep currents in high-latitude areas are not well developed and contourite deposits may provide a good tool for inferring the circulation patterns (Hernández-Molina et al., 2006). In this area, deep SW-trending currents may occur on the basin, and their acceleration by the topographic effects is responsible for the development of contourites. The turbidite channel on the SSI margin also seems to be affected by the NE-trending Bransfield Current (Grelowski et al., 1986; López et al., 1994, 1999; Gomis et al., 2002), which would force the curvature of the channel towards the northeast. The oceanographic control in the CBB is local and it is interpreted to have played a significant role only during interglacial stages, since the extension of the ice sheet would hinder the establishment of strong deep currents during the glacial advance and maximum and/or the glacial processes would obliterate their effect on the sedimentation.

4.3. AP *vs*. SSI margins

Major differences in the sedimentary systems can be observed between the two CBB margins (Fig. 3.4), including: (1) the relative importance of the main controlling factors (glacial/interglacial cyclicity predominates on the AP margin and tectonics and physiography predominate on the SSI margin); (2) the smaller size of the trough mouth fans on the SSI margin; (3) the absence of some features on the SSI margin (the succession of features on the troughs seafloor, iceberg plough marks and pockmark fields); and (4) the greater occurrence of slope apron systems on the SSI margin than on the AP margin.

The differences between the SSI and AP margins are interpreted as a "matter of size" effect. The physiography of the basin is determined by the recent rifting, about 4 Ma (Barker and Burrell, 1977; Anderson et al., 1990; Jeffers and Anderson, 1990; Barker, 2001; Galindo-Zaldívar et al., 2004). The opening of the basin occurred in a complex tectonic setting that gave rise to a markedly asymmetrical basin, with a narrow and steep SSI margin and a wide and gentler AP margin. Tectonics has controlled the development of both margins, but glacial/interglacial cyclicity has been more effective in modelling the evolution of the AP

margin. Here, the greater extension of the drainage areas, which occupy the entire AP, has produced thicker and wider ice sheets that have supplied higher amounts of sediment to the margin. As a result, wide slope platforms have developed on the AP margin, due to the coalescence of trough mouth fans from different glacial troughs. In contrast, tectonics and physiography are the main controls in the configuration of the SSI margin, and glacial/interglacial features are relatively poorly developed, as the result of the smaller size of ice sheets and the lower amount of available sediment on the narrow SSI margin.

IV. Post-rift seismic stratigraphic architecture of the Antarctic Peninsula margin, growth patterns and controlling factors

1. Introduction and dataset

This chapter is focused on the study of acoustic facies and the analysis of the seismic stratigraphy of the AP margin of the CBB. The relatively young age of the Bransfield Basin and its Plio-Quaternary sediment fill make this area particularly well suited for examining the stratigraphic record of climate change and glacial evolution in the northern Peninsula region.

Although few previous studies have dealt with this issue (Banfield and Anderson, 1995; Jeffers and Anderson, 1990; Prieto et al., 1999), this work provides a more detailed seismic stratigraphic analysis from the availability of new higher-resolution data. The general aims of this chapter are:

- The analysis of seismic sequences of the continental shelf to slope and the study of the factors that control the stratigraphic architecture in the AP margin;

- The establishment of a new constraint on the chronology of glacial cyclicity; and

- The interpretation of the effect of the Antarctic Peninsula Ice Sheet dynamics and its interaction with the local factors that have controlled the post-rift deposition on the AP margin of the CBB.

The seismic stratigraphic analysis is based on the study of single-channel airgun seismic reflection profiles acquired during the MAGIA99 cruise on board the R/V Hespérides (Fig. 4.1). Most lines were oriented perpendicular to the continental margin, from the continental shelf to the basin. Aditionally, the multibeam bathymetric dataset obtained during the GEBRA93 cruise were used for the interpretation of sedimentary features.
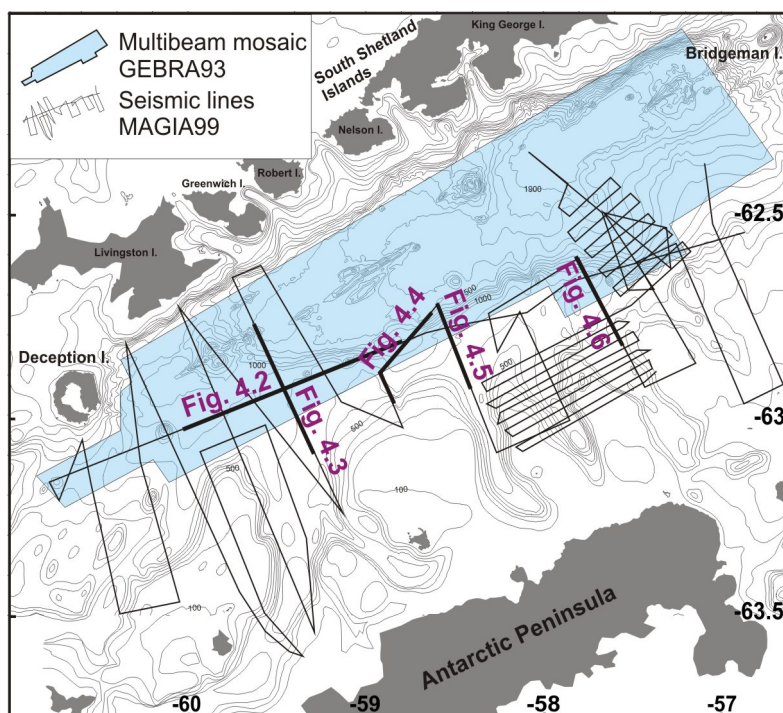

Figure 4.1. The dataset includes seismic lines obtained during the MAGIA99 cruise and a multibeam survey conducted during the GEBRA93 cruise, both on board the R/V Hespérides.

2. Seismic study: acoustic facies, stratigraphy and deposits

2.1. Acoustic facies analysis

The study of acoustic facies followed the method described by Damuth (1980). Five acoustic facies were differentiated based on acoustic amplitude, lateral continuity, geometry and reflection internal configuration. The acoustic facies are: Layered facies (L), with four subtypes, Parallel (LP), Oblique (LO), Wavy (LW) and Irregular (LI); Chaotic facies (Ch), with two subtypes, Indistinct (ChI) and Mounded (ChM); Semitransparent facies (S); Prolonged facies (P); and Hyperbolic facies (H). Descriptions of these facies are provided in Table 4.I.
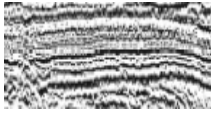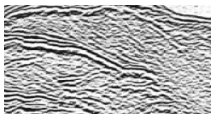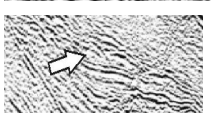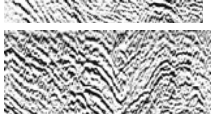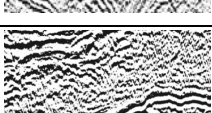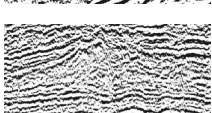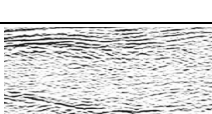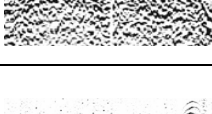
Type	Subtype	Seismic expression	Acoustic amplitude	Lateral continuity	Geometry	Internal configuration
Layered (L)	Parallel (LA)		Medium to high	High	Tabular	Parallel to subparallel
	Oblique (LO)		Low to medium	Medium	Wedged	Basinwards dipping
	Wavy (LW)		Medium	High	Irregular	Subparallel undulated layered
	Irregular (LI)		Medium to high	Low	Massive	Very deformed and folded
Chaotic (Ch)	Indistinct (ChI)		Medium to high	Very low to low	Massive	No internal organization
	Mounded (ChM)		Low	Low	Mounded or wedged	No internal organization
Semitransparent (S)			Low	No reflections	Mounded or tabular	No reflections
Prolonged (P)			High	High	Irregular	High-amplitude bottom reflection, with no underlying reflections
Hyperbolic (H)			Medium to high	Low	Irregular	Hyperbolic bottom reflections with no underlying reflections

Table 4.I. Characteristics of the acoustic facies identified on the AP margin.

2.2. Seismic stratigraphy

Based on the high-resolution seismic profiles (Figs. 4.2 to 4.6), the stratigraphic succession is composed of acoustic basement overlaid by a basal sequence composed of irregular reflections dominated by Prolonged and Layered Irregular facies on the shelf and upper slope, Hyperbolic facies on the floor of troughs and Layered Irregular and Oblique facies on the slope platforms and lower slope. The basal sequence is interpreted as the syn-rift sequence and it corresponds to the lower part of the Lower Sequence of Prieto et al. (1999) on the slope platforms and lower slope (Table 1.I). This syn-rift sequence outcrops at the base of the upper slope and at the most distal parts of troughs, where the seafloor is an erosion surface (Figs. 4.2 to 4.6).

Two seismic sequences, designated S1 and S2 from younger to older, overlie the syn-rift sequence. Their lower boundaries are prominent unconformities (U1 and U2, respectively), while the upper boundary of S1 is the present-day seafloor (Figs. 4.2 to 4.6). Sequences S1 and S2 have been correlated with sequences S1 and S2 of Jeffers and Anderson (1990), which are interpreted as post-rift sequences (Table 1.I). S1 and S2 pinch out in a landwards direction and unconformities U1 and U2 amalgamate in the same direction, to form an erosive surface that corresponds with the irregular seafloor (Figs. 4.2 to 4.6). These sequences are correlative along the slope, except in the eastern part, where the occurrence of sediment gravity flow processes during the post-rift period favored the vertical stacking of chaotic facies (Imbo et al., 2003) and the resolution of the available data make the definition of the outline of seismic sequences difficult (Figs. 3.4 and 3.12).

2.2.1. Lower Sequence S2

Sequence S2 was identified on the slope platforms and lower slope. The sequence overlies the U2 unconformity, onlapping the proximal slope platform and downlapping basinwards, where the lower limit deepens and cannot be detected in the seismic profiles (Figs. 4.2 to 4.6). The U2 isobath map shows that the slope formed a continuous NE-trending scarp, with no differentiation of slope platforms (Fig. 4.7A). The slope-break is especially abrupt in the eastern area (present-day EP), while it forms a ramp in the western area (present-day WP). The upper limit of S2 is the unconformity U1. The S2 isopach map indicates that this sequence represents the initial growth of the present-day EP and WP (Fig. 4.7B). Sequence S2 has a main depocenter on the EP, which is elongated in a direction parallel to the AP margin with a maximum thickness of 700 ms. On the WP, the thickness of S2 is generally less than 300 ms thick, except for a local 500 ms thick depocenter (Fig. 4.7B), and it is characterized by Oblique Layered facies forming wedges that prograde basinward.

Figure 4.2. Seismic profile and line drawing showing the interpretation of seismic sequences and units. This line crosses the WP in a WSW-ENE direction (see location of this line in Figure 4.1). Legend: S1: upper seismic sequence; S2: lower seismic sequence; U1 and U2: unconformities; m: multiple.
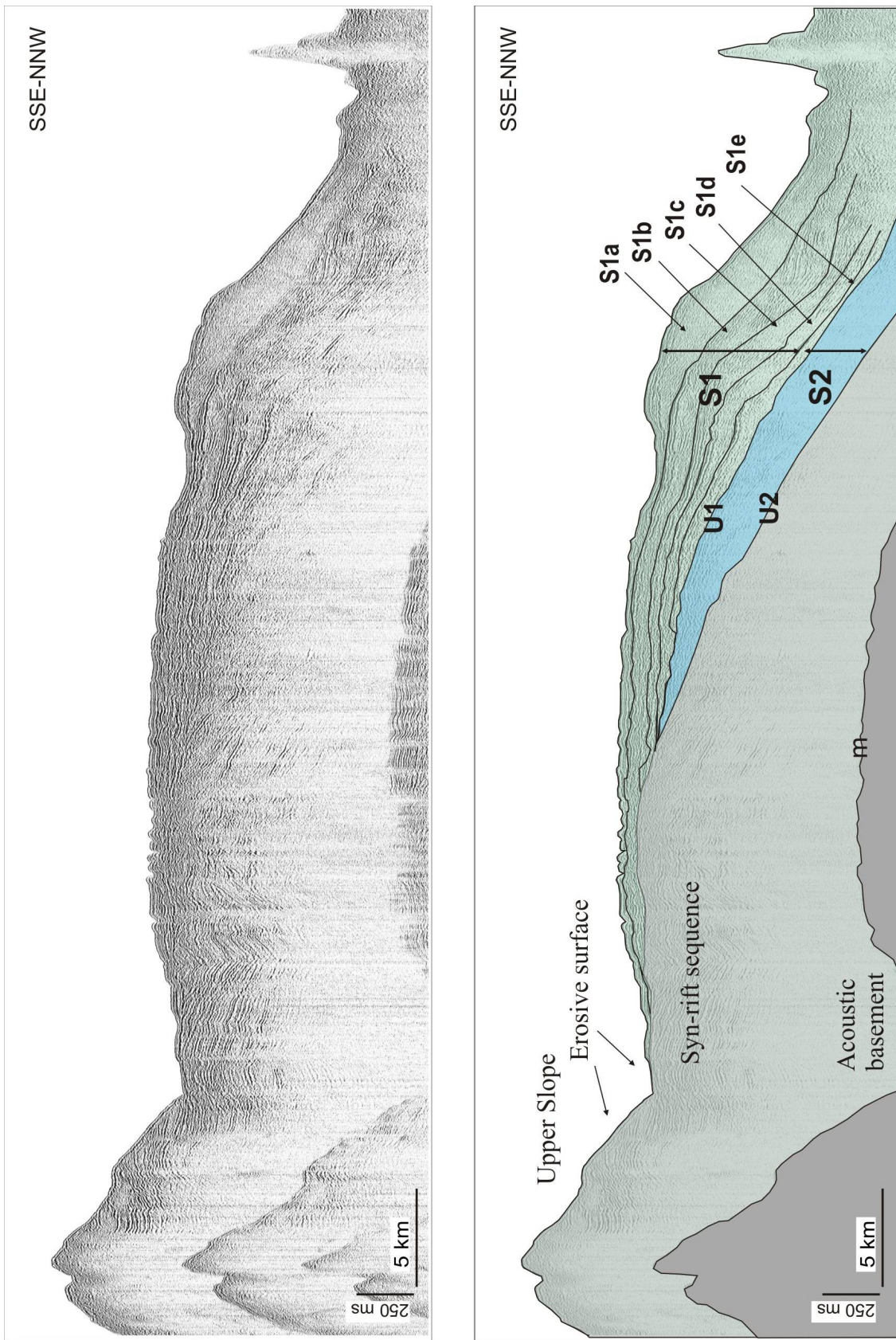
Figure 4.3. Seismic profile and line drawing showing the interpretation of seismic sequences and units. This line crosses the WP in a SSE-NNW direction (see location of this line in Figure 4..1). Legend: S1: upper seismic sequence; S2: lower seismic sequence. U1 and U2: unconformities; m: bottom multiple.
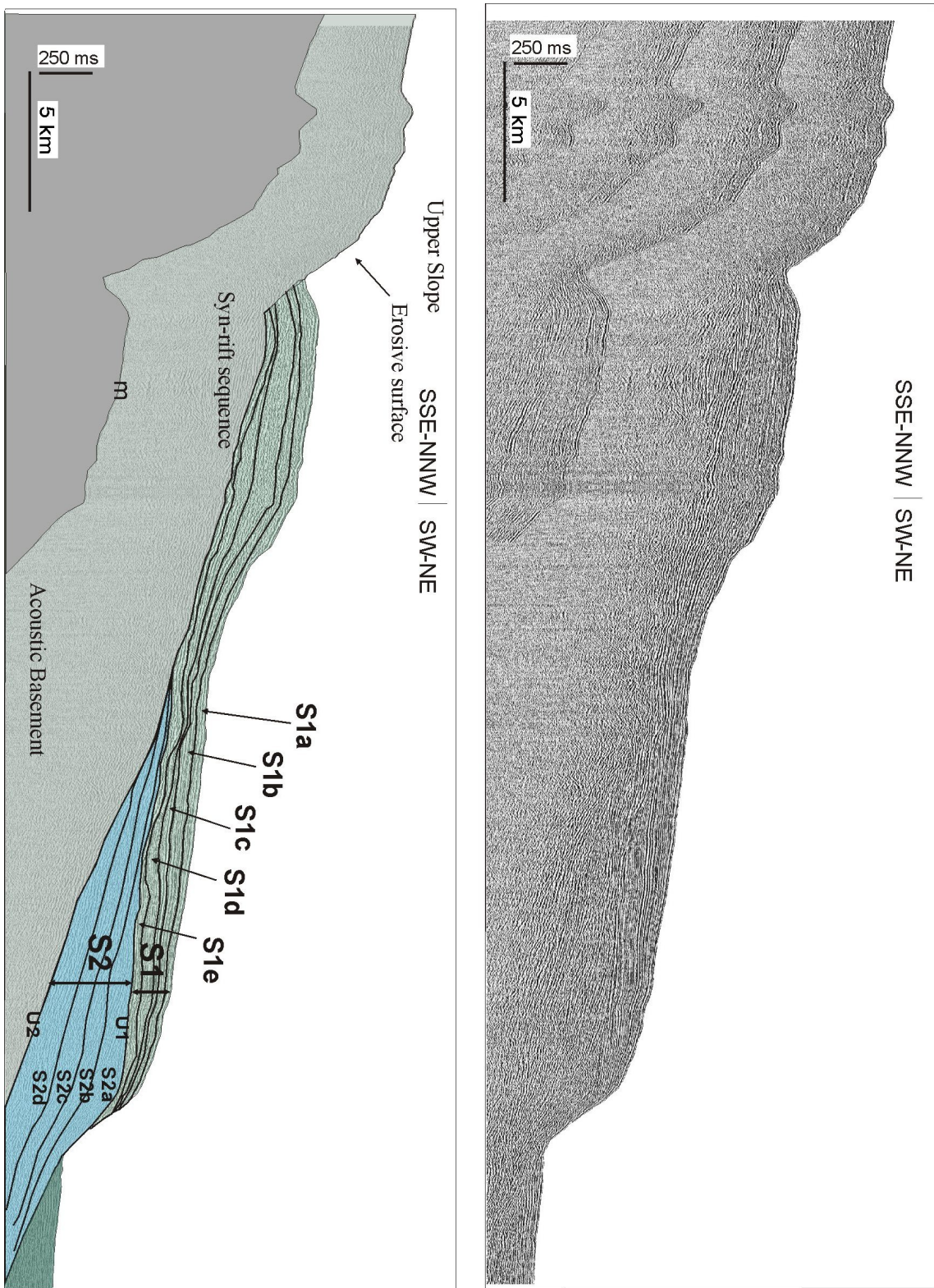
Figure 4.4. Seismic profile and line drawing showing the interpretation of seismic sequences and units. This line crosses the EP in a SSE-NNW direction (see location of this line in Figure 4.1). Legend: S1: upper seismic sequence; S2: lower seismic sequence. U1 and U2: unconformities; m: bottom multiple.
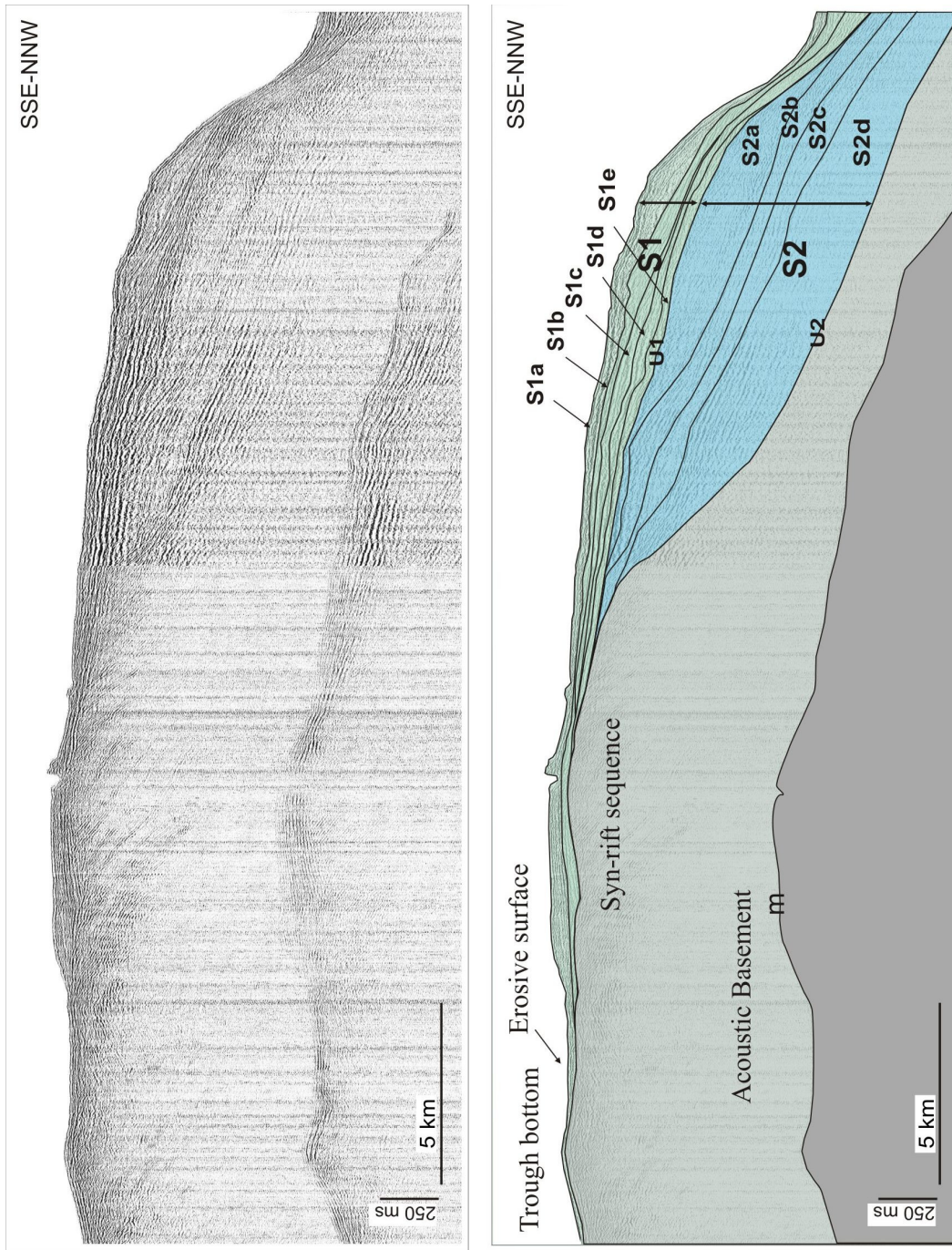
Figure 4.5. Seismic profile and line drawing showing the interpretation of seismic sequences and units. This line crosses the EP in a SSE-NNW direction (see location of this line in Figure 4.1). Legend: S1: upper seismic sequence; S2: lower seismic sequence. U1 and U2: unconformities; m: bottom multiple.
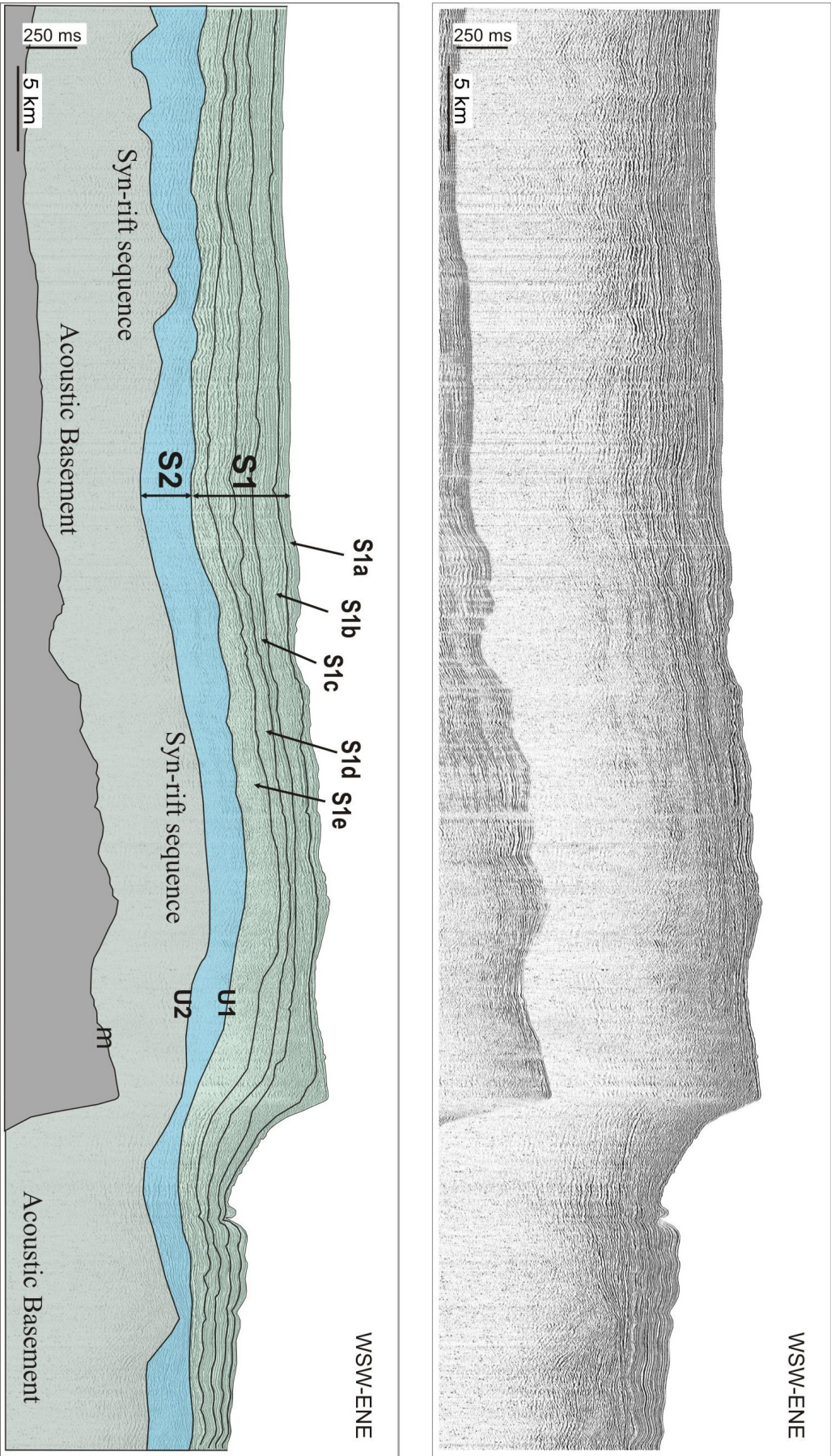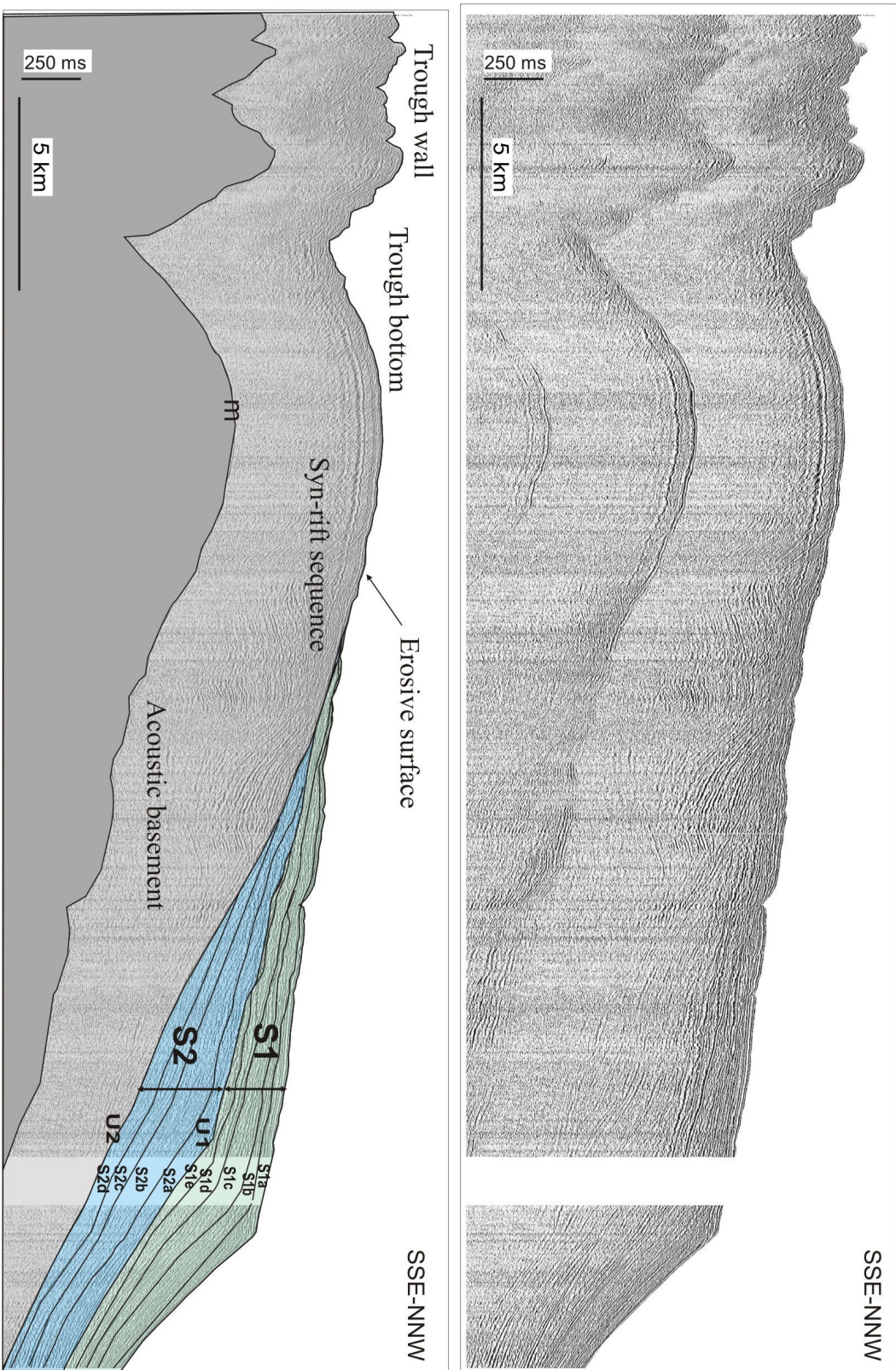
Figure 4.6. Seismic profile and line drawing showing the interpretation of seismic sequences and units. This line crosses the EP in a SSE-NNW direction (see location of this line in Figure 4.1). Legend: S1: upper seismic sequence; S2: lower seismic sequence. U1 and U2: unconformities; m: bottom multiple.

On the WP no seismic units can be differentiated within S2, but on the EP the seismic records show four units. They are designated S2d to S2a, from older to younger, and are bounded by the unconformities U2c to U2a (Figs. 4.4 to 4.6). Reflections onlap the unconformities in a landward direction and downlap towards the basin. The prograding character of units is represented by the geometry of the sedimentary packages, which reflects
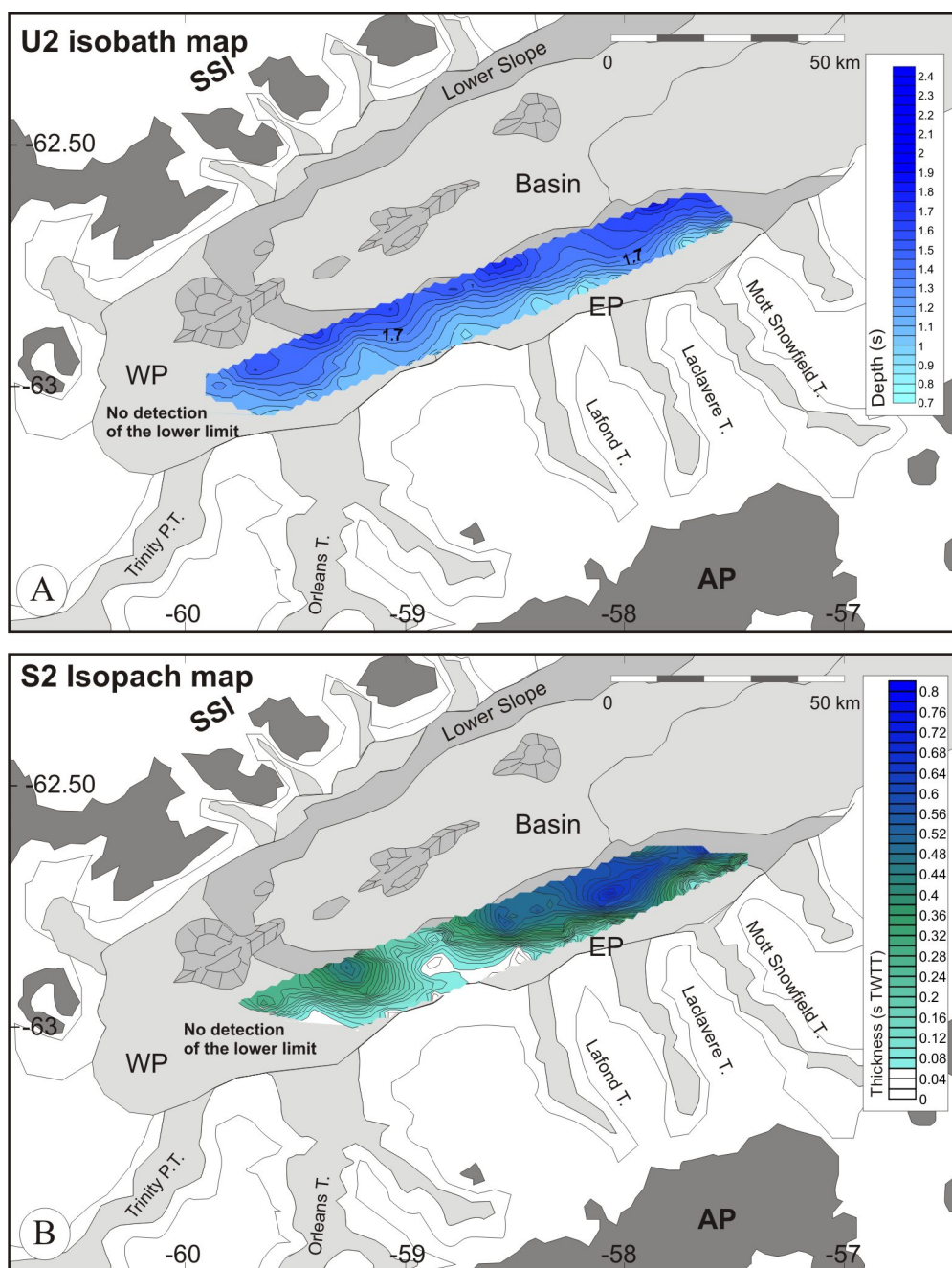
Figure 4.7. A) Isobath map of the unconformity U2. B) Isopach map of the unit S2. The lower limit cannot be detected on the WP.

basinwards growth of the margin. Units S2d to S2b show a similar distribution, with small depocenters (~200 ms) off the mouths of the troughs (Fig.4.8A to C). Unit S2a occurs mainly within a wide, 450-ms-thick depocenter on the EP-edge, between the mouths of the Laclavere and Mott Snowfield Troughs (Fig. 4.8D). The location of depocenters seaward of the mouths of glacial troughs indicates that the troughs were active during the deposition of S2. Seismic units S2d to S2a are characterized by Oblique Layered facies forming wedges that prograded basinward. Locally on the WP and proximal areas of the EP, Chaotic Indistinct facies form mounded bodies and Wavy Layered facies form irregular bodies (Figs. 4.2 to 4.6).
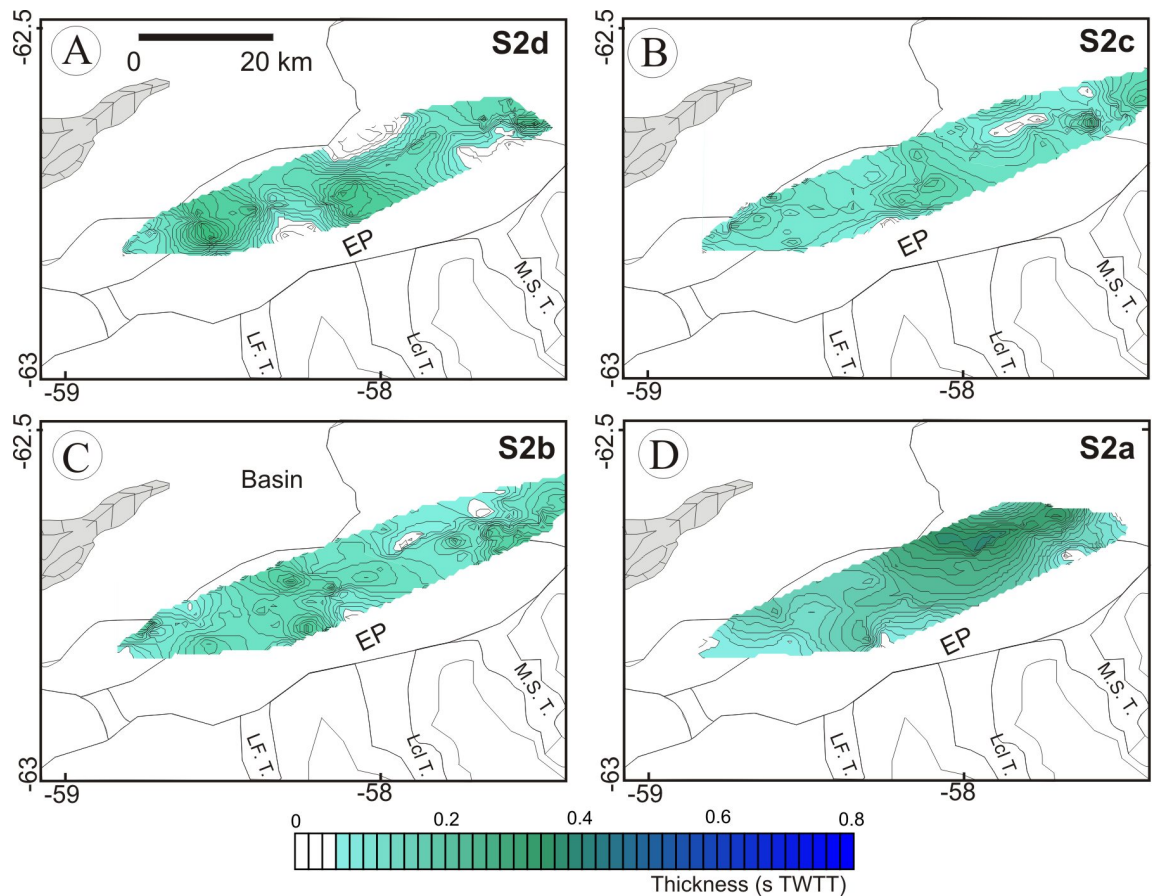
Figure 4.8. Isopach maps of the seismic units within the seismic sequence S2. These units can only be differentiated on the Eastern Platform and lower slope of the eastern part of the study area. Legend: LF.T: Lafond Trough; Lcl. T.: Laclavere Trough; M.S. T.: Mott Snowfield Trough.

2.2.2. Upper Sequence S1

The Upper Sequence S1 occurs on the continental slope, from the shelf break and within troughs down to the lower platform (Figs. 4.4 to 4.7). Sequence S1 overlies the U1 and has the seafloor as the upper limit. The contour map of the unconformity unconformity U1 shows that the template of the present-day physiography was already formed when this sequence was deposited, with the shelf dissected by troughs and a well-developed slope platform (Fig. 4.9A). The slope platform was continuous, with a linear AP margin-parallel WSW-ENE trend, and there was no differentiation between the western and eastern areas.
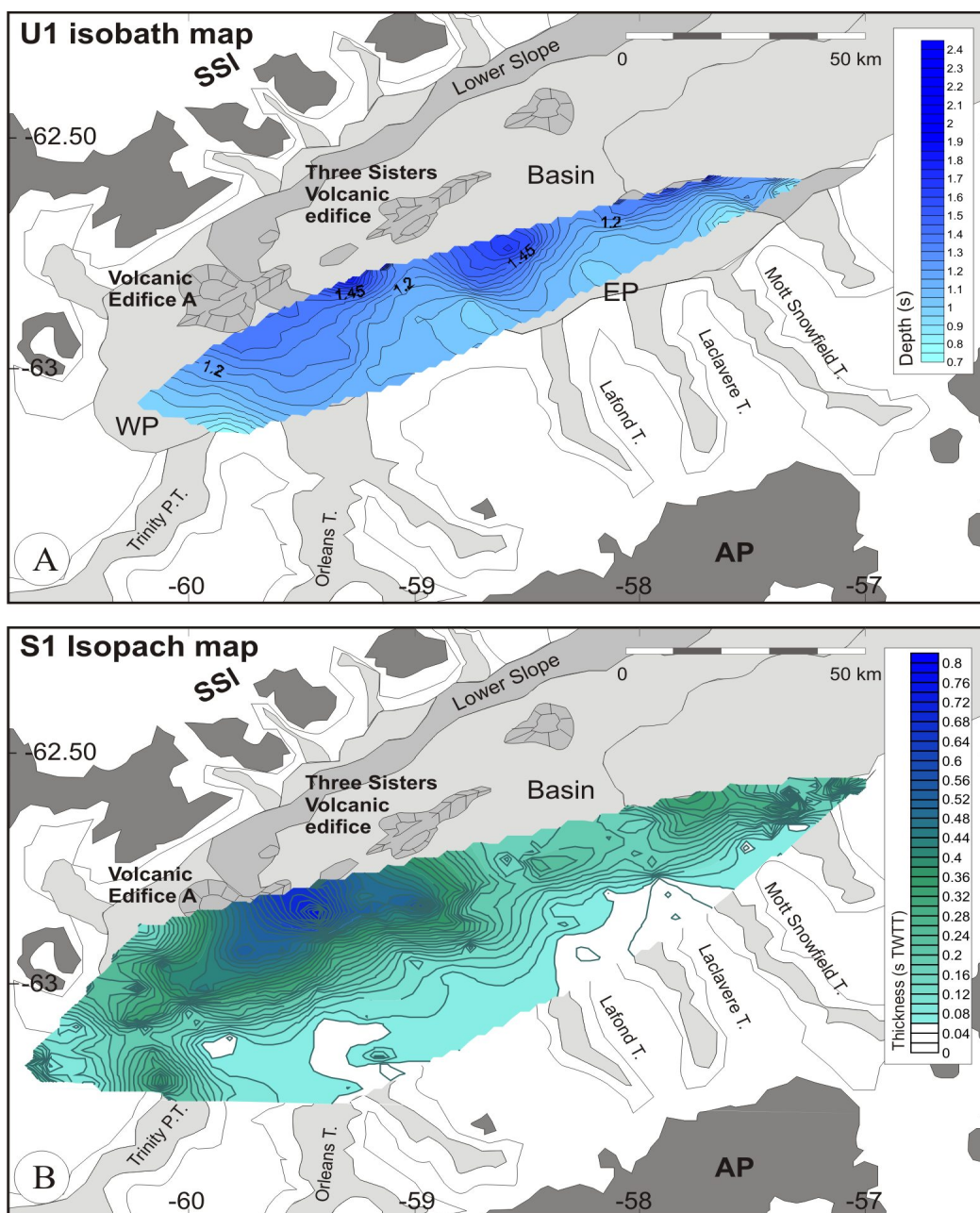
Figure 4.9. A) Isobath map of the unconformity U1. B) Isopach map of the unit S1.

The paleo-basin is located at about 1800 ms TWTT, beneath the present-day basin floor location of WP. The maximum depth (2.2 ms) occurs at the foot of the lower slope east of Volcanic Edifice A (Fig. 4.9A).

The main depocenter of S1 is located on the WP, off the Orleans Trough, and is oriented WSW-ENE (Fig. 4.9B). It represents infilling of the paleo-basin that marked the origin of the present-day WP, with a sediment thickness of more than 700 ms. Another large 400 ms thick depocenter occurs on the WP off the mouth of Trinity Passage Trough. On the platform edges, smaller 250 to 300 ms thick depocenters are located in the area between the WP and the EP and seaward of the mouths of the eastern troughs on the EP (250 to 300 ms thick).

Sequence S1 is composed of five seismic units (S1e to S1a, from older to younger) that, in general, display a common acoustic facies character (Figs. 4.4 to 4.6). The unconformities that bound the seismic units at the base become conformable or onlap surfaces on the proximal slope platforms and laterally correspond with downlap surfaces at the distal part of the slope platforms and lower slope. At the top, unconformities are erosive on the slope platforms and correspond with conformable surfaces at the most distal part of the slope platforms and lower slope. The vertical stacking pattern of the seismic units manifests both the aggradation and progradation that produce the upward and seaward outbuilding of the margin. The seismic units on the slope platforms display vertical and lateral changes in acoustic facies. Massive tabular packages of Chaotic Indistinct facies overlie the basal unconformity and, locally, bodies of Chaotic Mounded facies are also present. The top of the units is characterized by sheeted packages of Parallel Layered facies. On the platform-edges and lower slope, wedge-shaped packages of vertically stacked bodies with Oblique Layered facies are dominant and overlie the basal unconformity. Wavy Layered facies and Semitransparent facies occur only locally on the platform-edges and at the foot of steep scarps.

a) Seismic Unit S1e is laterally discontinuous and has been identified on the WP and locally on the EP, off the mouths of the easternmost troughs. The base of this sequence coincides with the unconformity U1 (Figs. 4.2, 4.3, 4.5 and 4.6). S1e depocenters occur mostly on the slope platform-edge, which is oriented in a direction parallel to the AP margin (Fig. 4.10). The main depocenter is 160 ms thick and occurs at a location east of the mouth of the Orleans Trough. Secondary WP (80 to 120 ms thick) depocenters are located on the WP, off the mouth of Trinity Passage trough. To the east, a small depocenter occurs on the EP in front of the Laclavere Trough (about 100 ms) and two depocenters occur on the WP-edge seaward of the easternmost troughs (100 and 120 ms).
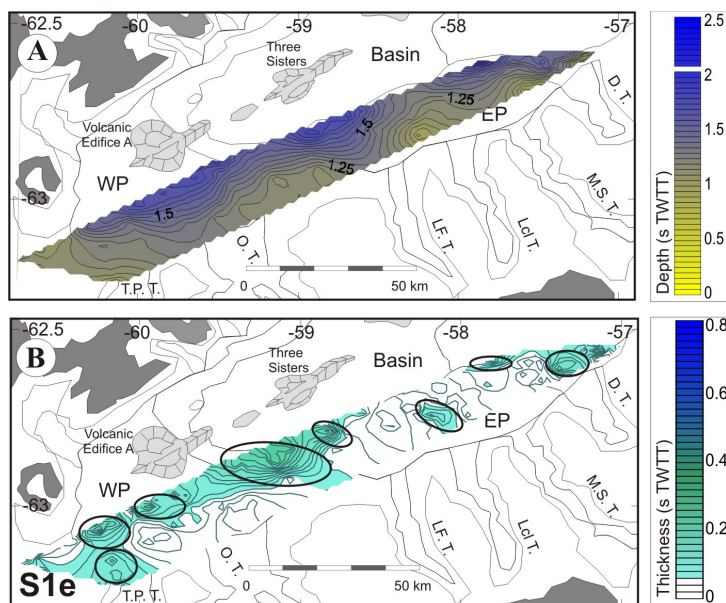
Figure 4.10. A) Isobath map of the unconformity U1 (base of S1e). B) Isopach map of the S1e seismic unit. Legend: LF.T: Lafond Trough; Lcl. T.: Laclavere Trough; M.S. T.: Mott Snowfield Trough. Circles mark the depocenters.

b) Seismic Unit S1d overlies the unconformity U1d. The contour map of U1d shows that the slope platform was continuous and the lower slope was more sinuous in plan view than the U1 surface. Unit S1d is mostly confined to the slope platform-edge (Figs. 4.2 to 4.6 and 4.11), with a main 160 ms thick depocenter off the Orleans Trough (160 ms) on the WP-edge and a secondary 100 ms thick depocenter at the mouth of the Mott Snowfield Trough on the EP-edge. A 100 ms thick sediment accumulation occurs on the platform-edge at the present-day limit between the WP and the EP. Another 110 ms thick depocenter occurs on the WP at the mouth of the Trinity Passage Trough.

Figure 4.11. A) Structure contour map of the base of seismic unit S1d. B) Isopach map of S1d. Legend: LF.T: Lafond Trough; Lcl. T.: Laclavere Trough; M.S. T.: Mott Snowfield Trough. Circles mark the depocenters.

91

c) The limit of Seismic Unit S1c is coincident at its southern margin with the limit of the underlying S1d unit, except in the mouth of the Lafond Trough, where seismic unit S1c is more extensive (Figs. 4.2 to 4.6). This seismic unit overlies the U1c unconformity, whose contour map shows a sinuous lower slope, located slightly to the south of the present-day position in the eastern area. Unit S1c is mostly confined to the slope platform-edges, and especially at their eastern extremes (Fig. 4.12). The maximum thickness of this unit is 170 ms in a wide rounded depocenter located off the mouth of the Orleans Trough. Other depocenters on the platform have elongate shapes parallel to the platform-edge, and occur on the present-day boundary between the WP and the EP (110 ms) and on the EP, off the Laclavere and Mott Snowfield Troughs (120 ms). A small depocenter also occurs on the WP at the mouth of the Trinity Passage Trough (100 ms thick).

Figure 4.12. A) Isobath map of the base of seismic unit S1c. B) Isopach map of S1c. Legend: LF.T: Lafond Trough; Lcl. T.: Laclavere Trough; M.S. T.: Mott Snowfield Trough. Circles mark the depocenters.

d) Seismic Unit S1b occurs above the U1b unconformity (Figs. 4.2 to 4.6). The contour map of this unconformity shows that the platform edge is sinuous and extended close to its present-day position, especially in the eastern area. Unit S1b is mainly concentrated in a wide, 240-ms-thick depocenter located on the WP, seaward of the Trinity Passage and Orleans troughs (Fig. 4.13). Smaller depocenters, 60 to 90 ms thick, occur on the EP in front of the mouth of troughs. S1b is very thin or almost non-existent at the boundary between the present-day WP and EP.

Figure 4.13. A) Structure contour map of the base of seismic unit S1b. B) isopach map of S1b. Legend: LF.T: Lafond Trough; Lcl. T.: Laclavere Trough; M.S. T.: Mott Snowfield Trough. Circles mark the depocenters.

e) Seismic Unit S1a overlies the U1a unconformity and its upper limit is the present-day seafloor (Figs. 4.2 to 4.6). It has relief very similar to the present-day seafloor, with the presence of a scarp separating the WP and the EP. The main depocenters occur at the platform-edge on both slope platforms. On the WP-edge, east of Volcanic Edifice A, the main depocenter has a circular shape and reaches a thickness of more than 250 ms (Fig. 4.14). A smaller depocenter 110 ms thick occurs off the Trinity Passage and Orleans troughs, while a uniform thickness of about 70 ms covers the rest of the WP. At the boundary between the EP and WP a small 80 ms thick depocenter exists. On the EP-edge, depocenters occur to the east of the mouths of the Laclavere (150 ms), Lafond (80 ms) and Mott Snowfield (120 ms) Troughs.
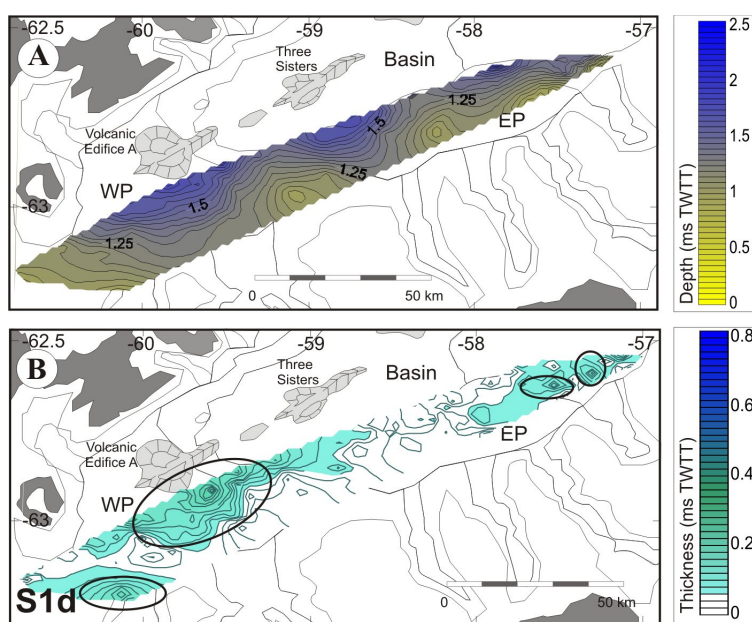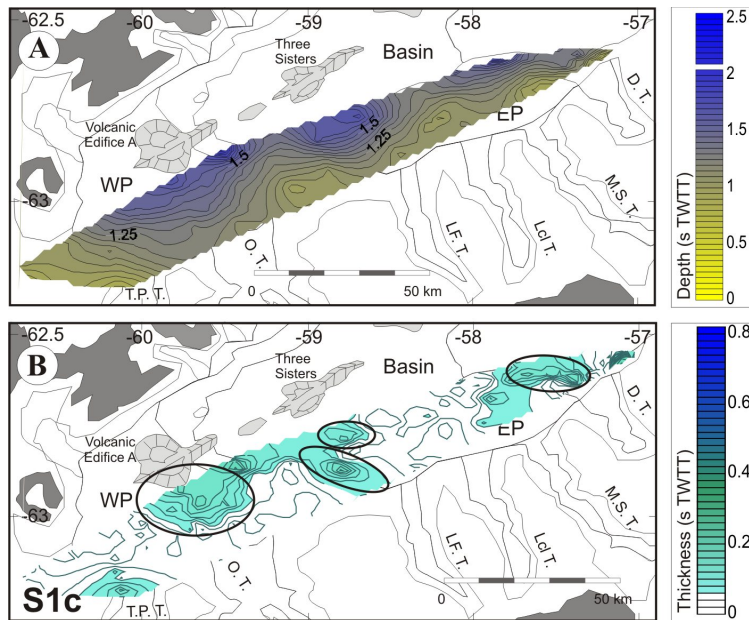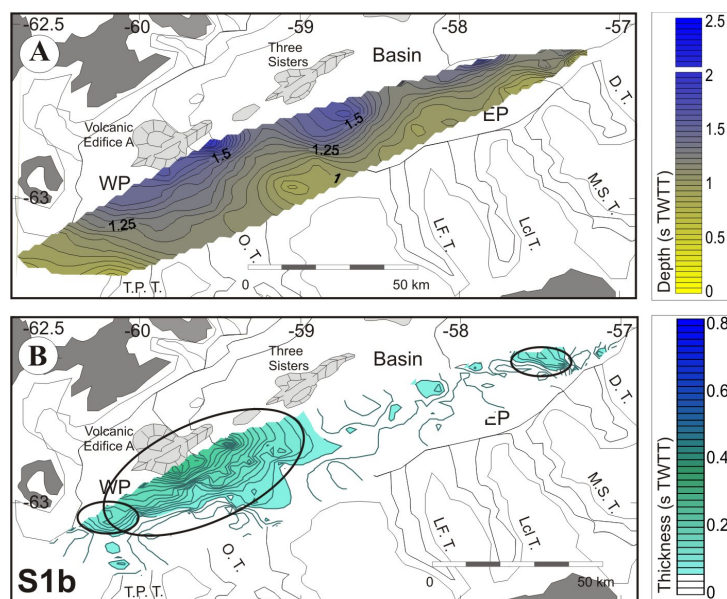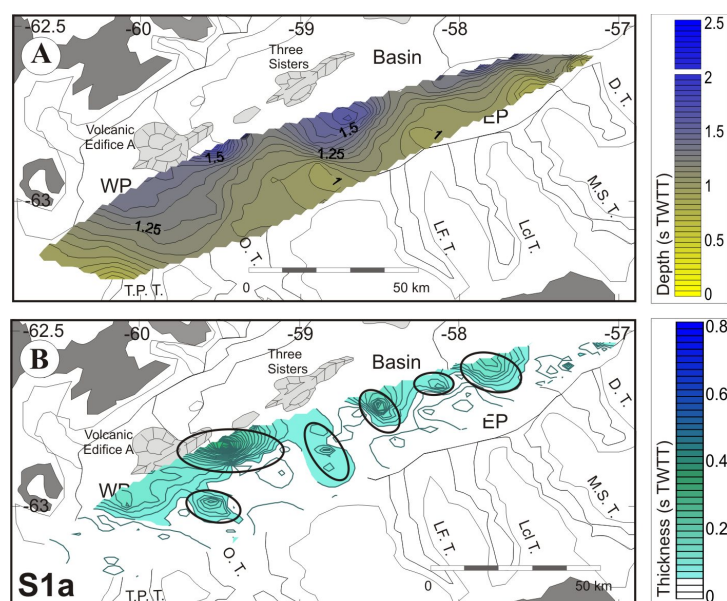

Figure 4.14. A) Isobath map of the base of seismic unit S1a. B) Isopach map of S1a. Legend: LF.T: Lafond Trough; Lcl. T.: Laclavere Trough; M.S. T.: Mott Snowfield Trough. Circles mark the depocenters.

93

3. Seismic depositional bodies

Different types of depositional bodies include till wedges, moraines, tunnel valleys, prograded wedges, trough mouth fans, glaciomarine drape and sediment gravity flow deposits (Figs. 4.15 and 4.16).

Till wedges form sheeted packages of Chaotic Indistinct facies that overlie the unconformities and occur at the base of all seismic units within S1, especially at the proximal parts of the slope platforms (Fig. 15B,E). These deposits are interpreted as the product of subglacial deposition at the base of the ice sheet (Shipp et al., 1999; Ó Cofaigh and Dowdeswell, 2001). Till wedges occur on the WP, particularly in the S1 seismic unit where they form packages up to 110 ms thick. The most recent ice sheet advance produced a till wedge whose upper surface is overprinted by glacial lineations (see Chapter III). Glacial lineations have a trough-parallel trend (N-NNW) on their proximal parts, and turn to a NE trend on the slope platforms, from the trough mouths (Fig. 4.15B,E).

Moraines occur on the WP in most seismic units of S1. They are characterized by Chaotic Mounded facies and form packages of chaotic reflections with flat bases, overlying unconformities and till sheets (Fig. 4.15F). Lateral moraines are interpreted to have been deposited along the margins of ice streams where the flow is relative slow, and may also have formed in the areas of confluence of two adjacent ice streams as ice stream boundary ridges (Anderson et al., 1992; Anderson, 1997). They consist of mounded packages of chaotic reflections with flat bases, like those identified on the WP and especially in seismic units S1c and S1b, off the mouths of the Trinity Passage and Orleans troughs (Fig. 4.15F).

Tunnel Valleys are channel-like depressions cut into till sheets and overlaid by draping stratified deposits. They occur in seismic unit S1d on the WP (Fig. 4.15G). Tunnel valleys are cut by subglacial meltwater where excess meltwater cannot be drained through an impermeable bed (Boulton et al., 1996; Eyles, 2006; Piotrowski, 1997b).

Prograded wedges form the distal edges of all seismic units of S1 and constitute almost the whole of S2 along both slope platform-edges and the lower slope. They include basinward prograded clinoforms, with the maximum thickness in front or slightly displaced to the east of the mouths of all troughs, and characterized by Layered Oblique facies (Fig. 4.16C). Their upper limit is an erosive surface that extends seaward into a conformable surface. The lower part of the clinoform onlaps landwards and downlaps seaward. These deposits are interpreted as sediment deposited at or near the grounding line of the ice sheet and are line-sourced (Alley et al., 1989; Punkari, 1997; Anderson, 1999; Dahlgren et al. 2005). They comprise glacigenic sediments transported and deposited by sediment gravity flows (Damuth, 1978; Laberg and Vorren, 1995; Vorren and Laberg, 1997).

94
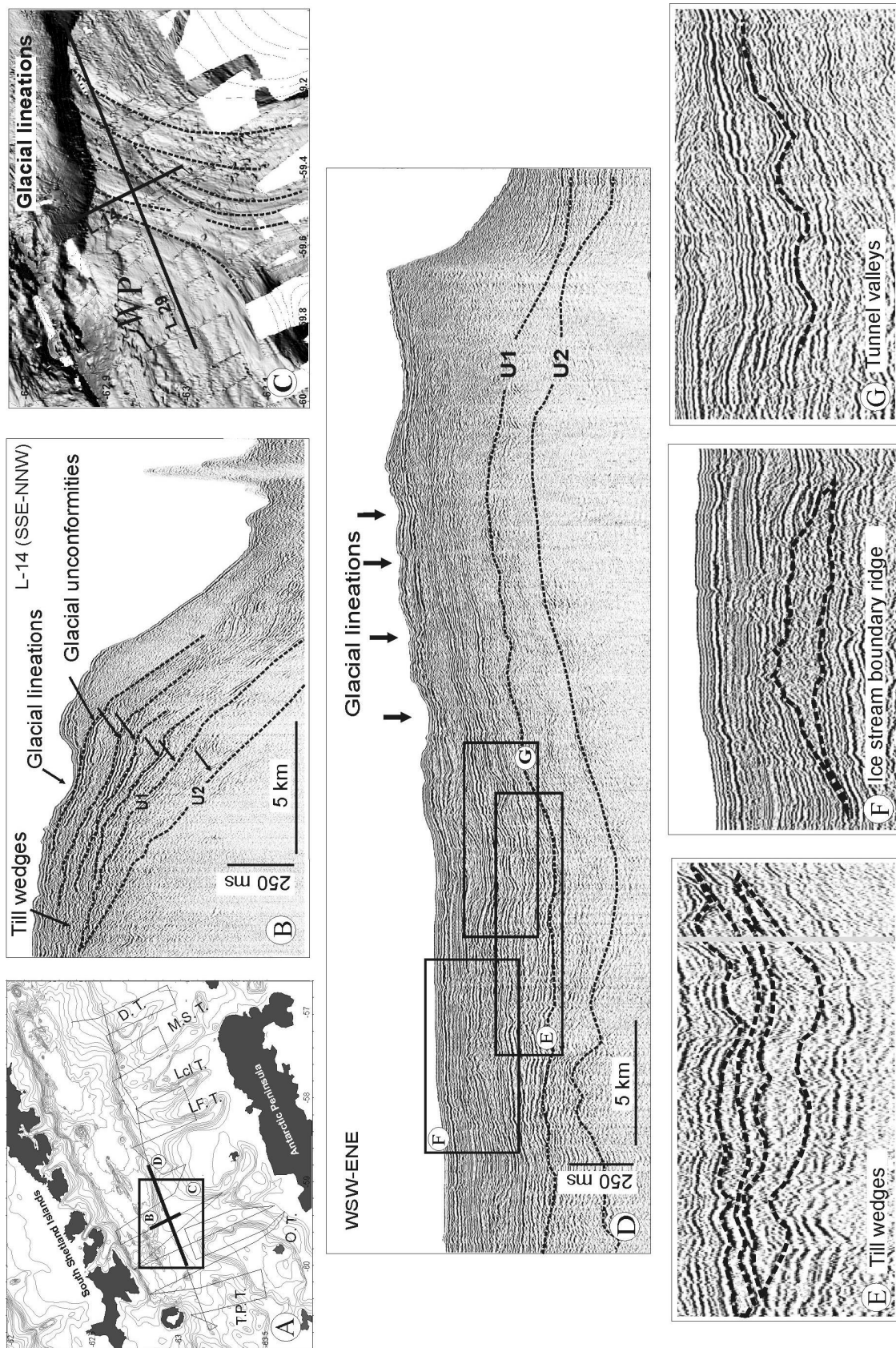
Figure. 4.15. Characterization of sedimentary features observed in seismic profiles and bathymetric data. A) Glacial troughs. B) Glacial lineations and glacial unconformities. C) Glacial lineations, modified from García et al., 2006). D) Seismic profile crossing the WP. E) Till wedges. F) Ice stream boundary ridges. G) Tunnel valleys (G). Legend: T.P.T.: Trinity Passage Trough; O.T.: Orleans Trough; LF T: Lafond Trough; Lcl. T.: Laclavere Trough; M.S. T.: Mott Snowfield Trough.

Trough mouth fans are considered as a special type of prograded wedges, which occur off the mouth of glacial troughs and are directly nourished by ice streams, where high point-sourced sediment supply occurs. They are fan-shaped depositional bodies characterized by Layered Oblique facies (Fig. 4.16B) (Davies et al., 1997). Depositional systems of this type have also been called "glacier-fed fan systems" (Dowdeswell et al., 1998) or "till deltas" (Laberg and Vorren, 1995).
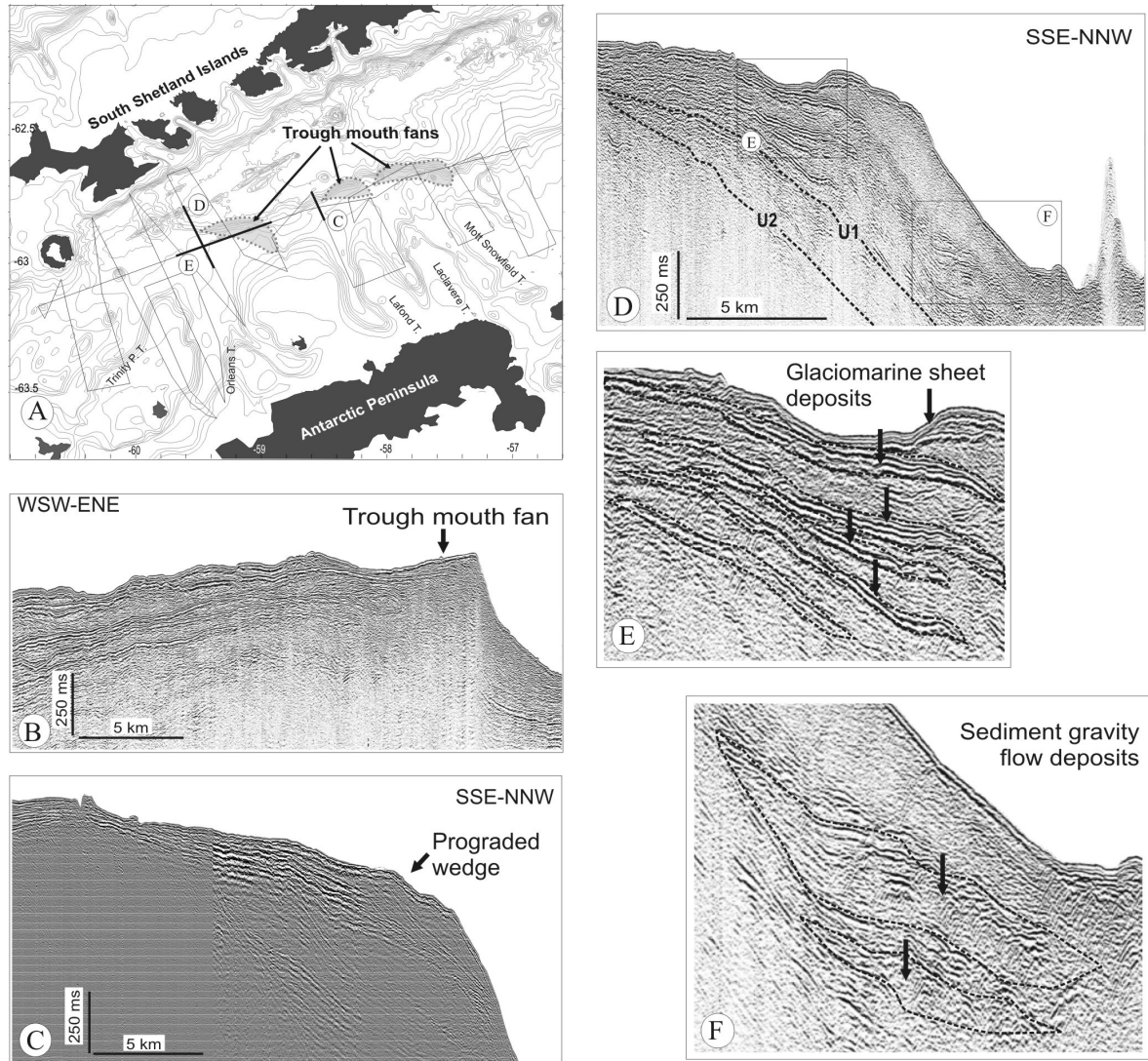
Figure 4.16. Seismic signature of deposits. A) map view showing the trough mouth fans (fans are outlined). B) Seismic profile across a trough mouth fan. C) Seismic profile across a prograded wedge. D), E) and F) Seismic profiles showing glaciomarine drape deposits and sediment gravity flow deposits.

Glaciomarine drape deposits occur in seismic records as sheets of Layered Parallel facies. Generally, they are located at the top of seismic units within S1 on the slope platforms overlying till sheets and moraines (Fig. 4.16E). They also form thin drapes on the distal parts of the bottom of troughs. These deposits are interpreted as the result of sedimentation by a combination of ice-rafting and a range of marine processes (Anderson, 1999).

Sediment gravity flow deposits are characterized in seismic records by Layered Wavy and Semitransparent facies (Fig. 4.16F). They occur in seismic units within S1 and are most prominent in the youngest unit, S1a. *Sediment gravity flow deposits* extend from the EP-edge to the basin floor, where they inter-tongue with hemipelagic deposits (Banfield and Anderson, 1995).

4. Discussion

4.1. Succession of processes during a glacial cycle in the CBB

The vertical stacking order of acoustic facies within seismic units shows a coherent pattern that indicates that each of the nine units is the result of a complete glacial-interglacial cycle. These cycles are designated C2d to C2a for the cycles associated with seismic units S2d to S2a of the Lower Sequence S2, and C1e to C1a for the cycles associated with seismic units S1e to S1a of the Upper Sequence S1. Each glacial-interglacial cycle includes two successive stages: ice sheet advance and glacial maximum, and ice sheet retreat and interglacial.

4.1.1. Ice sheet advance and glacial maximum

During the glacial acvance, the Antarctic Peninsula Ice Sheet advanced across the continental shelf, upper slope and slope platforms, producing the unconformities that bound the different units. Sediment transported in the basal layers of the ice sheet was deposited as till wedges on slope platforms and prograded wedges at the slope platform edge and lower slope. Sediment delivered to the margin by ice streams was deposited in trough mouth fans at two preferred locations of the slope platforms edge and lower slope: off the mouths of glacial troughs or displaced to the east. The occurrence of trough mouth fans within sequence S2 strongly indicates that troughs have been active since the start of the glacial activity on the CBB margin. Ice stream boundary ridges formed at the confluence of adjacent ice streams, specifically between the Trinity Passage and Orleans troughs in seismic units S1c and S1b (Fig. 4.15F). In conditions of less severe glacial climate, water melting at the base of the ice sheet was channelized and excavated tunnel valleys that drained meltwater away from the ice sheet margin (Fig. 4.15G).

4.1.2. Ice sheet retreat and interglacial

Moraines formed as the ice sheet retreated, indicating that the grounding line retreated episodically. Glaciomarine deposition dominated on the slope platforms and lower slope. During interglacial stages, the ice sheet retreated from the margin and glaciomarine sedimentary processes dominated, with the development of glaciomarine deposits at the top of units. In addition, sediment gravity flow processes occurred, especially along the EP-edge and the entire slope east of the Laclavere Trough. Sediment gravity flows were most likely the result of the excess pore pressure in sediments deposited rapidly during the ice sheet advance

and isostatic uplift after the retreat of the ice (Bryn et al., 2005; Solheim et al., 2005). In the CBB, sediment mass movements have also been attributed to other external triggering forces, which include the pre-existing tectonic framework and seismicity (Imbo et al., 2003; Casas et al., 2004).

4.2. Sedimentary architecture of the CBB margin: controlling factors

Based on the interpretation that each seismic unit is the result of an ice sheet advance and retreat cycle, the controlling factors on the post-rift stratigraphic architecture are analyzed in order to study the record of ice sheet evolution in the region. An important fact that cannot be neglected is that each advance of the ice sheet may have eroded the stratigraphic record of previous glacial cycles. Furthermore, not all the glacial cycles may have culminated in the ice sheet grounding at the platform edge, and short-lived glacial cycles may have produced stratigraphic packages that are too thin to be imaged on seismic records. Hence, the nine cycles identified in the seismic record should be considered a minimum number. Differences in the sedimentary architecture of the seismic sequences and units are influenced by the margin physiography and the climate.

4.2.1. Margin physiography and structural configuration over time

The stratigraphic architecture of the entire AP outer margin is made up of the stacking of thick prograded wedges and prominent trough mouth fans off glacial troughs, indicating that the outbuilding of the margin is the result of line-sourced sediment supply with point sources represented by ice streams, which led to the sinuous overall trend of the slope platforms edge. Glacial troughs were excavated by glacial erosion at the beginning of S2 deposition, as is indicated by the first occurrence of trough mouth fans in the lower part of this sequence, although the location and orientation of the troughs are interpreted to be structurally controlled (Jeffers and Anderson, 1990; Maestro et al., 2007).

The margin physiography at the beginning of deposition of each seismic sequence played an important role in controlling the distribution of seismic sequences S2 and S1. The spatial distribution of sediments on the CBB was determined by the progressive opening of the basin, which produced a northwestward migration of the depocenters (Fig. 4.17A, Prieto et al., 1998). A general tectonostratigraphic sketch of the CBB suggests that the opening of the basin occurred at a faster rate and/or during a more prolonged time period on the eastern area than in the western area, producing a progressively higher accommodation space in the first one (Fig. 4.17).

Sequence S2 started to develop after the initial opening of the Bransfield Basin. The basin was relatively shallow and the margin physiography at that time was characterized by a narrow and steep slope in the eastern area and a wider and gentler slope in the western area

(Figs. 4.7A and 4.9A). In the eastern area, sediment was deposited in thick prograded wedges and trough mouth fans that formed the ancestral EP (Fig 4.17B). In contrast, in the western area the prograding character of the stratigraphic architecture forming the ancestral WP was less pronounced (Fig 4.17B). This fact may be temptatively interpreted as the result of the wider and gentler physiography of the WP that allowed the distribution of the sediment supply along a larger area (Solheim et al., 1998), although the sediment supply from a larger drainage area (Orleans and Trinity Passage glacial troughs) was possibly higher.

Subsequently, during the time S1 was deposited, the ice sheet advance across the already well-developed WP and EP resulted in a more extensive distribution of S1, and the deposition of aggradational/progradational units, especially towards the SW (Fig. 4.9B). During this time, the rifting of the basin continued, with a more marked effect in the eastern area, where the progressive basin aperture combined with the tectonic subsidence led to the formation of a steeper slope platform with larger accommodation space. This led to a less pronounced prograding character of deposits in this area, when compared with the deposits of the WP, where the progradation was also enhanced by the higher sediment supply (Fig 4.17C).
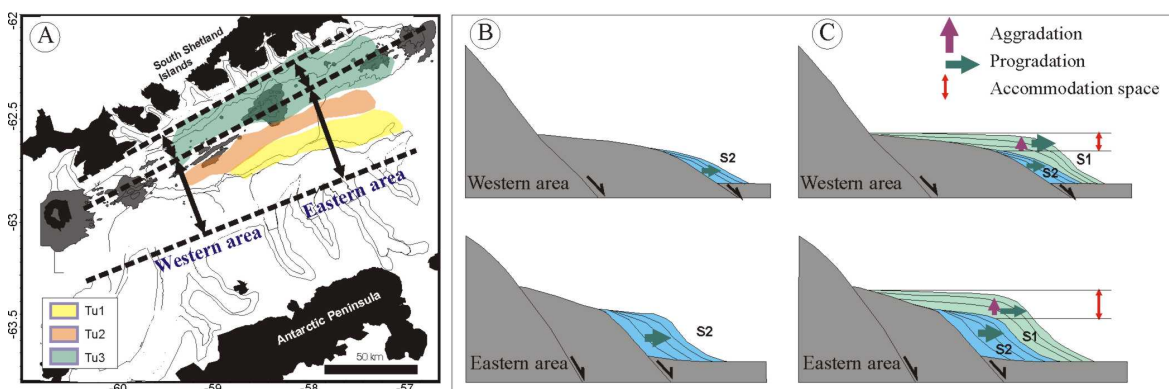
Figure 4.17. A) Scheme of the location of depocenters of tectonostratigraphic units (Tu1, Tu2 and Tu3 from older to younger) established by Prieto et al. (1998) and pattern of basin opening, inferred from the physiography and from the migration of depocenters (modified from Prieto et al., 1998). B) Stratigraphic architecture of the slope platforms showing the physiographic control on the progradational character of S2 on WP and EP. C) Stratigraphic architecture of the slope platforms showing the combined effect of the accommodation space and the character of glacial cycles on the differences in the progradational character of S1 between the WP and the EP and on the change in depositional style, from mainly progradational in S2 to progradational/aggradational in S1.

4.2.2. Climate

Climate was a major factor controlling the sedimentary evolution of the AP continental margin of the CBB (Jeffers and Anderson, 1990; Prieto et al., 1999), having affected the sedimentary architecture in two different scales. First, climate controlled the variations in sediment delivery patterns that led to the differences in the distribution and facies character between seismic units within each sequence. Second, glacial cycles determined the changes in

stratigraphic architecture between the two seismic sequences, S2 and S1. This interpretation allows the proposal of an age model for the AP margin of the CBB.

a) Variations in sediment delivery patterns

Differences in the distribution and facies character between seismic units within S2 on the EP are attributed to changes in ice flow pattern, which controlled sediment supply and deposition. Progradation of S2 was not uniform over time. Units S2d to S2b formed small and isolated depocenters, while S2a deposits compose a thick (up to 450 ms) and wide depocenter that occupies most of the present-day EP (Fig. 4.3). This may indicate that during the three first glacial cycles, C2d to C2b, the available sediment in the recently-opened basin was relatively low, while the deposition of S2a involved the glacigenic sediment deposited previously. Subunits cannot be differentiated on the WP, where S2 depocenters are concentrated on the present-day platform off the Trinity Passage Trough and on the present-day platform edge, slightly displaced to the east of the mouth of the Orleans Trough, although the penetration of the seismic source used in this study does not allow the recognition of the lower limit of S2 in the western parts of the WP.

Differences in the distribution, thickness and location of depocenters between seismic units of S1 may also record variations in the thickness of the ice sheets.
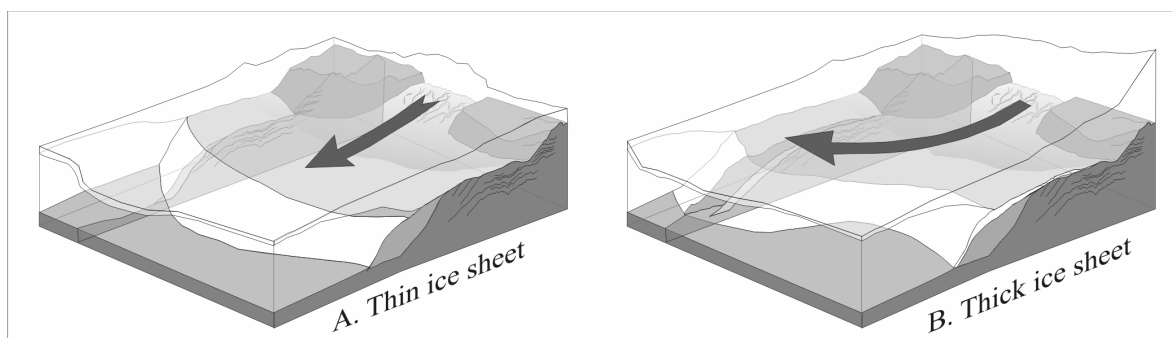
Figure 4.18. Models of glacial deposition dominated by different ice flow patterns. A) Thin ice sheet: the flow is constrained within glacial troughs and deposition occurs off the mouths of troughs; B) Thick ice sheet: the ice flow is towards the NE on the slope platforms and deposits are displaced to the east of the mouths of troughs.

- During cycles C1d and C1b, deposition was focused in prograded wedges on the slope platform at relatively proximal locations just off the mouths of troughs (Fig. 4.18A). This suggests that ice streams acted as sediment point sources topographically constrained by the glacial troughs. This fact may be interpreted in terms of the predomination of relatively thin ice sheets, which were more affected by topographic effects (Fig. 4.18A).

- During cycles C1e, C1c and C1a, ice streams flowed through glacial troughs in a north-northwest direction, but they turned eastwards as they reached the slope

100

platforms (Fig 4.18B). This is evidenced by two facts: i) the location of depocenters of seismic units S1e, S1c and S1a, which are displaced to the east of the mouths of troughs; and ii) the northeasterly direction of progradation, suggested by the change in trend of the glacial lineations associated with the most recent ice sheet expansion, from N-NNW within the glacial troughs to NE on the slope platforms (García et al., 2006a). This sediment dispersal pattern was most pronounced during deposition of unit S1a, which shows the maximum thickness of the five seismic units (250 ms). This fact may be related with a thicker ice sheet with a regional sloping direction towards the NE, that would affect the ice flow on the slope platforms, where the topographic constraint of the glacial troughs dissappears.

b) Control of glacial cycles and age model

Several attempts at establishing a chonostratigraphic framework for the CBB have been made, although the lack of datable sediment makes it difficult to corroborate age models. The strata below U2 have been correlated with the lower part of the Lower Sequence of Prieto et al. (1999), interpreted as a syn-rift sequence. Also, the opening of the CBB has been dated at 3.3 Ma (Galindo-Zaldívar et al., 1996, 2004), which provides a constraint for the age of seismic sequences S2 and S1.

The general pattern of stratigraphic architecture in the CBB from progradational (S2) to aggradational/progradational (S1) is similar to that which occurs on the Pacific Antarctic margin (Larter and Barker, 1989; Bart and Anderson, 1996). Rebesco et al. (2006) argued that this change in the stratigraphic architecture occurred at around 3.0 Ma and marked a time of change in the character of the ice sheet, from more temperate to more polar. However, the overall stratigraphic architecture is similar to that which occurs elsewhere in Antarctica, which Bartek et al. (1991) argue reflects the increased frequency of ice sheet grounding events associated with higher frequency climatic changes at this time. Furthermore, Bart and Anderson (1996, 2000) identified a number of glacial unconformities in progradational Miocene strata on the Pacific Antarctic margin.

Regardless of the cause of the change in stratigraphic architecture, the presence of subglacial seismic facies and features indicates that sequences S1 and S2 were deposited in a fully glaciated setting where the Antarctic Peninsula Ice Sheet advanced onto the continental shelf and upper slope. The timing of initial opening of the basin (3.3 Ma) and the thickness of sequences suggest that the U1 unconformity, which reflects a change from progradational to progradational/aggradational stratigraphic architecture, should be younger than 3.0 Ma. A sedimentary discontinuity that also marks a change in the recent stratigraphic architecture, from progradational/aggradational to aggradational, has been defined on the SW end of the South Shetland Trench (Jabaloy et al., 2003). These authors have assigned a mid- Pleistocene

age to the discontinuity, that coincides with a major change in the duration and character of glacial cycles in both hemispheres, designated as Mid-Pleistocene Revolution, MPR (Shackleton et al., 1990; Berger et al., 1994; Mangerud et al., 1996; Howard, 1997; Paillard, 1998).

Before the mid-Pleistocene, climatic oscillations were dominated by 100 ka cycles and modulated by 41 ka cycles. The reinforcement of glaciations due to the combination of cycles of different frequencies, in combination with the fact that the climate was globally warmer, led to the formation of thick ice sheets (Olsen et al., 2001; Oppenheimer, 2001). During this time, as S2 strata were being deposited, more prolonged sediment supply to the lower slope resulted in the formation of thick prograded wedges and trough mouth fans and the development of a prograding stratigraphic architecture (Fig. 4.17B,C).

After the mid-Pleistocene the frequency of grounding events reaching the slope platforms edge increased as a result of the predominance of 100 ka cycles. This change would have been responsible for the shift from predominant erosion to net accumulation and the development of the aggradational/progradational deposits (Solheim et al., 1996). The preservation of till wedges, prograded wedges and trough mouth fans, as well as the preservation of topset beds, also suggests increased subsidence at this time (Dahlgren et al., 2005) (Fig. 4.17B,C). The presence of tunnel valleys on seismic unit S1d indicates the availability of meltwater to carve the tunnels, but an interpretation in terms of glacial regime is difficult since these features have a very low preservation potential due to the erosion exerted by the subsequent ice sheet advance.
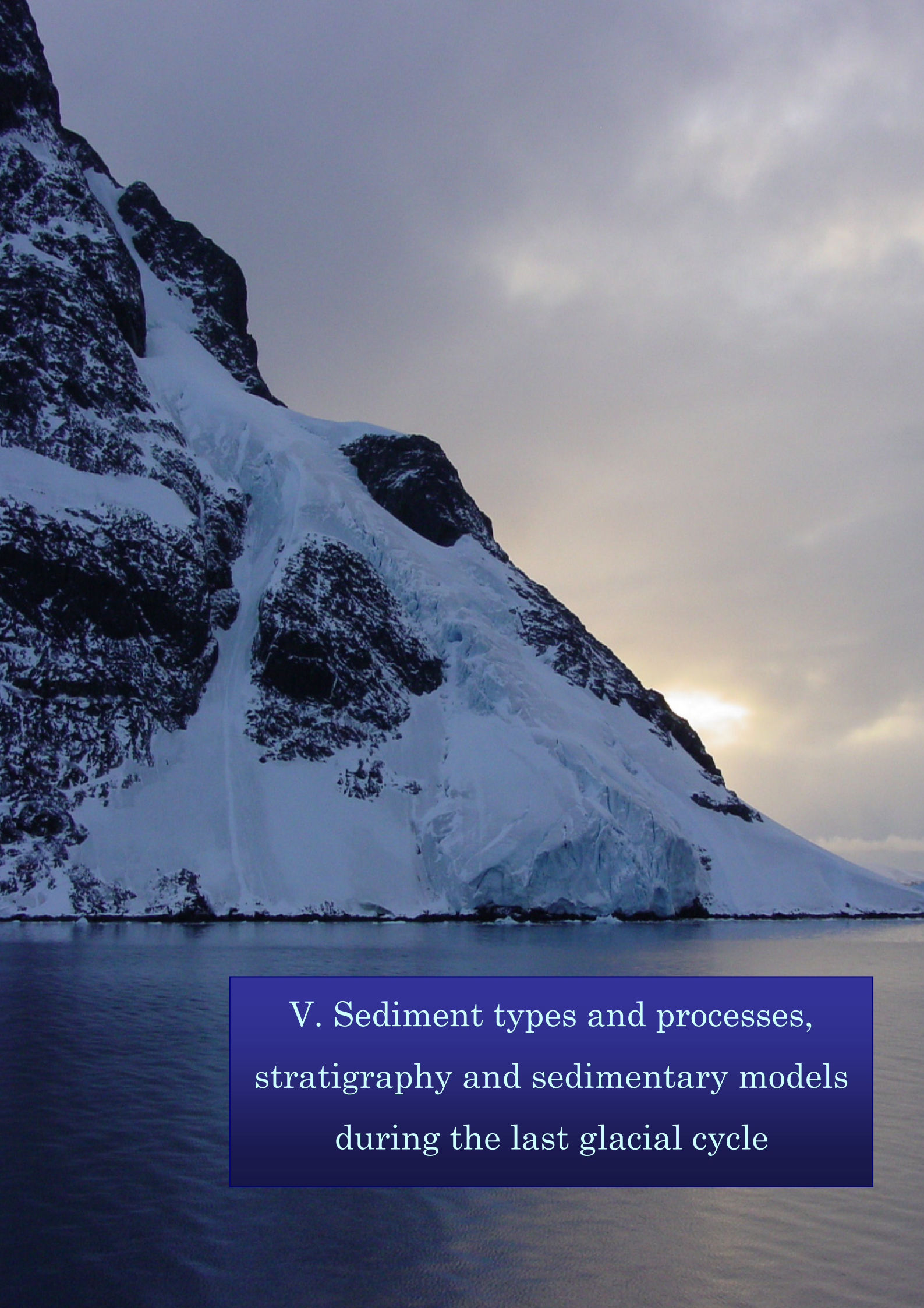
V. Sediment types and processes, stratigraphy and sedimentary models during the last glacial cycle

1. Introduction and dataset

Understanding the recent sedimentary processes on high-latitude continental margins is essential in order to obtain a better knowledge of glacial/interglacial cyclicity and the associated processes. The sedimentation in the CBB is very sensitive to the global climatic and eustatic oscillations (Willmott, 2007). On the AP the climate shows a recent rapid regional warming of 3.7 ± 1.6 ºC/century –several times the rate of global warming (Vaughan et al., 2003). This extremely sensitive climatic regime is reflected in the postglacial sedimentary record (Yoon et al., 1997; Fabrés et al., 2000; Willmott, 2007; Heroy et al., 2008). The aims of the sedimentological study were:

- To define the near-surface sediment types and sedimentary sequences of the CBB and their spatial and temporal distributions

- To characterize the stratigraphic models for each physiographic domain

- To establish the sedimentary processes with special interest in providing a regional perspective of the glacial, glaciomarine and marine sedimentary processes, and of the factors that controlled the most recent sedimentation in the CBB during the last glacial advance and maximum stage, and during the deglaciation and interglacial stages.

This study includes the analysis of 21 gravity sediment cores from the different depositional environments of the CBB defined in Chapter III (Figs. 5.1 and 5.2 and Table 5.I). The core sites were selected according to the seismic data, covering depths of 684-1930 m.
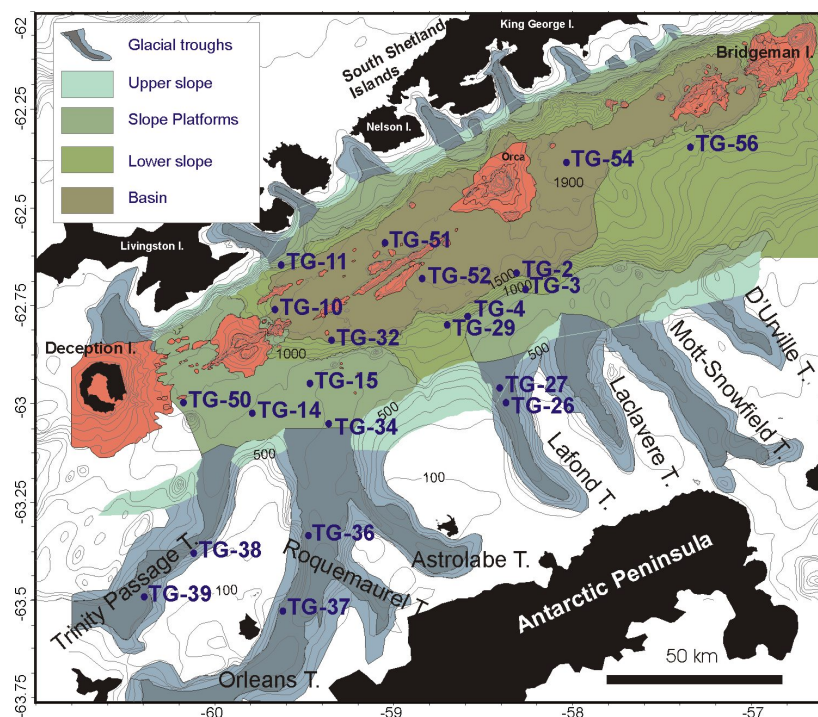
Figure 5.1. Location of the sediment cores. They cover the sedimentary environments identified in the CBB.

2. Core setting characterization

The depositional environments in which sediment cores were obtained include the inner and outer reaches of the continental shelf glacial troughs, the slope platforms, the lower continental slope and the basin (Fig. 5.1 and Table 5.I). These depositional environments have distinct morphological and acoustic characteristics.

Depositional environment	Core	Length (cm)	Latitude (º)	Longitude (º)	Water depth (m)
Inner reaches of glacial troughs	TG37	232	-63.5071	-59.610	822
	TG39	214	-63.4745	-60.3799	684
Outer reaches of glacial troughs	TG38	295	-63.363	-60.1052	1053
	TG36	300	-63.319	-59.4777	864
	TG27	250	-62.9418	-58.4119	755
	TG26	220	-62.9779	-58.3796	806
Slope platforms	TG50	83	-62.981	-60.1616	965
	TG34	264	-63.0337	-59.36	765
	TG14	261	-63.0062	-59.7804	903
	TG15	250	-62.9319	-59.4631	880
	TG11	268	-62.6296	-59.6215	790
Lower slope	TG3	84	-62.6912	-58.2742	1200
	TG4	230	-62.7611	-58.5905	1200
	TG29	120	-62.7827	-58.7051	1200
	TG56	240	-62.3303	-57.36	1500
Basin	TG32	151	-62.8216	-59.3435	1391
	TG2	148	-62.6501	-58.3209	1575
	TG10	209	-62.744	-59.6561	1366
	TG51	265	-62.5743	-59.048	1548
	TG52	324	-62.6646	-58.8403	1625
	TG54	76	-62.3695	-58.0463	1930

Table 5.I. Location and characteristics of the sediment gravity cores recovered from the depositional environments of the CBB.
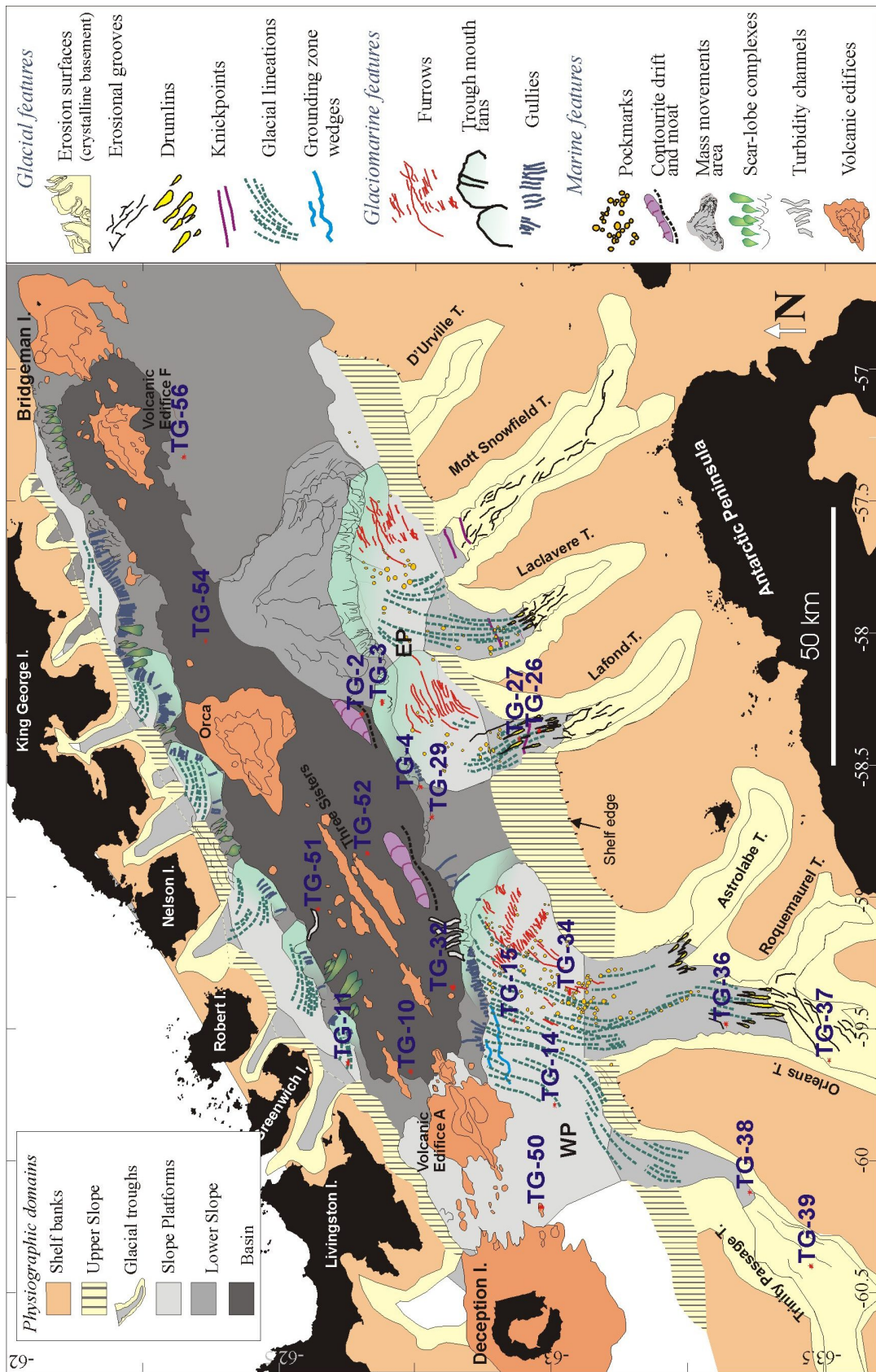
Figure 5.2. Physiographic and morphologic environments of the core sites. The physiography and morphology of the CBB are discussed in Chapter 3.

107
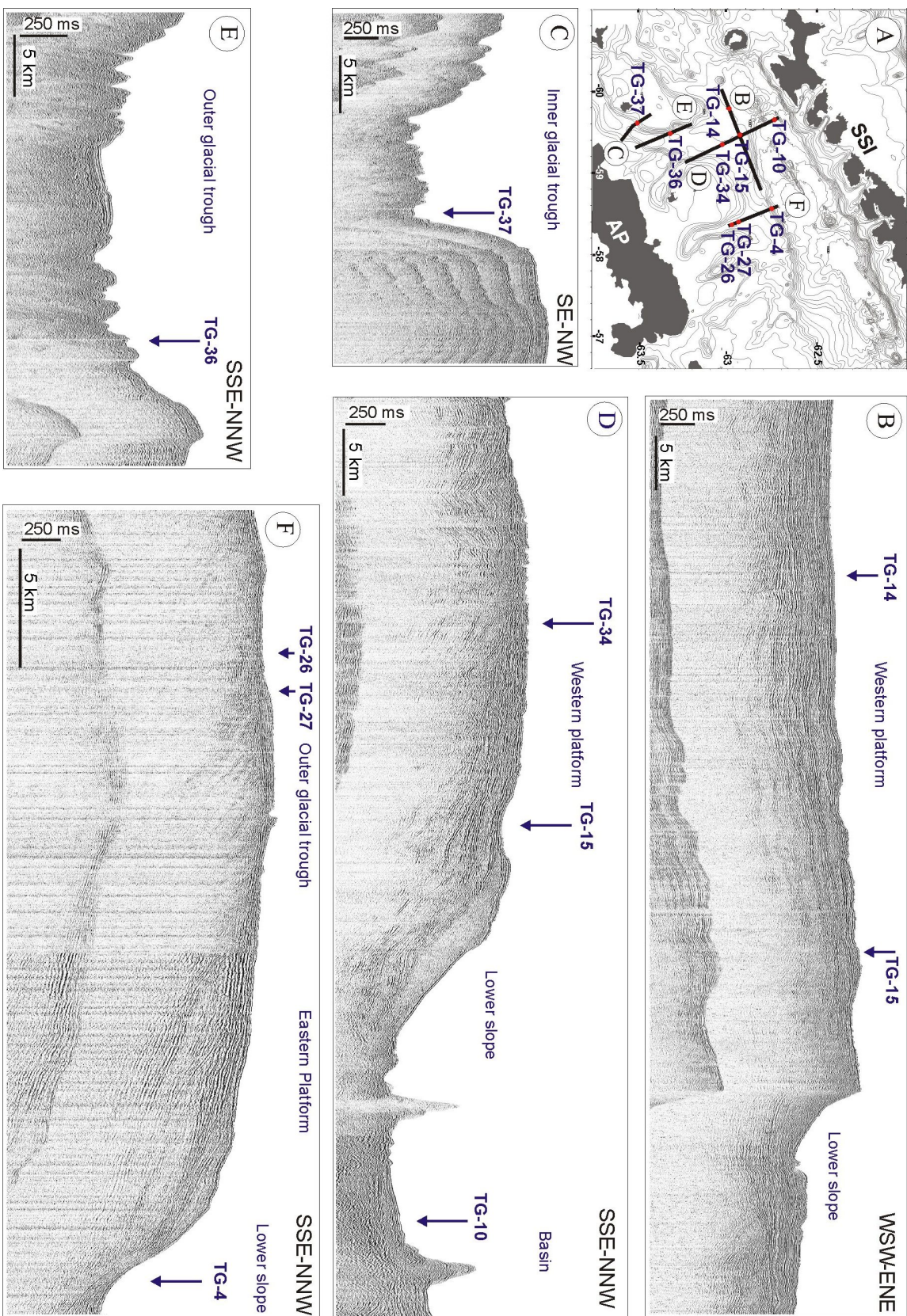
Figure 5.3. A) Location map. B) to E) High-resolution seismic profiles showing the location of sediment cores of the CBB. The facies character and the seismic stratigraphy are discussed in Chapters 3 and 4, respectively.

Sediment cores TG37 and TG39 were recovered in the proximal areas of the Trinity Passage and Orleans glacial troughs (Figs. 5.1 to 5.3E and Table 5.I). These areas are erosive surfaces with grooves where only a thin sedimentary cover can be locally identified. TOPAS profiles show hyperbolic non-penetrative echoes and airgun profiles show irregular hyperbolic echoes with chaotic subbottom reflections (Fig. 3.5). The sedimentological characteristics of core TG37 can be seen in Fig. 5.4.

Sediment cores TG38, TG36, TG27 and TG26 are located in the outer reaches of the Trinity Passage, Orleans and Lafond glacial troughs (Figs. 5.1 to 5.3E,F and Table 5.I), characterized as transitional areas from crystalline basement to sedimentary substrate. The predominant morphological features are drumlins and the proximal extremes of glacial lineations. Seismic profiles show continuous layered reflections overlying discontinuous reflections in the airgun profiles and transparent echoes in the TOPAS profiles (Fig. 3.6F). The sedimentological characteristics of core TG36 are shown in Figure 5.5.

Sediment cores TG50, TG34, TG14 and TG15 are located on the WP on the AP margin, and TG11 is located on the westernmost slope platform of the SSI margin (Figs. 5.1 to 5.3 and Table 5.I). Slope platforms are characterized by the presence of glacial lineations that show continuous layered reflections overlying discontinuous reflections in the airgun profiles and transparent echoes in the TOPAS profiles (Figs. 3.7 and 5.3B). TG34, TG15 and TG14 were recovered in a pockmark field, which is acoustically characterized in the TOPAS profiles as V- or U-shaped incisions in transparent deposits, filled in some cases with layered reflectors, and in airgun profiles as V-shaped incisions in the near-surface continuous layered reflectors (Fig. 3.12). The sedimentological characteristics of sediment cores can be seen in Figures 5.6 to 5.9.

Sediment cores TG3 and TG4 are located on the lower slope off the EP on the AP margin (Figs. 5.1 to 5.3F and Table 5.I). This area is characterized by the presence of trough mouth fans that show layered reflections forming a prograding stratigraphic pattern in the airgun profiles and indistinct non-penetrative bottom echoes or transparent echoes covered by continuous layered reflections in the TOPAS profiles (Figs. 3.9 and 5.3F). TG56 and TG29 were recovered on the lower slope, in areas unaffected by the presence of trough mouth fans. The sedimentological characteristics of the sediment cores recovered on the lower slope can be seen in Figures 5.10 to 5.13.

Finally, sediment cores TG32, TG2, TG10, TG51, TG52, and TG54 are located on the basin (Figs. 5.1 to 5.3D and Table 5.I). TG2 is located in a contourite moat at the foot of the lower slope, off the Eastern Slope platform, acoustically characterized by prolonged non-penetrative echoes in TOPAS profiles (Fig. 3.15). The rest of cores were recovered at different locations of the basin. The basin is morphologically characterized by a draping sheet that shows continuous parallel layered reflectors on seismic profiles (Fig. 3.11). The sedimentary

characteristics of most of the sediment cores recovered from the basin can be seen in Figures 5.14 to 5.18.

Figure 5.4. Sedimentological characteristics of sediment core TG37, including X-ray image and log, density, magnetic susceptibility, grain size log and carbonate content. This core is located in the inner reaches of the Orleans Trough (Fig. 5.1)

110

Figure 5.5. Sedimentological characteristics of sediment core TG36, including X-ray image and log, density, magnetic susceptibility, grain size log and carbonate content. This core is located in the outer reaches of the Orleans Trough (Figs. 5.1 and 5.2)

TG 34. Western Platform

| Depth (m) | X-ray image | X-ray log | Sediment type | Density (g/cc) | Magnetic Susceptibility (S.I.) | Grain size (%) | Carbonate content (%) |

Sediment type

Laminated
- Finely
- Regularly
- Flow-in
- Indistinct

- Brecciated
- Bioturbated
- Massive

Texture
- Gravel
- Sand
- Silt
- Clay

Figure 5.6. Sedimentological characteristics of sediment core TG34, including X-ray image and log, density, magnetic susceptibility, grain size log and carbonate content. This core is located on the WP (Figs. 5.1 and 5.2)

Figure 5.7. Sedimentological characteristics of sediment core TG14, including X-ray image and log, density, magnetic susceptibility, grain size log and carbonate content. This core is located on the WP (Figs. 5.1 and 5.2)

Figure 5.8. Sedimentological characteristics of sediment core TG15, including X-ray image and log, density, magnetic susceptibility, grain size log and carbonate content. This core is located on the WP (Figs. 5.1 and 5.2)
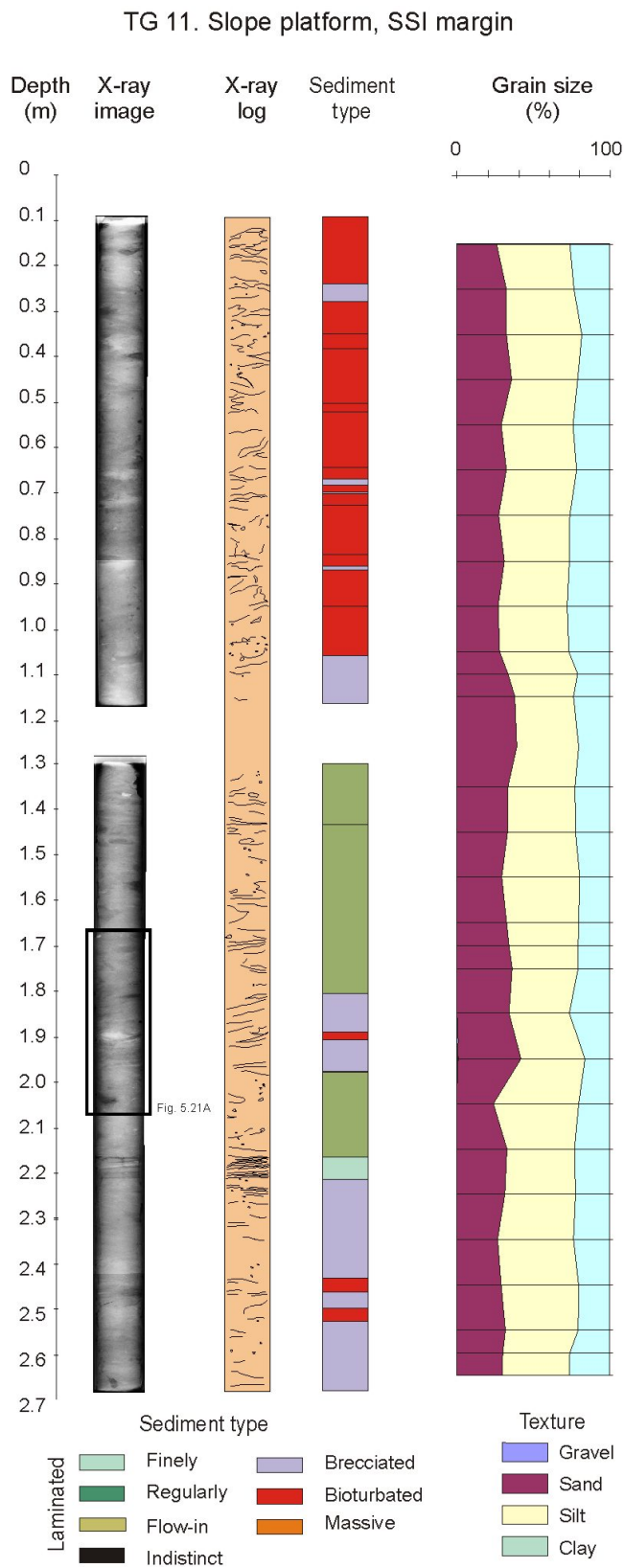
Figure 5.9. Sedimentological characteristics of sediment core TG11, including X-ray image and log and grain size log. This core is located on the SSI westernmost slope platform (Figs. 5.1 and 5.2)

TG 4. Basin
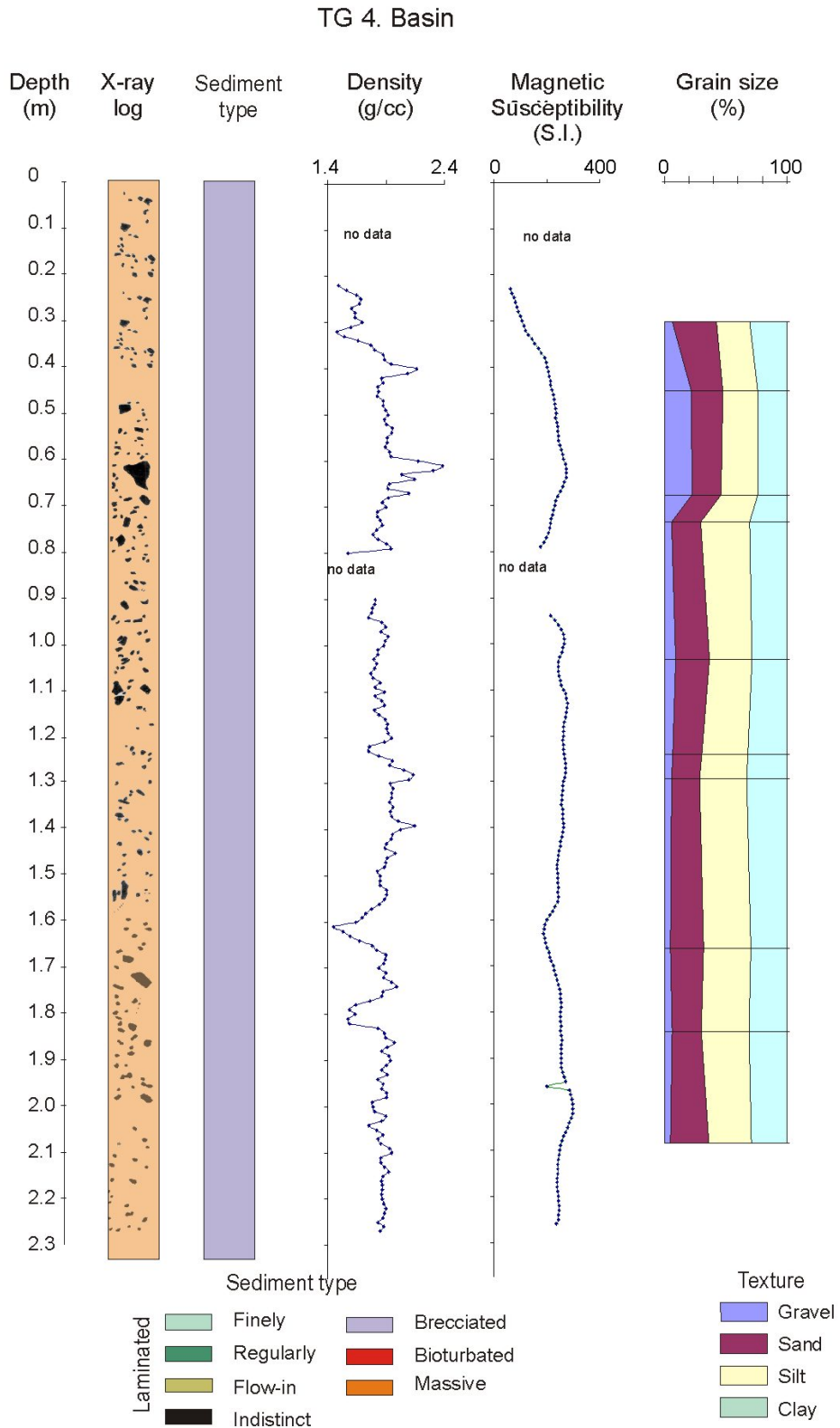
Figure 5.10. Sedimentological characteristics of sediment core TG4, including X-ray log, density, magnetic susceptibility and grain size log. This core is located on the lower slope (Figs. 5.1 and 5.2)

TG 3. Lower Slope
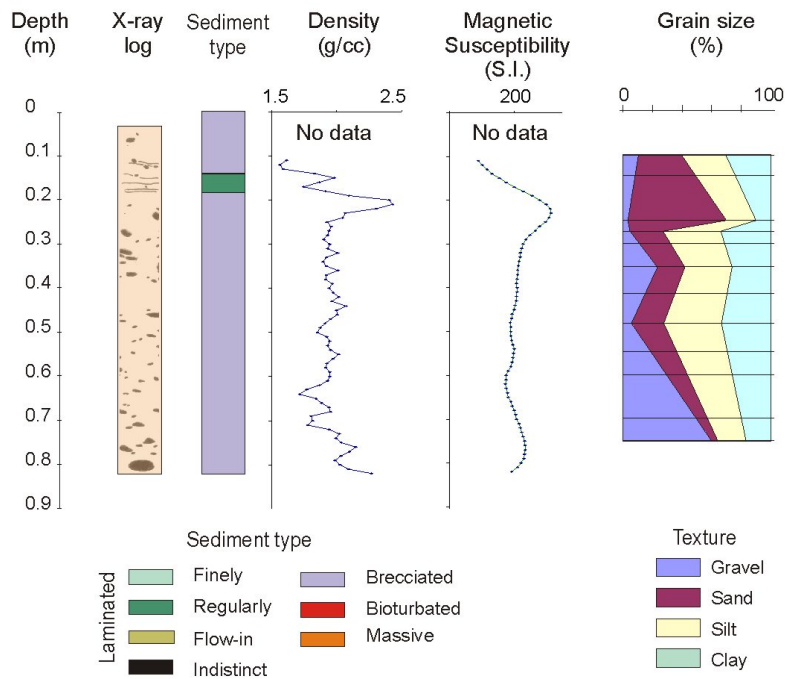
Figure 5.11. Sedimentological characteristics of sediment core TG3, including X-ray log, density, magnetic susceptibility and grain size log. This core is located on the lower slope (Figs. 5.1 and 5.2)

TG 29. Lower slope
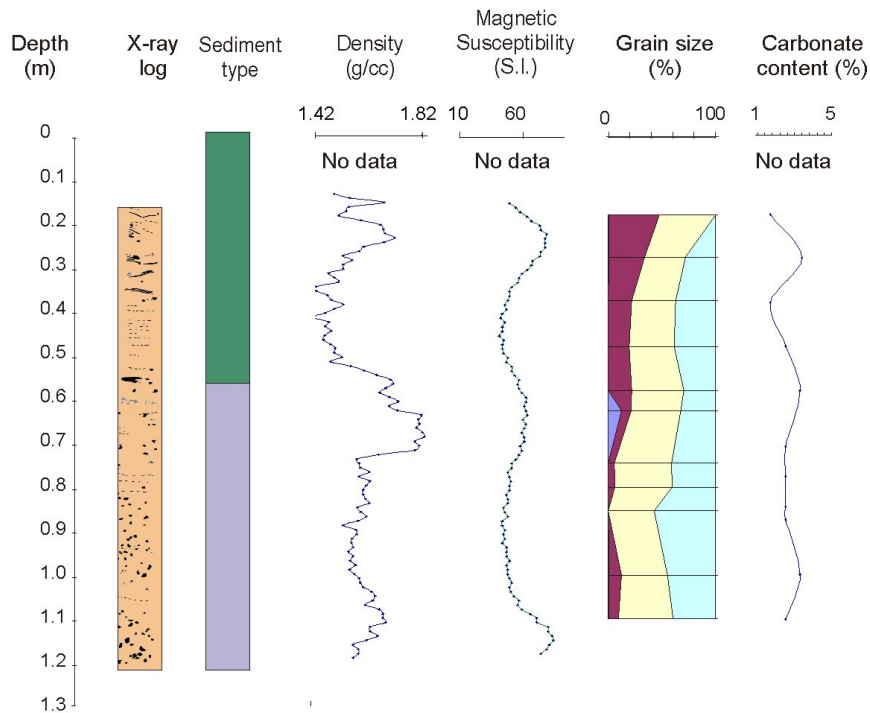
Figure 5.12. Sedimentological characteristics of sediment core TG29, including X-ray log, density, magnetic susceptibility, grain size log and carbonate content. This core is located on the lower slope (Figs. 5.1 and 5.2)

117
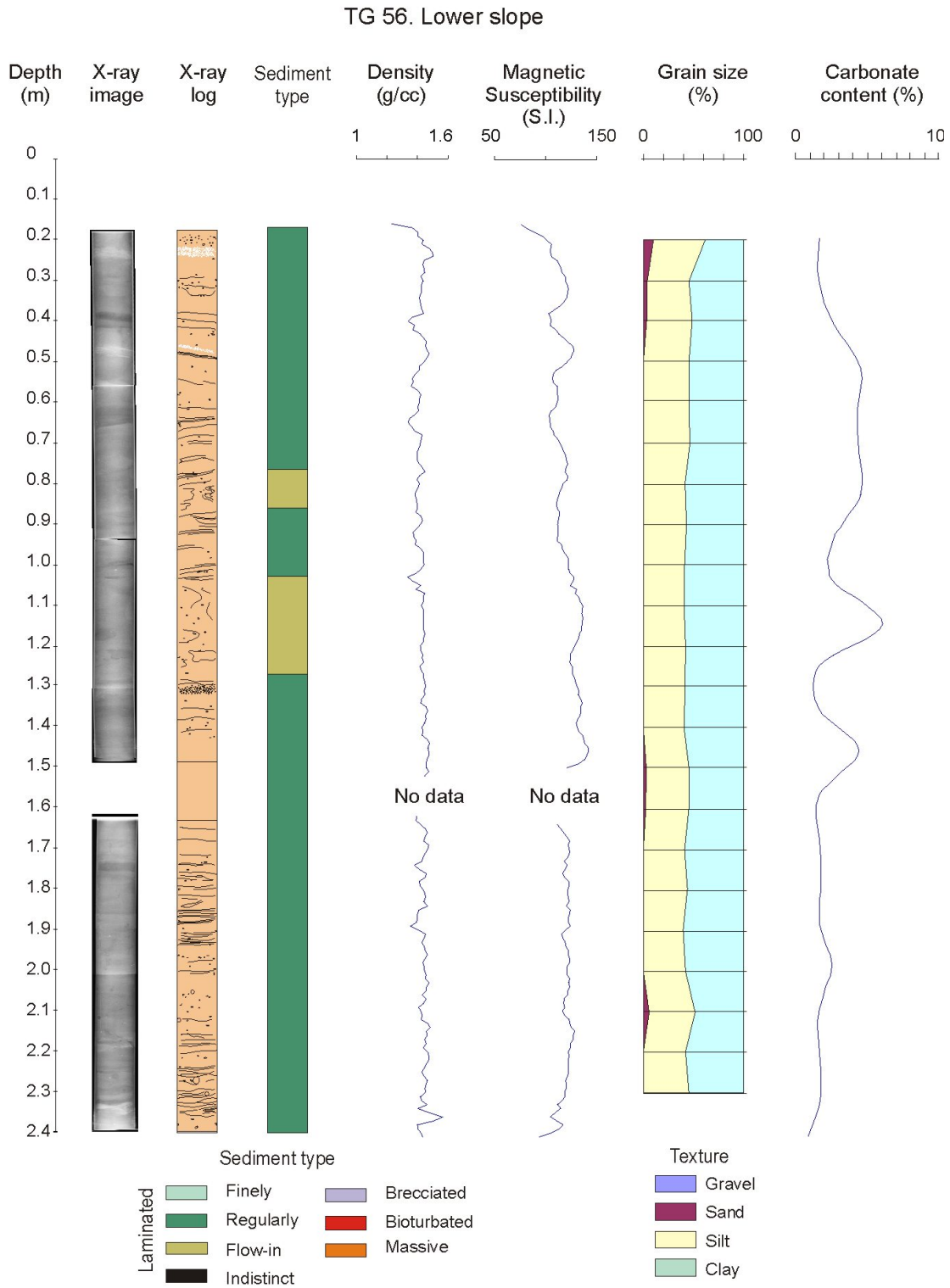
Figure 5.13. Sedimentological characteristics of sediment core TG56, including X-ray log, density, magnetic susceptibility, grain size log and carbonate content. This core is located on the lower slope (Figs. 5.1 and 5.2)

TG 10. Basin
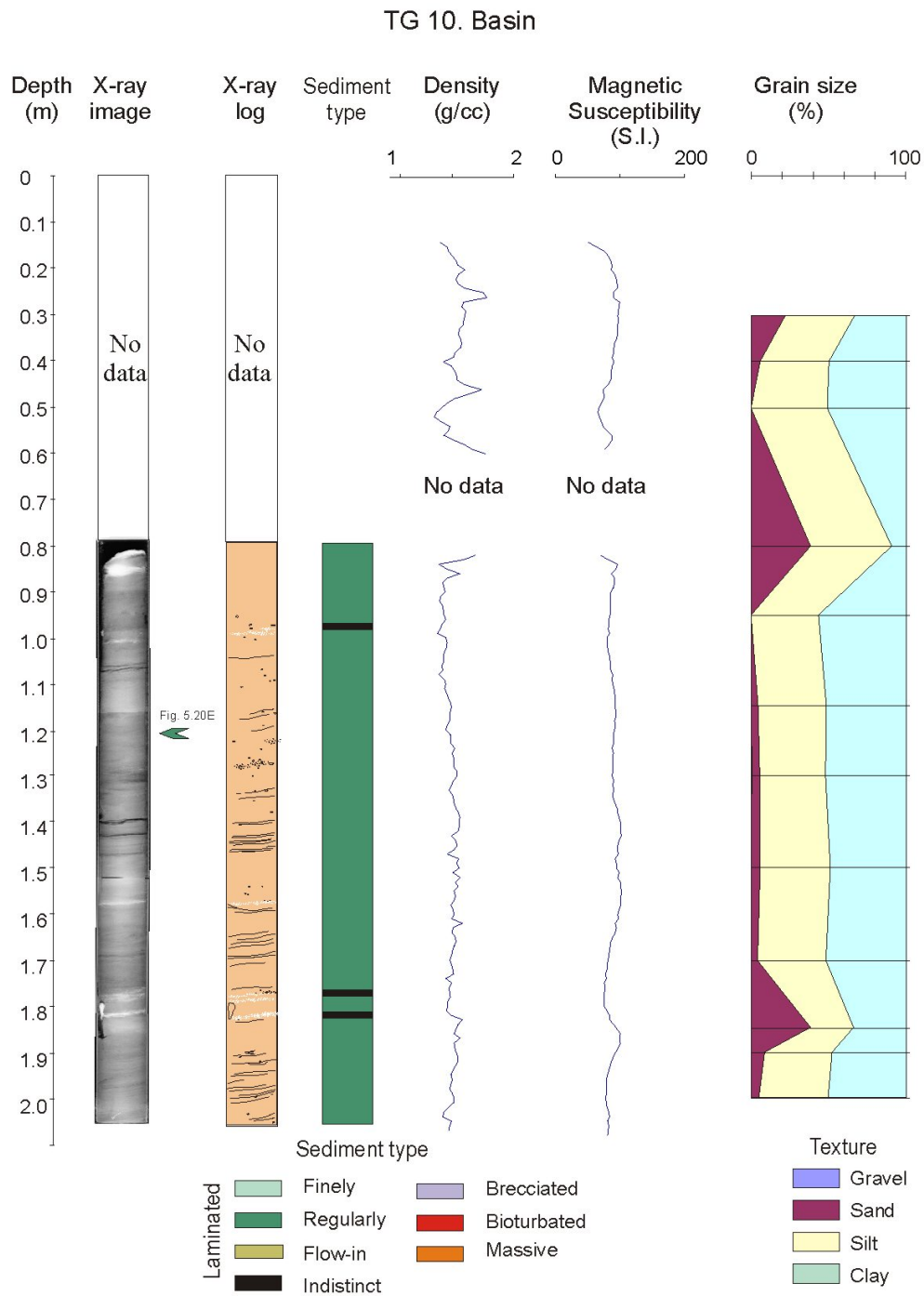
Figure 5.14. Sedimentological characteristics of sediment core TG10, including X-ray log, density, magnetic susceptibility and grain size log. This core is located on the eastern part of the basin (Figs. 5.1 and 5.2)
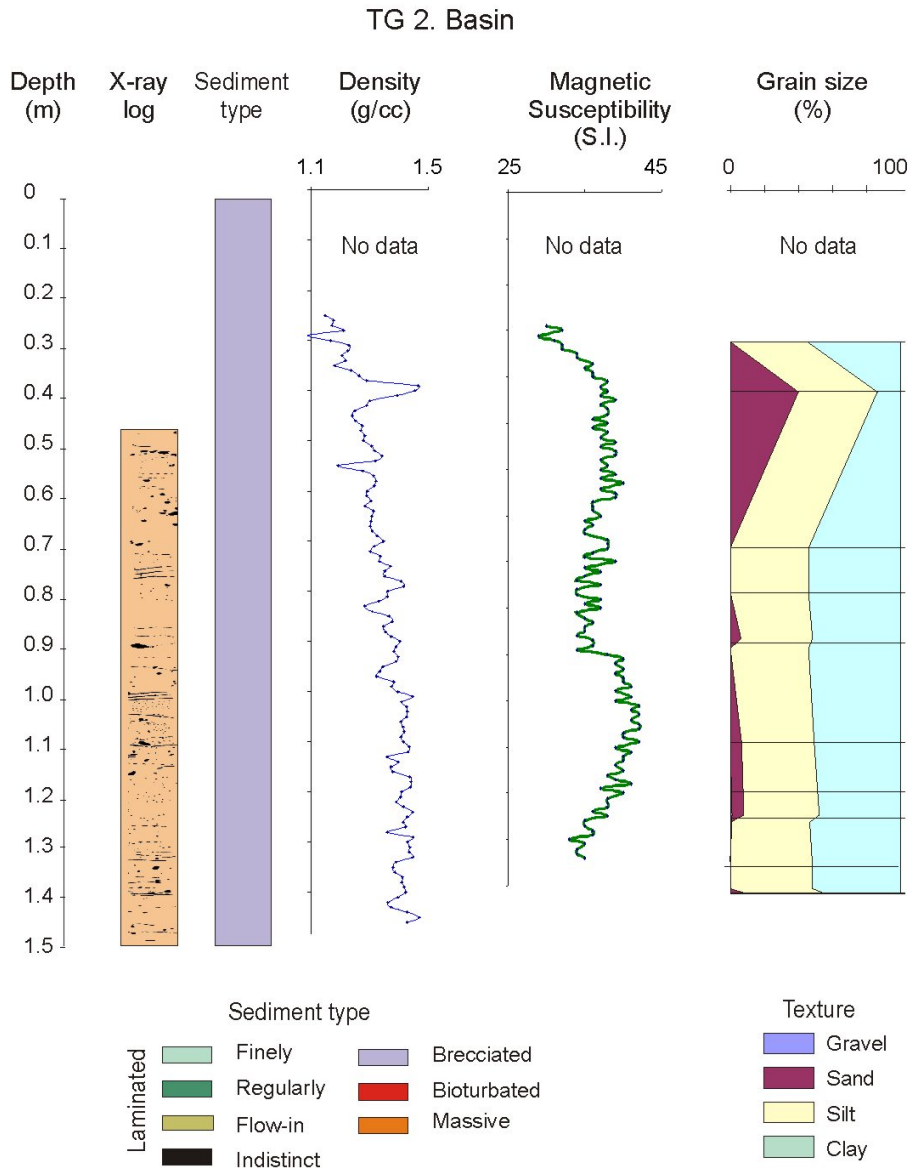
Figure 5.15. Sedimentological characteristics of sediment core TG2, including X-ray log, density, magnetic susceptibility and grain size log. This core is located on the basin, at the foot of the lower slope off the EP (Figs. 5.1 and 5.2)
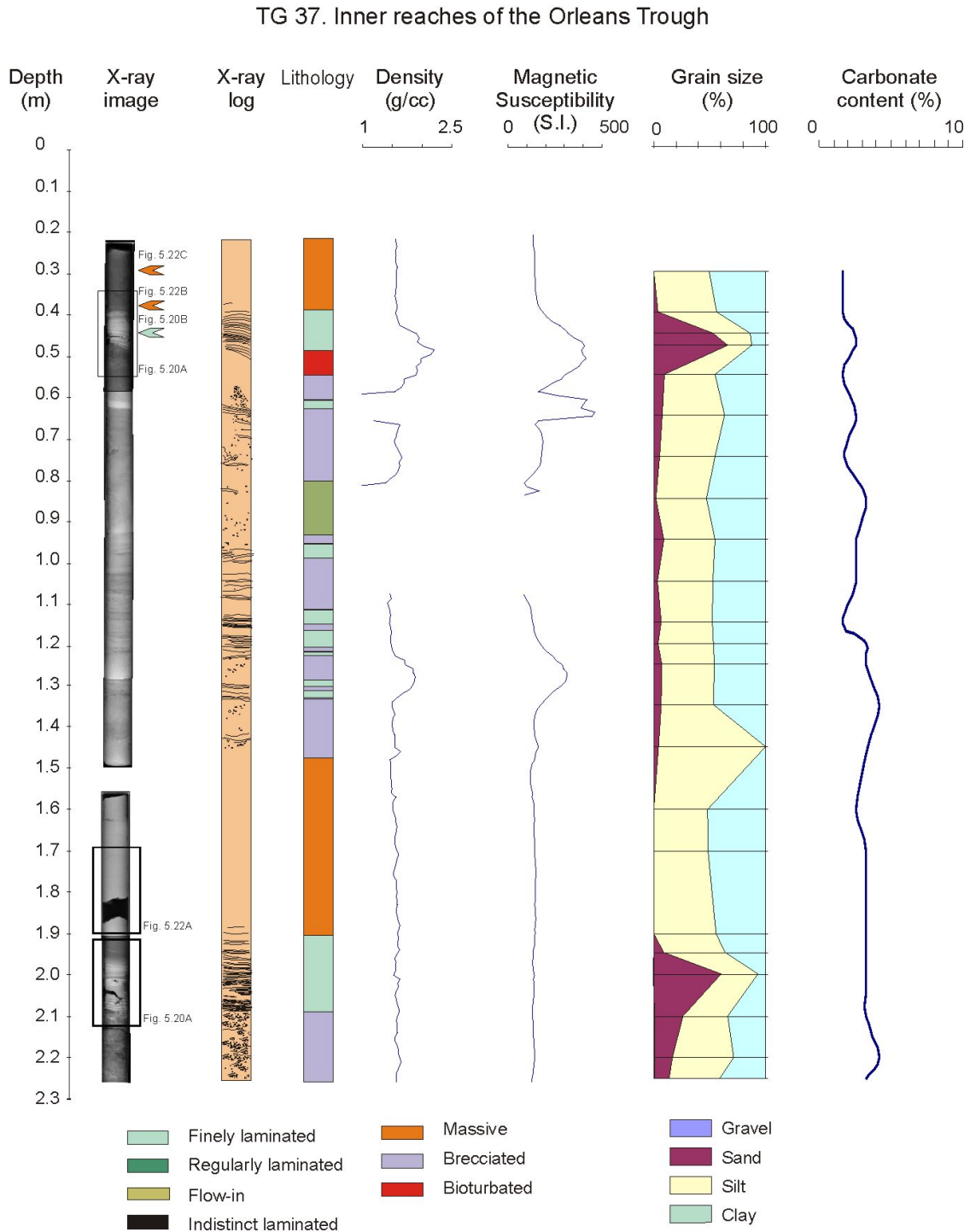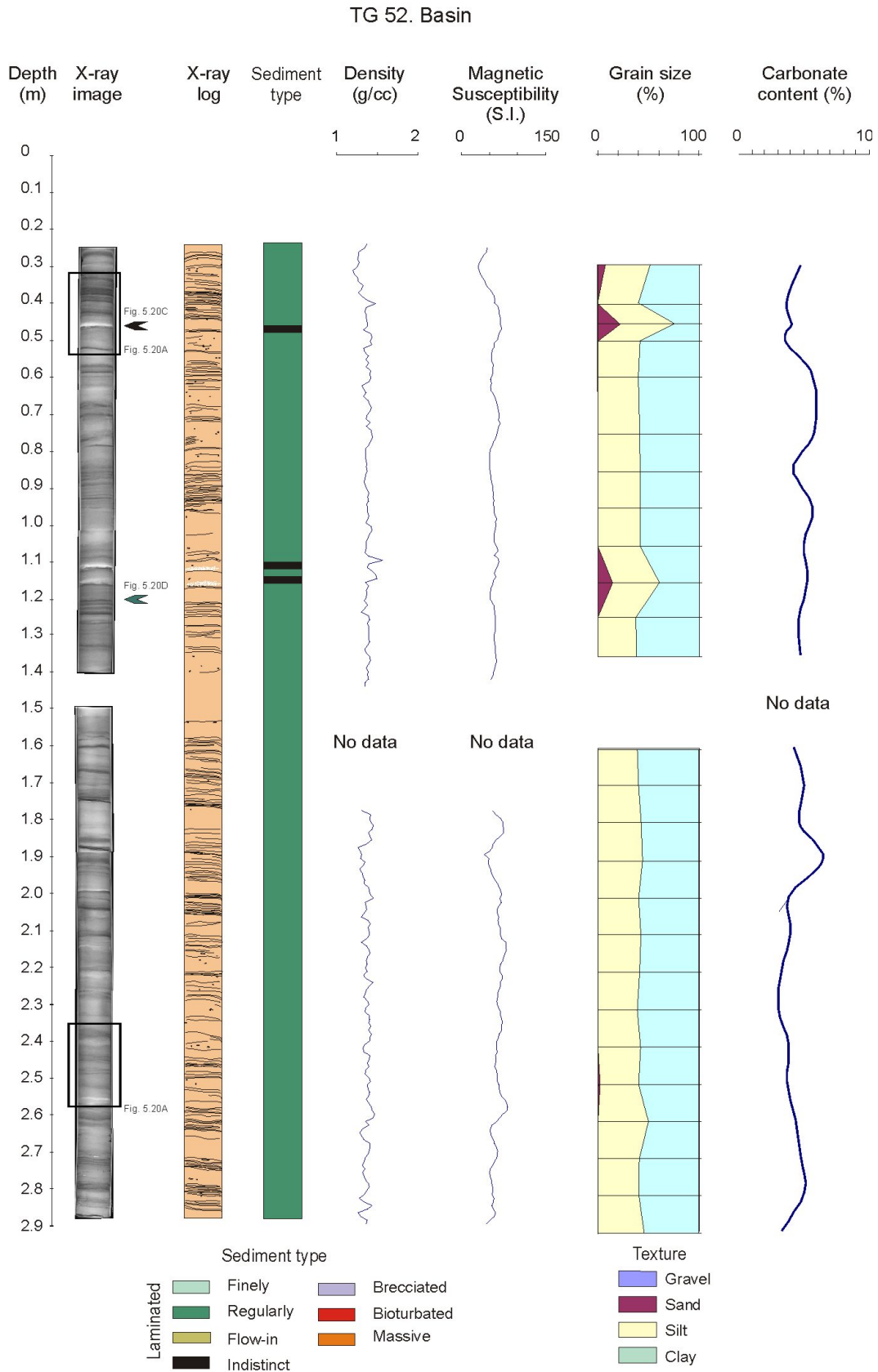
Figure 5.16. Sedimentological characteristics of sediment core TG52, including X-ray image and log, density, magnetic susceptibility, grain size log and carbonate content. This core is located on the basin (Figs. 5.1 and 5.2)
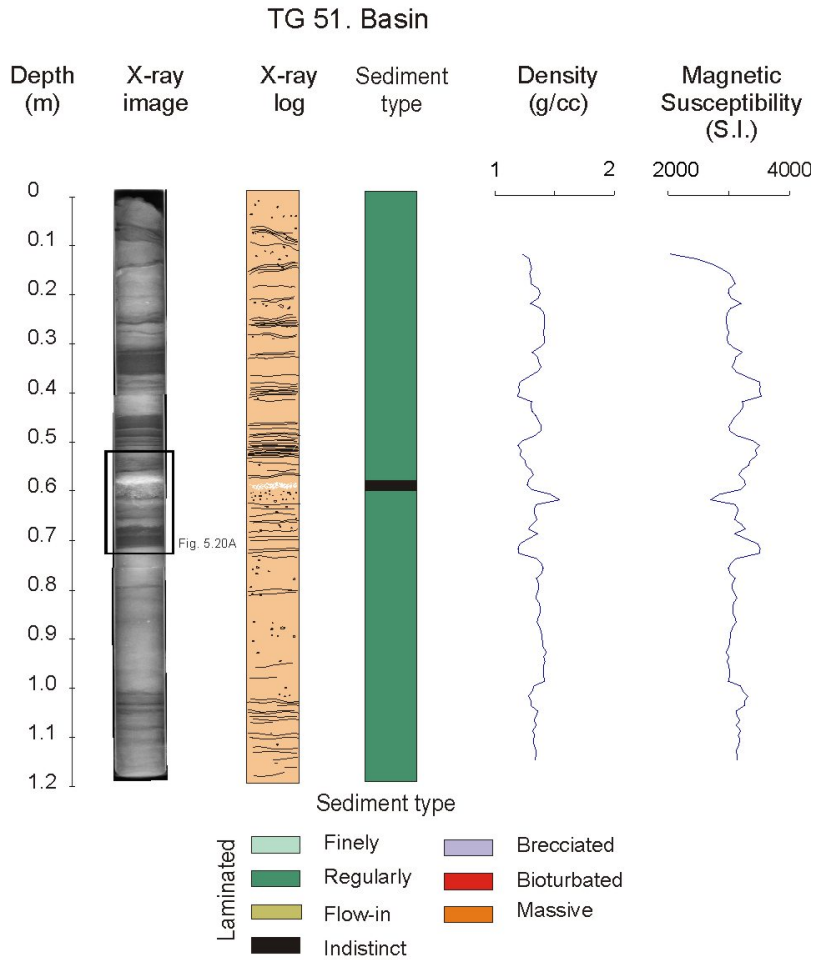
Figure 5.17. Sedimentological characteristics of sediment core TG51, including X-ray image and log, density and magnetic susceptibility. This core is located on the basin (Figs. 5.1 and 5.2)
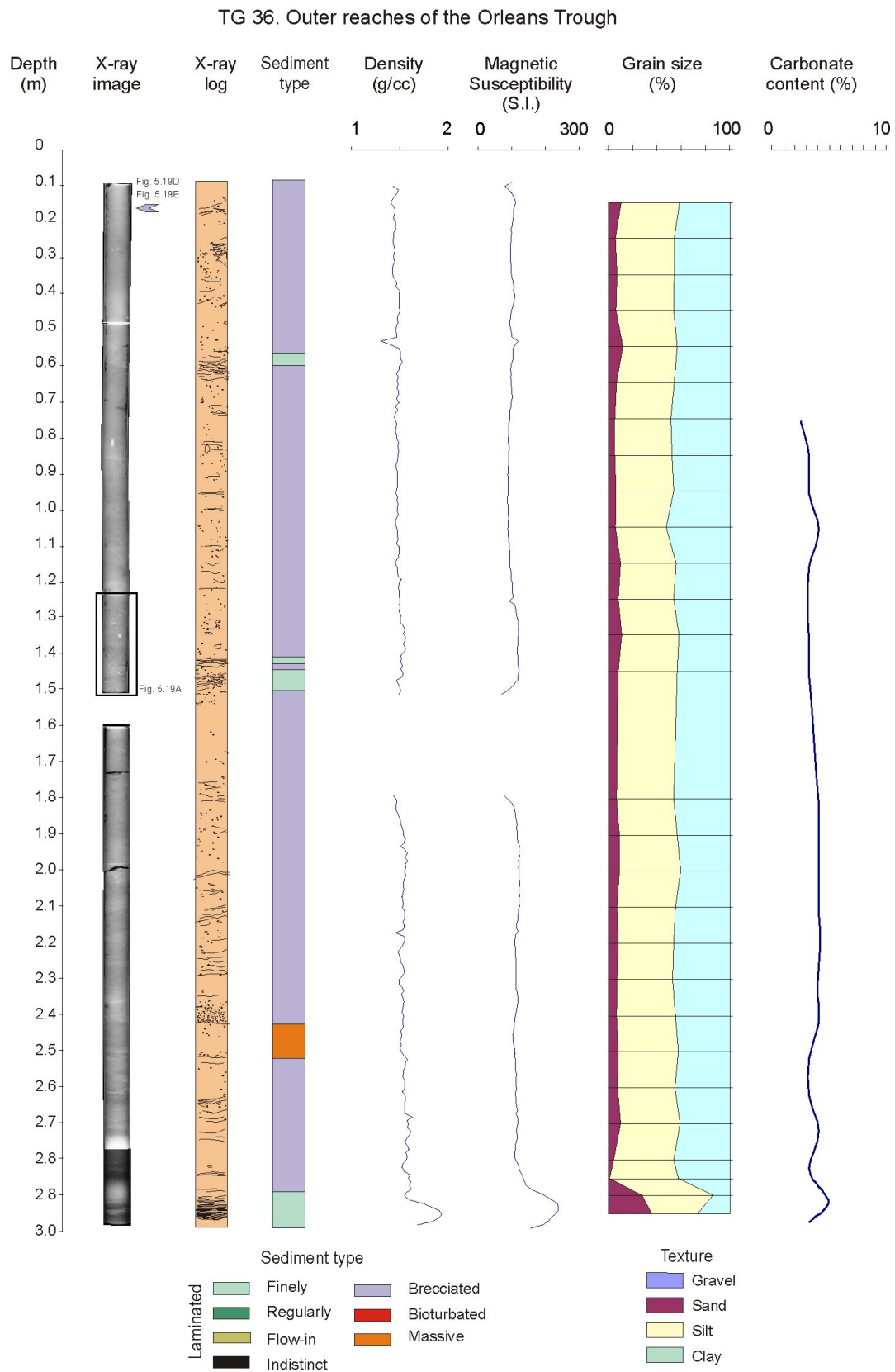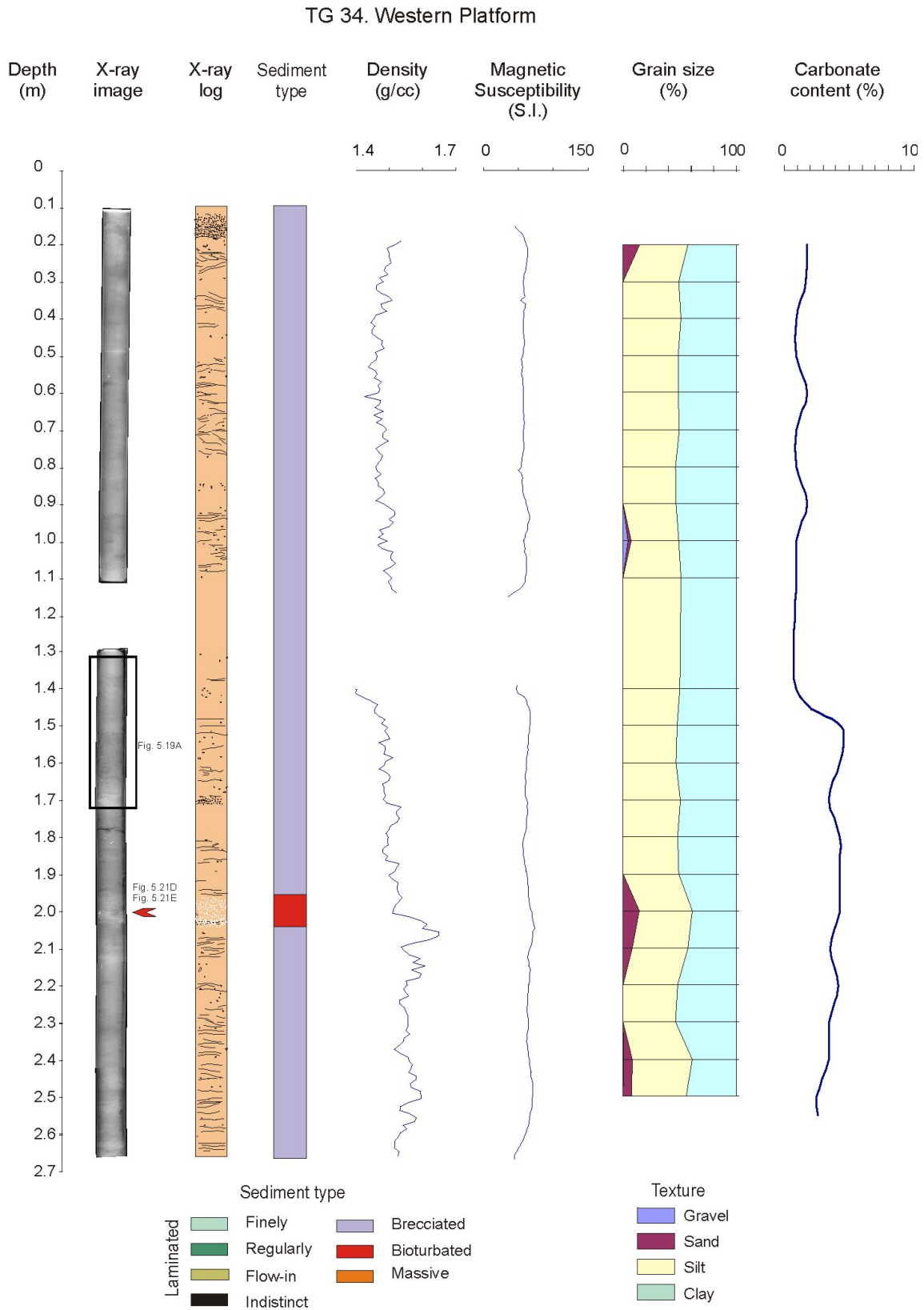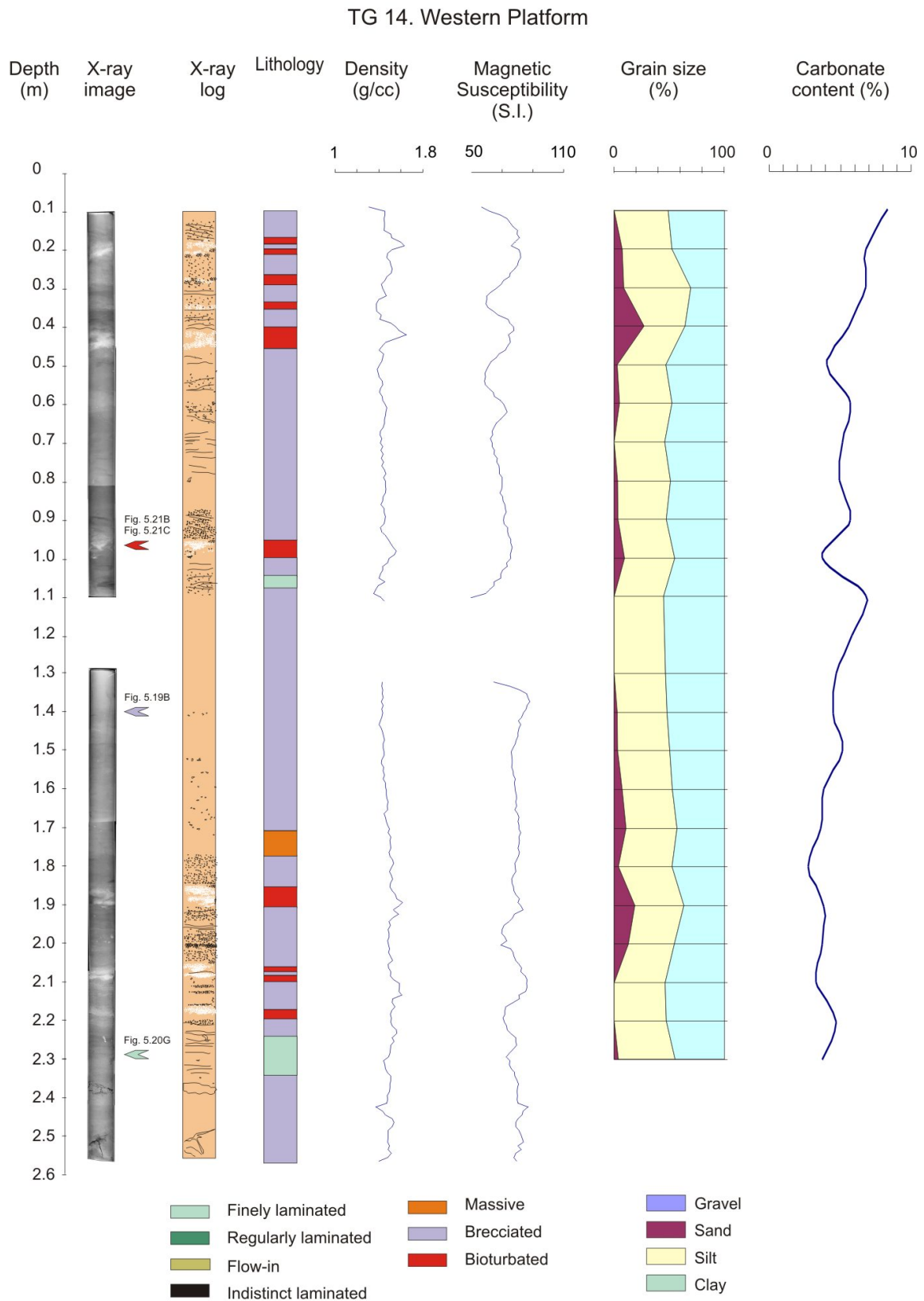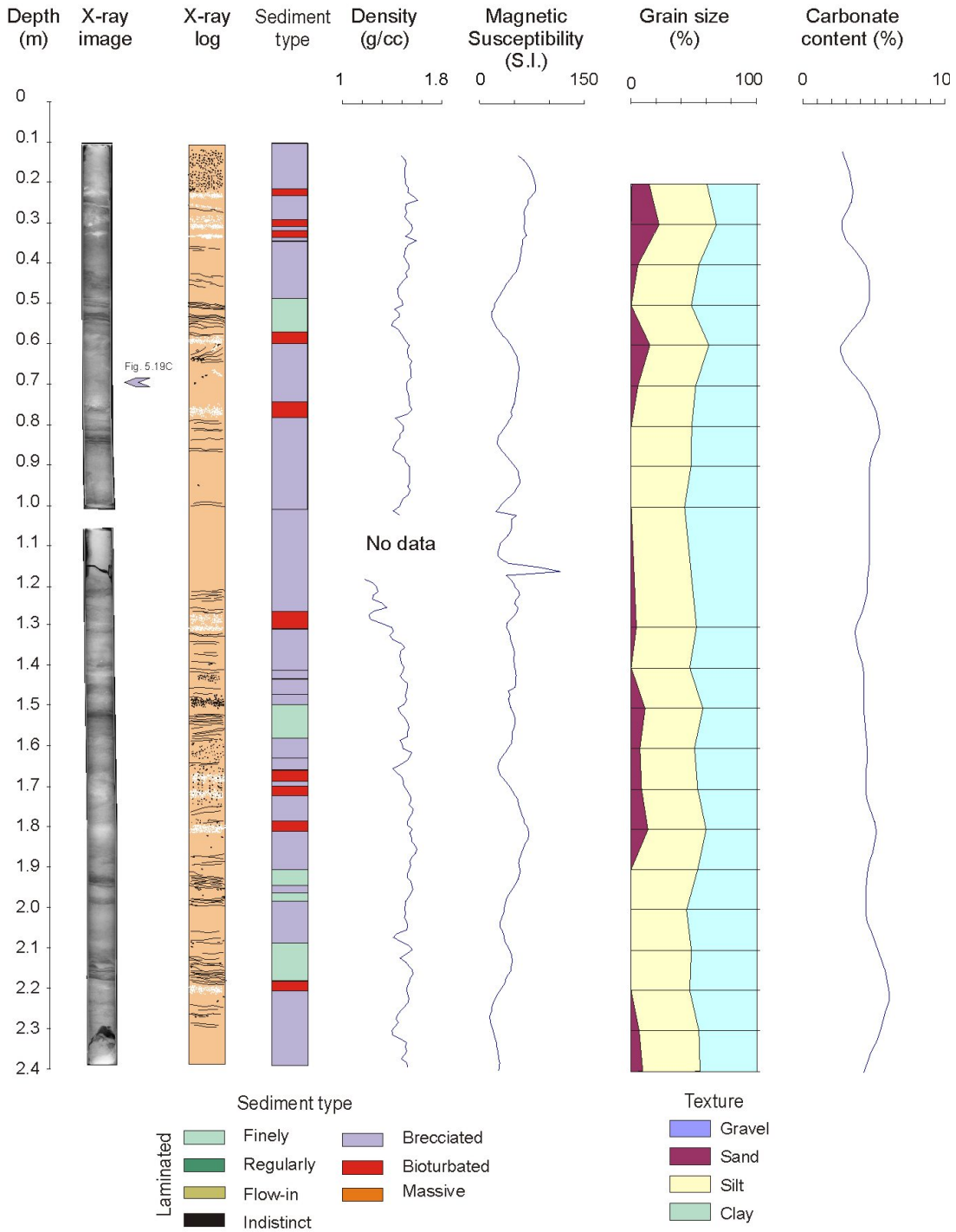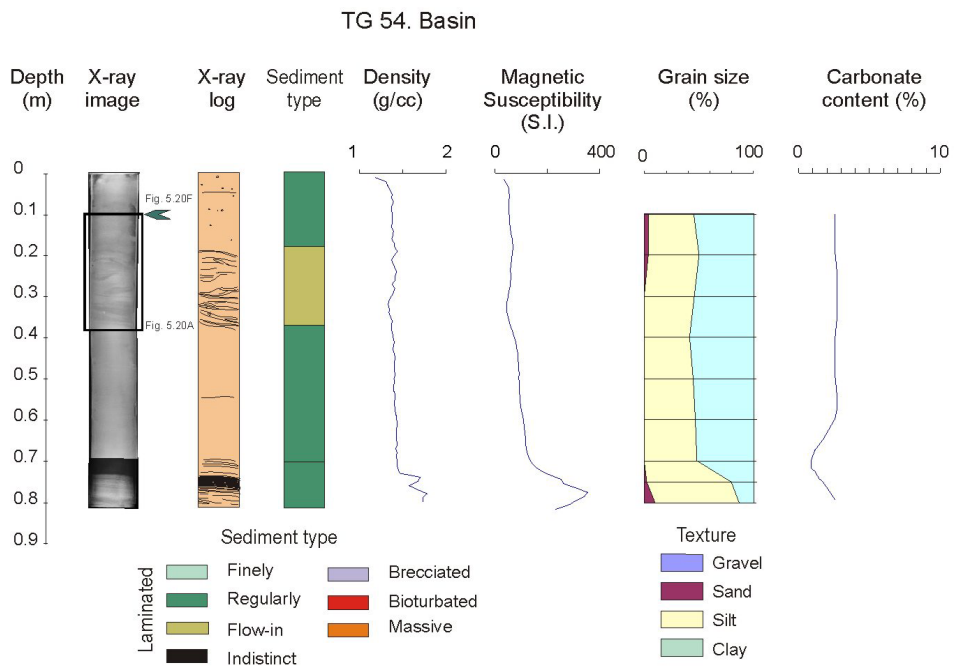

Figure 5.18. Sedimentological characteristics of sediment core TG54, including X-ray image and log, density, magnetic susceptibility, grain size log and carbonate content. This core is located on the basin (Figs. 5.1 and 5.2)

122

3. Major sediment types

Sediment types were defined on the basis of the grain size and the structures observed in X-ray images and split cores. Other qualitative and quantitative parameters were also considered, including the composition of the sand fraction, the qualitative composition of the pelitic fraction, carbonate content, color (Munsell color scale), and physical properties such as magnetic susceptibility and bulk density. Four major sediment types were distinguished and labeled on the basis of the sedimentary structures: 1) Brecciated; 2) Laminated; 3) Bioturbated; and 4) Massive (Table 5.II).

Sediment type	Brecciated	Laminated	Bioturbated	Massive
Structure	Structureless to weakly stratified Clasts	Regularly: mm- to cm- thick dark and light levels Finely: mm-thick light and dark levels Flow-in: deformed layers Indistinct: light massive to laminated mottles	Blurred structures and white mottling	No structure
Texture	Sandy mud Mud	Mud Sandy silt Muddy sand	Mud Sandy silt Muddy sand	Mud
Sand composition	Terrigenous, light and magnetic minerals, volcanic glass and dark fragments	Terrigenous (light and magnetic minerals). Indistinctly laminated: magnetic minerals and volcanic glass Biogenous: spicules	Light with magnetic minerals and volcanic glass	Terrigenous, low percentage of biogenous
Fine composition	Terrigenous with little biogenous	Coarse terrigenous and fine biogenous	Terrigenous and biogenous	Terrigenous and biogenous
Color	Grayish to brownish	Brownish to grayish	Grey olive	Olive brown
CaCO$_3$	2-8%	1-7%	2-4%	<4%
Density	1.5-2.4 g/cc	Mean: 1.4 g/cc	Peak (up to 2 g/cc)	Mean: 1.5 g/cc
MS	50-400 S.I.	100-400 S.I.	50-80 S.I. Max: 400 S.I.	120-150 S.I.

Table 5.II. Main characteristics of the sediment types differentiated in this study.

3.1. Brecciated sediment type

This sediment type is identified on the continental shelf glacial troughs, slope platforms, lower continental slope and basin of the CBB (Figs. 5.4 to 5.12 and 5.15). It is characterized by a dark gray matrix with light gray clasts in negative X-ray images (Fig. 5.19A). It is predominantly structureless to weakly stratified, with the matrix displaying a massive to blurred structure, but subhorizontal and inclined linear structures and indistinct laminations are also identifiable (Figs. 5.4 to 5.12, 5.15 and 5.19A). Some intervals are characterized by a relatively high concentration of clasts that display a chaotic and erratic distribution within the matrix. Some clasts show a weak to moderate preferential orientation, and others seem to be deformed soft clasts with an orientation subparallel to the stratification. The clasts are heterometric (0.2 to 3 cm long) and subangular to subrounded in shape and have low to high sphericity. Based on charts for *a visu* estimation of particle percentage (Swanson, 1981), their abundance varies from common to abundant, ranging between 11 and 60% and they form indistinct levels in which their presence is relatively high.
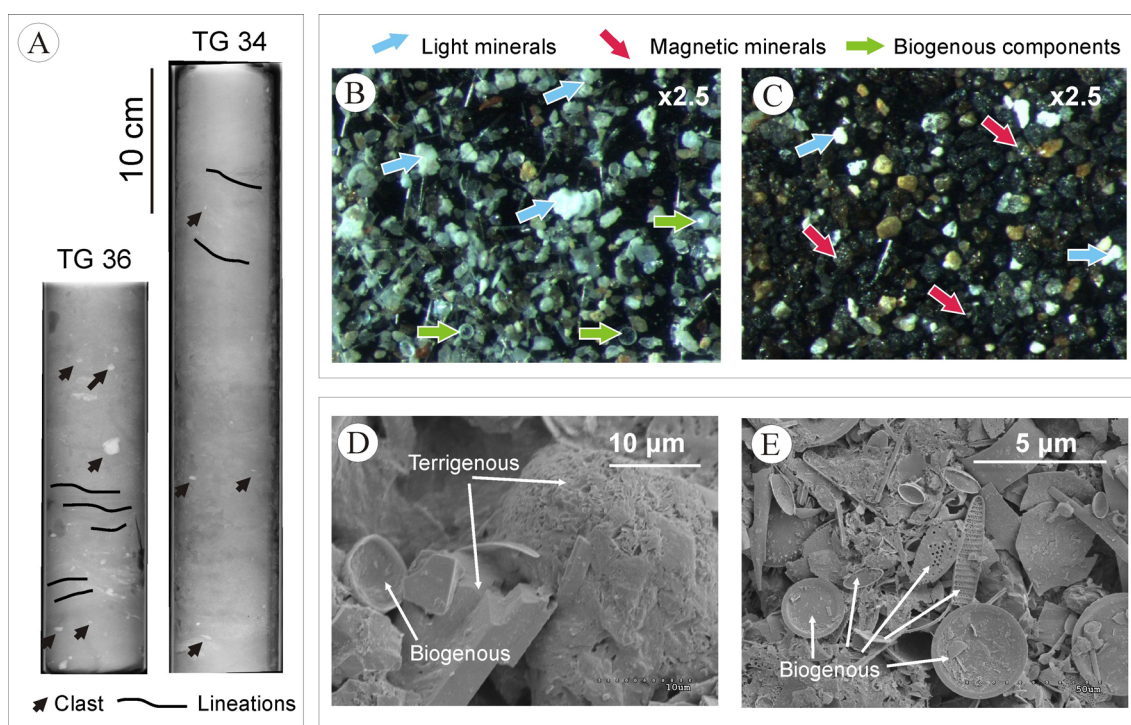
Figure 5.19. Characteristics of the brecciated sediment type. A) X-ray images showing the presence of heterometric clasts and linear structures. B) and C) Photographs of the sand fraction, showing the presence of light and magnetic minerals and biogenous components. D) and E) Electronic microscope images showing the terrigenous and biogenous composition of the pelitic fraction. For images location, see Figures 5.5 to 5.8.

The matrix is formed by sandy mud (about 40% silt, 30% clay and 24% sand) and mud (about 53% silt, 46% clay and 5% sand). In cores from the lower slope the matrix shows an upward grading (Figs. 5.11 and 5.12). The sand fraction composition is terrigenous (>85%),

with mostly light and magnetic minerals, volcanic glass and dark rock fragments (Fig. 5.19B,C). The biogenous fraction is dominated by spicules. In the clast-rich levels the sand fraction is mostly dominated by magnetic minerals, volcanic glass and rock fragments (Fig. 5.19C). The pelitic fraction is also dominated by poorly-sorted terrigenous material, with predomination of clay-like fragments. The biogenic fraction is poorly-sorted and is composed of fragmented diatoms, including *Thalassiosira, Porosira, Actinocyclus* and *Nitzschia* among others (Fig. 5.19D,E).

The brecciated sediment type shows a wide range of colors, from grayish to brownish colors (5YR 4/4, 5Y 5/4, 5Y 5/6, 5GY 3/2, 5GY 4/1, 10Y 4/1, 10Y 4/2). Carbonate content is low but shows relative peaks with values ranging from 2 to 8%. The brecciated sediment type has density values ranging from 1.5 to 2.4 gr/cc, and susceptibility values ranging from 50 to 400 SI. The vertical distributions of density and magnetic susceptibility do not display an overall trend but are marked by isolated peaks that coincide with the presence of large clasts or clusters of clasts (Figs. 5.10 and 5.12).

3.2. Laminated sediment type

This sediment type is identified in all the physiographic domains of the CBB (Figs. 5.4 to 5.9, 5.11 to 5.14 and 5.16 to 5.18). It can be subdivided into four subtypes, based on the characteristics of the laminated structure in the X-ray images and split cores: regularly laminated, finely laminated, flow-in structures and indistinct laminated (Fig. 5.20).

- The *regularly laminated subtype* is identified on the lower continental slope and basin (Figs. 5.11 to 5.14 and 5.16 to 5.18). This subtype displays levels of alternating light, dark and very dark tones in negative X-ray images, which are arranged forming intervals with millimetric to centimetric thick laminas. The lower boundary of the laminated levels is generally sharp, irregular-and erosive, and scour-and- fill structures can be identified.

- The *finely laminated subtype* can be found on the continental shelf glacial troughs and slope platforms (Figs. 5.4, 5.5, 5.7 to 5.9). These levels are arranged forming relatively finely laminated (millimetric) intervals. Cross laminations are identified at the bottom of some levels and parallel laminations predominate towards the top (Fig. 5.20A).

- The *flow-in structures subtype* is identified in the laminated sediments of the inner areas of the continental shelf glacial troughs, lower slope and basin (Figs. 5.4, 5.9, 5.13 and 5.18). It displays a flow-in structure characterized by deformed layers (undulating or contorted in vertically- and horizontally-oriented patterns), folded structures and the presence of sparse clasts (Figs. 5.4, 5.9, 5.13, 5.18 and 5.20A).

- The *indistinct laminated subtype* occurs in the sediment cores of the western part of the basin (Figs. 5.14, 5.16 and 5.17). It is characterized by very light tones in the negative X-ray images and a massive to weakly laminated structure.
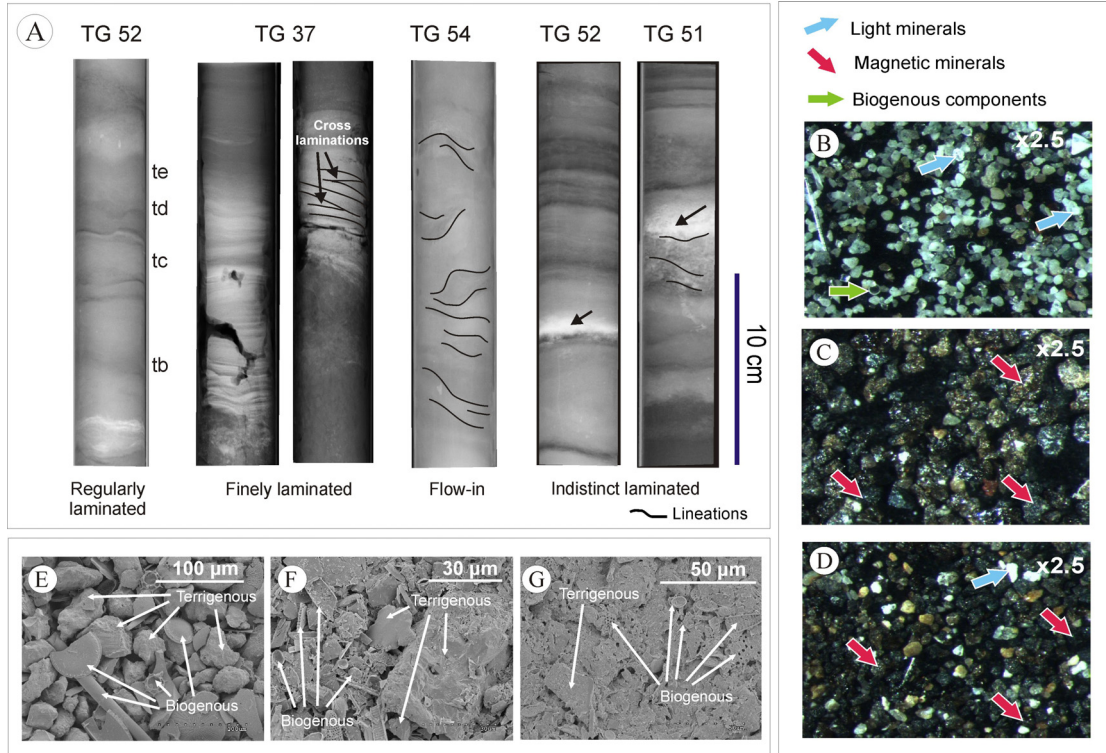
Figure 5.20. Characteristics of the laminated sediment type. A) X-ray images showing the different sub-types and their most important structures. B) to D) Photographs of the sand fraction, showing the presence of light and magnetic minerals and biogenous components. E) to G) Electronic microscope images showing the terrigenous and biogenous composition of the pelitic fraction. For images location see Figures 5.4, 5.7, 5.14 and 5.16 to 5.18.

The dominant texture of the laminated sediments is mud (about 42% silt, 24% sand and 33% clay), sandy silt (about 52% silt and 47% sand) and muddy sand (about 66% sand, 21% silt, 12% clay). The laminated sediments commonly represent fining upward levels of sandy silt to mud and from muddy sand to mud (Figs. 5.11, 5.16 and 5.18). Also texturally uniform levels are identified. Clasts up to 1.5 cm long rarely occur within this sediment type and their abundance decreases or totally disappears toward the top of the laminated levels.

The sand fraction composition is mainly terrigenous (>80%), composed of mostly light minerals with magnetic minerals, volcanic glass and rock fragments (Fig. 5.20B,C,D). The biogenous components consist mostly of spicules. In particular, the indistinct laminated subtype is exclusively composed of magnetic minerals and volcanic glass characterized by light brown to black blocky fragments with vesicle content. The pelitic fraction comprises two sizes: the coarser one is mainly composed of terrigenous material, and the finer one of fragments of diatoms, mostly *Thalassiosira*, *Porosira* and *Nitzschia* (Fig. 5.20E,F,G).

The color varies according to the sediment core location. On the continental shelf glacial troughs, slope platforms and lower continental slope the predominant colours are olive brown (5Y 4/4) with mottles of olive gray (10Y 5/4), olive gray (10Y 5/4), and dark greenish gray (5GY 4/1). On the basin the predominant colour is grayish olive (10Y 4/2), and the laminations have a wide range of colors: olive gray (5Y 3/2), brownish black (5Y 2/1) and moderate olive brown (5Y 4/4). Carbonate content ranges from 1 to 7%. Magnetic susceptibility ranges from 100 to 400 S.I. and generally decreases towards the top. The densitiy values in this sediment type are relatively constant, with a mean value of about 1.4 g/cc.

3.3. Bioturbated sediment type

Bioturbated sediments are characterized in negative X-ray images by the presence of blurred structures and white mottling, which disturb the original massive to indistinct laminated structure (Fig. 5.21A). Clasts are sparse in these levels. The bioturbated sediments display a similar texture and sand fraction composition to that of laminated sediments, being composed of mud (about 40% silt, 35% clay and 25% sand,), sandy silt (about 42% silt, 34% sand and 26% clay) and muddy sand (about 47% sand, 30% silt and 23% clay).
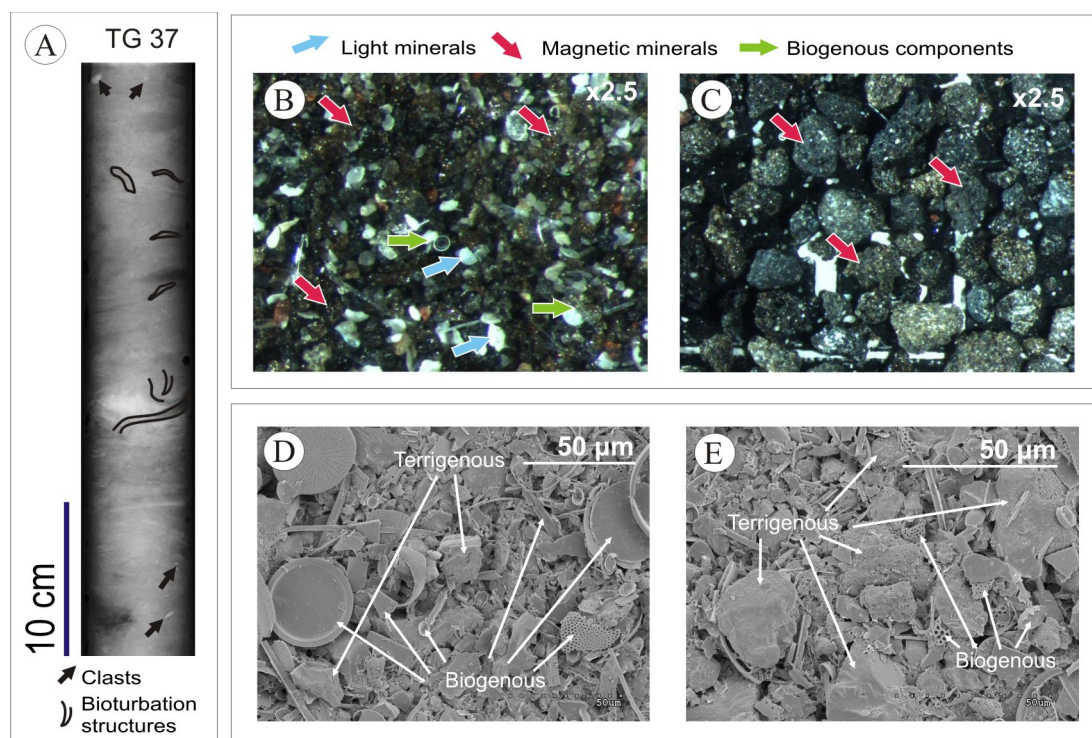
Figure 5.21. Characteristics of the bioturbated sediment type. A) X-ray image showing the presence of spare clasts and bioturbation structures. B) and C) Photographs of the sand fraction, showing the presence of light and magnetic minerals and biogenous components. D) and E) Electronic microscope images showing the terrigenous and biogenous composition of the pelitic fraction. For figures location see Figures 5.6, 5.7 and 5.9.

The sand fraction consists of light with magnetic minerals, or mostly magnetic minerals and volcanic glass (Fig. 5.21B,C). The pelitic fraction is dominated by poorly sorted

terrigenous material with a finer biogenous fraction composed of diatoms, both complete and fragmented (*Thalassiosira, Porosira, Nitzschia*) (Fig. 5.21D,E).

Gray olive colors predominate in this type of sediment (dark greenish gray 5GY 4/1, olive greenish gray 5GY 3/2 and grayish olive 10Y 4/1). The carbonate content ranges from 2 to 4%. Magnetic susceptibility ranges from 50 to 80 S.I., except for the level identified in sediment core TG37 in the inner basins of the Orleans Trough, where values reach 400 S.I. (Fig. 5.4). Density generally shows a peak in the bioturbated levels, reaching values of up to 2 g/cc.

3.4. Massive sediment type

This facies is identified in the continental shelf glacial troughs and on the slope platforms (Figs. 5.4, 5.5 and 5.7). The massive sediment type displays a uniform appearance in both the core sections and the X-ray images, with no internal sedimentary or organic structures (Fig. 5.22). Erratic clasts (<5%) can be observed.

The massive sediment type consists of about 50 % clay, 48 % silt and 2% sand. The sand fraction includes terrigenous components (mostly light minerals) with relatively low percentage (<30%) of spicule fragments and unidentifiable biogenous fragments (Fig. 5.22B). The pelitic fraction is poorly sorted and dominated by heterometric terrigenous and biogenic particles composed of fragments of diatoms (*Thalassiosira, Porosira, Nitzschia*) (Fig. 5.22C).

The massive sediment type displays a general moderate olive brown color (5Y 4/4), mottled with olive gray (10Y 5/4). The carbonate content is generally less than 4%. Magnetic susceptibility shows values of 120-150 S.I., and the density is relatively constant, with a mean value of 1.5 g/cc.
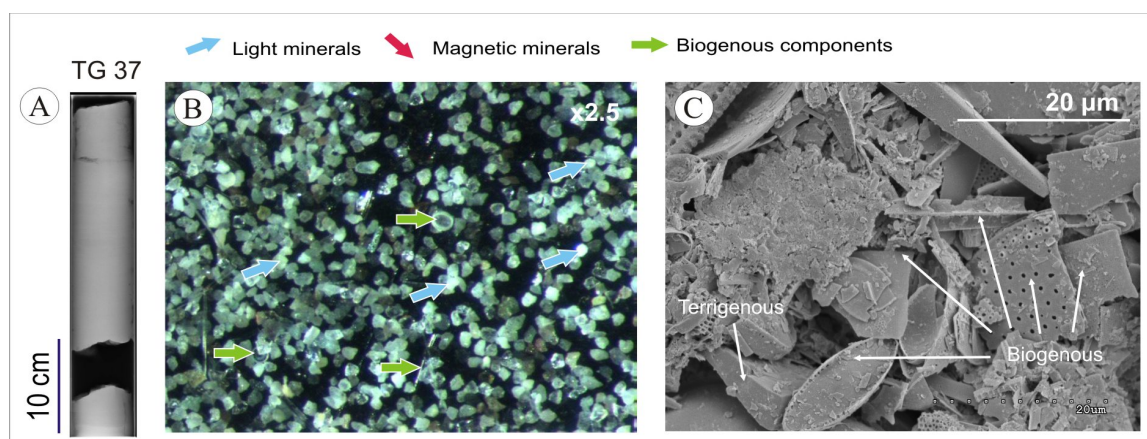
Figure 5.22. Characteristics of the massive sediment type. A) X-ray image. B) Photograph of the sand fraction, showing the predominance of light minerals and biogenous components. C) Electronic microscope image showing the terrigenous and biogenous composition of the pelitic fraction.

4. Definition of sedimentary sequences

The major sediment types present in the sediment cores can be divided into major assemblages that have sedimentological affinities. Each sequence is defined according to a sediment type succession that reflects deposition resulting from either a specific sedimentary processes (e.g., glacial turbid layers/meltwater plumes, turbidity currents, and mass flow) or regionally large-scale environment events (e.g., climatic changes significant enough to alter the ice sheet, eustatic oscillation and/or biogenic production). Seven major sequences are distinguished (Table 5.III): 1) Subglacial diamicton; 2) Compound glaciomarine; 3) Turbid glacial meltwater; 4) Proglacial diamicton; 5) Turbidite; 6) Flow-in; and 7) Contourite.

Depositional environment	Core	Subglacial diamicton	Compound glaciomarine	Turbid glacial meltwater	Proglacial diamicton	Turbidite	Flow-in	Contourite
Inner reaches of glacial troughs	TG37	X	X	X			X	
Outer reaches of glacial troughs	TG36		X	X				
Slope platforms	TG34		X					
	TG15		X	X				
	TG14		X	X				
	TG11		X	X			X	
Lower slope	TG3				X		X	
	TG4				X			
	TG29				X	X		
	TG56						X	
Basin	TG2							X
	TG10					X		
	TG51					X		
	TG52					X		
	TG54					X	X	

Table 5.III. Sedimentary sequences identified in the sediment cores illustrated in the figures of this chapter.

4.1. Subglacial diamicton

This sequence is identified in the inner reaches of the Orleans Trough (Table 5.III and Fig. 5.23). Subglacial diamicton has a sandy mud matrix-supported clasts fabric and is composed of brecciated sediments that have the highest percentage of clasts (60%). The clasts are interpreted as ice-rafted debris (IRD) on the basis of their heterometric size, shape and distribution. Linear structures representing shear structures are also identified (Fig. 5.19A). The sequence has a sharp upper boundary and a thickness of at least 14 cm, occupying the bottom of core TG37 (the lower boundary was not recovered).

The shear structures and oriented fabric displayed by the diamicton sequence suggest that it can be interpreted as soft glacial diamicton. This interpretation is supported by the physiographic location in the inner areas of a glacial trough and by the identification of compound glaciomarine sequences overlying the sequence (Fig. 5.23). Soft diamicton is the product of the deformation and reworking of lodgement diamicton (Evans et al., 2005) and reflects the effect of glacial erosion due to the action of ice sheets (Murdmaa et al., 2006).

4.2. Compound glaciomarine sequence

This sequence predominates in the continental shelf glacial troughs (TG37 and TG36, Fig. 5.25 and Table 5.III) and slope platforms (Table 5.III and Fig. 5.24). It consists of levels (a few centimeters to 180 cm thick) of brecciated sediment displaying a crude stratification and weak lamination, with thin (3-10 cm) clast-rich levels and intercalations of layers of massive and bioturbated sediment type. The boundaries with the structureless mud are sharp, and those with the bioturbated mud are diffuse. The detailed analysis of the X-ray images shows centimetric levels characterized by a lower laminated light-toned section that change towards the top to a uniform and/or crudely laminated dark-tone section, and this can be tentatively associated with a fining upward succession (Figs. 5.6 to 5.8).

The levels of brecciated sediment are interpreted as the result of the interplay of glaciomarine processes (Fig. 5.23). Sparse IRD distributed throughout the compound glaciomarine sequence result from the relatively continuous rain-out of basal debris from the ice shelf and/or icebergs calved from the ice shelf, while the clast-rich levels (up to 50%) indicate the massive presence of IRD and suggest the occurrence of three processes: a) pulses of increased rain-out of debris from the base of the ice shelf and icebergs (Lucchi et al., 2002; Heroy et al., 2008); b) quasi-instantaneous dumping of sediment accumulated on the iceberg surface and deposited after the iceberg calving or overturning (Dowdeswell et al., 1994); and c) the basal level of the deposition of IRD-charged flows from sediment-laden plumes emanating from the grounding line, in the cases in which IRD-rich levels form the lower part of fining-upward levels of brecciated sediment. The bioturbated levels intercalated with the brecciated sediment are interpreted in terms of a decrease in the sedimentation rates during pulses of

cessation of the glacial/glaciomarine processes (Ó Cofaigh et al., 2001). The levels of massive sediment may also be the result of the cessation of glacial/glaciomarine sedimentation, as suggested by the lack of any structure or IRD within these levels.
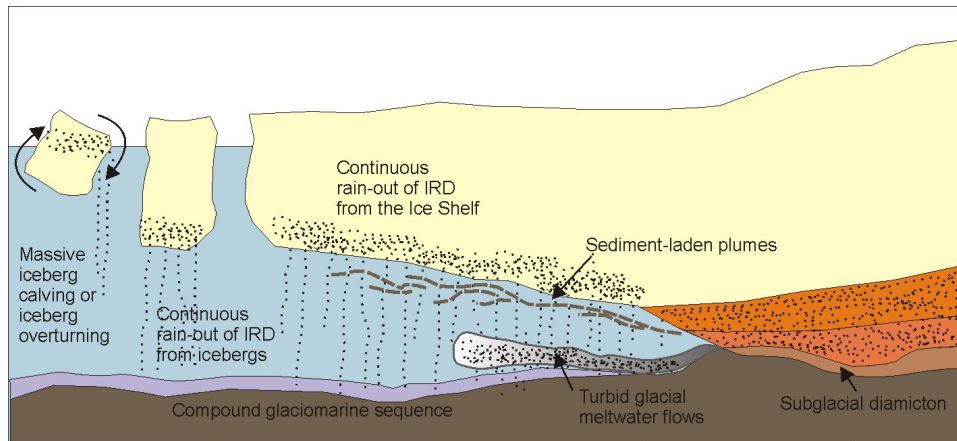
Figure 5.23. Scheme of the glaciomarine processes involved in the deposit of IRD within the compound glaciomarine sequence.

4.3. Turbid glacial meltwater sequence

This sequence is deposited in the continental shelf glacial troughs (Fig. 5.24 and Table 5.III), and on the slope platforms (Fig. 5.25 and Table 5.III) and occurs interbedded with compound glaciomarine sequences. The turbid glacial meltwater sequence consists of 3 to 20 cm-thick levels of finely laminated sediment subtype composed of mud or silt, and fining-upward sediments ranging from sand and silt to mud. The fining-upward sequence displays cross and/or parallel lamination at the base (lighter in X-ray images) that changes to indistinct lamination and lack of structures (darker in X-ray images) toward the top (Fig. 5.20A). The upper part of this sequence is absent in many of these sequences, which are considered as top-cut sequences. Likewise, many of these sequences have irregular and sharp bottom limits, in some cases with scour-and-fill structures, which are interpreted as erosive limits (Figs. 5.24 and 5.25).

This sequence is interpreted as glaciomarine sediment deposited by pulses of dense turbid meltwater flows formed seaward of the grounding zone (Hesse et al., 1997; Lucchi et al., 2002; Escutia et al., 2003; Murdmaa et al., 2006). The fine lamination, lack of bioturbation in the structureless mud, incomplete sequences, and erosive lower limits may indicate high-energy deposition of turbid flows. These glacio-marine processes could occur as sporadic events of turbid meltwater current discharge, as suggested by the interbedding of this sequence with the compound glaciomarine sequences, displaying erosive and sharp boundaries that indicate a sharp change in the environmental conditions.

4.4. Proglacial diamicton

This sequence is exclusively identified on the lower continental slope (TG3, TG4 and TG29, Fig. 5.26 and Table 5.III) and consists of 15 to 230 cm-thick levels of brecciated sediment displaying a matrix-supported IRD fabric, interbedded with centimetric levels of laminated mud. The high percentages of IRD (up to 60%) and its large size are the differential characteristic of the proglacial diamicton. This sediment is predominantly structureless, although a poor stratification can be identified, as evidenced by the fining-upward grain size trend of the matrix in levels up to 30 cm thick, and by the presence of centimetric bands of faint parallel lamination where IRD appear oriented and deformed with a lamination-parallel trend (Fig. 5.26).

The main glaciomarine sedimentary process responsible for the formation of the proglacial diamicton is the massive rain-out of glacigenic debris from the proximal basal zone of the ice shelf and calved icebergs and the lateral transport of turbid meltwater flows from the grounding line (Evans et al., 2005). The rain-out of IRD from the ice shelf and icebergs could explain the presence of clusters of IRD observed in some cores (TG29 and TG4, Fig. 5.26). This mechanism of transport and deposition through the water column, without the effect of a later lodgement process, is consistent with the results from consolidation tests obtained in this sediment by Casas et al. (2004).

The generally undeformed IRD and the absence of shear structures suggests that this sequence represent non-deformed till, while the local weak stratification may record debris transport by mass flows and/or reworking of the original proglacial diamicton by sub-aqueous mass flows. The latter interpretation is supported by the steep regional slope (10 to 18º) and the presence of mass movement features affecting the near-surface sediments (Casas et al., 2004).

4.5. Turbidite sequence

This sequence comprises <10 to tens of cm-thick intervals in the lower slope and basin sediment record (Figs. 5.26 and 5.27 and Table 5.III). It is defined as an upward-fining sequence from silty sand to mud, corresponding mostly to the regularly laminated sediment subtype. The turbidite sequence displays various terms defined by Bouma (1962), although none of the cores register the complete Bouma sequence. The Bouma terms identified are from Tb to Te, but most of them are Td and Te, displaying the characteristics of the muddy turbidites. The X-ray images show that many rhythms are truncated at the top and/or the bottom (Tb-e, Tb-d, Td-e) indicating that those turbidity sequences are base- and top-cut (Figs. 5.25 and 5.26). The lower boundaries of the levels within the turbidite sequence are sharp and/or erosive and the upper boundaries are sharp.

Layers of volcanic sediment can be differentiated within the turbidite sequences. These layers are 1-4 cm thick and are composed of an indistinct layered sediment subtype. The shallower layer can be correlated along the western part of the basin because it occurs at similar core depths (50-85 cm) in the three sediment cores recovered in this area (Fig. 5.27). Two deeper layers of similar characteristics can only be identified in sediment core TG52 at core depths of 110 and 115 cm and in sediment core TG50 at a core depth of 183 cm. Although the composition of the layers and the location of the cores where they have been identified strongly indicate that the sediment composing these layers has a volcanic origin, their sedimentary structure indicates rapid deposition from sediment gravity flows, mainly as proximal sandy and/or silty turbidites.

The above features indicate that turbidite sequences have been deposited from marine processes represented by turbidity flows with different types of sedimentary charge, i.e., finer- and coarser-grained turbidity flows, or diluted and denser turbidity flows. These flows would affect the glacigenic sediment deposited at or near the grounding line of the ice sheet and the volcanoclastic sediment from the volcanic edifices (Alley et al., 1989; Laberg and Vorren, 1995; Punkari, 1997; Vorren and Laberg, 1997; Casas et al., 2004; Dahlgren et al. 2005).

4.6. Flow-in sequence

This sequence is identified in the inner reaches of the Orleans glacial trough, on the SSI slope platform, on the AP lower slope and in the basin (Figs. 5.24 to 5.27 and Table 5.III). It forms layers tens of cm thick and is characterized by the flow-in laminated sediment subtype. The presence of abrupt angular contacts and the highly disturbed structures of this sequence, interbedded with compound glaciomarine deposits on the slope platform and with turbidites in the basin suggests that this sequence is formed by sediment reworked by plastic deformation.

4.7. Contourite sequence

The contourite sequence (about 30 cm thick) is identified at the foot of the lower slope (Fig. 5.27 and Table 5.III), in an area morphologically characterized as a contourite moat (Fig. 5.2). It is composed of brecciated sediment facies that show some IRD-rich levels (up to 2 cm long IRD, in a proportion of up to 11%) which occur in beds with a predominant orientation, whereas IRD is sparse in the rest of the sequence (Casas et al., 2004). This sequence is interpreted as the result of bottom current activity that influences the deposition of sediments reaching the basin, arising from glaciomarine or mass wasting processes. The presence of IRD suggests the glacigenic character of the sediment forming this sequence. The difference in the IRD concentration at different levels may indicate variations in the intensity of the bottom currents and the oriented IRD suggests the occurrence of strong bottom currents (McCave and Tucholke, 1986).
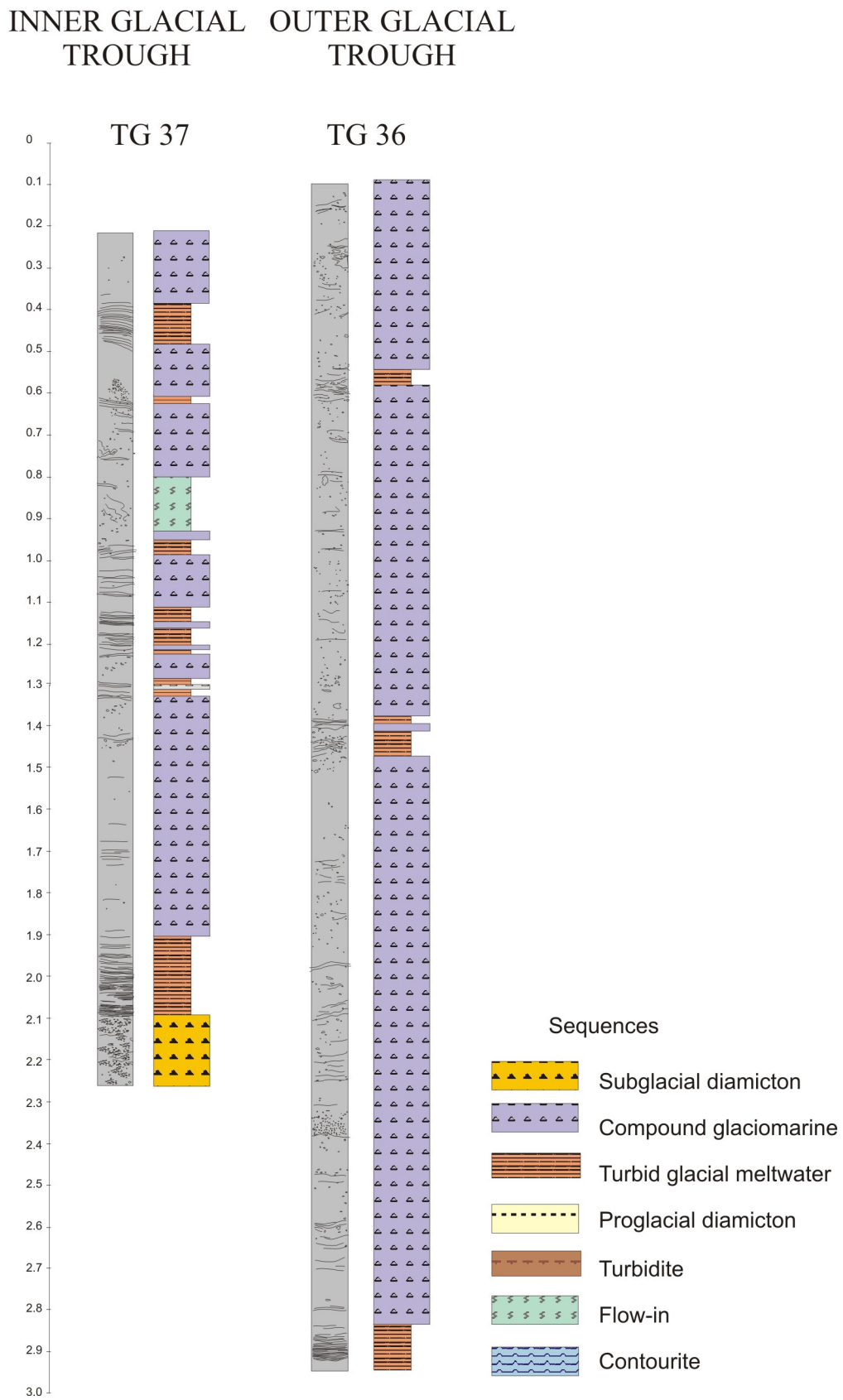
Figure 5.24. Sequences defining the stratigraphy of sediment cores from the inner (TG37) and outer (TG36) glacial trough. See location of cores in Fig. 5.1. The X-ray log shows the structural criteria in the definition of sequences.

WESTERN SLOPE PLATFORM

SSI SLOPE PLATFORM

TG 34   TG 14   TG 15   TG 11

Sequences

Subglacial diamicton — Turbidite

Compound glaciomarine — Flow-in

Turbid glacial meltwater — Contourite

Proglacial diamicton
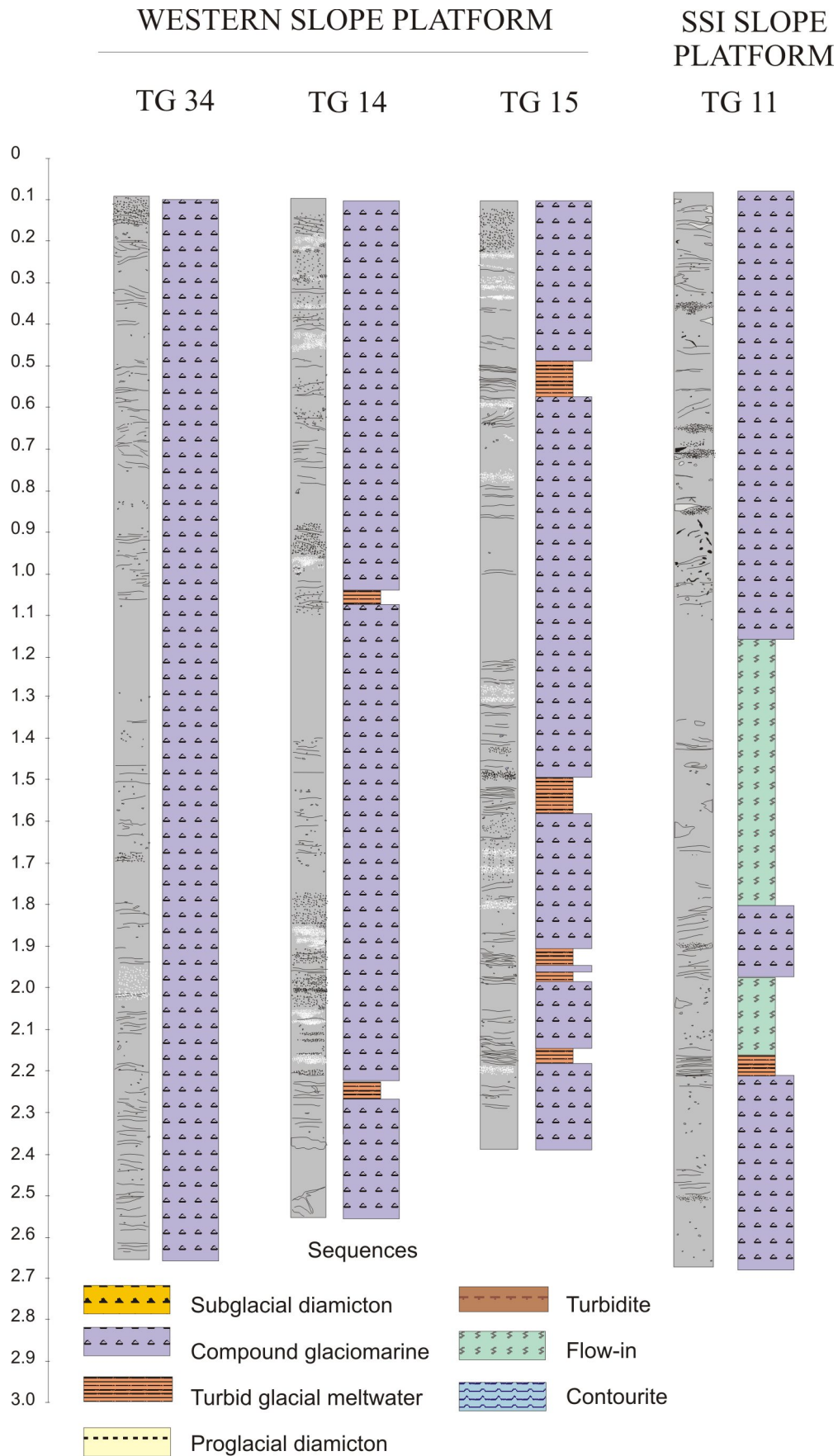
Figure 5.25. Sequences defining the stratigraphy of sediment cores from the AP (TG34, TG15 and TG14) and SSI (TG11) slope platforms. See location of cores in Fig. 5.1. The X-ray log shows the structural criteria in the definition of sequences.

135

LOWER SLOPE
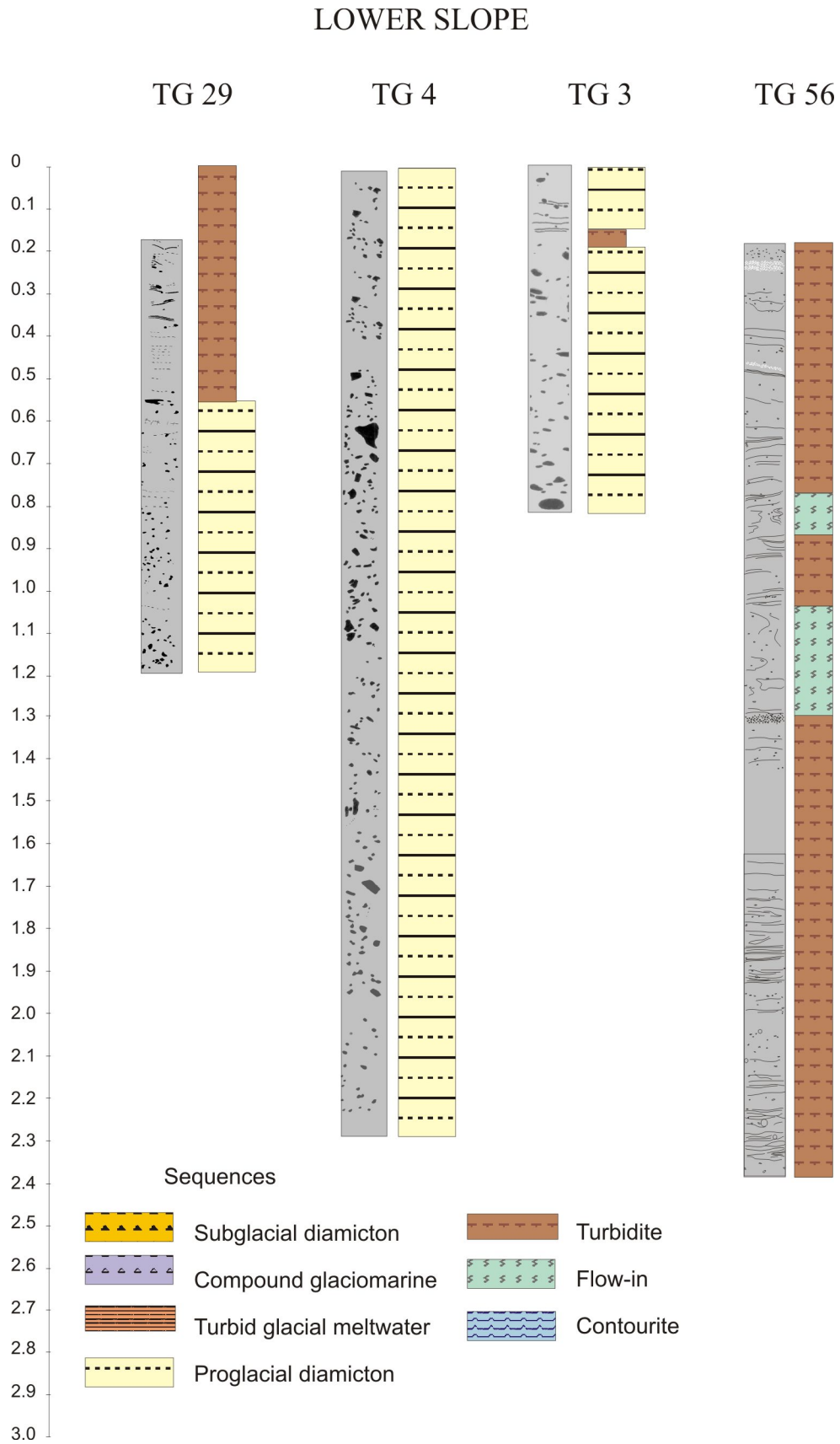
Figure 5.26. Sequences defining the stratigraphy of sediment cores from the lower continental slope of the AP margin. See location of cores in Fig. 5.1. The X-ray log shows the structural criteria in the definition of sequences.
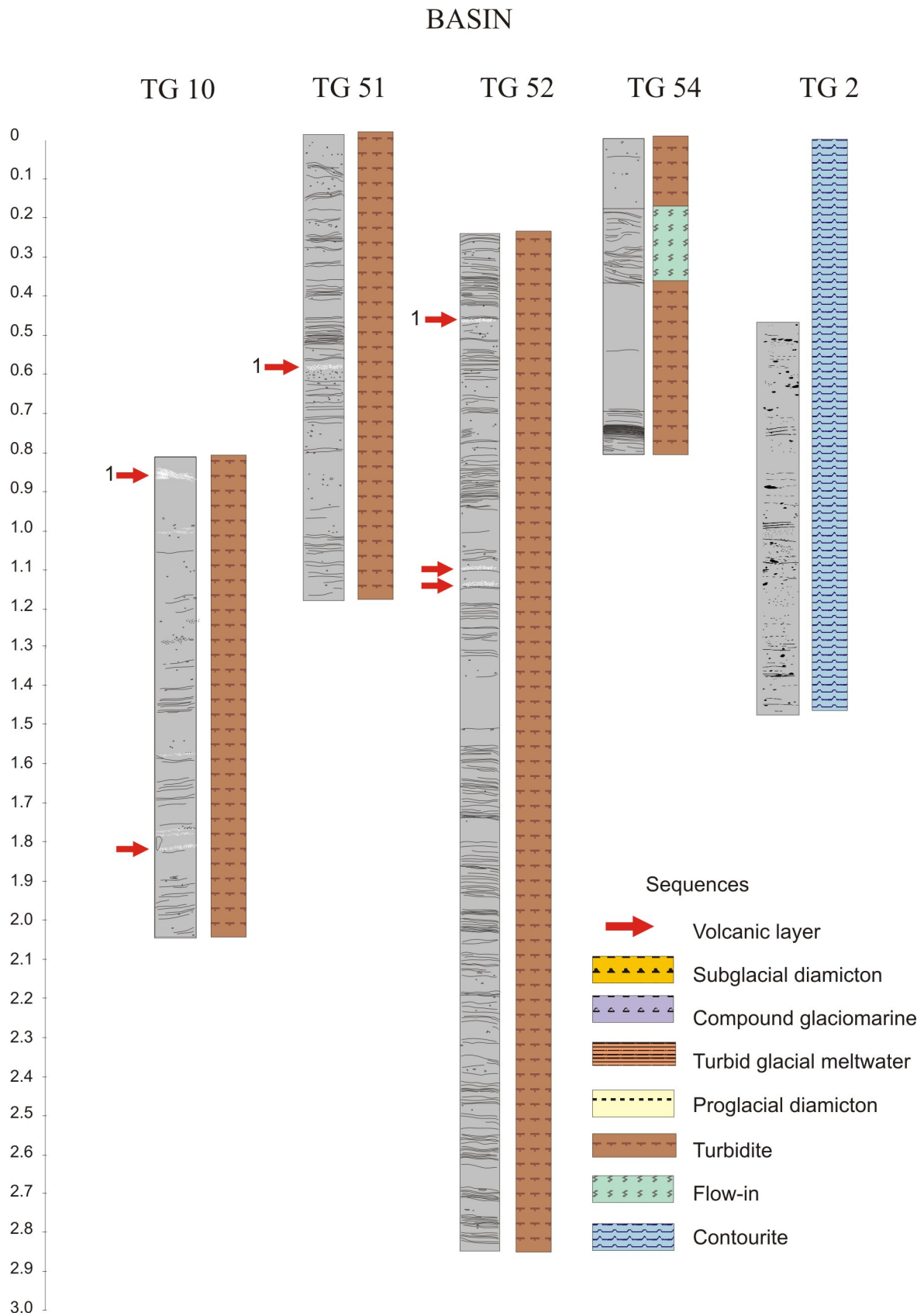
Figure 5.27. Sequences defining the stratigraphy of sediment cores from the CBB basin. See location of cores in Fig. 5.1. The X-ray log shows the structural criteria in the definition of sequences. Number 1 indicates the volcanic layer that can be correlated between cores of the western area of the basin.

5. Discussion: spatial and temporal variability of the near-surface stratigraphy

The mapping of the sedimentary sequences composing the surficial sediment of the CBB (Fig. 5.28) reveals a close relationship between the sedimentary processes (glacial, glaciomarine and marine) that predominate in the different physiographic domains and the resulting near-surface stratigraphy. The slope platforms glacial troughs show a compound glaciomarine sequence. Only the area of the WP located between Deception Island and Volcanic Edifice A is characterized by turbidite sequences. The lower slope has a proglacial diamicton sequence, except in the area between the EP and WP, which is characterized by turbidite sequences. With the exception of the area at the foot of the lower slope off the Lafond glacial trough, which presents a contourite sequence, the basin is mostly characterized by turbidite sequences.
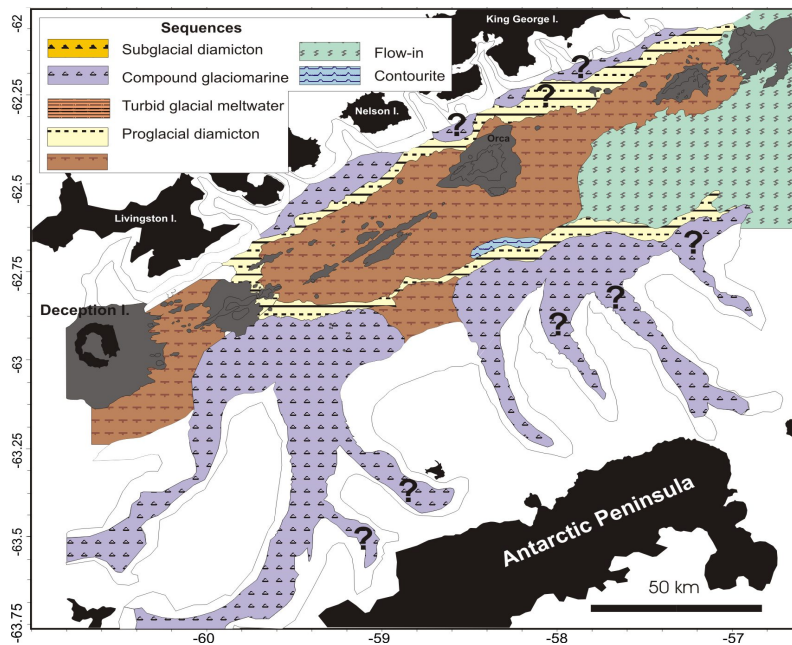
Figure 5.28. Surficial distribution of sedimentary sequences in the CBB. The extrapolation to the entire CBB was based on the integration of sedimentological and seismic data. Note the strong correlation between the surficial sequences and the physiographic domains.

The results of this study show that sequences are not generally correlatable across the CBB or even within a single physiographic domain though in the latter a general succession of sedimentation patterns can be recognized (Fig. 5.28). Because of this, the regional distribution of sequences is differentiated according to the physiographic domains in which they occur: continental shelf glacial troughs, slope platforms, lower continental slope and basin.
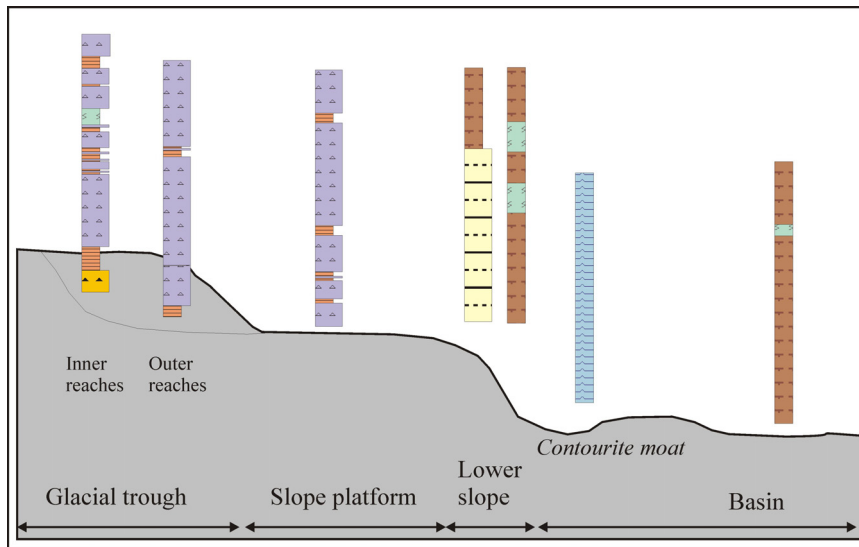
Figure 5.29. General distribution of sedimentary sequences in the physiographic domains of the CBB. See legend on Fig. 5.28.

5.1. Stratigraphic model of the continental shelf glacial troughs

The glacial troughs display two different stratigraphic models based on the location: inner and outer (Figs. 5.24 and 5.29). The stratigraphy of the inner reaches of the glacial trough comprises a basal subglacial diamicton sequence overlaid by compound glaciomarine sequences interbedded with different levels (at least eight) of turbid meltwater sequences and a level of flow-in sequence. The compound glaciomarine sequences are characterized by coarser-grain sediments and a greater presence of glacial debris than those deposited on the slope platforms. The flow-in sequence may be the result of debris flows from the steep walls of the Orleans Trough (Camerlenghi et al., 2001). The stratigraphy of the outer reaches of the glacial troughs is defined by the compound glaciomarine sequence with interbedded levels of turbid meltwater sequences.

5.2. Stratigraphic model of the slope platforms

The stratigraphy of the AP slope platforms consists mostly of compound glaciomarine sequences with interbedded levels of turbid glacial meltwater sequences (Figs. 5.25 and 5.29). The greatest variability occurs in the outer slope platforms. In contrast, cores from the inner slope platforms show a low variability and in some cases are only represented by the compound glaciomarine sequence. The compound glaciomarine sequences in this domain are characterized by numerous bioturbated and IRD-rich levels. On the SSI slope platforms (TG11), the stratigraphy is similar, but higher percentages of glacial debris and bioturbation are observed, especially toward the top of cores (Fig. 5.25).

5.3. Stratigraphic model of the lower continental slope

The stratigraphy of the lower continental slope comprises two distinct models (Figs 5.26 and.5.29): a) proglacial diamicton sequences locally interbedded with turbidite sequences in sediment cores from the lower continental slope off the eastern slope platform (TG29 and TG3); and b) turbidite sequences with interbedding of flow-in sequences in the near-surface sediment east of the Gebra-Magia slide complex area (Fig. 5.26).

5.4. Stratigraphic model of the basin

The stratigraphy of the basin comprises two distinct sequence models (Figs. 5.27 and 5.29): a) turbidite sequences, or turbidite sequences with interbedded levels of flow-in sequences; and b) contourite sequences. The basin stratigraphy of the basin is mostly defined by the vertical succession of turbidite sequences, locally interbedded with flow-in sequences in the eastern sector of the lower continental slope. The flow-in sequence represents remolding of the turbidite sequences. The correlation of turbidites through basins has been described many times and various criteria have been used to perform it (Weaver et al., 1986; Weaver and Rothwell, 1987; Davies et al., 1997). However, in this work, it was not possible to correlate all the identified turbidites. Only the correlation of one volcanic layer was possible, based on the similar core depth, texture, sand fraction composition and physical properties (Fig. 5.27).

The contourite sequence is defined in core TG2 from the contourite moat located on the basin, at the foot of the lower slope (Fig. 5.2). This sequence is composed of contouritic mud and silt, and was defined based on the geomorphological environment in which it occurs, which explains the strictly process-related sequence. From a sedimentological point of view, the recognition of contourites –and especially of muddy contourites– is difficult because they usually occur associated with fine turbidites, displaying similar textural and acoustic characteristics and both types of deposit commonly have a stratigraphic continuity (Stow and Lovell, 1979; Howe, 1995; Stoker et al., 1998).

5.5. Glacial cyclicity, morphology, physiography, sediment source and oceanography as controlling factors of the sedimentary products

The stratigraphy and spatial and temporal distribution of the sedimentary sequences are the geological criteria that distinguish the global factors (glacial cycles) from the local factors (morphology and physiography, sediment source and oceanography) that have governed the recent sedimentary history of the CBB.

5.5.1. Global factor: last glacial-interglacial cycle

The sediment types, sedimentary sequences and stratigraphic models defined in this study indicate that the sedimentary record may fit into the last glacial-interglacial cycle, in spite of the lack of dating for the sediment core samples. The last glacial advance was a period

when the AP ice sheet and ice streams within it advanced along the AP and SSI margins. The last deglaciation in the CBB started at 17340 cal yr B.P. in the more distal areas of the AP margin and finished at about 9000 cal yr B.P. in the inner areas of glacial troughs (Heroy and Anderson, 2005; Heroy et al., 2008). The last glacial-interglacial cycle has conditioned the sedimentary processes (subglacial, proglacial, glaciomarine and open-marine) and the variations in the sedimentation rate in the CBB. The evolution over time of these processes since the decay of ice sheet in each physiographic domain of the CBB is interpreted in relation to this last cycle as follows:

- Last glacial advance and glacial maximum period

The CBB continental shelf glacial troughs and slope platforms were dominated by the direct influence of subglacial erosive processes resulting from the seaward advance of the ice sheet. The mapping of the megascale lineations indicates that the grounding line reached down to 1000 m depths, i.e., down to the slope platform edges (Figs. 3.17 and 5.2). A massive soft diamicton is found in the inner reaches of glacial troughs (Fig. 5.24). This muddy matrix-supported IRD sediment with shear structures and deformed IRD would represent the subglacial deformation till deposited during this stage (Fig. 5.30A). The subglacial diamicton could have been deposited subglacially in the inner reaches of glacial troughs, even when the deglaciation had already started on the distal margin areas. This subglacial diamicton sequence may be correlated with the over-compacted diamicton or basal till identified in a similar setting of the Trinity Passage glacial trough and also in the Marion Cove embayment on the SSI margin (Yoon et al., 1997; Heroy et al., 2008), with an age of >9000 y BP. Although not recovered in most sediment cores, sub-glacial diamicton is interpreted to compose the acoustically transparent, non-penetrative echoes underlying the sedimentary drape in TOPAS seismic profiles (See Chapter III; Pudsey et al., 1994; Ó Cofaigh et al., 2005; García et al., 2006b).

During this stage, mass flows and sediment-laden plumes from the ice mass front moving downslope and rain-out of ice shelf basal debris favored the deposition of massive proglacial diamicton on the lower continental slope when the grounding zone reached the slope platform edge (Fig. 5.30A). This sediment was probably inherently unstable and underwent mass movements that reworked and transported the proglacial diamicton downslope. However, these processes could also have occurred during the initial stages of deglaciation, when iceberg calving and strong sediment supply from meltwater favored a high IRD delivery.

The last glacial advance and maximum period is not recorded in the cores from the basin. This statement is based on the correlation between the basin cores and the sediment core GEBRA1 recovered from the same area. The GEBRA 1 core is 2.5 m long and has been interpreted to record the sedimentation during a period of about 1950 yr BP (Fabrés et al., 2000). The basin cores of this study are <2.5 m long so, assuming similar deposition processes and rates, they would have a similar age.
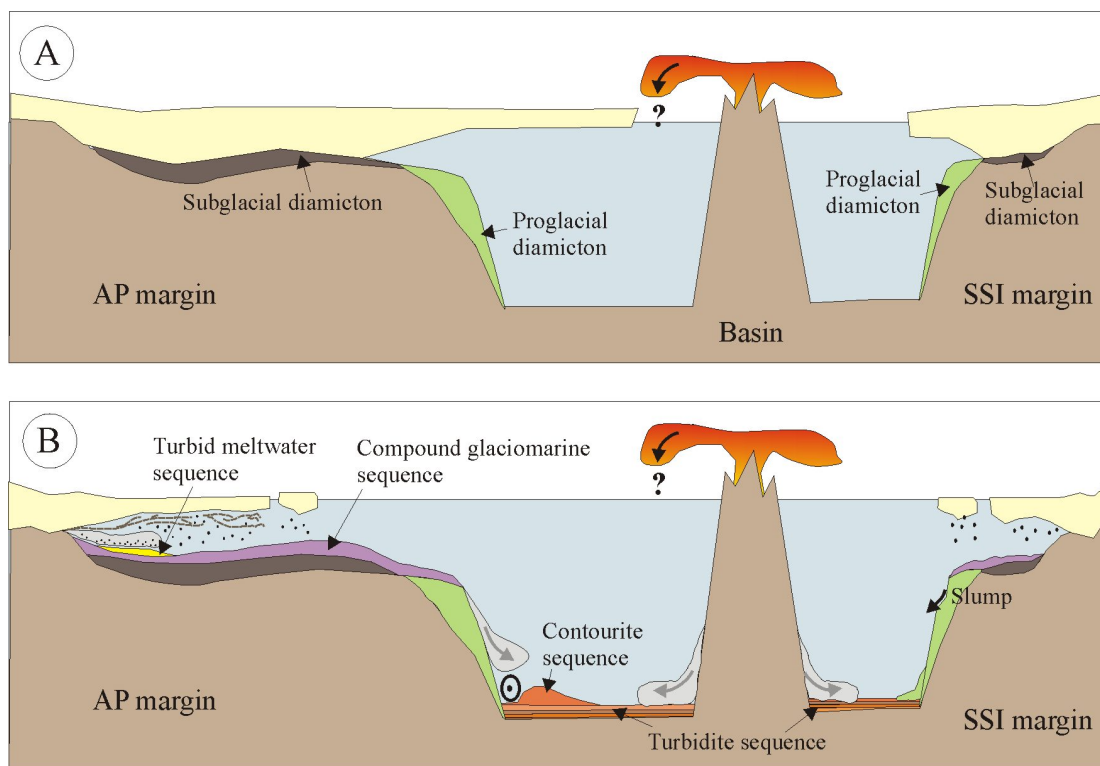
Figure 5.30. Sedimentary products associated with the sequences identified on the sediment cores from the CBB, in relation to: A) the glacial advance and glacial maximum stage; and B) the deglaciation and interglacial stage.

- Last deglaciation and interglacial

On the continental shelf glacial troughs and slope platforms subglacial processes were progressively replaced by proglacial glaciomarine processes (i.e., rain-out of debris, sediment laden plumes and turbid dense meltwater flows) and later by open marine processes (vertical settling), as the ice sheet and associated sedimentary environments migrated landward during the deglaciation (Fig. 5.30B). The interpretation of all these processes indicates that the deglaciation and interglacial stages were characterized on the glacial troughs and slope platforms by sub-ice shelf processes that gave rise the compound glaciomarine sequence. The sedimentary structures strongly indicate that sub-ice shelf deposition was mostly characterized by successive pulses of sediment-laden plumes and rain-out of debris, occasionally interrupted by pulses of dense turbid layers (Fig. 5.29B). As the AP ice sheet migrated landward, the slope platforms became less affected by these

processes, and only the most important turbid meltwater flows escaping from the grounding line deposited on them. This translated in the occurrence of two processes within the compound glaciomarine sequences: a) bioturbation and b) deposition of IRD-rich layers. Both processes suggest relatively low sedimentation rates and a reduction of the glacigenic supply, which led to the concentration of IRD (De Santis et al., 1997; Ó Cofaigh et al., 2001) and also allowed the development of bioturbation processes.

The high variability of sedimentary sequences on the continental shelf glacial troughs during the deglaciation and interglacial stage, especially the interbedding of up to eight levels of turbid glacial meltwater sequence, was the result of a relatively proximal location to the ice mass. This area is more likely to record the effect of meltwater plumes than the outer reaches of the glacial troughs, where the predominance of the compound glaciomarine sequence with only a few intervals of turbid glacial meltwater sequence reflects the distal environment, but may also reflect the effect of local factors. In this case, a higher post-glacial sedimentation rate may explain the sedimentary stratigraphy, although other local factors affect the glacial dynamics of the ice streams during the deglaciation, such as the bathymetry, the ice flux and the erodibility of the bedrock (Faleide et al., 1996; Solheim et al., 1998; Ó Cofaigh et al., 2005).

Simultaneously, the lower continental slope represented an area of sediment bypass or very low or even no deposition, as suggested by the exposure of proglacial sediments, which were deposited during the previous glacial period (Fig. 5.30A). The lower slope also reflects the influence of mass-movements represented by turbidity flows (Fig. 5.30B).

On the basin this period was dominated by open-marine processes that controlled the transport and distribution of sediments. These processes comprise mostly mass movement processes and bottom currents (Fig. 5.30B). All these processes involve the reworking of glacigenic sediment deposited during the glacial advance and last glacial maximum, and possibly the iceberg rafting, as suggested by the presence of IRD affecting the turbidites. Most of the basin is dominated by turbidity flows responsible for the stacking of turbidite sequences. The area located basinwards of the Magia-Gebra slide complex is characterized by a flow-in sequence interbedded within the turbidite sequence, representing a mass flow event that reached the basin after being channelized along the slide complex. Finally, the local effect of bottom currents is represented by the contourite sequence at the foot of the lower slope.

- IRD on the CBB: a key to understanding the variation of glacial and glaciomarine sedimentation over time

The variability of the stratigraphy over time and the spatial distribution of sequences suggest that the occurrence of IRD-rich layer may have paleoenvironmental and paleoclimatic significances. The more important spatial control on the sediment delivery was the distance from the ice sheet. Sediments with higher percentages of IRD are interpreted as being deposited subglacially and/or in proximal proglacial environments. Thus, the identification of this type of sediment on the lower slope is related to the glacial advance and maximum, and its identification on the slope platforms is related to the deglaciation stage. Disperse IRD within sediment suggests distal proglacial environments and is related to the deglaciation and interglacial periods, especially where the presence of IRD increases landward, together with an increase in bioturbated layers in a seaward direction.

- AP *vs.* SSI margins

Sedimentation on the SSI margin (TG11, Fig. 5.25) indicates that the slope platform records similar sedimentary processes to that of the AP slope platforms, but shows a higher variability. More numerous levels of bioturbated and IRD-rich layers within the compound glaciomarine sequence would indicate a more frequent occurrence of pulses of IRD deposition and/or decreased sedimentation rate. This would be explained by the reduced size of the SSI margin, where a smaller ice sheet would form. The sedimentary processes on this margin would therefore be more affected by any change in the ice sheet dynamics. The flow-in sequence identified at the top of the core may be related to the relatively high gradients in this area.

5.5.2. Local factors

5.5.2.1. Morphology and physiography

The high variability of morphosedimentary features in the different physiographic domains (Chapter III) indicates the wide range of mechanisms of transport and deposit occurring in the CBB during the last glacial cycle, especially during the glacial advance and glacial maximum stage. The variability shown in this sedimentological study suggests that the deglaciation and interglacial stage recorded in the near-surface stratigraphy was also characterized by the occurrence of a wide range of processes. This makes it difficult to correlate individual sedimentary sequences between different physiographic domains, and even within the same domain.

144

In general, the physiography of the CCB has conditioned the occurrence of any kind of glacial and glaciomarine sedimentation throughout both margins of the CBB, from the continental shelf down to the edge of the slope platforms. In contrast, this sedimentation was restricted to the continental shelves in most open Antarctic margins, whereas the distal continental margins were mainly affected by distal glaciomarine and marine processes (Alley et al., 1989; Anderson, 1999). This may be explained in terms of the AP ice sheet advances and retreats affecting the entire area, from the shelf down to the edge of the slope platforms in the CBB, whereas on the open margins the grounding line only reached the shelf break. The CBB margins are characterized by the presence of slope platforms that are separated from the continental shelf by a very narrow (<10 km) and steep (up to 23º) upper slope (see Chapter III). Thanks to this morphologic configuration, the seafloor of glacial troughs and the slope platforms practically form a single, flat-lying surface, through which the AP ice streams advanced and retreated at least nine times during the post-rift stage (see Chapter IV). This surface would therefore represent a sedimentary environment similar to the open Antarctic continental shelves.

The uneven morphology of the slope platform edge and lower slope of the AP margin probably explains why the near-surface stratigraphy of the cores sampled on the lower slope is different even though they are all located at 1200 m water depth (TG3, TG4 and TG29, Fig. 5.26). This different stratigraphy suggests that sedimentary processes changed alongslope. The stratigraphy of cores TG3 and TG4 is composed of massive diamicton, whereas westwards, TG29 comprises poorly stratified diamicton changing topward to turbidites. We interpret these lateral variations in terms of the varying distance from the grounding zone and the uneven volume of debris release along the lower continental slope. Hence, the presence of massive diamicton occurs off the mouths of glacial troughs (Fig. 5.3); here, the grounding zone of the ice sheets reached a more distal position during the last glacial period, and the glaciomarine processes (debris release from ice-shelves and icebergs) played a more important role. In contrast, the presence of turbidites overlying the poorly stratified diamicton occurs in areas where the grounding zone reached a more proximal position (Prieto et al., 1999) and the marine conditions arrived earlier, favoring the predominance of marine processes (turbidity flows) over glaciomarine processes.

5.5.2.2. Sediment source control on the recent sedimentation

The sediment source, directly related to morphological/physiographic configuration of the CBB, has controlled the spatial distribution of sediments (Fig. 5.31). The CBB has a semiradial arrangement of hinterland entry point sources and a radial arrangement for the submarine entry point sources (Pilkey and Hokanson, 1991). The semiradial distribution refers to the northwest and southeast location of the AP and SSI hinterland areas and

adjacent margins that together represent the areas eroded by the AP ice sheet that moved with a convergent pattern on the CBB, towards the NE from the AP margin and towards the SE from the SSI margin (Fig. 5.31A,B). This resulted in a similar zonation of sedimentary sequences in both proximal margins, including glacial, sub-ice shelf and turbid meltwater flows on the shelf and slope, and marine processes (turbidity flows, mass-flows and bottom currents) in the basin (Figs. 5.29 and 5.30).
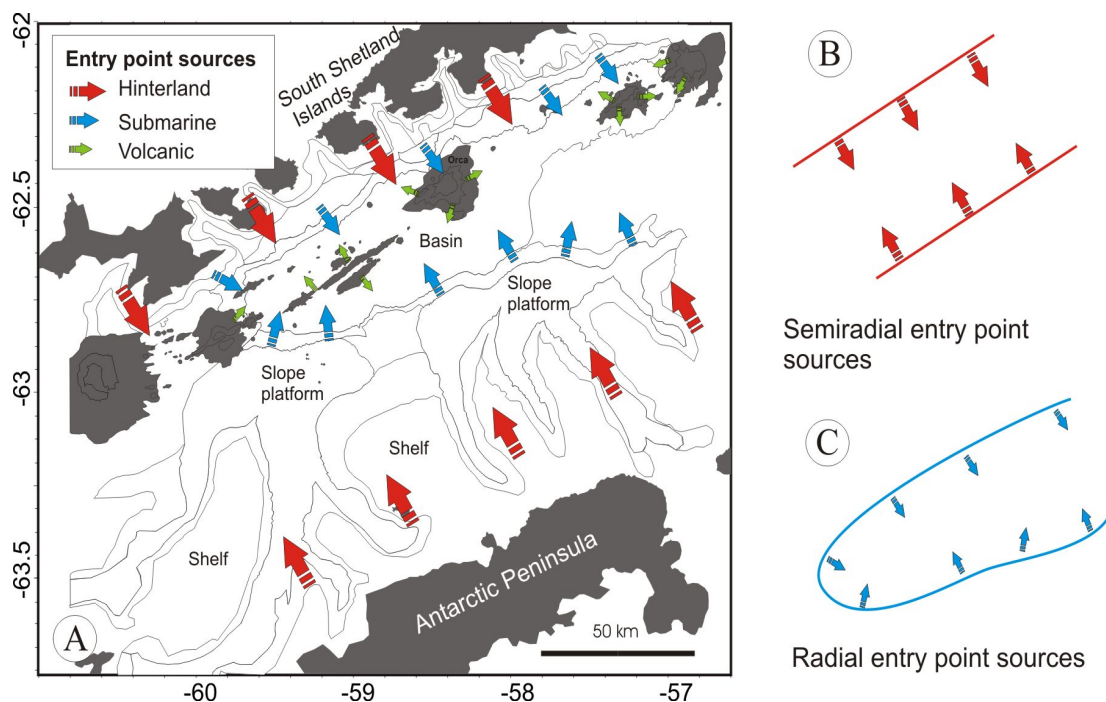
Figure 5.31. A) Distribution of the hinterland, submarine and volcanic sediment entry points in the CBB. B) Radial arrangement of hinterland entry points. C) Semiradial arrangement of submarine entry points.

The radial distribution for submarine entry point sources refers to the situation of the trough mouth fans that acted as sediment source areas around the basin (Fig. 5.31A,C). This distribution allowed the turbidity flows and related flows reaching the basin to come from practically all the areas surrounding the basin, and in consequence the turbidite sequences predominated over the entire basin. Radial distributions may contribute with an uneven occurrence of turbidity events, favoring their spatial variability, which could also explain why it was impossible to correlate the basin turbidites, at least with the sedimentological parameters used in this study. Likewise, in the basin the volcanic submarine edifices are also sporadic sources for the turbidity flows (Fig. 5.28B), as suggested by the volcanic layers identified within the turbidite sequences (Fig. 5.27). Although similar volcanic layers in the CBB have been attributed to turbidite flows from Deception Island (Fabrés et al., 2000), other studies indicate that other volcanic centres have contributed ash to the CBB (Fretzdorff and Smellie, 2002). The identification of volcanoclastic layers in the western part of the basin and their stratigraphic correlation suggest that the Three Sisters volcanic edifice was the most

probable source for volcanic layers, which deposited through instability processes on its flanks (Fig. 5.30B). The distribution of sediment throughout the basin is also affected by the volcanic edifices, which act as a topographic barrier for the sediment dispersion (Fig. 5.3; Lee et al., 2005).

5.5.2.3. Oceanographic control on the recent sedimentation

The oceanographic control in the CBB played a local role in the development of contourite deposits in the basin, at the foot of the lower slope off the AP margin. As discussed in Chapter IV, contourite drifts and moats resulted from the deep current acceleration and concentration due to the interaction of deep flows with the seafloor topography. The location of contourite deposits in the CBB indicates that the main topographic features affecting the oceanographic flow patterns were the Three Sisters and Orca volcanic edifices.

VI. Synthesis and conclusions

1. Post-rift sedimentary evolution of the CBB: physiography and morphology, sedimentary dynamics, stratigraphy and near-surface deposits

This PhD Thesis studies the sedimentary evolution of the CBB through multi-scale, multi-resolution and multi-temporal analyses. The multi-scale approach comprises spatial perspectives ranging from regional (tens of kilometers) to local (tens of meters); the multi-resolution approach comprises the use of several methods for the data gathering and analysis (Fig. 6.1). Acoustic, seismic and sedimentological data were obtained and a great variety of methods were used to analyze them: computer programs for seismic processing and geology visualization offering a metric and decametric resolution from regional to local contexts, and sedimentological analyses with a centimetric to micrometric resolution. Both the multi-scale and multi-resolution analyses were used to establish a multi-temporal approach for the interpretation of the sedimentary processes and evolution:

- The Pliocene-Quaternary approach includes the study of the stratigraphic architecture of the CBB, with the analysis of the factors that have controlled the AP margin growth pattern.

- The Late Pleistocene-Holocene approach analyses the morphology and sedimentary systems that developed on the CBB during the last glacial/interglacial cycle. Climate is considered as the main controlling factor, and the physiography, tectonics and oceanography as secondary factors.

- Finally, the Holocene approach studies the sedimentary processes occurring on the CBB during the last deglaciation, and the effect of the morphology/physiography, sediment source and oceanography on the sedimentary environments.

1.1. Detailed physiographic characterization of the CBB

The interpretation of the new seafloor mapping of the CBB has allowed a new and more detailed characterization of the physiographic domains of the AP and SSI margins, i.e., the continental shelf, upper slope, discontinuous slope platforms, lower slope and basin.

The slope platforms are relatively wide and flat areas that represent about 65% of the CBB continental slope. Their occurrence is unique in comparison with other glacial environments, and this study provides clues to understanding their role in the development of the stratigraphic architecture of the CBB and in the growth pattern variability, which changes spatially and over time.
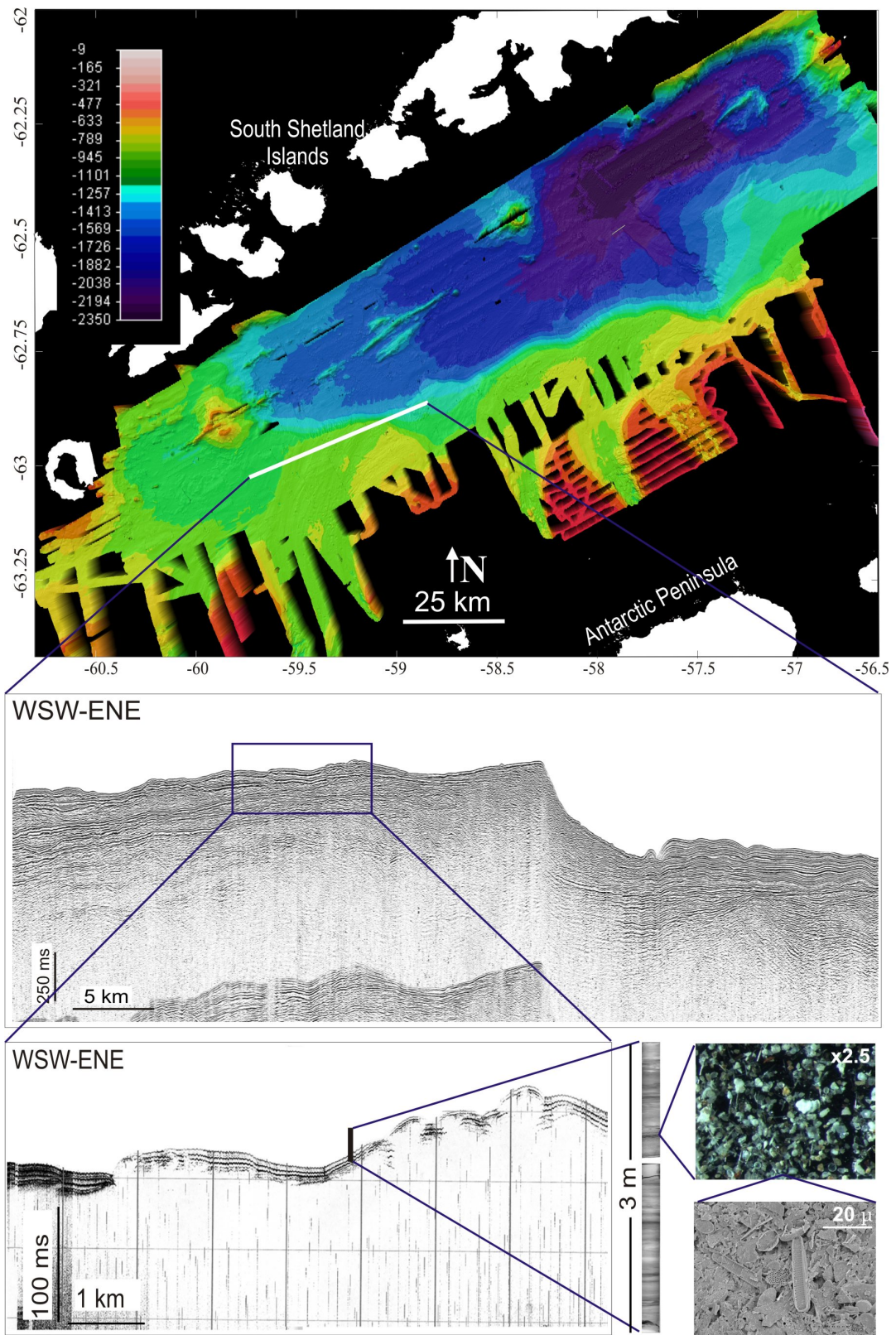
Figure 6.1. Different scale data used for the multi-scale approach to the study of the post-rift sedimentary evolution of the CBB, from regional bathymetric mosaics to scanning electronic microscope imagery.

1.2. CBB sedimentary dynamics during the last glacial cycle

The last glacial cycle has been characterized in terms of the sedimentary systems that developed during the entire cycle and the last deglaciation and interglacial interval has been studied with more detail based on the recent sedimentary record. The interpretation of the new seafloor mapping has provided a new and more detailed characterization of the sedimentary systems of the CBB and offers clues to some aspects of the sedimentary evolution. Several sedimentary systems have been identified in each physiographic domain: glacial-glaciomarine, slope-basin, seabed fluid outflow and contourite systems. They are composed of architectural elements of different orders of magnitude, from a few to hundreds of metres in relief and thickness, and from a few hundred meters to several kilometers in length.

The sedimentary dynamics of the CBB during the last glacial cycle is revealed through the development of sedimentary systems and the architectural elements composing them. The major elements of the glacial-glaciomarine system are erosional surfaces, glacial troughs (with architectural elements of minor hierarchy, such as erosional grooves, drumlins, knickpoints and glacial lineations), grounding zone wedges, furrows and a draping sheet. Most of these elements were deposited during the ice sheet advance and glacial maximum and their distribution and characteristics indicate that the ice sheet moved with an eastward direction on the slope platforms of both margins and that the development of trough mouth fans off the ice streams caused the sinuous plan-view shape of the AP and SSI margins. During the ice-sheet retreat and interglacial stage glaciomarine and marine processes dominated in the CBB.

The glacial dynamics during the last cycle is overprinted by a secondary/local control of tectonics, physiography and oceanography. The interplay among all these factors governs the development of the slope-basin system, the seabed fluid outflow system and the contourite system. The first one includes trough mouth fans, slope aprons (composed of scar-and-lobe complexes), the Gebra-Magia slide complex (composed of scar, slides, mass transport deposits and mass flow deposits), and turbidity systems (including gullies and turbidite channels). The seabed fluid outflow system is defined by a single architectural element, pockmarks grouped forming fields, and the contourite systems by two elements, drift and moat.

The study of the recent sedimentation allows the interpretation of sedimentary processes during the last glacial cycle to be refined. Likewise, it provides a better understanding of the overprint of secondary local controlling factors on the main global factor represented by glacial cyclicity. The most important processes reflected in the sedimentary record (subglacial, proglacial, glaciomarine and open-marine) have occurred in distinct sedimentary environments on the CBB, related to the relative distance from the grounding zone. The sedimentary stratigraphic models in each physiographic domain explain the building of the AP and SSI margins and adjacent basin as the result of the continuous

redistribution of sediments by the last glacial advance and maximum and the subsequent retreat of the AP ice sheet. Each stage of the glacial cycle originates distinct sedimentary sequences.

- The glacial advance and maximum stage is typified by subglacial soft diamicton sequences in the glacial trough and proglacial massive diamicton on the upper slope.

- The deglaciation and interglacial stage comprises: compound glaciomarine sequences, interbedded with turbid glacial meltwater sequences and flow-in sequences in the continental shelf glacial troughs and slope platforms; turbidite and flow-in sequences on the lower slope; and turbidite and contourite sequences on the basin. The sediment source –mostly in terms of entry points– has controlled the similar zonation of sequences in the AP and SSI margins and the spatial distribution of turbidites and volcanoclastic sediment. Oceanography plays a local control in the development of contourite deposits on the lower slope and basin.

The deglaciation stage is interpreted to have occurred as a relatively rapid event, interrupted by small-scale stages of pause and/or readvance of the grounding zone. This is suggested by the preservation of morphological features that developed during the previous ice sheet advance and glacial maximum stage along the entire slope platforms and may be explained by the markedly warm character of interglacials after 900 ky (Mangerud et al., 1996). The occurrence of at least two stages of stillstand and/or readvance of the grounding zone during the deglaciation stage is suggested by the grounding zone wedges and also by the set of glacial lineations that overlap older ones with a different trend on the WP. These facts may be related to a major event of glacial readvance reported from James Ross Island between around 7000 and 6000-5000 yr BP (Hjort et al., 1992; Ingólfsson et al., 1992). Staggered glacial retreat patterns similar to that occurring in the CBB have been documented in other areas of the Antarctic Peninsula, Ross Sea and Weddell Sea (Pope and Anderson, 1992; Evans et al., 2005; Ó Cofaigh et al., 2005), although the ice stream dynamics during the deglaciation is variable and depends on local factors (bathymetry, ice stream drainage basin size, ice flux, erodibility of the bedrock) and on the glacial thermal regime (Faleide et al., 1996; Solheim et al., 1998; Ó Cofaigh et al., 2005).

1.3. Post-rift stratigraphic architecture and growth patterns

The seismic stratigraphy of the AP margin of the CBB consists of two post-rift seismic sequences, S2 and S1. Sequences S2 and S1 include a variety of sedimentary features related to the ice sheet advance during glacial maxima and ice sheet retreat during interglacials. Thus, deposition on the CBB margin has been dominated by glacial and glaciomarine sedimentary processes throughout most of the post-rifting stage. The seismic stratigraphic

analysis can be used to establish the post-rift stratigraphic architecture and growth patterns of the AP margin, which can be divided into two stages: post-rift to mid-Pleistocene and mid-Pleistocene to Holocene.

1.3.1. Post-rift to mid-Pleistocene stage

After the rifting that led to the opening of the Bransfield Basin the dominant sedimentary processes that conditioned the basin infilling were glacial and glaciomarine processes governed by climatic cycles of 100 ka and modulated by cycles of 41 ka. The distribution of the seismic depositional bodies was controlled by the entry points of sediment sources (glacial troughs) and by the physiography of a young rift basin. Sequence S2 was deposited during this stage, forming thick prograded wedges and trough mouth fans on the WP and the EP of the AP margin. On the EP four subunits can be differentiated, S2d to S2a. The three older units occur in small isolated depocenters, while the recentmost one forms a wider depocenter on the EP edge. Progradation was the result of the deposit of thick erosive ice sheets and structurally-controlled ice streams that eroded glacial troughs along the AP margin. The margin outbuilding is the result of the deposition of thick prograded wedges and trough mouth fans off the mouths of glacial troughs on the distal continental margin.

The progradation that characterized the stratigraphic architecture of the AP margin is the result of the interplay between the low accommodation space in the shallow, recently-opened (in geological terms) CBB and the sediment supply. Sediment transported by the ice sheet and ice streams was enough to fill the accommodation space forming prograding packages that progressively produce the basinward progradation of the margin (Fig. 6.2A). Successive advances of the ice sheet produced rather different progradational styles along the slope. On the EP, the margin was narrower and steeper, and wedges with a very large progradational component (up to 10 km) were formed. In contrast, on the WP the margin was wider and less steep and deposition was more widespread, resulting in less progradation (up to 5 km). The non-preservation of the topset of prograding wedges is the result of the major erosion exerted by the ice sheet advance during the relatively longer glacial cycles that characterized the post-rift to Mid-Pleistocene stage.

This scenery favored the formation of slope platforms, which contrasts with the typical deposition in glaciated continental margins of both the Northern and Southern Hemispheres, where prograding wedges and trough mouth fans deposit at the shelf-edge and on the lower continental slope (Fig. 6.2B) and part of the sediment is distributed along the continental rise and in deep basins (Vorren et al., 1989; Kuvaas and Kristoffersen, 1991; Alonso et al., 1992; Anderson and Bartek, 1992; Bart et al., 1994; King et al., 1996).
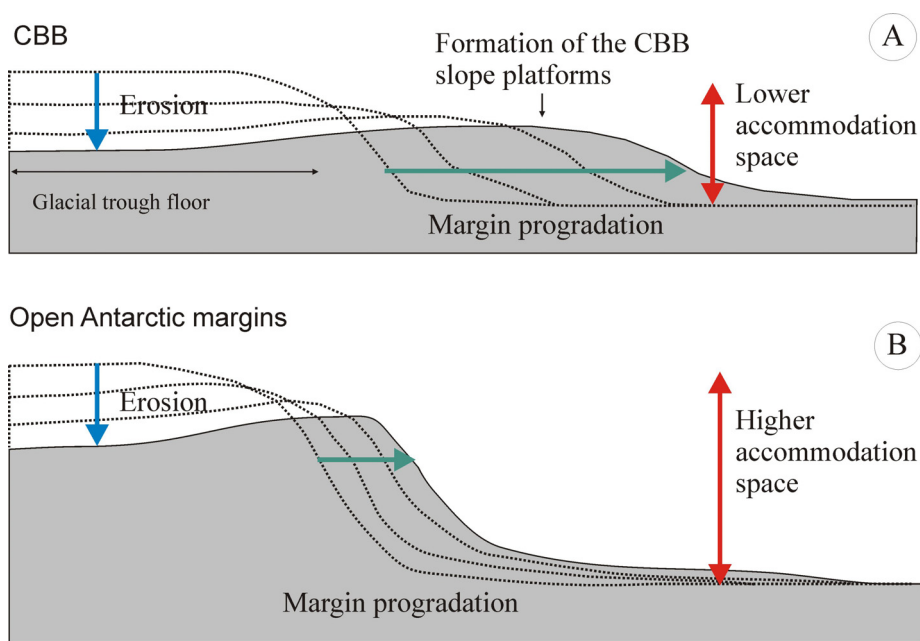
Figure 6.2. Sketch of the stratigraphic architecture in relation to the effect of the accommodation space on the margin progradation. A) Topographic profile along a glacial trough of the CBB. B) Topographic profile along a typical open Antarctic margins.

1.3.2. Mid-Pleistocene to Holocene stage

After the Mid-Pleistocene, the glacial and glaciomarine sedimentary processes continued being dominant, but were governed by climatic cycles of 100 ky. During this stage, sequence S1 was deposited. It is composed of five subunits, S1e to S1a, which are relatively thinner but display similar seismic facies to S2. Sequence S1 deposits are thicker and more extensive on the WP than on the EP, and individual seismic units form rounded depocenters off the mouths of troughs and elongate, platform-edge-parallel depocenters along the eastern CBB. Two alternating ice flow regimes with different sediment delivery patterns can be differentiated during the deposition of S1e to S1a subunits. Subunits S1e, S1c and S1a were deposited by relatively thick ice sheets that sloped toward the north-northeast. Glacial troughs directed the flow of ice streams on the continental shelf. Off the glacial troughs on the slope platforms, ice flow turned to the northeast, resulting in the formation of slope depocenters to the east of the glacial troughs. In contrast, deposition of subunits S1d and S1b occurred preferentially off the mouths of troughs, in relation with thinner ice sheets and discrete ice streams flowing within glacial troughs.

During this stage, the predominant frequency of climatic cycle of 100 ky favored the increase in frequency of grounding events and the availability of sediment previously deposited on the margin during the previous stage led to the formation of thinner and faster-flowing ice sheets. In combination with the continuous opening of the basin and the

156

subsequent increase in accommodation space, this led to a prograding-aggrading architecture pattern. The shallower depth of the WP, together with the higher sediment supplied by the larger drainage area of the Trinity Passage and Orleans troughs, resulted in a more pronounced prograding pattern on the WP (up to 13 km) than on the EP. Here, in some cases the slope platform edge was maintained in the same position or even migrated landwards after deposition of S1. The preservation of the slope platform deposits and topsets of prograded wedges and trough mouth fans suggests the effect of tectonic and/or sedimentary subsidence during this stage.

2. New insights into the glacial sedimentary models: refining and filling the gaps in the knowledge of the CBB sedimentary evolution

The results of this study allow the glacial sedimentary models on the CBB to be refined, since they provide detailed and high-resolution characterizations of the sedimentary systems and their dynamics and feed-back interactions, the sedimentary processes and the interplay among their global and local controlling factors, and the stratigraphic architecture and its temporal and spatial variability in this area.

2.1. Sedimentary models on the CBB

Two different sedimentary models can be differentiated in the CBB, based on the stratigraphic architecture, the elements forming sedimentary systems that determine different hierarchies of sedimentary systems and the recent sedimentary stratigraphy of the environments. These models are: 1) the *Margin domain*; and 2) the *Basin domain*.

2.1.1. Margin domain model

This domain includes the shelf, upper slope, slope platforms and lower slope. It reflects the most dramatic changes caused by the effect of glacial and glaciomarine processes. The stratigraphic architecture of the AP and SSI margin is characterized mostly by the glacial erosion of the shelf, upper slope and proximal areas of the slope platforms, and the deposition of glacigenic sediment forming the slope platforms and lower slope. The succession of glacial cycles produced the progressive basinwards growth of the margin and determined the occurrence of glacial and glaciomarine processes on the slope platforms and lower slope, contrasting with the general scheme of other glacial margins where deposition occurs on the lower slope and continental rise. This is the most differential characteristic of the CBB, which can be interpreted as an anomalous quasi landlocked shallow basin.

The margin domain represents an entire sediment-dispersal system that suffers the most dramatic sedimentary changes. When the ice sheet and ice streams move seaward, this domain is affected by wild subglacial erosion and proglacial, glaciomarine and marine deposition; and when the ice sheet retreats, it is affected by glaciomarine and marine

deposition resulting from the combination of the marine and subglacial processes, seafloor scouring of the drifting icebergs and seafloor reworking by the expulsion of water from compacting sediment. Therefore, in this domain the pathways followed by the sediment from source to sink are totally governed by the glaciations.

The stratigraphic record studied from the seismic and sedimentological approaches indicates that sedimentary products deposited during the glacial advances and glacial maximum stages of each cycle are responsible for most of the CBB margin post-rift sedimentary record. The predominating glacial nature of the margin domain is suggested by several facts: 1) Unconformities bounding the seismic sequences and units represent the widespread subglacial erosion during the glacial advance and glacial maximum of each cycle; 2) The bulk of seismic units making up the margins are composed of seismic depositional bodies of glacial and glaciomarine origin produced mostly during the ice sheet advance and glacial maximum. These bodies include till wedges, prograded wedges and trough mouth fans. Glaciomarine drape deposits and moraines, related with glaciomarine and marine processes during the deglaciation and interglacial stage of the glacial cycle, are quantitatively less important on the CBB margin post-rift infilling; and 3) The glacial-glaciomarine sedimentary system includes most of the morphological features identified on this domain. Most of them (erosion surfaces, glacial troughs, glacial lineations and furrows) are related to the glacial advance and glacial maxima, while only grounding zone wedges on the slope platforms and the draping sheet were deposited during the deglaciation and interglacial stages.

In general, the sedimentary products of the glacial advance and glacial maxima predominated in comparison with those of the deglaciation and interglacial stage, regardless of the frequency of the climatic cycles. This minimizes the effect of the differences in characteristics of the climatic cycles on the margin out-building, contrasting with middle-latitude margins, where the identification of several systems tracts allows the interpretation of differences in the symmetry, frequency and amplitude of climatic cycles. In the CBB and in high-latitude glacially-controlled continental margins in general, the effect of glacial erosion and deposition (regressive and lowstand systems tracts) tends to rework the sedimentary products of the deglaciation and interglacial stages (transgressive and highstand systems tracts) of the previous cycles. Also, the predominance of the climatic factors in the control of the sedimentary infilling obliterates the effect of the tectonic factors in the sedimentary record, even though the CBB is characterized as a tectonically active basin. This could be due to the faster dynamics of ice sheet fluctuations in comparison with regional tectonic movements, which do not modify the trend of the ice sheet displacement within each glacial cycle, but alter the long-term margin accommodation space changes at a multi-cycle time scale (e.g., the S1 and S2 scale). The development of the slope-basin sedimentary system on the lower slope and

the presence of volcanic edifices that locally control sedimentation on the basin are also related to structural and physiographic factors.

2.1.2. Basin domain model

The CBB basin is mostly affected by marine and oceanographic processes that predominate when the ice sheet and ice streams retreat landward. In this domain, the sediment pathways from source to sink are governed by local factors as indicated by the sedimentary systems and the recent sedimentation. Sedimentary processes governing the sedimentation in this domain are related to mass wasting (turbidites and related flows, slumps), bottom current circulation processes (contourites) and occasional vertical settling of IRD. Also the instabilities affecting the flanks of volcanic edifices in the basin produce volcanoclastic sediments that are deposited on the basin, as indicated by the volcanic layers identified within the basin turbidite sequence.

2.2. AP *vs.* SSI

Based on the complex present-day architectural model and the sedimentary records, two types of margins can be differentiated in the CBB: the relatively starved SSI margin and the constructional AP margin. The sedimentary model of the SSI margin results from the interaction between the relatively narrow shelf and steep slope, which are an imprint of the tectonic configuration, and the glacial and glaciomarine processes associated with a smaller ice-sheet development. In this scenario, the outbuilding of the sedimentary systems is limited and they develop as small, isolated features whose location, nature and geometry are conditioned by the physiographic template. The higher variability of sediment sequences on the SSI margin, with numerous levels of bioturbated and clast-rich layers within the compound glaciomarine sequence would indicate a higher variability of the ice shelf that can be also explained by the small size of the margin. However, the present-day architecture model of the AP margin does not reflect this structural template because the glacial, glaciomarine and marine processes have helped to develop larger sedimentary systems whose outbuilding has favored their vertical stacking and lateral coalescence, forming a constructional margin. In fact, the AP margin features are similar to those of glaciomarine passive margins.

2.3. Interplay among global and local factors controlling the post-rift sedimentary evolution of the CBB: identification of their effect on the resulting sedimentary products

The present-day physiography, morphology and seismic and sedimentary stratigraphy of the CBB are the result of the interplay of a variety of controlling factors that determine the potential for preservation and the resulting distribution and geometry of the different deposits accumulated on the CBB during the post-rift stage (Fig. 6.1).

As discussed in Section 4, the most important factor in the control of the evolution of the CBB is related to the glacial changes that determine the succession of glacial/interglacial cycles. Factors such as the frequency of grounding events, the thermal glacial regime and the thickness and extent of the AP ice sheet conditioned the stratal pattern, facies and distribution of the different types of deposits on the CBB. In particular, the most important control of the sedimentary evolution of the CBB is related to the ice sheet advance and glacial maximum stages of each glacial/interglacial cycle. The control exerted by the glacial factor is modulated by other factors such as tectonics, physiography and sediment supply, which affect the sedimentary evolution of the CBB in different ways.

The tectonic imprint on the general physiographic configuration is inherited from the processes involved in the basin opening, which caused a markedly asymmetry between the margins and a differential opening rate between the western and eastern areas. This led to the differences in the sedimentary systems and processes between the SSI and AP margins (mostly in relation to the size of the ice sheet), and also the variability of the stratigraphic architecture along the AP margin. Tectonic subsidence may have been responsible for the preservation of the slope platform aggrading deposits. Tectonics also determines the location of volcanic edifices along the axis of the CBB and the related sedimentary processes, and marks the preferential NW-SE trending weak zones where glacial troughs were eroded on the AP and SSI margins.

The control of the physiographic factor is related to the location of the different domains, and to their migration along the margin during the successive glacial cycles, which is directly related to the rate of advance and retreat of the grounding zone. The physiographic domains have a clear correlation with the spatial distribution of the sedimentary systems and with the sedimentary stratigraphic models established in the CBB. This correlation allows the two distinct sedimentary models to be differentiated: the margin domain model that includes the continental shelf and slope, and the basin domain model that includes the basin

The sediment supply is mostly determined by the size of the AP ice sheet drainage area, which has an impact on the sedimentation rate and thickness of deposits, and also on the nature of the subglacial substrate, which determines the speed and erosive capability of the ice flows. Sediment supply also has a direct impact on the development of sedimentary systems, especially on the lower slope of the SSI and AP margins and on the basin. The spatial arrangement of the entry point sources –semiradial for hinterland sources and radial for the submarine sources– has a direct effect on the spatial distribution of sedimentary systems.

Finally, oceanography plays a local role on the development of contourite features and in the reworking of the rest of the sedimentary deposits on the basin. Although the deep

circulation in the CBB is not well known, the presence of volcanic edifices and the physiography of the basin are interpreted to affect the deep oceanographic flows.
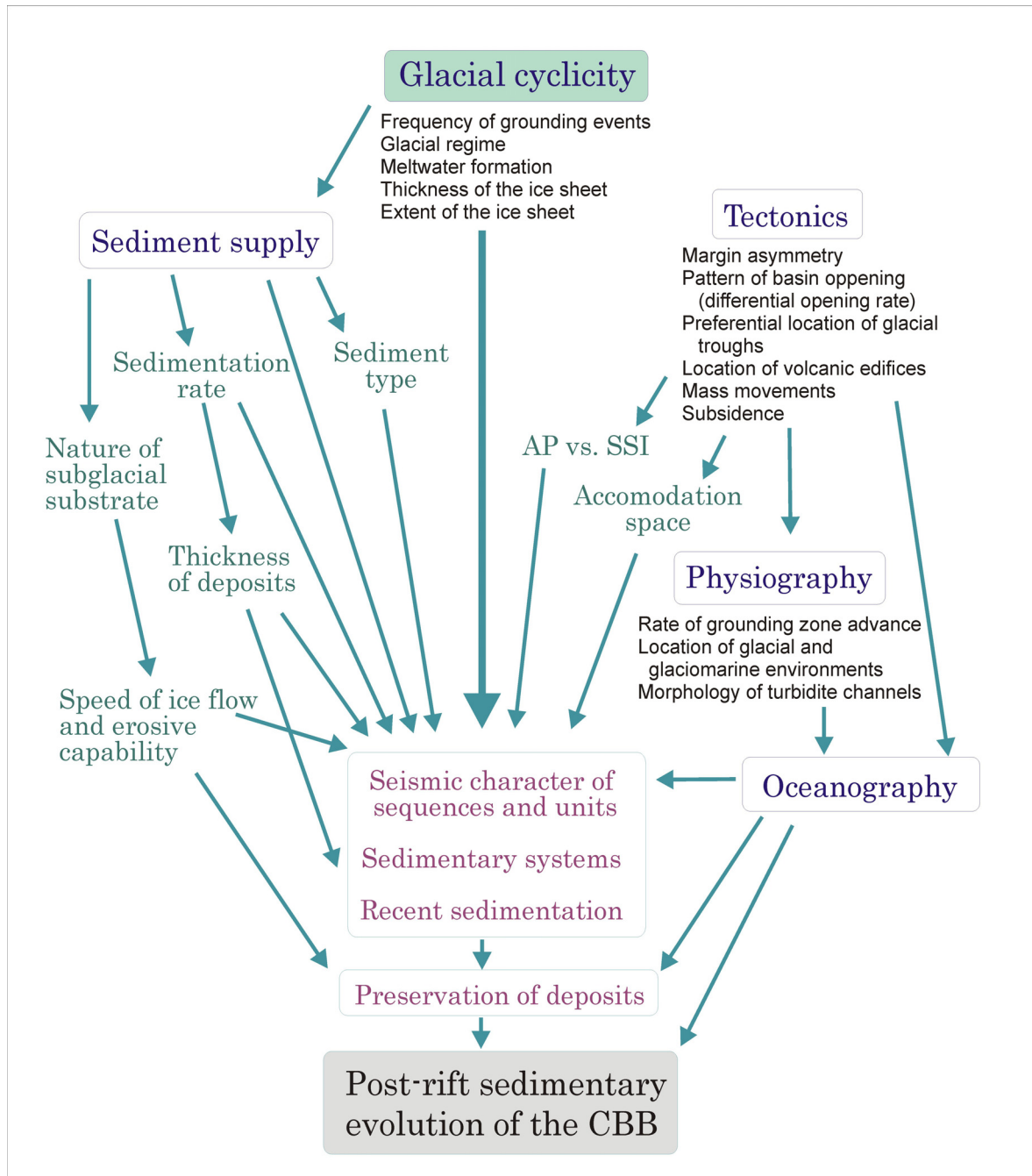

Figure 6.3. Diagram showing the complex interaction between the factors controlling the post-rift sedimentary evolution of the CBB. The major factor is related with glacio-eustatic changes, and sediment supply, tectonics, physiography and oceanography act as secondary, modulating factors.

3. Outstanding questions

This research work has provided a better knowledge of the post-rift sedimentary evolution of the CBB, through multi-scale, multi-resolution and multi-temporal approaches. As a result, new sedimentary models have been proposed, the interplay of the main global and local controlling factors has been analyzed and the sedimentary and architectural products have been defined with confidence. However, during the scientific process that has provided these results, many new questions have also arisen, that should be properly addressed.

The physiographic and morphological study (Chapter III) has allowed the definition of different sedimentary systems and the analysis of their controlling factors. Some interesting issues regarding these interpretations are:

- The relationships between the instability features –especially the Gebra-Magia slide valley complex- with the glacial cyclicity: What are the triggering mechanisms that originated these features, and are they related to any stage of the glacial cycle?

- The characterization of the deep currents in the CBB can be refined on the base of the analysis of contourite features (drifts and moats) on the basin. The location and character of these features may help to better constraint the present-day circulation in an area where oceanographic studies are inherently difficult to perform, and may also provide clues to paleo-circulation interpretations.

- The present-day morphology of the CBB gives detailed information of the sedimentary processes occurring during the last glacial cycle, but especially during the glacial advance and glacial maximum stage. However, most of these processes did not occur simultaneously on the basin, e.g., subglacial processes on the inner glacial troughs coexisted with open-marine processes on the distal margin. On the other hand, sedimentary processes during the deglaciation stage can not be identified, at least with the resolution of the methods used in this study, and the glacial dynamics during this stage still remains unknown.

The stratigraphic study performed in Chapter IV has provided new insights into the seismic stratigraphy of the CBB, through the analysis of higher resolution data, but some questions should still be addressed:

- A study of the chronology of the structural features of the CBB and their relationship with the seismic sequences and units, as well as a better definition of the lower limit of the Lower Sequence (S2) should be performed to better understand the effect of tectonic subsidence/uplifting and sedimentary subsidence, the different evolution of the SSI and AP margins and the structural control on the stratigraphic architecture. Such study would help to define a paleogeographic reconstruction of the CBB

162

sedimentary upbuilding over time in relation to the paleostructural and paleoenvironments scenarios as the basin opened.

- The sequence stratigraphy models, which have been traditionally applied to low- and mid-latitude continental margins, present different problems when applied to glaciated margins. The dynamic view of the stratigraphic architecture upbuilding related to sea level changes could be correlated with the margin upbuilding related to glacial cycles; in general, the ice sheet advance would correspond to a regressive stage, the glacial maximum to a lowstand stage, the deglaciation to a transgressive stage, and the interglacial to a highstand stage. But when approached, this correlation is not direct, since the unconformities that bound seismic units and sequences have not a direct relation to the sea level and would represent polygenetic surfaces. This indicates that the spatial and temporal significance of sequence boundaries and discontinuities for glaciated margins should be revised if a sequence stratigraphic study is approached.

The sedimentological study presented in this research work (Chapter V) has allowed the sedimentary processes during the deglaciation and interglacial stage to be refined. However, a better understanding of these processes would be obtained if some issues were addressed:

- Chronological constraints for the sedimentary sequences though datations would be necessary to define the chronology of the deglaciation events and also to correlate the results of this work with other studies based on samples from the study area that have been published in the literature.

- This study manifests the great diversity of diatom species in the sedimentary record of the CBB. Their detailed study in terms of diatoms assemblages would provide detailed information on the paleoceanography and paleoclimatic conditions of the CBB, and could constitute an important input for climatic and oceanographic reconstructions in the CBB.

References

Alley, R.B., Blankenship, D.D., Rooney, S.T., Bentley, C.R., 1989. Sedimentation beneath ice shelves- The view from ice stream B. Marine Geology 85, 101-120.

Alonso, B., Anderson, J.B., Díaz, J.I., Bartek, K.R., 1992. Pliocene-Pleistocene seismic stratigraphy of the Ross Sea: Evidence for multiple ice sheet grounding episodes. Antarctic Research Series 57, 93-103.

Anderson, J.B., 1997. Grounding zone wedges on the Antarctic continental shelf, Weddell Sea. In: Davies, T.A., Bell, T., Cooper, A.K., Josenhans, H., Polyak, L., Solheim, A., Stoker, M.S., Stravers, J.A. (Eds.) Glaciated Continental Margins: an atlas of acoustic images. pp. 98-99. Chapman and Hall, London.

Anderson, J.B., 1999. Antarctic Marine Geology. Cambridge University Press, Cambridge. 289 pp.

Anderson, J.B., Bartek, L.R., 1992. Cenozoic glacial history of the Ross Sea revealed by intermediate resolution seismic reflection data combined with drill site information. In: Kennet, J.P., Warnke, D.A. (Eds.), The Antarctic Paleoenvironment: A perspective on global change. Antarctic Research Series 56, 231-263.

Anderson, J.B., Wright, R., Andrews, B., 1986. Weddell Fan and associated abyssal plain, Antarctica: morphology, sediment Processes, and factors influencing sediment supply. Geo-Marine Letters 6, 121-129.

Anderson, J.B., Pope, P.G., Thomas, M.A., 1990. Evolution and hydrocarbon potential of the Northern Antarctic Peninsula continental shelf. In: St. John, B. (Ed.), Antarctica as an Exploration frontier: hydrocarbon potential, geology and hazards. AAPG Studies in Geology 31, 1-12.

Anderson, J.B., Kennedy, D.S., Smith, M.J., Domack, E.W., 1991. Sedimentary facies associated with Antarctica's floating ice masses. In: Anderson, J.B., Ashley, G.M. (Eds.), Glacial marine sedimentation. Paleoclimatic significance. Geological Society of America Special Paper 261. Boulder, Colorado.

Anderson, J.B., Shipp, S.S., Bartek, L.R., Reid, D.E., 1992. Evidence for a grounded ice sheet on the Ross Sea continental shelf during the late Pleistocene and preliminary paleodrainage reconstruction, in: Elliot, D.H. (Ed.), Contributions to Antarctic research III. American Geophysical Union Antarctic Research Series 57, pp. 39-42.

Anderson, J.B., Wellner Smith, J., Lowe, A.L., Mosola, A.B., Shipp, S.S., 2001. Footprint of the Expanded West Antarctic Ice Sheet: Ice stream history and behaviour. GSA Today 11, 4-9.

Anderson, J.B., Shipp, S.S., Lowe, A.L., Wellner, J.S., Mosola, A.B., 2002. The Antarctic ice Sheet during the Last Glacial Maximum and its subsequent retreat history: a review. Quaternary Science Reviews 21, 49-70.

Assmann, K., Hellmer, H.H., Beckmann, A., 2003. Seasonal variation in circulation and water mass distribution on the Ross Sea continental shelf. Antarctic Science 15 (1), 3–11.

Banfield, L.A., Anderson, J.B., 1995. Seismic facies investigation of the Late Quaternary glacial history of Bransfield Basin, Antarctica. In: Cooper, A.K., Barker, P.F., Brancolini, G. (Eds.), Geology and Seismic Stratigraphy of the Antarctic Margin. Antarctic Research Series 68, 123-140.

Banfield, L.A., Anderson, J.B., 1997. Grounding zone and associated proglacial seismic facies from Bransfield Basin, Antarctica. In: T.A. Davies, T. Bell, A.K. Cooper, H. Josenhans, L. Polyak, A. Solheim, M.S. Stoker, J.A. Stravers (Eds.) Glaciated Continental Margins: an atlas of acoustic images. pp. 100-103. Chapman and Hall, London.

Barnes, P.W., Reimnitz, E., 1997. Morphology and stratigraphy related to the nearshore boundary of the Stamukhi Zone. In: T.A. Davies, T. Bell, A.K. Cooper, H. Josenhans, L. Polyak, A. Solheim, M.S. Stoker, J.A. Stravers (Eds.) Glaciated Continental Margins: an atlas of acoustic images. pp. 222-223. Chapman and Hall, London.

Barker, D.H.N, Austin, Jr., J.A., 1994. Crustal diapirism in Brasnfield Strait, West Antarctica: Evidence for distributed extension in marginal-basin formation. Geology 22, 657-660.

Barker, P.F., 1972. Magnetic lineations in the Scotia Sea. In: Adie, R.J. (Ed.), Antarctic Geology and Geophysics. Universitets Forlaget, Oslo.

Barker, P.F., 1982. The Cenozoic subduction history of the Pacific margin of the Antarctic Peninsula: ridge crest-trench interactions. Journal of the Geological Society of London 139, 787-801.

Barker, P.F., 2001. Scotia Sea regional tectonic evolution: implications for mantle flow and palaeocirculation. Earth-Science Reviews 55, 1-39.

Barker, P.F., Burrell, J., 1977. The opening of Drake Passage. Marine Geology 25, 15-34.

Barker, P.F., Dalziel, I.W.D., 1983. Progress in geodynamics in the Scotia Arc region. In: Cabre, R. (Ed.), Geodynamics of the Eastern Pacific Region, Caribean and Scotia Arcs. American Geophysical Union, Geodynamics Series 9, 137-170.

Barker, P.F., Camerlenghi, A., 2002. Glacial history of the Antarctic Peninsula from Pacific margin sediments. In: Barker, P.F., Camerlenghi, A., Acton, G.D., Ramsay, A.T.S. (Eds), Proceedings of the Ocean Drilling Program, Scientific Results, 178, 1-40.

Barker, P.F., Barrett, P.J., Cooper, A.K., Huybrechts, P., 1999. Antarctic glacial history from numerical models and continental margin sediments. Palaeogeography, Palaeoclimatology, Palaeoecology 150, 247–267.

Barnes, P.W., Reimnitz, E., 1997. Morphology and stratigraphy related to the nearshore boundary of the Stamukhi Zone. In: T.A. Davies, T. Bell, A.K. Cooper, H. Josenhans, L. Polyak, A. Solheim, M.S. Stoker, J.A. Stravers (Eds.) Glaciated Continental Margins: an atlas of acoustic images. pp. 222-223. Chapman and Hall, London.

Bart, P.J., Anderson, J.B., 1995. Seismic record of glacial events affecting the Pacific margin of the northwestern Antarctic Peninsula. In: Cooper, A.K., Barker, P.F., Brancolini, G. (Eds.), Geology and Seismic Stratigraphy of the Antarctic Margin. Antarctic Research Series 68, 75-95.

Bart, P.J., Anderson, J.B., 1996. Seismic expression of depositional sequences associated with expansion and contraction of ice sheets on the northwestern Antarctic Peninsula continental shelf. Geological Society, London, Special Publications 117, 171-186.

Bart, P.J., Anderson, J.B., 1997a. Glacial uncorformities on the Antarctic continental margin, an example from the Antarctic Peninsula. In: Davies, T.A., Bell, T., Cooper, A.K., Josenhans, H., Polyak, L., Solheim, A., Stoker, M.S., Stravers, J.A. (Eds.), Glaciated Continental Margins: an atlas of acoustic images. Chapman and Hall, London, pp. 43-45.

Bart, P.J., Anderson, J.B., 1997b. Grounding zone wedges on the Antarctic continental shelf, Antarctic Peninsula. In: Davies, T.A., Bell, T., Cooper, A.K., Josenhans, H., Polyak, L., Solheim, A., Stoker, M.S., Stravers, J.A. (Eds.), Glaciated Continental Margins: an atlas of acoustic images. Chapman and Hall, London, pp. 96-97.

Bart, P.J., Anderson, J.B., 2000. Relative temporal stability of the Antarctic Ice Sheets during the late Neogene based on the minimum frequency of outer shelf grounding events. Earth and Planetary Science Letters 182, 259–272.

Bart, P.J., De Batist, M., Miller, H., 1994. Neogene collapse of glacially-deposited, shelf-edge deltas in the Weddell Sea: Relationships between deposition during glacial periods and sub-marine fan development. Terra Antarctica 1(2), 317-318.

Bartek, L. R., Vail, P. R., Anderson, J. B., Emmet, P. A., Wu, S., 1991. Effect of cenozoic ice sheet fluctuations in Antarctica on the stratigraphic signature of the Neogene. J. Geophys. Res. 96 (B4), 6753-6778.

Belderson, R.H., Kenyon, N.H., Wilson, J.B., 1973. Iceberg plough marks in the northeast Atlantic. Palaeogeography, Palaeoclimatology, Palaeoecology 13 (3), 215-224.

Benn, D.I., 1995. Fabric signature of till deformation, Breidamerkurjokull, Iceland. Sedimentology 42, 735–747.

Benn, D.I., Evans, D.J.A., 1996. The interpretation and classification of subglacially deformed sediments. Quaternary Science Reviews15, 23–52.

Bennett, M.R., Glasser, N.F., 1996. Glacial geology: ice sheets and landforms. Wiley, Chichester. 364 pp.

Bentley, M.J., Anderson, J.B., 1998. Glacial and marine geological evidence for the ice sheet configuration in the Weddell Sea-Antarctic Peninsula region during the Last Glacial Maximum. Antarctic Science 10 (30), 309-325.

Berger, W.F., Yasuda, M.K., Bickert, T., Wefer, G., Takayamat, T., 1994. Quaternary time scale for Ontong Java plateau: Milankovitch template for ocean drilling program site 806. Geology 22, 463–467.

Bindoff, N.L., Rosenberg, M.A., Warner, M.J., 2000. On the circulation and water masses over the Antarctic continental slope and rise between 80 and 150 degrees E. Deep-Sea Research Part II 47, 2299–2326.

Blum, P., 1997. Physical properties handbook: a guide to the shipboard measurement of physical properties of deep-sea cores. ODP Tech. Note, 26. Available from World Wide Web: <http://www-odp.tamu.edu/publications/tnotes/tn26/INDEX.HTM>.

Bougamont, M., Tulaczyk, S., Joughin, I., 2003. Response of subglacial sediments to basal freeze-on: Application in numerical modelling of the recent stoppage of Ice Stream C, West Antarctica, Journal of Geophysical Research 108, 2223, doi:10.1029/2002JB001936.

Boulton,G.S., Caban, P.E., van Gijssel, K., Leijnse, A., Punkari, M., van Weert, F.H.A., 1996. The impact of glaciation on the groundwater regime of Northwest Europe. Global and Planetary Change 12, 397-413.

Bouma, A.H., 1962. Sedimentology of Some Flysch Deposits: a Graphic Approach to Facies Interpretation. Elsevier, Amsterdam. 168 pp.

Bugge, T., Belderson, R.H., Kenyon, N.H., 1988. The Storegga Slide. Philosophical Transactions of the Royal Society of London. Series A, Mathematical and Physical Sciences, 325 (1586), 357-388.

Bryn, P., Berg, K., Forsberg, C.F., Solheim, A., Kvalstad, T.J., 2005. Explaining the Storegga Slide. Mar.Petrol.Geol. 22, 11-19.

Camerlenghi, A., Domack, E., Rebesco, M., Gilbert, R., Ishman, S., Leventer, A., Brachfeld, S., Drake, A., 2001. Glacial morphology and post-glacial contourites in northern Prince Gustav Channel (NW Weddell Sea, Antarctica). Marine Geophysical Researches 22, 417-443.

Canals, M., Baraza, J., Bart, P.J., Calafat, A.M., Casamor, J.L,, De Batist, M., Ercilla, G., Farrán, M., Francés, G., Gràcia, E., Ramos-Guerrero, E., Sanz, J.L., Sorribas, J., Tassone, A., 1994. La Cuenca Central de Bransfield (NW de la Península Antártica): primeros resultados de la campaña GEBRA'93. Geogaceta 16, 122-125.

Canals, M., Urgeles, R., Calafat, A.M., 2000. Deep sea-floor evidence of past ice streams off the Antarctic Peninsula. Geology 28 (1), 31-34.

Canals, M., Casamor, J.L., Urgeles, R., Calafat, A.M., Domack, E.W., Baraza, J., Farran, M., De Batist, M., 2002. Seafloor evidence of a subglacial sedimentary system off the northern Antarctic Peninsula. Geology 30 (7), 603-606.

Casas, D., Ercilla, G., Estrada, F., Alonso, B., Baraza, J., Lee, H., Kayen, R., Chiocci, F., 2004. Physical and geotechnical properties and assessment of sediment stability on the continental slope and basin of the Bransfield Basin (Antarctic Peninsula). Marine Geores. & Geotech. 22 (4), 253-278.

Clark, C.D., Tulaczik, S.M., Stokes, C.R., Canals, M., 2003. A groove-ploughing theory for the production of mega-scale glacial lineations, and implications for ice-stream mechanics. Journal of Glaciology 49 (165), 240-256.

Clausen, L., 1998. The Southeast Greenland glaciated margin: 3D stratal architecture of shelf and deep sea. The Geological Society of London, Special Publications 129, 173-203.

Cochonat, P., Piper, D.J.W., 1995. Source area of sediments contributing to the "Grand Banks" 1929 turbidity current. In: T.A. Davies, T. Bell, A.K. Cooper, H. Josenhans, L. Polyak, A. Solheim, M.S. Stoker, J.A. Stravers (Eds.) Glaciated Continental Margins: an atlas of acoustic images. pp. 12-13. Chapman and Hall, London.

Cook, A.J., Fox, A.J., Vaughan, D.G., Ferrigno, J.G., 2005. Retreating glacier fronts on the Antarctic Peninsula over the past half-century. Science 308, 541-545.

Cooper, A.K., Barrett, P.J., Hinz, K., Traube, V., Leitchenkov, G., Stagg, H.M.J., 1991. Cenozoic prograding sequences of the Antarctic continental margin: a record of glacio-eustatic and tectonic events. Marine Geology 102, 175-213.

Cowan, E.A., 2001. Identification of the glacial signal from the Antarctic Peninsula since 3.0 Ma at Site 1101 in a continental rise sediment drift. In: Barker, P.F., Camerlenghi, A., Acton, G.D., and Ramsay, A.T.S. (Eds.) Proceedings of the Ocean Drilling Program, Scientific Results 178, 1-22.

Dahlgren, K.I.T., Vorren, T.O., Stoker, M.S., Nielsen, T., Nygard, A., Sejrup, H.S., Sejrup, H.P., 2005. Late Cenozoic prograded wedges on the NW European continental margin: their formation and relationship to tectonics and climate. Marine and Petroleum Geology 22, 1089-1110.

Damuth, J.E., 1978. Echo character of the Norwegian-Greenland Sea: relationship to Quatemary sedimentation. Marine Geology 28, l-36.

Damuth, J.E., 1980. Use of high-frequency (3.5-12 kHz) echograms in the study of a near-bottom sedimentation precesses in the deep-sea: a review. Marine Geology 38, 51-75.

Davies, T.A., Bell, T., Cooper, A.K., Josenhans, H., Polyak, L., Solheim, A., Stoker, M.S., Stravers, J.A. (Eds.), 1997. Glaciated Continental Margins: an atlas of acoustic images. Chapman and Hall, London, 315 pp.

Davies, T.L., Van Niel, B., Kidd, R.B., Weaver, P.P.E., 1997. High-resolution stratigraphy and turbidite processes in the Seine Abyssal Plain, northwest Africa. Geo-Marine Letters 17, 147-153.

De Angelis, H., Skvarca, P., 2003. Glacier surge after ice shelf collapse. Science 299, n. 5612, 1560-1562.

De Santis, L., Anderson, J.B., Brancolini, G., Zayatz, I., 1997. Glaciomarine deposits on the continental shelf of Ross Sea, Antarctica. In: T.A. Davies, T. Bell, A.K. Cooper, H. Josenhans, L. Polyak, A. Solheim, M.S. Stoker, J.A. Stravers (Eds.) Glaciated Continental Margins: an atlas of acoustic images. pp. 110-113. Chapman & Hall.

De Santis, L., Brancolini, G., Donda, F., 2003. Seismo-stratigraphic analysis of the Wilkes Land continental margin (East Antarctica): influence of glacially driven processes on the Cenozoic deposition. Deep Sea Research Part II: Topical Studies in Oceanography 50, 1563-1594.

Dingle, R.V., Lavelle, M., 1998. Antarctic Peninsular cryosphere: Early Oligocene (c. 30 Ma) initiation and a revised glacial chronology. Journal of the Geological Society 155 (3), 433-437.

Domack, E.W., 2002. A Synthesis for Site 1098: Palmer Deep. In: Barker, P.F., Camerlenghi, A., Acton, G.D., and Ramsay, A.T.S. (Eds.), Proceedings of the Ocean Drilling Program, Scientific Results 178, <http://wwwodp.tamu.edu/publications/178_SR/ VOLUME/CHAPTERS/SR178_34.PDF

Domack, E., Amblàs, D., Gilbert, R., Brachfeld, S., Camerlenghi, A., Rebesco, M., Canals, M., Urgeles, R., 2006. Subglacial morphology and glacial evolution of the Palmer deep outlet system, Antarctic Peninsula. Geomorphology 75, 125-142.

Dowdeswell, J.A., Sharp, M.J., 1986. Characterisation of pebble fabrics in modern terrestrial glacigenic sediments. Sedimentology 33, 699–710.

Dowdeswell, J.A., Bamber, J.L., 2007. Keel depths of modern Antarctic icebergs and implications for sea-floor scouring in the geological record. Marine Geology 243, 120-131.

Dowdeswell, J.A., Whittington, R.J., Marienfeld, P., 1994. The origin of massive diamicton facies by iceberg rafting and scouring, Scoresby Sund, East Greenland. Sedimentology 41, 21-35.

Dowdeswell, J.A., Kenyon, N.H., Elverhøi, A., Laberg, J.S., Hollender, F.-J., Mienert, J., Siegert, M.J., 1996. Large-scale sedimentation on the glacier-influenced Polar North Atlantic margins: Long-range side-scan sonar evidence. Geophysical Research Letters 23 (24) 3535-3538.

Dowdeswell, J.A., Elverhøi, A., Spielhagen, R., 1998. Glacimarine sedimentary processes and facies on the polar North Atlantic margins. Quaternary Science Reviews 17, 242-272.

Dowdeswell, J.A., Whittington, R.J., Jennings, A.E., Andrews, J.T., Mackensens, A., Marienfeld, P., 2000. An origin for laminated glacimarine sediments through sea-ice build-up and suppressed iceberg rafting. Sedimentology 47, 557-576.

Dowdeswell, J.A., Ó Cofaigh, C., Pudsey, C.J., 2004. Continental slope morphology and sedimentary processes at the mouth of an Antarctic palaeo-ice stream: Marine Geology 204, 203-214.

Drewry, D.J., Morris, E.M., 1992. The response of large ice sheets to climatic change. Antarctica and environmental change. Philosophical Transactions: Biological Sciences, 338, 234-242.

Drewry, D.J., Jowan, S.R., Jankowski, E., 1982. Measured properties of the Antarctic ice sheet: Surface configurations, ice thickness, volume and bedrock characteristics. Annals of Glaciology 3, 83-91.

Ercilla, G., Baraza, J., Alonso, B., Canals, M., 1998. Recent geological processes in the Central Bransfield Basin (Western Antarctic Peninsula). In Stoker, M.S., Evans, D., Cramps, A. (Eds), Geological Processes on Continental Margins: Sedimentation, Mass-Wasting and Stability. Geological Society of London, Special Publications 129, 205-216.

Ercilla, G., Alonso, B., Estrada, F., Chiocci, F.L., Baraza, J., Farrán, M., 2000. El Sistema Turbidítico del Magdalena: Procesos geológicos recientes (Mar Caribe). In: Alonso, B., Ercilla, G. (Eds.), Valles Submarinos y Sistemas Turbidíticos Modernos, pp. 203–228. CSIC, Madrid.

Escutia, C., Warnke, D., Acton, G.D., Barcena, A., Burckle, L., Canals, M., Frazee, C.S., 2003. Sediment distribution and sedimentary processes across the Antarctic Wilkes Land margin during the Quaternary. Deep-Sea Research II 50, 1481-1508

Evans, H.B., 1965. GRAPE- A device for continuous determination of material density and porosity. SPWLA, 6th Annual Symposium 2, B1-B25.

Evans, J., Dowdeswell, J., ÓCofaigh, C., 2004. Late Quaternary submarine bedforms and ice-sheet flow in Gerlache Strait and on the adjacent continental shelf, Antarctic Peninsula: Journal of Quaternary Science 19, 397–407.

Evans, J., Pudsey, C.J., ÓCofaigh, C., Morris, P., Domack, E., 2005. Late Quaternary glacial history, flow dynamics and sedimentation along the eastern margin of the Antarctic Peninsula Ice Sheet. Quaternary Science Reviews 24, 741–774.

Eyles, N., 2006. The role of meltwater in glacial processes. Sedimentary Geology 190, 257-268.

Eyles, N., de Broekert, P., 2001. Glacial tunnel valleys in the Eastern Goldfields of Western Australia cut below the Late Paleozoic Pilbara ice sheet. Palaeogeography, Palaeoclimatology, Palaeoecology 171, 29-40.

Fabrés, J., Calafat, A.M., Canals, M., Bárcena, M.A., Flores, J.A., 2000. Bransfield Basin fine-grained sediments: late-Holocene sedimentary processes and Antarctic oceanographic conditions. The Holocene 10, 703-718.

Fagan, B.M., 2001. The Little Ice Age: How climate made History, 1300-1850. Basic Books, 272 p.

Faleide, J.I., Solheim, A., Fiedler,A., Hjelstuen, B.O., Andersen, E.S., Vanneste, K., 1996. Late Cenozoic evolution of the western Barents Sea-Svalbard continental margin. Global and Planetary Change 12, 53-74.

Faugères, J.C., Stow, D.A.V., 1993. Bottom current controlled sedimentation: a synthesis of the contourite problem. Sedimentary Geology 82, 287-297.

Faugères, J.C., Mézerais, M.L., Stow, D.A.V., 1993. Contourite drift types and their distribution in the North and South Atlantic Ocean basins. Sedimentary Geology 82, 189-203.

Faugères, J.C., Stow, D.A.V., Imbert, P., Viana, A., 1999. Seismic features diagnostic of contourite drifts. Marine Geology 162, 1-38.

Fitzgerald, P.G., Sandford, M., Barrett, P.J., Gleadow, A.J.W., 1986. Asymmetric extension associated with uplift and subsidence in the Transantarctic Mountains and Ross Embayment. Earth and Planetary Science Letters 81, 67-78.

Fretzdorff, S., Smellie, J.L., 2002. Electron microprobe characterization of ash layers in sediments from the central Bransfield basin (Antarctic Peninsula): evidence for at least two volcanic sources. Antarctic Science 14 (4), 412-421.

Galindo-Zaldívar, J., Jabaloy, A., Maldonado, A., Sanz de Galdeano, C., 1996. Continental fragmentation along the South Scotia Ridge transcurrent plate boundary (NE Antarctic Peninsula). Tectonophysics 258, 275-301

Galindo-Zaldivar, J., Gamboa, L., Maldonado, A., Nakao, S., Bochu, Y., 2004. Tectonic development of the Bransfield Basin and its prolongation to the South Scotia Ridge, northern Antarctic Peninsula. Marine Geology 206, 267-282.

Gamboa, L.A.P., Maldonado, P.R., 1990. Geophysical investigations in the Bransfield Strait and in the Bellingshausen Sea. In: St. John, B. (Ed.), Antarctica as an Exploration Frontier: Hydrocarbon Potential, Geology, and Hazards. American Association of Petroleum Geologists, Studies in Geology 31, 127–142.

García, M.A., Castro, C.G., Ríos, A.F., Doval, M.D., Roson, G., Gomis, D., López, O., 2002. Water masses and distribution of physico-chemical properties in the Western Bransfield Strait and Gerlache Strait during Austral summer 1995/1996. Deep-Sea Research II: Topical Studies in Oceanography 49, 585-602.

García, M., Ercilla, G., Alonso, B., 2006a. Caracterización morfológica del margen continental de la Cuenca de Bransfield. Procesos sedimentarios durante el último periodo glacial. VII Spanish Simposium on Polar Studies, Granada (Spain). Abstracts volume, 113-115.

García, M., Anderson, J.B., Ercilla, G., Alonso, B., 2006b. Glaciomarine sedimentation of the Central Bransfield Basin shelf. Conference on External controls on deep water depositional systems: Climate, sea-level and sediment flux. London Geological Society. Abstracts volume, 41-42.

Gilbert, R., Domack, E.W., Camerlenghi, A., 2003. Deglacial history of the Greenpeace Trough: ice sheet to ice shelf transition in the northwestern Weddell Sea. In: E. Domack, A. Leventer, A. Burnett, R. Bindschadler, P. Convey & M. Kirby (Eds.), Antarctic Peninsula Climate Variability: Historical and Paleoenvironmental Perspectives, pp. 195-204. Antarctic Research Series, 79. American Geophysical Union.

Gleadow, A.J.W., Fitzgerald, P.G., 1987. Uplift history and structure of the Transantarctic Mountains: new evidence from fission track dating of basement apatites in the Dry Valleys area, southern Victoria Land. Earth and Planetary Science Letters 82, 1-14.

Gomis, D., García, M.A., López, O., Pascual, A., 2002. Quasi-geostrophic 3D circulation and mass transport in the western Bransfield Strait during Austral summer 1995/96. Deep-Sea Research II, 49, 603-621.

González-Casado, J.M., Giner-Robles, J.L, López-Martínez, J., 2000. Bransfield Basin, Antarctic Peninsula: Not a normal backarc basin. Geology 28 (11), 1043-1046.

Gordon, A.L. Taylor, H.W., Georgi, D.T., 1977. Antarctic oceanographic zonation In: Dunbar, M.J. (Ed.), Polar Oceans, Arctic Institute of North America, Calgary. pp. 45–76.

Gràcia, E., Canals, M., Farrán, M., Prieto, M.J., Sorribas, J., GEBRA Team, 1996. Morphostructure and Evolution of the Central and Eastern Bransfield Basins (NW Antarctic Peninsula): Marine Geophysical Researches 18, 429-448.

Grelowski, A., Majewicz, A., Pastuszak, M., 1986. Mesoscale hydrodynamic processes in the region of Bransfield Strait and the southern part of Drake Passage during BIOMASS-SIBEZ 1983/84. Polish Polar Research 7 (4), 353-369.

Gribchenko, Y.N., Kurenkova, E.I., 1997. The main stages and natural environmental setting of late Palaeolithic human settlement in Eastern Europe. Quaternary International 41-42, 173-179.

Grobe, H., Mackensen, A., 1992. Late Quaternary climate cycles as recorded in sediments from the Antarctic continental margins. In: Kennett, J.P., Watkins, N.B. (Eds.), The Antarctic Paleoenvironment. American Geophysical Union, Antarctic Research Series 56, 349-376.

Haflidason, H., Sejrup, H.P., Nygård, A., Mienert, J., Bryn, P., Lien, R., Forsberg, C.F., Berg, K., Masson, D., 2004. The Storegga Slide: architecture, geometry and slide development. Marine Geology 213, 201-234.

Harrington, P.K., 1985. Formation of pockmarks by porewater escape. Geo-Marine Letters 5, 193-197.

Harris, P.T., O'Brien, P.E., 1998. Bottom currents, sedimentation and ice-sheet retreat facies successions on the Mac Robertson shelf, East Antarctica. Marine Geology 151, 47-72.

Hart, J.K., Roberts, D.H., 1994. Criteria to distinguish between subglacial glaciotectonic deformation and glaciomarine sedimentation, I. Deformation styles and sedimentology. Sedimentary Geology 91, 191–213.

Hawkes, D.D., 1962. The structure of the Scotia Arc. Geological Magazine 99, 85-91.

Hepp, D.A., Mörz, T., Thiede, J., W.C. Dullo, 2004. Reconstruction of Antarctic ice-sheet history from drift sediments. Geophysical Research Abstracts 6, 06413. SRef-ID: 1607-7962/gra/EGU04-A-06413

Hepp, D.A., Mörz, T., Grützner, J., 2006. Pliocene glacial cyclicity in a deep-sea sediment drift (Antarctic Peninsula Pacific Margin). Palaeogeography, Palaeoclimatology, Palaeoecology 231, 181-198.

Hernández-Molina, F.J., Larter, R.D., Rebesco, M., Maldonado, A., 2004. Miocene changes in bottom current regime recorded in continental rise sediments on the Pacific margin of the Antarctic Peninsula. Geophysical Reseach Letters 31, L22606, doi:10.1029/2004GL020298.

Hernández-Molina, F.J., Larter, R.D., Rebesco, M., Maldonado, A., 2006. Miocene reversal of botttom water flow along the Pacific Margin of the Antarctic Peninsula: Stratigraphic evidence from a contourite sedimentary tail. Marine Geology 228, 93-116.

Heroy, D.C., Anderson, J.B., 2005. Ice-sheet extent of the Antarctic Peninsula region during the Last Glacial Maximum (LGM)- Insights from glacial geomorphology. G.S.A.Bulletin 117, 1497-1512.

Heroy, D.C., Sjunneskog, C.S., Anderson, J.B., 2008. Holocene climate change in the Bransfield Basin, Antarctic Peninsula: evidence from sediment and diatom analysis. Antarctic Science 20, 69-87.

Hesse, R., Khodabakhsh, S., Klaucke, I., Ryan, W.B.F., 1997. Asymmetrical turbid surface-plume deposition near ice-outlets of the Pleistocene Laurentide ice sheet in the Labrador Sea. Geo-Marine Letters 17, 179–187.

Hesse, R., Klauck I., Khodabakhsh, S. Piper, D., 1999. Continental slope sedimentation adjacent to an ice margin. III. The upper Labrador Slope. Marine Geology 155, 249–276.

Hillenbrand, C.D., Fütterer, D.K., 2001. Neogene to Quaternary deposition of opal on the continental rise west of the Antarctic Peninsula. ODP Leg 178, Sites 1095, 1096, and 1101 In: Barker, P.F., Camerlenghi, A., Acton, G.D., and Ramsay, A.T.S. (Eds.), Proceedings of the ODP, Scientific Results 178, 1–33.

Hillenbrand, c.D., Ehrmann, W., 2005. Late Neogene to Quaternary environmental changes in the Antarctic Peninsula region: evidence from drift sediments. Global and Planetary Change 45, 165-191.

Hjort, C., Ingólfsson, Ó, Björck, S., 1992. The last major deglaciation in the Antarctic Peninsula region – A review of recent Swedish Quaternary research. In: Yoshida et al. (Eds.), Recent Progress in Antarctic Earth Science, 741-732. Terrapub, Tokyo.

Hofmann, E.E., 1985. The large-scale horizontal structure of the Antarctic Circumpolar Current from FGGE drifters. Journal of Geophysical Research 90 (4), 7087-7097.

Howard, W.R., 1997. A warm future in the past. Nature 388, 418–419.

Howe, J.A. 1995. Sedimentary processes and variations in slope-current activity during the glacial-interglacial episode on the Hebrides slope, northern Rockfall Trough, North Atlantic Ocean. Sedimentary Geology 96, 201-230.

Imbo, Y., De Batist, M., Canals, M., Prieto, M.J., Baraza, J., 2003. The Gebra Slide: a submarine slide on the Trinity Peninsula Margin, Antarctica. Marine Geology 193, 235-252.

Ingólfsson, Ó, Jhort, C., Björk, C., Smith, R.I.L., 1992. Late Pleistocene and Holocene glacial history of James Ross Island, Antarctic Peninsula. Boreas 21, 209-222.

Jabaloy, A., Balanyá, J.C., Barnolas, A., Galindo-Zaldívar, J., Hernández-Molina, F.J., Maldonado, A., Martínez-Martínez, J.M., Rodríguez-Fernández, J., Sanz de Galdeano, C., Somoza, L., Suriñach, E., Vázquez, J.T., 2003. The transition from an active to a passive margin (SW end of the South Shetland Trench, Antarctic Peninsula). Tectonophys 366, 55-81.

Jaeger, J.M. Nittrouer, C.A. Demaster, D.J. Kelchner C., Dunbar, R.B., 1996. Lateral transport of settling particles in the ross sea and implications for the fate of biogenic material. Journal of Geophysical Research-Oceans 101, 18479–18488.

Jeffers, J.D., Anderson, J.B., 1990. Sequence Stratigraphy of the Bransfield Basin, Antarctica: Implications for Tectonic History and Hydrocarbon Potential. In: St John, B. (Ed.), Antarctica as an Exploration Frontier: Hydrocarbon Potential, Geology and Hazards. AAPG. Studies in Geology 31, 13-29.

Jin, Y.K., Larter, R.D., Kim, Y., Nam, S.H., Kim, K.J., 2002. Post-subduction margin structures along Boyd Strait, Antarctic Peninsula. Tectonophysics 346, 187-200.

Josenhans, H., 1997. Subglacial channels in Hudson Bay, Canada. In: T.A. Davies, T. Bell, A.K. Cooper, H. Josenhans, L. Polyak, A. Solheim, M.S. Stoker, J.A. Stravers (Eds.) Glaciated Continental Margins: an atlas of acoustic images. pp. 62-63. Chapman & Hall.

Judd, A., Hovland, M., 2007. Seabed fluid flow. The impact on geology, biology and the marine environment. Cambridge University Press.

Kelley, J.T., Dickson, S.M., Belknap, D.F., Barnhardt, W.A., Henderson, M., 1994. Giant sea-bed pockmarks: evidence for gas escape from Belfast Bay, Maine. Geology 22, 59-62.

King, E.L., Sejrup, H.P., Haflidason, H., Elverhøi, A., Aarseth, I., 1996. Quaternary seismic stratigraphy of the North Sea Fan: glacially-fed gravity flow aprons, hemipelagic sediments, and large submarine slides. Marine Geology 130, 293-315.

King, E.L., Haflidason, H., Sejrup, H.P., Løvlie, R., 1998. Glacigenic debris flows on the North Sea trough mouth fan during ice stream maxima. Marine Geology 152, 217-246.

Klepeis, K. A., Lawver, L.A., 1994. Bathymetry of the Bransfield Strait, southeastern Shackleton Fracture Zone and South Shetland Trench. Antarct. J. U. S. 28, 103–104.

Kuijpers, A., Dalhoff, F., Brandt, M.P., Hümbs, P., Scott, T., Zotova, A., 2007. Giant iceberg plow marks at more than 1 km water depth offshore West Greenland. Marine Geology 246, 60-64. doi: 10.1016/j.margeo.2008.05.010.

Kuvaas, B., Leitchenkov, G., 1992. Glaciomarine turbidite and current-controlled deposits in Prydz Bay, Antarctica. Marine Geology 108, 365-381.

Kuvaas, B., Kristoffersen, Y., 1991. The Crary Fan: A trough-mouth fan on the Weddell Sea continental margin, Antarctica. Marine Geology 97, 345-362.

Laberg, J.S., Vorren, T.O., 1995. Late Weichselian submarine debris flow deposits on the Bear Island trough mouth fan. Marine Geology 127, 45-72.

Larter R.D., Barker, P.F., 1989, Seismic stratigraphy of the Antarctic Peninsula Pacific margin: a record of Pliocene-Pleistocene ice volume and paleoclimate, Geology17, 731-734.

Larter R.D., Barker, P.F., 1991. Effects of ridge crest-trench interaction on Antarctic-Phoenix spreading: forces on a young subducting plate. Journal of Geophysical Research 96, 19586-19607.

Larter, R.D., Cunningham, A.P., 1993. The depositional pattern and distribution of glacialinterglacial sequences on the Antarctic Peninsula Pacific margin. Marine Geology 109, 203-219.

Larter, R.D., Vanneste, L.E., 1995. Relict subglacial deltas on the Antarctic Peninsula outer shelf. Geology 23 (1), 33-36.

Lawver, L.A., Sloan, B.J., Barker, D.H.N., Ghidella, M., Von Herzen, R.P., Keller, R.A., Klinkhammer, G.P., Chin, C.S., 1996. Distributed, active extension in Bransfield Basin, Antarctic Peninsula: Evidence from multibeam bathymetry. GSA Today 6, 1-6.

Lee, J.I., Park, B.-K., Jwa, Y.J., Yoon, H.I., Yoo, K.C., Kim, Y., 2005. Geochemical characteristics and the provenance of sediments in the Bransfield Strait, West Antarctica. Marine Geology 219, 81-98.

Leventer, A., Domack, E., Barkoukis, A., McAndrews, B., Murray, J., 2002. Laminations from the Palmer Deep: a diatom based interpretation. Paleoceanography 17, doi:10.1029/2001PA000624.

Leventer, A., Domack, E., Dunbar, R., Pike, J., Stickley, C., Maddison, E., Brachfeld, S., Manley, P., McClennen, C., 2006. Marine sediment record from the East Antarctic margin reveals dynamics of ice sheet recession. GSA Today 16 (12), doi: 10.1130/GSAT01612A.1.

Licht, K.J., Dunbar, N.W., Andrews, J.T., Jennings, A.E., 1999. Distinguishing subglacial till and glacial marine diamictons in the western Ross Sea, Antarctica: Implications for a last glacial maximum grounding line: Geological Society of America Bulletin 111, 91-103.

Lien, R., Solheim, A., Elverhøi, A., Rokoengen, K., 1989. Iceberg scouring and sea bed morphology on the eastern Weddell Sea shelf, Antarctica. Polar Research 7 (1), 43-57.

Llave, E., García, M., Pérez, C., Sayago, M., Farrán, M., Ercilla, G., Somoza, L., León, R., Maestro, A., Medialdea, T., Hernández-Molina, F.J., Alvarez, R., Durán, R., Mohamed, K., 2008. Morphological feature analyses of the Prestige half-graben on the SW Galicia Bank. Marine Geology 249, 7-20.

López, O., García, M.A., Sánchez.-Arcilla, A., 1994. Tidal and residual currents in the Bransfield Strait, Antarctica. Annales Geophysicae 12, 887-902.

López, O., García, M.A., Gomis,D., Rojas, P., Sospedra, J., Sánchez-Arcilla, A., 1999. Hydrographic and hydrodynamic characteristics of the eastern basin of the Bransfield Strait (Antarctica). Deep-Sea Research I 46, 1755-1778.

Lowe, A.L., Anderson, J.B., 2003. Evidence fro abundant subglacial meltwater beneath the paleo-ice sheet in Pine Island Bay, Antarctica. Journal of Glaciology 49 (164), 125-138.

Lucchi, R.G., Rebesco, M., Camerlenghi, A., Busetti, M., Tomadin, L., Villa, G., Persico, D., Morigi, C., Bonci, M.C., Giorgetti, G., 2002. Mid-late Pleistocene glacimarine sedimentary processes of a high-latitude, deep-sea sediment drift (Antarctic Peninsula Pacific margin). Marine Geology 189, 343-370.

MacLean, B., 1997. Submarine lateral moraine in the south central region of Hudson Strait, Canada. In: T.A. Davies, T. Bell, A.K. Cooper, H. Josenhans, L. Polyak, A. Solheim, M.S. Stoker, J.A. Stravers (Eds.) Glaciated Continental Margins: an atlas of acoustic images. pp. 86-87. Chapman & Hall.

Maestro, A., Somoza, L., Rey, J., Martínez-Frías, J., López-Martínez, J., 2007. Active tectonics, fault patterns, and stress field of Deception Island: A response to oblique convergence between the Pacific and Antarctic plates. Journal of South America Earth Sciences 23 (2-3), 256-268.

Maldonado. A., Aldaya, F., Balanyá. J.C., Galindo-Zaldívar, J.. Jabaloy. A., Larter, R.D., Rodríguez-Fernández. J.. Roussanov. M., Sanz de Galdeano. C., 1994. Cenozoic continental margin growth patterns m the northern Antarctic Peninsula. Terra Antarctica 1, 311-314.

Maldonado, A., Barnolas, A., Bohoyo, F., Galindo-Zaldívar, J., Hernández-Molina, J., Lobo, F., Rodríguez-Fernández, J., Somoza, L., Vázquez, J.T., 2003. Contourite deposits in the central Scotia Sea: the importance of the Antarctic Circumpolar Current and the Weddell Gyre flows. Palaeogeography, Palaeoclimatology, Palaeoecology 198, 187-221.

Mandryk, C.A.S., Josenhans, H., Fedje, D.W., Mathewes, R.W., 2001. Late Quaternary paleoenvironments of Northwestern North America: implications for inland versus coastal migration routes. Quaternary Science Reviews 20, 301-314.

Mangerud, J., Jansen, E., Landvik, J.Y., 1996. Late Cenozoic history of the Scandinavian and Barents Sea ice sheets. Global and Planetary Change 12, 11-26.

Marshall, D., 1995. Topographic steering of the Antarctic Circumpolar Current. Journal of Physical Oceanography 25 (7), 1636-1650.

Masson, D.G., Huggett, Q.J., Brunsden, D., 1993. The surface texture of the Saharan Debris Flow deposit and some speculations on submarine debris flow processes. Sedimentology 40, 583-598.

McCave, I.N., Tucholke, B.E., 1986. Deep current controlled sedimentation in the western North Atlantic. In: Vogt, P.R., Tucholke, B.E. (Eds.), The Geology of North America, vol. M, The Western North Atlantic Region, pp. 451–468. Geological Society of America, Boulder, Colorado.

McKay, R.M., Dunbar, G.B., Naish, T.R., Barrett, P.J., Carter, L., Harper, M., 2008. Retreat history of the Ross Ice Sheet (Shelf) since the Last Glacial Maximum from deep-basin sediment cores around Ross Island. Palaeogeography, Palaeoclimatology, Palaeoecology 260, 245-261.

McMullen, K., Domack, E., Leventer, A., Olson, C., Dunbar, R., Brachfeld, S., 2006. Glacial morphology and sediment formation in the Mertz Trough, East Antarctica. Palaeogeography, Palaeoclimatology, Palaeoecology 231, 169– 180.

Miller, K.G., Wright, J.D., Fairbanks, R.G., 1991. Unlocking the Ice House: Oligocene–Miocene oxygen isotopes, eustasy, and margin erosion. Journal of Geophysical Research 96, 6829-6848.

Mitchum R.M.J., Vail, P.R., Thompson III, S., 1977a. Seismic stratigraphy and global changes of sea level, Part 2: The depositional sequence as a basic unit for stratigraphic analysis. In: Payton, C.E. (Ed.), Seismic Stratigraphy –Applications to Hydrocarbon Exploration. American Association of Petroleum Geologists, Memoir, 53-62.

Mitchum, R.M.J., Vail, P.R., Sangree, J.B., 1977b. Seismic stratigraphy and global changes of sea level, Part 6: Stratigraphic interpretation of seismic reflection patterns in depositional sequnces. In: Payton, C.E. (Ed.), Seismic Stratigraphy –Applications to Hydrocarbon Exploration. American Association of Petroleum Geologists, Memoir, 117-133.

Murdmaa, I., Ivanova, E., Duplessy, J.C., Levitan, M., Khusid, T., Bourtman, M., Alekhina, G., Alekseeva, T., Belousov, M., Serova, V., 2006. Facies system of the Eastern Barents Sea since the last glaciation to present. Marine Geology 230, 275-303.

Naveira Garabato, A.C., Heywood, K.J., Stevens, D.P., 2002a. Modification and pathways of Southern Ocean Deep Waters in the Scotia Sea. Deep-Sea Research I 49, 681–705.

Naveira Garabato, A.C., McDonagh, E.L., Stevens, D.P., Heywood, K.J., Sanders, R.J., 2002b. On the export of Antarctic Bottom Water from the Weddell Sea. Deep-Sea Research II 49, 4715–4742.

Naveira Garabato, A.C., Stevens, D.P., Heywood, K.J., 2003. Water mass conversion, fluxes and mixing in the Scotia Sea diagnosed by an inverse model. Journal of Physical Oceanography 33, 2565–2587.

Naveira-Garabato, A.C., Polzin, K.L., King, B.A., Heywood, K.J., Visbeck, M., 2004. Widespread intense turbulent mixing in the Southern Ocean. Science 303 (5655) 210-213.

Nygård, A., Sejrup, H.P., Haflidason, H., Bryn, P., 2005. The glacial North Sea Fan, southern Norwegian Margin: architecture and evolution from the upper continental slope to the deep-sea basin. Marine and Petroleum Geology 22, 71–84.

O'Brien, P.E., Leitchenkov, G., Harris, P.T., 1997. Iceberg plough marks, subglacial bedforms and grounding zone moraines in Prydz Bay, Antarctica. In: T.A. Davies, T. Bell, A.K. Cooper, H. Josenhans, L. Polyak, A. Solheim, M.S. Stoker, J.A. Stravers (Eds.) Glaciated Continental Margins: an atlas of acoustic images. pp. 228-231. Chapman & Hall.

O'Brien, P.E., De Santis, L., Harris, P.T., Domack, E., Quilty, P.G., 1999. Ice shelf grounding zone features of western Prydz Bay, Antarctica : sedimentary processes from seismic and sidescan images. Antarctic Science 11, 78-91.

O'Brien, P.E., Cooper, A.K., Richter, C., 2001. Leg 188 summary: Prydz Bay-Cooperation Sea, Antarctica. Proceedings of the Ocean Drilling Program. Initial Reports, 1096-2158.

Ó Cofaigh, C., Dowdeswell, J.A., 2001. Laminated sediments in glacimarine environments: diagnostic criteria for their interpretation. Quaternary Science Reviews 20, 1411-1436.

Ó Cofaigh, C., Dowdeswell, J.A., Pudsey, C.J., 2001. Late Quaternary iceberg rafting along the Antarctic Peninsula continental rise and in the Weddell and Scotia Seas. Quaternary Research 56, 308-321.

Ó Cofaigh, C., Dowdeswell, J.A., Allen, C.S., Hiemstra, J.F., Pudsey, C.J., Evans, J., Evans, D.J.A., 2005. Flow dynamics and till genesis associated with a marine-based Antarctic palaeo-ice stream. Quaternary Science Reviews 24, 709-740.

Olsen, L., Sveian, H., Bergstrøm, B., Selvik, S.F., Lauritzen, S.E., Stokland, Ø., Grøsfjeld, K., 2001. Methods and stratigraphies used to reconstruct Mid- and Late Weichselian palaeoenvironmental and palaeoclimatic changes in Norway. Norges geologiske undersøkelse Bulletin 438, 21-46.

Oppenheimer, M., 2001. Global warming and the stability of the West Antarctic Ice Sheet. Nature 393, 325-332.

Orsi, A.H., Nowlin, W.D., Whitworth III, T., 1993. On the circulation and stratification of the Weddell Gyre. Deep-Sea Research I 40 (1), 169-203.

Orsi, A.H., Whitworth III, T. Nowlin, W., 1995. On the meridional extent and fronts of the Antarctic Circumpolar Current. Deep-Sea Research I 42 (5), 641-673.

Orsi, A.H., Johnson, G.C., Bullister, J.L., 1999. Circulation, mixing and production of Antarctic Bottom Water. Progress in Oceanography 43, 55–109.

Osterman, L.E., Poore, R.Z., Barron, J., 2001. Climate variability of the Holocene, Site 1098, Palmer Deep, Antarctica. In: Barker, P.F., Camerlenghi, A., Acton, G.D., Ramsay, A.T.S. (Eds.). Proceedings of the Ocean Drilling Program, Scientific Results 178, 1–45. http://www-odp.tamu.edu/publications/178_SR/VOLUME/CHAPTERS/SR178_07.PDF

Ottesen, D., Rise, L., Knies, J., Olsen, L., Henriksen, S., 2005. The Vestfjorden-Trænadjupet palaeo-ice stream drainage system, mid-Norwegian continental shelf. Marine Geology 218, 175-189.

Paillard, D., 1998. The timing of Pleistocene glaciations from a simple multiple-state climate model. Nature 391, 378–381.

Pilkey, O.H., Hokanson, C., 1991. A proposed classification for submarine basins plains. In: Osborne, R.H. (Ed.), From shoreline to abyss: Contributions in Marine Geology in Honor of Francis Parker Shepard. Society of Economic Paleontologists and Mineralogists, Special Publication 46, 249-258.

Piotrowski, J.A., 1997a. Subglacial groundwater flow during the last glaciation in northwestern Germany. Sedimentary Geology 111, 217-224

Piotrowski, J.A., 1997b. Subglacial hydrology in north-western germany during the last glaciation: groundwater flow, tunnel valleys and hydrological cycles. Quaternary Science Reviews 16 (2), 169-185.

Polish Academy of Sciences, Institute of Ecology, 1990. Mapa Batymetryczna Ciesniny Brasfielda (Bransfield Strait), 1:14000.

Polyak, L., Forman, S.L., Herlihy, F.A., Ivanov, G., Krinitsky, P., 1997. Late Weichselian deglacial history of the Svyataya (Saint) Anna Trough, northern Kara Sea, Arctic Russia. Marine Geology 143, 169-1188.

Pope, P.G., Anderson, J.B., 1992. Late Quaternary glacial history of the Northern Antarctic Peninsula's western continental shelf: evidence from the marine record. Contributions to Antarctic Reseach III. Antarctic Research Series 57, 63-91

Posamentier, H.W., Jervey, M.T., Vail, P.R., 1988. Eustatic controls on clastic deposition I –conceptual framework. Special Publications Society for Sedimentary Geology 42, 109-124.

Powell, R.D., 1984. Glacimarine processes and inductive lithofacies modelling of ice shelf and tidewater glacier sediments based on quaternary examples. Marine Geology 57, 1-52.

Prieto, M.J., Canals, M., Ercilla, G., De Batist, M., 1998. Structure and geodynamic evolution of the Central Bransfield Basin (NW Antarctica) from seismic reflection data. Marine Geology 149, 17-38.

Prieto, M.J., Ercilla, G., Canals, M., De Batist, M., 1999. Seismic stratigraphy of the Central Bransfield Basin (NW Antarctic Peninsula): interpretation of deposits and sedimentary processes in a glacio-marine environment. Marine Geology 157, 47-68.

Pudsey, C.J., 2000. Sedimentation on the continental rise west of the Antarctic Peninsula over the last three glacial cycles. Marine Geology 167, 313-338.

Pudsey, C.J., Camerlenghi, A., 1998. Glacial-interglacial deposition on a sediment drift on the Pacific Margin of the Antarctic Peninsula. Antarctic Science 10, 286-308.

Pudsey, C.J., Barker, P.F., Larter, R.D., 1994. Ice sheet retreat from the Antarctic Peninsula shelf. Continental Shelf Research 14, 1647-1675.

Pudsey, C.J., Barker, P.F, Larter, R.D., 1997. Glacial flutes and iceberg furrows, Antarctic Peninsula. In: Davies, T.A., Bell, T., Cooper, A.K., Josenhans, H., Polyak, L., Solheim, A., Stoker, M.S., Stravers, J.A. (Eds.), Glaciated Continental Margins: an atlas of acoustic images. Chapman and Hall, London, pp. 58-59.

Punkari, M., 1997. Subglacial processes of the Scandinavian Ice Sheet in Fennoscandia inferred from flow-parallel features and lithostratigraphy. Sedimentary Geology 111, 263-283.

Rack, W., Rott, H., 2004. Pattern of retreat and disintegration of the Larsen B ice shelf, Antarctic Peninsula. Annals of Glaciology 39, 505-510.

Raymo, M.E., Lisiecki, L.E., Nisancioglu, K.H., 2006. Plio-Pleistocene Ice Volume, Antarctic Climate, and the Global $\delta^{18}O$ Record. Science 313, 492-495.

Reading, H. G., 1986, Sedimentary environments and facies. Elsevier, New York. 615 pp.

Rebesco, M., Larter, R.D., Camerlenghi, A., Barker, P.F., 1996. Giant sediment drifts on the continental rise of the Antarctic Peninsula. Geo-Marine Letters 16, 65-75.

Rebesco, M., Larter, R.D., Barker, P.F., Camerlenghi, A., Vanneste, L.E., 1997. The history of sedimentation on the continental rise west of the Antarctic Peninsula. In: Barker, P.F., Cooper, A.K. (Eds.), Geology and Seismic Stratigraphy of the Antarctic Margin (Pt. 2). Antarctic Research Series 71, 29-50.

Rebesco, M., Camerlenghi, A., Geletti,R., Canals, M., 2006. Margin architecture reveals the transition to the modern Antarctic ice sheet ca. 3 Ma. Geology 34 (4), 301-304.

Rintoul, S.R., Hughes, C.W., Olbers, D., 2001. The Antarctic Circumpolar Current system. In: Siedler, G., Church, J., Gould, J. (Eds.), Ocean circulation and climate: observing and modelling the global ocean. International Geophysics Series 77, 271-302.

Rise, L., Ottesen, D., Berg, K., Lundin, E., 2005. Large-scale development of the mid-Norwegian margin during the last 3 million years. Marine and Petroleum Geology 22, 33-44.

Rott, H., Skvarca, P., Nagler, T., 1996. Rapid collapse of Northern Larsen Ice Shelf, Antarctica. Science 271 (5250), 788-792.

Saanumi, A.A., 2006. Ice sheet grounding zone deposits on Ross Sea continental shelf (Antarctica): Seismic facies analysis and P-wave reflectivity attributes. MSc Thesis, Louisiana State University and A&M College. 104 pp.

Scambos, T.A., Bohlander, J.A., Shuman, C.A., Skvarca, P., 2004. Glacier acceleration and thinning after ice shelf collapse in the Larsen B embayment, Antarctica. Geophysical Research Letters 31, L18402, doi:10.1029/2004GL020670.

Shackleton, N.J., Berger, A., Peltier, W.R., 1990. An Alternative astronomical calibration on the Lower Pleistocene time scales based on ODP Site 677. Tran. R. Soc. Edinburgh. Earth Sci. 81, 251–261.

Shaw, J., Kvill, D., Rains, B., 1989. Drumlins and catastrophic subglacial floods. Sedimentary Geology 62, 177-202.

Shaw, J., 2002. The meltwater hypothesis for subglacial bedforms. Quaternary International 90, 5-22

Shipp, S.S., Anderson, J.B., 1997. Drumlin field on the Ross Sea continental shelf, Antarctica. In: T.A. Davies, T. Bell, A.K. Cooper, H. Josenhans, L. Polyak, A. Solheim, M.S. Stoker, J.A. Stravers

(Eds.) Glaciated Continental Margins: an atlas of acoustic images. pp. 52-53. Chapman and Hall, London.

Shipp, S., Anderson, J., Domack, E., 1999. Late Pleistocene-Holocene retreat of the West Antarctic Ice-Sheet system in the Ross Sea: Part 1-Geophysical results. Geological Society of America Bulletin 111, 1486-1516.

Sjunneskog, C., Taylor, F., 2002. Postglacial marine diatom record of the Palmer Deep, Antarctic Peninsula (ODP Leg 178, Site 1098) 1. Total diatom abundance. Paleoceanography 17(3), 10.1029/2000PA000563.

Solheim A., Andersen, E.S., Elverhøi, A., Fiedler, A., 1996. Late Cenozoic depositional history of the western Svalbard continental shelf, controlled by subsidence and climate. Glob. Planet. Change 12, 135-148.

Solheim, A., 1997. Ice-marginal and ice-contact features. Overview. In: Davies, T.A., Bell, T., Cooper, A.K., Josenhans, H., Polyak, L., Solheim, A., Stoker, M.S., Stravers, J.A. (Eds.), Glaciated Continental Margins: an atlas of acoustic images. Chapman and Hall, London, pp. 75-76.

Solheim, A., Faleide, J.I., Andersen, E., Elverhøi, A., Forsberg, C.F., Vanneste, K., Uenzelmann-Neben, G., Channell, J.E.T., 1998. Late Cenozoic seismic stratigraphy and glacial geological development of the East Greenland and Svalbard-Barents Sea continental margins. Quaternary Science Reviews 17, 155-184.

Solheim, A., Berg, K., Forsberg, C.F., Bryn, P., 2005. The Storegga Slide complex: repetitive large scale sliding with similar cause and development: Mar. Petrol. Geol. 22, 97-107.

Stoker, M.S., Akhurst, C., Howe, J.A., Stow, D.A.V., 1998. Sediment drifts and contourites on the continental margin, off Northwest Britain. Sedimentary Geology 115 (1–4), 33–52.

Stokes, C.R., Clark, C.D., 2001. Palaeo-ice streams. Quaternary Science Reviews 20, 1437-1457.

Stokes, C.R., Clark, C.D., 2002. Are long subglacial bedforms indicative of fast ice flow? Boreas 31 (3), 239-249.

Stow, D.A.V., Lovell, J.P.B., 1979. Contourites: their recognition in modern and ancient sediments. Earth Science Reviews 14, 251-291.

Stow, D.A.V., Pudsey, C.J., Howe, J.A., Faugères, J.C., Viana, A.R., 2002. Deep-water Contourite Systems: Modern Drifts and Ancient Series, Seismic and Sedimentary Characteristics. Memoirs, vol. 22. Geological Society of London.

Swanson, R.G., 1981. Sample examination manual. Methods in Exploration Series, AAPG.

Taylor, F., Sjunneskog, C., 2002. Postglacial marine diatom record of the Palmer Deep, Antarctic Peninsula (ODP Leg 178, Site 1098) II: Diatom assemblages. Paleoceanography, 10.1029/2000PA000584.

ten Brink, U.S., Schneider, C., Johnson, A.H., 1995. Morphology and stratal geometry of the Antarctic continental shelf: insights from models. Antarctic Research Series 68, 1-24.

Tittman, J., Wahl, J.S., 1965. The physical foundations of formation density logging (Gamma-Gamma). Geophysics 30, 284-294.

Ussler III, W., Paull, C.K., Boucher, J., Friederich, G.E., Thomas, D.J., 2003. Submarine pockmarks: a case study from Belfast Bay, Maine. Marine Geology 202, 175–192.

Vail, P.R., 1987. Seismic stratigraphy interpretation procedure. In: Bally, A.W. (Ed.), Seismic stratigraphy I and II. American Association of Petroleum Geologists Studies in Geology, Memoir, pp 1-10.

Vail, P.R., Mitchum, R.M.J., Thompson, S., 1977. Seismic stratigraphic and global changes of sea level, part 4: global cycles of relative changes of sea level. American Association of Petroleum Geologists, 26: 63-81.

Vail, P.R., Mitchum Jr., R.M., Todd, R.G., Widmier, J.M., Thompson III, S., Sangree, J.B., Bubb, J.N., Hatlelid, W.G., 1977. Seismic stratigraphy and global changes of sea level. In: Payton, C.E. (Ed.), Seismic Stratigraphy- Applications to Hydrocarbon Exploration. AAPG Memoir 26, 49-205.

Vail, P.R., Audemard, F., Bowman, S.A., Eisner, P.N., Pérez-Cruz, C., 1991. The stratigraphic signature of tectonics, eustasy and sedimentology –an overview. In: Einsele, G., Ricken, W., Seilacher, A. (Eds.), Cycles and events in stratigraphy. Springer-Verlag, pp. 617-659.

Van Wagoner, J.C., Posamentier, H.W., Mitchum, R.M., Vail, P.R., Sarg, J.F., Loutiti, T.S., Hardenbol, J., 1988. An overview o the fundamentals of sequence stratigraphy, and key definitions. In: Wilgus, C.K., Ross, C.A., Posamentier, H.W., Van Wagoner, J.C., Kendall, C. (Eds.), Sea level changes: an integrated approach. Special Publication of the Society of Economic Paleontologists and Mineralogists, Tulsa, Oklahoma, pp. 39-45.

Vatan, A., 1967. Manuel de Sédimentologie. Technip, Paris. 397 pp.

Vaughan, D.G., Marshall, G.J., Connolley, W.M., Parkinson, C, Mulvaney, R., Hodgson, D.A., King, J.C., Pudsey, C.J., Turner, J., 2003. Recent rapid regional climate warming on the Antarctic Peninsula. Climatic Change 60, 243–274.

Vera, J.A., 1994. Asociaciones de facies. Estratigrafía: principios y métodos. Rueda, Madrid, pp. 157-195.

Vorren, T.O., Laberg, J.S., 1997. Trough mouth fans - palaeoclimate and ice-sheet monitors. Quaternary Science Reviews 16, 865-881.

Vorren, T.O., Lebesbye, E., Andreassen, K., Larsen, K.B., 1989. Glacigenic sediments on a passive continental margin as exemplified by the Barents Sea. Marine Geology 85, 251-272.

Vorren, T.O., Laberg, J.S., Blaume, F., Dowdeswell, J.A., Kenyon, N.H., Mienert, J., Rumohr, J., Werner, F., 1998. he Norwegian-Greenland Sea continental margins: morphology and late quaternary sedimentary processes and environment. Quaternary Science Reviews 17, 273-302.

Weaver, P.P.E., Rothwell, R.C., 1987. Sedimentation on the Madeira Abyssal Plain over the last 300 000 years. In: Weaver, P.P.E., Thomson, J. (Eds.), Geology and Geochemistry of Abyssal Plains. Geological Society of London, Special Publication 31, 71-86.

Weaver, P.P.E., Searle, R.C., Kuijpers, A., 1986. Turbidite depositional and the origin of the Madeira Abyssal Plain. In: Summerhayes, C., Shackleton, N.J. (Eds.), North Atlantic Palaeoceanography. Geological Society of London Special Publications 21, 131-143.

Weaver, P.P.E., Wynn, R.B., Kenyon, N.H., Evans, J., 2000. Continental margin sedimentation, with special reference to the north-east Atlantic margin. Sedimentology 47, 239-256.

Webb, D.L., 1993. Seabed and sub-seabed mapping using a parametric system. Hydrographic Journal 68, 5-13.

Weiss R. F., Oestlund, H. G., Craigh, H., 1979. Geochemical studies of the Weddell Sea. Deep-Sea Research 26, 1093-1120.

Wellner, J.S., Lowe, A.L., Anderson, J.B., 2001. Distribution of glacial geomorphic features on the Antarctic continental shelf and correlation with substrate: implications for ice behavior. Journal of Glaciology 47 (158), 397-411.

Wellner, J.S., Heroy, D.C., Anderson, J.B., 2006. The death mask of the Antarctic Ice Sheet: comparison of glacial geomorphic features across the continental shelf. Geomorphology 75 (1-2), 157-171.

Whitworth, T.I., 1980. Zonation and geostrophic flow of the Antarctic Circumpolar Current at Drake Passage. Deep-Sea Research 27, 497–507

Whitworth, T., Nowlin, W.D., 1987. Water masses and currents of the Southern Ocean at the Greenwich Meridian. Journal of Geophysical Research 92 (6), 6462-6476.

Willmott, V., 2007. Registros sedimentarios marinos del Holoceno en la Península Antártica septentrional. PhD Thesis, University of Barcelona. 212 pp.

Willmott, V., Canals, M., Casamor, J.L., 2003. Retreat history of the Gerlache-Boyd ice stream, Northern Antarctic Peninsula: an ultra-high resolution acoustic study of the deglacial and post-glacial sediment drape. In: Domack, E.W., Leventer, A., Burnett, A., Bindschadler, R., Convey, P., Kirby, M.E. (Eds.), Antarctic Peninsula Climate Variability: a historical and palaeoenvironmental perspective. Antarctic Research Series 79, American Geophysical Union, Washington D.C., 183-194.

Willmott, V., Domack, E. W., Canals, M., Brachfeld, S., 2006. A high resolution relative paleointensity record from the Gerlache-Boyd paleo-ice stream region, northern Antarctic Peninsula. Quaternary Research 66, 1-11.

Willmott, V., Domack, E. W., Canals, M., in press. Glacio-marine sediment drifts from Gerlache Strait, Antarctic Peninsula. In: Glasser, N., Hambrey, M.J. (Eds.), Glacial Sedimentary Processes and Products. International Association of Sedimentologists, Special Publication.

Wilson, C., Kinkhammer, G.P., Chin, C.S., 1999. Hydrography within the Central and East Basins of the Bransfield Strait, Antarctica. Journal of Physical Oceanography 29, 465-479.

Yoon, H.I., Han, M.W., Park, B.-K., Oh, J.-K, Chang, S.-K., 1997. Glaciomarine sedimentation and palaeo-glacial setting of Maxwell Bay and its tributary embayment, Marian Cove, South Shetland Islands, West Antarctica. Marine Geology 140, 265-282.

Yoon, H.I., Park, B.K., Kim, Y., Kan, C.Y., 2002. Glaciomarine sedimentation and its Paleoclimatic implications on the Antarctic Peninsula shelf over the last 15000 years. Palaeogeography, Palaeoclimatology, Palaeoecology 185, 235–254.